OPTIMISATION OF ADVANCED BIOFUEL THERMOCHEMICAL CONVERSION PHENOMENA FOR PRODUCING BIOENERGY VIA GASIFICATION

Edris Madadian

Department of Bioresource Engineering

McGill University

Quebec, Canada

January 2017

A Thesis Submitted to McGill University in partial fulfilment of the requirement for the degree of Doctor of Philosophy

This thesis is dedicated to the pearls of my life, my beautiful parents for their love, endless support and encouragement

Abstract

With the need for developing a more sustainable world there is a desire to shift from fossil fuels to biofuels, produced using the concept of biorefineries. Within the last few decades, thermochemical conversion technologies have gained a great deal of attention for producing advanced biofuels. In this context, the present thesis elaborated different aspects of biomass gasification technology, as a representative of thermochemical pathways, and suggested potential solutions to enhance the efficacy of the process. To fulfill this goal, different types of biomass feedstock were used to examine the potential of bioenergy production through a down-draft gasification reactor.

The first study was an assessment of pelletized woody biomass to identify potential combustion failure during the decomposition of pelletized biomass in a down-draft reactor. The average temperature of the combustion and reduction zones were recorded at 838 °C and 754 °C, respectively. There was a pressure drop observed within the reactor from top of the main reactor where the pressure was 0.07 kPa in the combustion zone and where the pressure was measured from -1.30 kPa to -1.64 kPa. The pressure drop was hypothesized to be caused by bridging of the feedstock, which was the result of the physical properties of the feedstock. The air leak due to weak sealing was considered as another option for this failure, which did not feed the combustion zone and resulted in less syngas.

In a second study, a parametric investigation on six different biomass feedstocks was performed in which the result indicated a greater potential of switchgrass to result in higher yield of syngas. It was also demonstrated that the variations in syngas components were smaller at higher temperatures while H_2/CO ratio showed greater variation between individual feedstocks.

In the third study, gasification of composite biomass feedstock was examined. A composite paper fiber and waste plastic pellet was tested in the down-draft gasifier. For this study, four different plastic percentages of 0%, 2%, 5%, and 10% mixed with fiber were studied. The results showed that higher plastic-containing feedstock has a higher energy content; however, the higher plastic content potentially causes mechanical performance issues inside the reactor and does not necessarily guarantee syngas with a greater calorific value. The variation in temperature and pressure resulted in the generation of clinkers and interrupted the normal operation of the reactor. The clinkers were analyzed using ICP-MS and predominantly contained aluminum, silicon, calcium and sodium that originate from the fiber and plastic.

A fourth study determined the thermo-chemo-mechanical properties of the composite paper fiber and plastic waste. Thermogravimetric analysis (TGA) and differential scanning calorimetry (DSC) were used to evaluate thermal behavior of the material. The results reported that the higher volume fraction of plastics (5% and 10%) in the pellets resulted in thermal degradation occurring in three main stages while only two stages were measured for the lower fractions of plastic contained pellets (2% and 0%). The DSC results showed that the glass transition of the composite pellets, when taking place under endothermic reactions, occurred when the plastic content increased in the composite pellets. The thermal conductivity of the composite pellets was measured using the Hot-Disk Transient Plane Source (TPS) technique. The TPS results showed that composite pellets with higher volume-fractions of plastics possessed a lower thermal conductivity which was due to the lower thermal conductivity of the shredded plastics compared to the fibers in the matrix of the pellets.

In the fifth study, the composite material was analyzed mechanically to identify the physical strength during the degradation in the down-draft reactor. For these mechanical experiments, the

biomass feedstocks were blended with a 5% volume fraction of plastics but pelletized in different diameters. The composite pellets were compressed longitudinally and laterally using a universal testing machine to evaluate their mechanical properties such as stress-strain behaviour and elastic and plastic properties of biomass. The compression test results showed that pellets with larger diameters have higher elastic limits. In the transverse direction, there was no certain relationship between stress-strain values and pellet size. Due to unknown origin of the plastic waste, the type of plastics used in the composites were predicted using the rule of mixtures, based on the Young's modulus of the pellet, the wood fiber alone, and the volume fractions of the plastic constituents. The results indicated the possibility of the presence of the polymers such as ethylene vinyl acetate (EVA) and Surlyn in the composite pellets. In the same study, the angle of repose of the composite wood pellets ranged between 25^{o} for the 14 mm diameter pellet to 41^{o} for the 5 mm diameter. This phenomenon implied that the pellets with smaller diameters have a lower chance of slumping in the feeding drum during gasification. The angle of repose increased with the moisture content and decreased with the bulk density in all measured composite pellets. These characteristics impacted the flow properties of the composite pellets inside the downdraft gasifier and resulted in higher temperatures during the thermochemical conversion. The chemical analysis showed the existence of minerals (specifically aluminum and calcium) in the composition of the composite plastic pellets which could cause changes in their multiphysics properties as well as their thermal energy value.

The sixth study defined a thermodynamic model to study the effect of equivalence ratio (ER) on the reactions temperature and producer gas during the decomposition of biomass in a down-draft gasifier. The model was created using MATLAB and CONTERA programming platform. The composition of the producer gas was estimated by calculating the minimum Gibbs free energy.

The results showed that when the amount of air as gasifying agent oxidant was small, the order of produced gases resulted in $H_2 > CO > CH_4 > CO_2$. As ER increased, the production of hydrogen and methane, gradually decreased, while the amount of carbon monoxide and carbon dioxide remained constant. By increasing the ER, the lower heating value of the gas linearly dropped from 13 MJ Nm^{-3} to 6.4 MJ Nm^{-3} at ER 0.31 and kept decreasing at higher ER values. Increasing moisture content strongly degraded the gasifier performance in terms of heating value of the syngas from around 35% (from 9.4 MJ Nm^{-3} to 6.1 MJ Nm^{-3}). The higher moisture content resulted in lower production of syngas which consequently caused reduction in cold gas efficiency (CGE).

Résumé

Avec la nécessité de développer un monde plus durable, il y a un désir de passer des combustibles fossiles aux biocarburants, produits à l'aide du concept des bioraffineries. Au cours des dernières décennies, les technologies de conversion thermochimique ont gagné beaucoup d'attention pour produire des biocarburants avancés. Dans ce contexte, la présente thèse a élaboré différents aspects de la technologie de la gazéification de la biomasse, en tant que représentant des voies thermochimiques, et a suggéré des solutions potentielles pour améliorer l'efficacité du procédé. Pour atteindre cet objectif, différents types de matières premières de biomasse ont été utilisés pour examiner le potentiel de la production de bioénergie à travers d'un réacteur de gazéification

La première étude était une évaluation de la biomasse ligneuse granulée afin d'identifier une défaillance potentielle de la combustion lors de la décomposition de la biomasse granulée dans un réacteur à courant descendant. La température moyenne des zones de combustion et de réduction a été enregistrée respectivement à 838°C et 754°C. Il y a eu une chute de pression observée dans le réacteur depuis le haut du réacteur principal où la pression était de 0,07 kPa dans la zone de combustion et où la pression a été mesurée de -1,30 kPa à -1,64 kPa. On a supposé que la chute de pression était causée par le pontage de la charge qui était le résultat des propriétés physiques de la charge d'alimentation. La fuite d'air dû à une étanchéité faible a été considérée comme une autre option pour cette défaillance qui n'a pas alimenté la zone de combustion et a abouti à moins de gaz de synthèse.

Dans une deuxième étude, une étude paramétrique sur six différentes matières premières de biomasse a été réalisée dans lequel le résultat a indiqué un plus grand potentiel de switchgrass pour

obtenir un rendement plus élevé de gaz de synthèse. Il a également été démontré que les variations des composants de gaz de synthèse étaient plus faibles à des températures plus élevées tandis que le rapport H_2/CO présentait une plus grande variation entre les charges d'alimentation individuelles.

Dans la troisième étude, on a examiné la gazéification de la charge de biomasse composée. On a testé une pastille de fibre de papier composite et de déchets de plastique dans le gazéificateur à courant descendant. Pour cette étude, quatre pourcentages différents de plastique (0%, 2%, 5%, et 10%) mélangés avec de la fibre, ont été étudiés. Les résultats ont montré qu'une matière première contenant un pourcentage de matières plastiques élevé a une teneur en énergie plus élevée; cependant, la teneur en matière plastique plus élevée entraîne potentiellement des problèmes de performances mécaniques à l'intérieur du réacteur et ne garantit pas nécessairement un gaz de synthèse de plus grand pouvoir calorifique. La variation de température et de pression a entraîné la production de mâchefers et a interrompu le fonctionnement normal du réacteur. Les mâchefers ont été analysés en utilisant ICP-MS et contiennent principalement de l'aluminium, du silicium, du calcium, et du sodium qui proviennent de la fibre et du plastique.

Une quatrième étude a déterminé les propriétés thermo-chimio-mécaniques de la fibre de papier composite et des déchets de plastique. L'analyse thermogravimétrique (TGA) et la calorimétrie différentielle à balayage (DSC) ont été utilisées pour évaluer le comportement thermique du matériau. Les résultats indiquent que la fraction volumique plus élevée de matières plastiques (5% et 10%) dans les pastilles a entraîné une dégradation thermique se produisant en trois étapes principales alors que seulement deux étapes ont été mesurées pour les fractions inférieures de plastique contenu dans les pastilles (2% et 0%). Les résultats du DSC ont montré que la transition vitreuse des pastilles composites, lorsqu'elles se produisaient sous des réactions endothermiques,

se produisait lorsque la teneur en matière plastique augmentait dans les pastilles composites. La conductivité thermique des pastilles composites a été mesurée en utilisant la technique de source de flux transitoire à disque chaud (TPS). Les résultats de TPS ont montré que les pastilles composites avec des fractions volumiques supérieures de matières plastiques possédaient une conductivité thermique plus faible qui était dû à la conductivité thermique plus faible des matières plastiques déchiquetées par rapport aux fibres dans la matrice des pastilles.

Dans la cinquième étude, le matériau composite a été analysé mécaniquement pour identifier la résistance physique pendant la dégradation dans le réacteur à courant descendant. Pour ces expériences mécaniques, les matières premières de biomasse ont été mélangées avec une fraction volumique de 5% de matières plastiques, mais ont été granulés dans différents diamètres. Les pastilles composites ont été comprimées longitudinalement et latéralement à l'aide d'une machine d'essai universelle pour évaluer leurs propriétés mécaniques telles que le comportement contrainte-déformation et les propriétés élastiques et plastiques de la biomasse. Les résultats des essais de compression ont montré que les pastilles de plus grands diamètres ont des limites élastiques plus élevées. Dans la direction transversale, il n'y avait pas de relation certaine entre les valeurs de contrainte-déformation et la taille de pastille. En raison de l'origine inconnue des déchets plastiques, le type de plastique utilisé dans les composites a été prédit selon la règle des mélanges basée sur le module de Young de la pastille, la fibre de bois seule, et les fractions volumiques des constituants plastiques. Les résultats indiquent la possibilité de présence des polymères éthylène-acétate de vinyle (EVA) et Surlyn dans les pastilles composites. Dans la même étude, l'angle de repos des pastilles de bois composées variait entre 25^{o} pour la pastille de 14 mm de diamètre jusqu’à 41^{o} pour le diamètre de 5 mm. Ce phénomène impliquait que les pastilles de diamètres plus petits avaient une plus faible chance de s'affaisser dans le bidon d'alimentation pendant la

gazéification. L'angle de repos augmente avec la teneur en humidité et diminue avec la densité apparente dans toutes les pastilles composites mesurées. Ces caractéristiques ont influé sur les propriétés d'écoulement des pastilles composites à l'intérieur du gazéificateur de fuite et ont donné lieu à des températures plus élevées pendant la conversion thermochimique. L'analyse chimique a montré l'existence de minéraux (spécifiquement l'aluminium et le calcium) dans la composition des pastilles de plastique composites qui pourraient provoquer des changements dans leurs propriétés multiphysiques ainsi que leur valeur d'énergie thermique.

La sixième étude a défini un modèle thermodynamique pour étudier l'effet du rapport d'équivalence (ER) sur la température des réactions et sur le gaz producteur lors de la décomposition de la biomasse dans un gazéificateur de fuite. Le modèle a été créé avec la plateforme de programmation MATLAB et CONTERA. La composition du gaz producteur a été estimée en calculant l'énergie libre minimale de Gibbs. Les résultats ont montré que lorsque la quantité d'air comme agent oxydant était faible, l'ordre des gaz produits était H_2 > CO > CH_4 > CO_2. À mesure que l'ER augmente, la production d'hydrogène et de méthane diminue progressivement, tandis que la quantité de monoxyde de carbone et de dioxyde de carbone reste constante. En augmentant l'ER, la valeur de chauffage inférieure du gaz a chuté linéairement de 13 MJ Nm^{-3} jusqu'à 6,4 MJ Nm^{-3} à ER 0,29 et a continué de baisse à des valeurs plus élevées de ER. L'augmentation de la teneur en humidité a fortement dégradé la performance du gazéificateur en termes de valeur calorifique du gaz de synthèse pour environ 35% (de 9,4 MJ Nm^{-3} à 6,1 MJ Nm^{-3}). La teneur en humidité plus élevée a entraîné une production plus faible de gaz de synthèse, ce qui a provoqué une réduction de l'efficacité du gaz froid (CGE).

ACKNOWLEDGMENTS

First and foremost, I would like to thank my parents, Mohammadreza and Rafat, for the endless love and support. Without their support, I may not have found myself at McGill University, nor had the courage to engage in this task and see it through.

At the very outset, I would like to express my sincere gratitude to my supervisor, Professor Mark Lefsrud, for the continuous support of my Ph.D. studies and research, for his patience, motivation, enthusiasm, and immense knowledge.

I am particularly thankful to my co-supervisor and Chair of the Bioresource Engineering Department, Professor Valerie Orsat, for the scientific support and insightful comments and advice she made throughout my doctorate program.

I am also thankful for the advice of Professor Hamid Akbarzadeh within the last year of my Ph.D. Program. I would also like to acknowledge and thank for the help and technical support provided by Mr. Scott Manktelow, Mr. Yvan Gariepy and Ms. Helene Lalande during the experimental sessions of the work.

This research also benefited tremendously from the many friends at McGill University. Special thanks to Mr. Camilo Perez Lee, Mr. Yves Roy, Mr. Emmet Austin, Ms. Andrea Beck, Ms. Jauharah Khudzari, Ms. Debora Parrine, Ms. Monica Baledon, Mr. Hossein Rahimipour, Ms. Fatemeh Mafi, Dr. Leila Amiri and Dr. Nima Gharib, for countless hours spent discussing fruitful ideas. Thanks also goes to the amazing people in the Bunker who made there a pleasant environment to work in.

Finally, this research is funded by BioFuelNet Canada, a network focusing on the development of advanced biofuels. BioFuelNet is a member of the Networks of Centres of Excellence of Canada program.

Contribution of Authors

In accordance with the guidelines of the Faculty of Graduate Studies and Research of McGill University "Guidelines for a Manuscript Based Thesis Preparation", the prepared manuscripts and contribution of authors are presented below.

Edris Madadian is the principal author of this work, supervised by Professor Mark Lefsrud from the Department of Bioresource Engineering, McGill University, Quebec, Canada. The entire construction, assembly and experimentations were performed in the McGill Technical Service unit (Machine Shop), of the Bioresource Engineering Department.

Professor Mark Lefsrud, the supervisor and director of the thesis, co-authored all manuscripts, and provided scientific guidance in the planning and execution of the work as well as co-editing and reviewing manuscripts.

Professor Valerie Orsat, the co-supervisor of this thesis, co-authored three chapters (2^{nd}, 3^{rd}, and 6^{th}) and made valuable comments to improve the manuscripts.

Professor Hamid Akbarzadeh co-authored the manuscript extracted from the fifth and sixth chapters and made contribution by reviewing the articles and involving the Thermtest Instrument Company from New Brunswick to perform the thermal conductivity tests.

Mr. Camilo Perez Lee and Mr. Yves Roy, co authored the first and the second manuscripts, and provided technical assistance during fabrication the gasifier, preparing the feedstocks and conducting the experiments.

Ms. Christine Crowe co-authored the fourth manuscript extracted from the fourth chapter. She made contribution by supplying the composite feedstocks, helping in running the experiments, and assisting in reviewing the manuscript.

Dr. Leyla Amiri, co-authored the last manuscript extracted from the eighth chapter and made contribution by assisting in simulation part of the work. She also helped in validation of the model by comparing the results with the ones from the experiments.

Details of the papers published, accepted and submitted are provided below:

A. Journal Papers

1. **Madadian E.**, Lefsrud M., Perez Lee C., Roy Y., (2014). Green energy production: The potential of using biomass gasification. *Journal of Green Engineering, 4*(2), 101-116.
2. **Madadian E.**, Lefsrud M., Perez Lee C., Roy Y., & Orsat V. (2016). Gasification of pelletized woody biomass using a downdraft reactor and impact of material bridging. *Journal of Energy Engineering*, 04016001.
3. **Madadian E.**, Lefsrud M., & Orsat V. (2016). A comparative study of temperature impact on air gasification of various types of biomass in a research-scale down-draft reactor. *Energy & Fuels*, DOI: 10.1021/acs.energyfuels.6b03489.
4. **Madadian E.**, Crowe C., & Lefsrud M. (2016). Evaluation of Composite Fiber-Plastics Biomass Clinkering Under the Gasification Conditions. *The Journal of Cleaner Production* (Under revision).
5. **Madadian E.**, Akbarzadeh A.H., & Lefsrud M. (2016). Pelletized Composite Wood Fiber Mixed with Plastic as Advanced Solid Biofuels: Thermo-Chemical Analysis. *Waste and Biomass Valorization*, DOI:10.1007/s12649-017-9921-1.
6. **Madadian E.**, Akbarzadeh A.H., Orsat V., & Lefsrud M. (2016). Pelletized Composite Wood Fiber Residues Mixed with Plastic Wastes as Advanced Solid Biofuels: Physico-Chemo-Mechanical Analysis. *Waste and biomass valorization* (Under revision).
7. **Madadian E.**, Amiri L., & Lefsrud M. (2016). Thermodynamics behaviour of wood pellet gasification using a down-draft reactor. *Energy & Fuels* (Under revision).

B. Papers presented at conferences

1. **Madadian E.**, Lefsrud M., Orsat V., Perez Lee C., Roy Y., "Gasification of biomass feedstock for producing bioenergy", International Conference & Exhibition on Clean Energy, Ottawa, Canada, September 2013.
2. **Madadian E.**, Lefsrud M., Perez Lee C., Roy Y., "Harvest and Post-Harvest Densification", Advanced biofuels symposium, Ottawa, Canada, June 2014.
3. **Madadian E.**, Lefsrud M., Orsat V., Perez Lee C., Roy Y., "Gasification of waxed cardboard feedstock using an air-blown downdraft gasifier", Northeast agricultural and biological engineering conference (NABEC), Kemptville (Ontario), Canada, July 2014.
4. **Madadian E.**, Lefsrud M., Roy Y., "Gasification of waxed cardboard feedstock using an air-blown downdraft gasifier", General meeting of wood pellet association of Canada and UBC pellet workshop, Vancouver, Canada, November 2014.
5. **Madadian E.**, Lefsrud M., "Influence of physical characteristics of feedstock on gasification operation in a down-draft reactor", Advanced biofuels symposium, Montreal, Canada, June 2015.
6. **Madadian E.**, Lefsrud M., Perez Lee C., Roy Y., "Gasification of pelletized woody biomass in a downdraft reactor", American society of agricultural and biological engineers (ASABE), Annual international meeting, Montreal, Canada, July 2015.
7. **Madadian E.**, Lefsrud M., "Thermodynamics behaviour of wood pellet gasification using a down-draft reactor", American society of agricultural and biological engineers (ASABE), Annual international meeting, New Orleans, Louisiana, USA 2015.
8. **Madadian E.**, Lefsrud M., Akbarzadeh A.H. "Thermo-chemical analysis of composite wood fiber and plastics for producing advanced biofuels", Advanced biofuels symposium, Vancouver, Canada, June 2016.

Table of Contents

List of Tables

List of Figures

Glossary

ABS	Acrylonitrile butadiene styrene
APL	All Power Labs
ASTM	American society for testing materials
BFN	BioFuelNetwork (Canada)
CFP0%	Composite pellet with 0% plastics content
CFP2%	Composite pellet with 2% plastics content
CFP5%	Composite pellet with 5% plastics content
CFP10%	Composite pellet with 10% plastics content
CGE	Cold gas efficiency
DIN	Deutsches Institut für Normung
DIS	Draft international standard
DSC	Differential scanning calorimetry
EEA	European environment agency
FC	Fixed carbon
GC	Gas chromatography
GCU	Gasifier control unit
GEK	Gasifier’s experimenter’s kit
HCs	Hydrocarbons
HDPE	High-density polyethylene
HHV	Higher heating value
ICP-MS	Inductively coupled plasma mass spectrometry

IPCC	Intergovernmental panel on climate change
ISO	International organization for standardization
LDPE	Low-density polyethylene
LHV	Lower heating value
MC	Moisture content
MSW	Municipal solid waste
NAA	Neutron activation analysis
NOXs	Nitrogen oxides
P	Porosity
PE	Polyethylene
PET	Polyethylene terephthalate
PP	Polypropylene
PPM	Parts per million
PS	Polystyrene
PVC	Polyvinyl chloride
SEM	Scanning electron microscopy
TCD	Thermal conductivity detector
TGA	Thermogravimetric analysis
TPS	Transient plane source
USB	Universal serial bus
VM	Volatile matter
WPCs	Wood-plastic composites

CHAPTER 1

1. INTRODUCTION

1.1. Background

Energy is an important concern in sustainable development, leading to significant environmental pressures at global, national, regional, and local levels (Del Río and Burguillo 2009, Stigka, Paravantis et al. 2014). The energy industry serves as the foundation for developing economies and improving quality of life, in combination with environmental protection (Maria and Tsoutsos 2004, Stigka, Paravantis et al. 2014).

Historically, the energy demands of humans were relatively simple, comprising space heating and cooking (Rutter and Keirstead 2012). Possibly as early as two million years ago, our ancestors advanced from using fire to keep warm to using fire to cook food (Wrangham, Jones et al. 1999, Rutter and Keirstead 2012). The first formal energy systems likely co-evolved over this period with changes in diet and agricultural practices. For early civilization, work and heat were separate energy functions: work was provided by human and animal labor and heat was provided by burning biomass. By the 19th Century, mankind began to understand that heat and work were both forms of energy and that engines could be developed to convert heat into work (Towler 2014).

Throughout history, the most successful civilizations have maximized their energy throughput. The higher the energy use, the higher the standard of living the more the culture progressed. The source of energy has changed over time with a concomitant increase in energy throughput, moving from human labor to biomass combustion, animal labor, hydrocarbon combustion, hydroelectric power, and atomic and nuclear energy. In the year 1800, the primary source of energy was biomass combustion—mostly trees that were burned to provide heat for homes and factory furnaces. Some

coal was also being burned in steam engines and in the few existing factory furnaces. This was a small and insignificant energy source compared to burning wood. Circa 1910, coal overtook biomass as the primary source of energy in the world. By this time, coal was being widely used to generate electricity, make steel and as the primary transportation fuel to drive locomotive engines. It was not until the 1960s that oil overtook coal as the primary energy source in the world. Natural gas was always seen as a by-product of oil production and often it was simply burned at the field unless a market for it could be found. Commencing in approximately 1940, natural gas became a commodity for marketing as an industrial fuel and to generate electricity in gas turbines. Hydroelectric power plants generate electricity from the release of water trapped in dams. This form of energy was first developed to drive mills to grind grain (Rutter and Keirstead 2012). With the development of large hydroelectric power plants around 1900, its use expanded greatly. Nuclear power plants that generate electricity were developed in the 1950s.

In modern civilization, hydrocarbon energy is the ruler: it is so inexpensive hence fuelled economic growth, raised the standard of living for the vast majority of people, and had profound environmental impact on a global scale (Towler 2014). Nuclear power is the sixth leading source of energy in the world, behind oil, coal, natural gas, biomass, and hydroelectricity (Towler 2014, Ferrer-Castán, Morales-Barbero et al. 2016). Wind, solar, and other sources of energy barely register on the scale. There is a great deal of interest in further developing these sources of energy because they are clean and renewable, but their use has been limited to date by cost and reliability issues (Towler 2014).

Urban areas consume approximately 70% of global energy and—in light of a growing population and increasing densification of urban areas—this share is expected to further increase in the future (Harter, Weiler et al. 2017). Urban energy systems represent the “the combined processes of

acquiring and using energy" to meet the energy service demands of an urban population. Activities in a modern city are supported by a diverse range of energy services: building heating and cooling, indoor and outdoor space lighting, electric power for appliances, mobility services, communications, and more (Sharp, Jaccard et al. 2009, Rutter and Keirstead 2012). Energy consumers are driven by their demand for energy services, and the costs associated with these services are crucial for understanding energy consumption patterns. The cost of the energy services generally combines the price of energy and the efficiency of the energy technology used (Fouquet 2016).

1.2. The Green Economy

In recent years, economic understanding around the world is evolving to embrace "the green economy", the concept that the United Nations (UN) has been developing since the 1990s. The green economy focuses on renewable, alternative (to hydrocarbon combustion) energy sources to fuel sustainable development, instead of depleting natural resources directly for development—an approach that is not forward-looking (Karakul 2016). The concept of the green economy has gradually gained prominence among academics and policy-makers (Gasparatos, Doll et al. 2017). In a green economy, growth in income and employment is driven by public and private investments that reduce carbon emissions and pollution, enhance energy and resource efficiency, and prevent the loss of biodiversity and ecosystem services (Bina 2013, Harter, Weiler et al. 2017). In 2015, more than two decades after the UN Framework Convention on Climate Change (UNFCCC) was established, the UNFCCC mechanism brought together 195 countries to sign into a new international climate agreement (the Paris Agreement) (Griffiths 2017).

1.3. Future energy transition

Carbon dioxide (CO_2) emission from fossil fuel combustion in energy systems is acknowledged as the paramount factor causing global climate change. In addition to increasingly coordinated global efforts to address climate change, the energy landscape around the world has been rapidly evolving in recent years because of the rise of cost-competitive new sources of oil and gas supply, dramatic volatility in international oil and gas prices, and emergence of various types of renewable energy as cost-competitive energy sources (Griffiths 2017). These factors have motivated national, regional, and local governments and some in the private sector to substitute conventional with renewable energy sources (Aghaei and Alizadeh 2013). Countries, states and cities are establishing plans, milestones, and targets for future renewable energy systems (Pachauri, Allen et al. 2014, Thellufsen and Lund 2016).

Many aspects of future energy transitions are highly uncertain. The expression "energy transition" indicates a long-term structural change in energy systems (Guidolin and Guseo 2016). The worldwide transition to renewable energy technologies raises new and important governance questions. Each technology proposed within global climate change mitigation policy produces different costs and benefits from local to international levels (Kelly-Richards, Silber-Coats et al. 2017). The building blocks to understand energy transitions include theory, empirical evidence and analysis, and simulation exercises (Fouquet and Pearson 2012).

Within energy transitions, renewable energy is the primary energy resource. Renewable energy is a clean or inexhaustible energy like wind or solar power. The most important benefit of renewable energy systems is lower environmental pollution compared to conventional energy sources. Although oil and gas are expected to remain important sources of energy, the share of renewable energy sources is expected to increase significantly to 30–80% in 2100 (Demirbas 2005). Biomass,

wind, and geothermal energy are commercially competitive and are progressing relatively rapidly (Fridleifsson 2001). Known global renewable energy reserves are presented in Table 1.1.

Table 1.1. Global renewable energy resources (Goldemberg 2000, Demirbas 2005)

Resource	Capacity (MW)	Approximate annual output ($TWh.Year^{-1}$)
Biomass	35000	185
Wind	20000	50
Geothermal	8200	44
Small hydroelectric	3000	15
Solar photovoltaic	1200	1
Solar thermal	350	0.2

1.1.Biomass and biofuel

Biomass in this context refers to biological material that can be used as fuel for transport or an energy source to produce industrial or domestic heat and electricity (Bessou, Ferchaud et al. 2011). In recent years, biomass has gained significant attention as a potential renewable energy source for a future sustainable energy mix (Raheem, Azlina et al. 2015). Primary producers (plants, algae, and cyanobacteria) create biomass and energy for cell functions by carbon fixation (photosynthesis) during growth. In comparison to fossil fuels such as natural gas and coal, which take millions of years to form, biomass is easy to grow, collect, use and replace quickly without depleting natural resources (Yue, You et al. 2014).

Biofuels—considered the most likely sources of energy to replace an important proportion of fossil fuels—are energy products obtained by pretreatment or conditioning (physical, thermochemical, chemical, or biological) of raw biomass. Biofuels are considered carbon-neutral: their use represents savings of greenhouse gases (GHGs) that are not counteracted by an increase in the

same emissions during the production and transformation of the raw materials (biomass). In other words, the CO_2 released during combustion of biofuels was initially taken from the atmosphere during growth of the biomass from which the biofuels were obtained (Bessou, Ferchaud et al. 2011).

Biofuels are broadly classified as primary and secondary. Primary biofuels are used in an unprocessed form (e.g. fuelwood, wood chips, pellets) for heating, cooking, or electricity production in small- and large-scale industrial applications. Secondary biofuels are produced from processing primary biofuels. They are in the form of solids (e.g. charcoal), or liquids (e.g. ethanol, biodiesel and bio-oil), or gases (e.g. biogas, synthesis gas and hydrogen) and can be used in vehicles and industrial processes. Secondary biofuels are further classified as first-, second-, third-, and fourth generation, based on the raw material and technology used for their production.

First-generation liquid biofuels gained significant attention in the 1990s. They are produced in a significant commercial quantity in several countries from sugars, grains, or seeds by a relatively simple process. However, the viability of their production is questionable: because they compete with the food supply, they have a high production cost. This favours the search for nonedible biomass for first-generation biofuel production.

Second-generation liquid biofuels are produced via biological or thermochemical processing from agricultural and forest lignocellulosic biomass that can be either nonedible residues of food crop production or nonedible whole plant biomass (energy crops). The nature of the source of biomass makes them a better option than first-generation biofuels because competition for food is eliminated. In addition, production per unit land area (land use efficiency) is higher. However, concerns remain regarding competing land use or required land use changes (Nigam and Singh 2011).

Third-generation biofuel production is essentially related to microalgae. Microalgae produce lipids, proteins, and carbohydrates that can be processed into a variety of biofuels such as biodiesel from transesterification, hydrogen and methane from anaerobic digestion (Hernandez, Solana et al. 2014), alcohols from saccharification and fermentation nonedible (Meyer and Weiss 2014), and bio oil and biocrude from pyrolysis and hydrothermal liquefaction, respectively (Demirbas 2011).

Biomass can be converted into useful biofuels and bio-chemicals via biorefinery technologies and biomass upgrading. A biorefinery integrates biomass conversion processes to produce fuels, power, and chemicals from biomass. Biomass upgrading processes include fractionation, liquefaction, pyrolysis, hydrolysis, fermentation, and gasification (Demirbas 2009) (Figure 1.1).

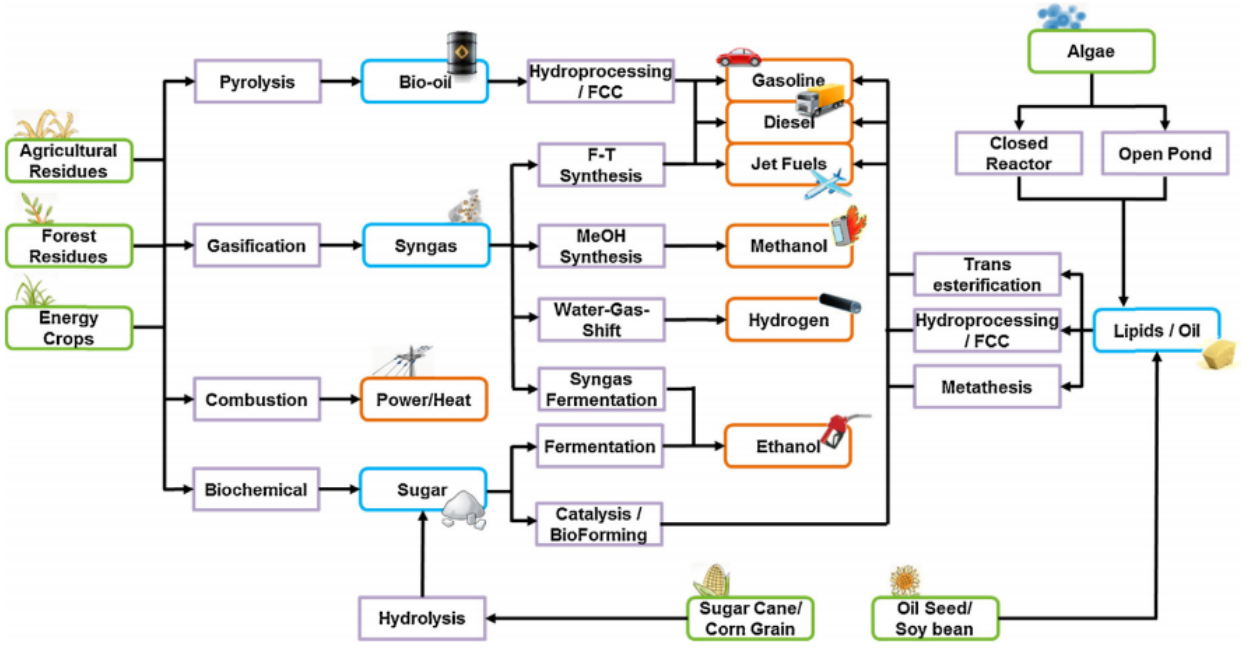

Figure 1.1. Conversion pathways from terrestrial and aquatic biomass to intermediates and to final biofuel products (Yue, You et al. 2014)

The development of fourth-generation biofuels is ongoing and has not generated as much attention because policy and other needs for first-, second-, and third-generation biofuels are more pressing (Awudu and Zhang 2012). There is no formal definition for the term fourth-generation biofuels. They have been defined as biofuels created from processes other than first-generation ethanol and biodiesel, second-generation cellulosic ethanol, and third-generation biofuels (Awudu and Zhang 2012). A second definition is crops that are genetically engineered to consume more CO_2 from the atmosphere than they will produce during combustion as a fuel (Demirbas 2011). Some fourth generation technology pathways include: pyrolysis, gasification, upgrading, solar-to-fuel, and genetic manipulation of organisms to secrete hydrocarbons (Chakrabortty, 2008). "nonedible Advanced biofuels" include bioethanol made from celluloses, hemicelluloses, sugar, starch, and waste, as well as biomass-based biodiesel, biogas, biohydrogen, and other fuels made from cellulosic biomass or other non-food crops (Altun 2011, Demirbas 2011, Ertas and Alma 2011).

Fourth-generation biofuel research began in 2009 (Leung, Wu et al. 2010), whereas the majority of research into first-generation biofuels was carried out between 2006 and 2010. In the case of third- and fourth-generation biofuels, a reduction in GHG emission can be obtained by recycling the CO_2 produced during fermentation as a carbon source for algae cultivation (Leung, Wu et al. 2010, Singh and Gu 2010).

1.4. Food versus fuel debate

The food versus fuel debate relates to many biofuel feedstocks such as corn, sugarcane, and soybeans, which are key sources of food being substituted for energy. Production of crops for bioenergy may displace food-related crops, which can increase the cost and decrease the

availability of foodstuffs, including plant and animal-based foods (Duku, Gu et al. 2011, Awudu and Zhang 2012). Thus, second-, third- and fourth- generation biofuel feed stocks such as cellulosic grass, switchgrass, silvergrass, and algae are currently being explored. These raw materials are not used for food, and provide higher conversion rates and lower cultivation costs (Awudu and Zhang 2012). Biofuels provide the prospect of new economic opportunities for people in rural areas in oil importing and developing countries. Renewable energy sources that use indigenous resources have the potential to provide energy services with zero or near-zero emissions of air pollutants and GHGs (Najafi, Ghobadian et al. 2009, Leung, Wu et al. 2010, Demirbas 2011).

The substitution of oil in the production of liquid fuels is highly problematic, since currently only biofuels can replace oil directly in most applications. Biofuels exhibit lower land use efficiency and energy return on energy investment rates than oil-based fuels (Mediavilla, de Castro et al. 2013). Significant environmental benefits can be obtained by using biomass fuels in direct combustion, gasification, or pyrolysis systems, although some uncertainties remain. CO_2, SO_2, and ash production will typically be far lower for biomass power systems than for coal combustion and conversion systems (Bain, Overend et al. 1998).

In an effort to achieve a higher efficiency through a biomass thermochemical conversion pathways, this project aims at a detailed investigation on performance of gasification as one of the potential thermochemical conversion technologies to produce biofuels from different types of feedstock. This is achieved through technical evaluation of the technology from thermal, chemical, and mechanical standpoints. In the following chapters, after reviewing the major pathways from biomass to biofuels, and discussing the main properties of the feedstocks, fuel products and intermediates, a detailed description of gasification technology using a down-draft reactor will be

presented. The output of this study improves the performance of gasification technology and facilitates further decision-making in optimizing this technology for future work.

1.5. Objectives

The general objective of this thesis is to optimize gasification technology for producing biomass feedstock through thermo-chemo-mechanical investigation of different types of fuels during the course of decomposition inside a down-draft reactor. The specific objectives of this project are focused on two main topics:

1- Experimental investigation and mathematical modeling to enhance understanding of the fundamentals of advanced biofuels thermochemical conversion, particularly using gasification.

2- Thermal and mechanical characterization of composite advanced biofuels and their impact on the thermochemical conversion process through gasification.

3- Identification of failure scenarios in a down-draft reactor and suggested solutions to rectify the problems and optimize the efficiency of the process.

Connecting Text

Chapter 1 presented a historical overview of energy transition around the world to provide an understanding of the driving demands to promote the renewable energy sector. It provided information about the future energy transition and the role of renewables in developing a green economy. Then different sources of renewable energy were discussed focusing on the role of biofuels to cover a part of the conventional fuels for future.

Chapter 2 establishes the basis for the rest of the research work. The concept of green energy production using biomass gasification technology was investigated. The chapter further examines the essential requirements and experiments to analyse raw material (i.e. biomass feedstock). It elaborates the basics of the gasification in batch mode defining different zones during the process, and the intents to develop a unit for continuous mode. The information provided gives the basic understanding of the biomass thermochemical conversion pathways particularly during gasification, which is required for future chapters.

Chapter 2 is published as:

Madadian E., Lefsrud M., Perez Lee C., Roy Y., (2014). Green energy production: The potential of using biomass gasification. *Journal of Green Engineering, 4*(2), 101-116.

CHAPTER 2

2. GREEN ENERGY PRODUCTION: REVIEW OF BIOMASS GASIFICATION

Abstract

Bioenergy production from biomass gasification technology is reviewed as an environmentally friendly alternative to fossil fuels and a pilot downdraft gasifier equipment kit (GEK) is described. Biomass encompasses a wide range of feedstocks such as agricultural residues, energy crops, forestry materials, food waste, municipal solid waste, grains and starch crops. An efficient GEK unit produces syngas—predominantly a mixture of hydrogen gas and carbon monoxide—with a calorific value up to 20 MJ kg^{-1}. This syngas can be used in several processes, including for electricity generation, steam generation, transportation and hydrogen production, as well as chemical production, fertilizer manufacturing and consumer products. This research highlights the potential of biomass gasification as a viable alternative for bioenergy production and a substitute for fossil fuels.

Keywords: Biomass feedstock, Thermochemical reactions, Gasification, Renewable energy, Syngas

2.1. Introduction

According to the United States Census Bureau, the global human population will reach nine billion by the year 2050 (Statistics, Division et al. 1979). To sustain this growing population, more energy resources will be required and energy supply will become a more significant issue. The World Health Organization and the United Nations Development Programs estimated that an additional two billion people will require modern energy services to meet development goals (Mendu, Shearin et al. 2012). Within the last decades, between 80 and 90% of the world's liquid fuel needs were met by non-renewable sources (D'Sa 2005). Although fossil fuels have been critical in the development of our modern society; its use creates serious environmental problems such as global climate change, acid rain and air pollution. They are, at this point, not strong candidates as energy resources to meet future energy needs.

2.1.1. Green energy

Green energy can be considered a catalyst for energy security, sustainable development and social, technical, industrial and governmental innovations in a country. Loosely defined as the form and utilization of energy that has minimal or no negative environmental, economic and social impacts, green energy is essential to achieve the ultimate goal of sustainability. Energy diversity with local renewable (i.e. continually replenished) energy resources such as solar, hydroelectric power, biomass, wind, and geothermal can facilitate reaching sustainability goals (Midilli, Dincer et al. 2007). Approximately 10% of the global marketed energy consumption is from renewable energy sources, with a projection of 14% by 2035 (Demirbas 2009).

2.1.2. Biomass feedstocks

Biomass feedstock from agriculture, forestry, municipal, industrial and urban residues is the biological source material for biofuel end-products such as biodiesel, ethanol and methanol (Acton and Gregorich 1995, Jefferson, McCaughey et al. 2004). The worldwide annual production of biomass from terrestrial plants is 170–200 gigatons, of which approximately 70% is plant cell wall material (Nanda, Mohammad et al. 2014). However, only a small portion of global biomass is used for biofuel production; most is used for sugar production, electricity generation and compost for crop fields.

Table 2.1 summarizes composition and heating value (potential of producing calorific value) of various potential biomass feedstocks compared to coal. Among renewable feedstocks, sawdust has the highest heating value and dry sewage has the least. Woody biomass contains approximately 45% oxygen, whereas coal contains 6–17% oxygen. The high oxygen content of biomass is beneficial because less oxygen is needed for gasification; however biomass has a lower calorific value compared to coal and other fossil fuels (Milne, Evans et al. 1997).

Table 2.1. Composition of potential biomass gasifier feedstocks (Bridgwater and Evans 1993, Prins, Ptasinski et al. 2007)

	Ultimate Analysis (wt% dry basis)						Proximate Analysis (wt% dry basis)			
	C	**H**	**N**	**O**	**S**	**Ash**	**Moisture**	**Volatiles**	**Fixed Carbon**	**Heating Value (MJ kg^{-1})**
	(wt% dry basis)									
Agricultural Residues										
Saw dust	50.0	6.3	0.8	43.0	0.03	0.03	7.8	74.0	25.5	19.3
Bagasse	48.0	6.0	-	42.0	-	4.0	1.0	80.0	15.0	17.0
Corn cob	49.0	5.4	0.4	44.6	-	1.0	5.8	76.5	15.0	17.0
Short Rotation Woody Crops										
Beech wood	50.4	7.2	0.3	41.0	0	1.0	19	85.0	14.0	18.4
Herbaceous Energy Crops										
Switchgrass	43.0	5.6	0.5	46.0	0.1	4.5	8.4	73.0	13.5	15.4
Straw	43.5	4.2	0.6	40.3	0.2	10.1	7.6	68.8	13.5	17.0
Silvergrass	49.0	4.6	0.4	46.0	0.1	1.9	7.9	79	11.5	12.0
Municipal Solid Waste										
Dry sewage	20.5	3.2	2.3	17.5	0.6	56	4.7	41.6	2.3	8.0
Coals										
Sub-bituminous	67.8	4.7	0.9	17.2	0.6	8.7	31.0	43.6	47.7	24.6
Bituminous	61.5	4.2	1.2	6.0	5.1	21.9	8.7	36.1	42.0	27.0

2.1.3. Bioenergy conversion

Biomass can be converted into useful forms of energy using several processes. Factors that influence the choice of conversion process are the type and quantity of biomass feedstock, the desired form of the energy (i.e. end-use requirements), the environmental standards, the economic conditions and any other project-specific factors. Conversion process technologies can be classified as thermochemical or biochemical/biological. Within thermochemical conversion, four process options are available: combustion, pyrolysis, liquefaction and gasification. Biochemical conversion encompasses two process options: digestion (production of biogas, a mixture of mainly methane and carbon dioxide, CO_2) and fermentation (production of ethanol) (McKendry 2002). This review focuses on gasification technology as an environmentally friendly technique to produce bioenergy.

2.1.4. Gasification

Gasification technology has been receiving a great deal of attention in the past few decades. Gasification converts carbon-based materials into gaseous products. When air is used as the oxidant, the gaseous product is usually called producer gas, and when oxygen or steam is used, the product is termed synthesis gas (syngas). Syngas is an important feedstock for the chemical and energy industries, along with hydrocarbons traditionally produced from petroleum oil that can also be produced from syngas (Basu 2010). Figure 2.1 presents the worldwide growth of operating syngas capacity over time.

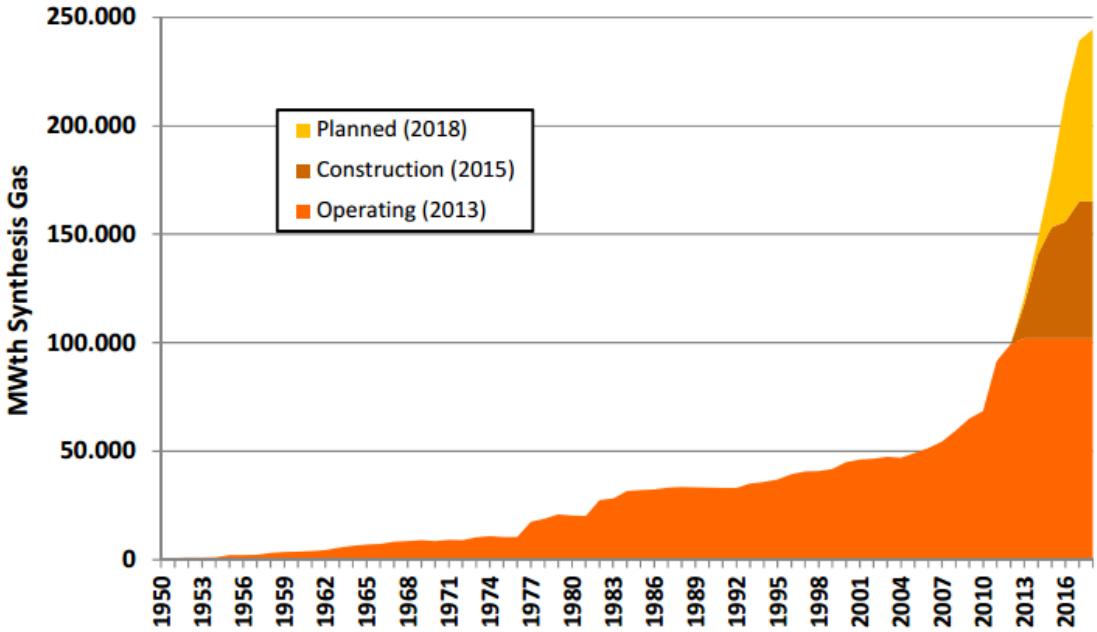

Figure 2.1. Cumulative worldwide gasification capacity and growth (Higman 2013)

Syngas is a combination of carbon monoxide (CO), hydrogen gas (H_2) and lesser amounts of hydrocarbons. Gasification improves the H_2/CO ratio in the produced syngas, which is required for liquid fuel synthesis (Zanzi, Sjöström et al. 2002, Kumabe, Hanaoka et al. 2007). In addition, inorganic matter present in biomass catalyzes the gasification of coal. Syngas composition depends on feedstock composition, type of gasification reactor, gasification agents and operating conditions. Many gasification configurations are available which can be classified into categories based on the factors listed in Table 2.2 (McKendry 2002).

Table 2.2. Classification of gasifier configuration (Sims 2003)

Classification factor	Gasifier configuration
Heat transfer	Internal heating – Autothermic or direct
	External heating – Heat exchange or direct
Reactant contact	Fixed bed
	Fluidized bed
	Suspension of solid fuel in reaction medium
Reactant flow	Updraft (co-current)
	Downdraft (counter-current)
Gasifying medium	Steam with oxygen
	Oxygen enriched air
	Air and hydrogen
Residue removal	Dry ash
	Slagging

The designs above were developed primarily for gasification of fossil fuels, but they have been adapted for biomass gasification. Currently operating biomass gasifiers can be divided into four major categories: (1) updraft fixed-bed, (2) downdraft fixed-bed, (3) bubbling fluidized bed, and (4) circulating fluidized bed. This review emphasizes on downdraft fixed-bed gasifying reactor. Fixed-bed gasifiers are more suitable for small-scale power generation and industrial heating applications (Salam, Kumar et al. 2010).

2.1.5. Biomass gasification

A research focus in recent years has been to estimate the efficiency and performance of the gasification process using various types of biomass (e.g. cornhusks, switchgrass, straw) (Brar, Singh et al. 2012). Biomass is very non-homogeneous in its natural state, which creates challenges in maintaining constant feed rates to gasification units. High oxygen and moisture contents result in a low heating value for syngas (typically < 2.5 MJ m^{-3}), which poses problems for downstream

combustors that are typically designed for a consistent medium-to-high heating value fuel (Ciferno and Marano 2002).

2.2. Generalized biomass gasification process

2.2.1. Feedstock analysis

Characteristics of biomass directly affect the amount of energy produced by gasification (Chiang, Chien et al. 2012). Feedstock samples are typically analyzed before processing for moisture content, fixed carbon, ash content and volatile matter based on standard American Society for Testing and Materials (ASTM) methods. Samples might be analyzed in the form in which they were received ("as received"), or they might be dried before analysis by heating to remove water ("dry basis") or combusted at a higher temperature to remove ash (Yin 2011). After drying, elemental analysis reports the composition of the feedstock biomass as mass percent of carbon, hydrogen and oxygen (the major components), as well as sulfur and nitrogen.

2.2.2. Gasification process

During gasification, feedstock is partially oxidized. A gas medium—air, pure oxygen, steam or a mixture of these gases—is required to maintain the process. Biomass feedstock and gasification reactants, which accelerate ignition of the feedstock, enter the gasifier at the top and travel in the same direction down the gasifier (Figure 2.2). A grate at the bottom of the unit holds the feedstock to prevent it from falling to the bottom. Syngas is removed from the bottom of the reactor. After ignition, the feedstock undergoes drying, pyrolysis, oxidation and reduction steps within the gasifier unit.

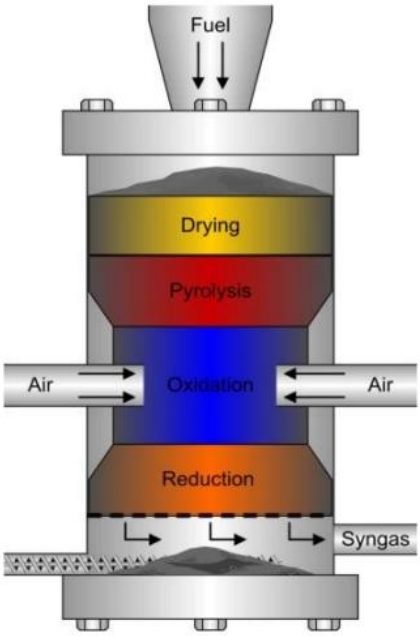

Figure 2.2. Schematic of downdraft gasifier and different stages occuring during the process

2.2.3. Drying

Although drying occurs in a gasifier reactor due to the high temperature generated at the oxidation stage, the moisture content of the feedstock should be reduced using pre-treatment operations (e.g. torrefaction) to meet gasifier specifications (Brar, Singh et al. 2012). High moisture content reduces the temperature achieved in the oxidation and reduction stages, resulting in incomplete gasification. Biomass moisture content should be less than 10–15% range prior to gasification (McKendry 2002). Forest residues and wood have a fiber saturation point at 30–31% moisture content (dry basis), and other biomass can have high moisture content as high at 90% (Amen-Chen, Pakdel et al. 2001).

2.2.4. Pyrolysis

Pyrolysis, also known as devolatilization, is the decomposition of the biomass feedstock by heat. It is endothermic and produces 75–90% of volatile materials in the form of gaseous and liquid hydrocarbons. The remaining non-volatile material with high carbon content is termed char (Ciferno and Marano 2002).

2.2.5. Oxidation

The oxidation zone is called the combustion zone. The combustible substance from a solid fuel is usually composed of elemental carbon, hydrogen and oxygen. During complete combustion, CO_2 is obtained from the carbon, and water is produced from the hydrogen and oxygen, resulting in steam. The combustion reaction is exothermic and yields a theoretical oxidation temperature of 900–1500°C (Obernberger and Thek 2008). Under typical gasification conditions, oxygen levels (including oxygen in the feedstock) are restricted to < 30% of that required for a complete combustion to take place (Stultz and Kitto 1992).

2.2.6. Reduction

Reduction of the combustion products is the final stage in the gasification process. In the reduction zone, the CO_2 and H_2O from the oxidation zone are reduced to CO and H_2 gas, the syngas components. At the end of the reduction stage, the syngas is typically cooled and removed from the reactor for further downstream processing.

2.3. Syngas conditioning

The syngas from the reactor immediately enters a cyclone filtering system to remove water, particulates and other impurities that could cause problems in turbines and other downstream applications. Cyclone filtering may be followed by water /venturi scrubbing or charcoal filtering, whereby charcoal from the filter is used as a feedstock in the gasifier. Examples of impurities include tars—mostly polynuclear hydrocarbons such as pyrene and anthracene—that can clog engine valves, cause deposition on turbine blades or fouling of a turbine system leading to poor performance and high maintenance requirements (Ciferno and Marano 2002). Conventional scrubbing systems are generally the technology of choice for tar removal from syngas. Removal of the tars by catalytically cracking the larger hydrocarbons reduces or eliminates this waste stream, eliminates the cooling inefficiency of scrubbing, and enhances the syngas quality and quantity. A cyclone can provide primary particulate control, but is not adequate to meet gas turbine specifications (Ciferno and Marano 2002). Water scrubbing can remove up to 50% of the tar in the product gas, and is followed by a venturi scrubber, with the potential to remove 97% of the remaining tars (Paisley and Anson 1998).

2.4. Pilot-Scale Gasifier Equipment Kit (GEK) Unit

The process of gasification was investigated in our laboratory using a pilot-scale downdraft gasifier (GEK Level 4, Model V3.1.0) provided by ALL Power Labs (Berkley, California, USA). The nominal thermal input of the unit is 10 kW (Figure 2.3). The feeder consists of a cylindrical stainless steel drum (feeding capacity 141,342 cm^3) and a drying bucket (volume 39,100 cm^3). The GEK unit was initially assembled for batch operation, but has been improved for continuous operation using a screw biomass conveyor connected to a motor. The feedstock in the drying

bucket is dried using a cyclone column connected at the bottom of the bucket. The drum can hold enough feedstock to support many hours of continuous operation.

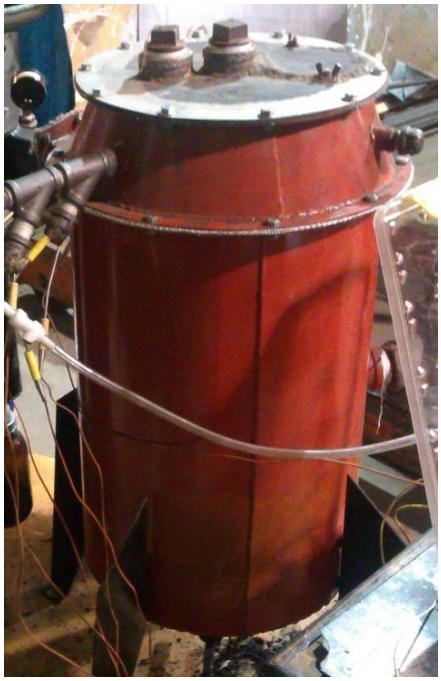

Figure 2.3. Pilot-scale GEK gasification reactor

The main reactor is a cylindrical vessel (39.4 cm height, 35.5 cm diameter) equipped with air nozzle supports to provide the reactant, as well as gas lines to transport the syngas into the filtering system (Figure 2.4). The bottom of the reactor is filled with wood charcoal up to approximately 10 cm below the reactor lid, to provide fuel for the ignition of the system. The remainder of the vessel is filled with feedstock materials. A reticular grate at the bottom of the reactor holds the feedstock and allows only ash to pass through. A monometer is connected to the reactor frame to monitor pressure inside the reactor. A GEK gasifier control unit monitors and controls temperature

and pressure during the operation. For this purpose, nine thermocouples and three pressure indicators are installed in the unit.

Figure 2.4. Fully assembled gasifier equipment kit (GEK) unit

The charcoal filtering system is a cylindrical drum filled with charcoal media. The first 5 cm of space is filled with 2.5 cm diameter charcoal pieces and the remainder of the volume is filled with charcoal pieces that are 0.15–1.5 cm in size. A perforated disk is placed on the charcoal and two filter foams are placed on top of the disk.

Before starting the system, cold tests are required to check for air leaks in the gasification unit Cold tests are performed by connecting the compressor to the unit and increasing the air pressure to 12.7 cm of H_2O. After the cold tests, liquid fuel is injected into the ignition port and ignited with a propane torch. During the process, syngas exits the reactor from the bottom, enters the cyclone

and charcoal filtering chamber and is combusted in the flare burner. Waste ash passes through the grate and is collected from the bottom of the reactor with a rotary handgrip at the end of the cycle.

2.5. Market for syngas

The type of reactant used in the process determines the heating value of the syngas. Air-based gasifiers typically yield a producer gas containing relatively high nitrogen concentrations, with a heating value of 4–6 MJ m^{-3}. Oxygen and steam-based gasifiers produce a syngas containing relatively high concentrations of H_2 and CO, with a heating value of 10–20 MJ m^{-3} (Ciferno and Marano 2002).

The potential market for syngas is based on the assumption that syngas could replace fossil fuels in some regions. Approximately 30% of the world's primary energy consumption is for transportation fuels and the chemical industry. Figure 2.5 presents the data of the syngas market in 2006 and prospective syngas market around the world in 2040.

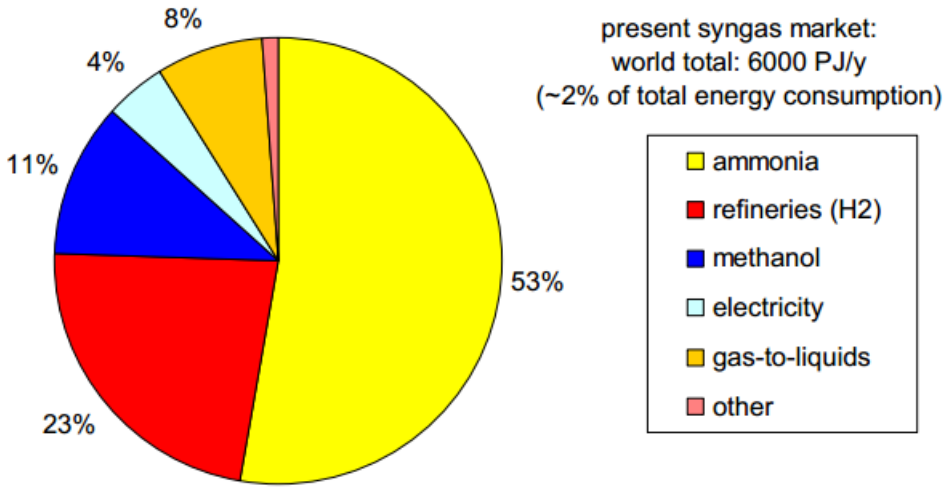

(a)

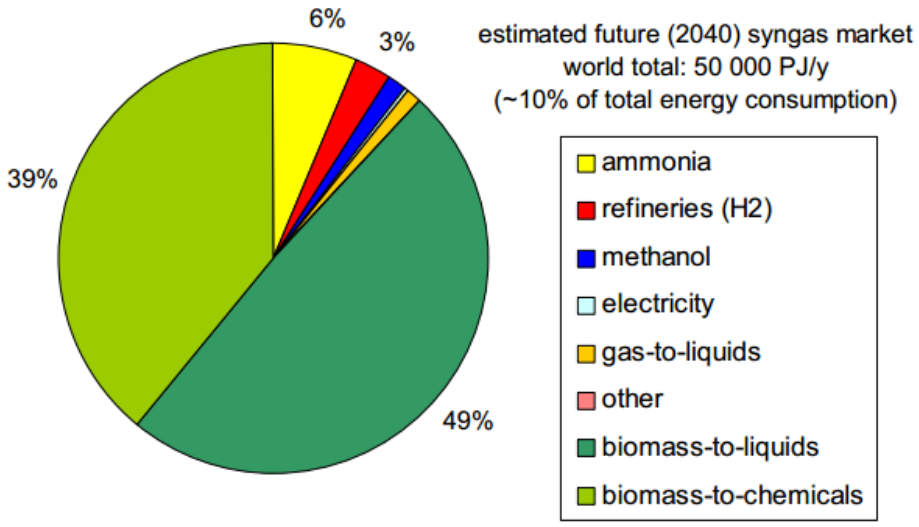

(b)

Figure 2.5. World syngas market (a) Current and (b) predicted in 2040 (IEA. 2006)

2.6. Conclusion

The production of renewable energy from biomass using a gasification system is an environmentally friendly method that helps reduce dependence on fossil fuels. Biomass gasification offers advantages over the direct burning of biomass in a boiler. For example, gasification can be used for very small-scale (up to 20 kW) decentralized power generation projects. A gasifier system is a simple device that can be made of fire bricks, steel or concrete and oil barrels. Since syngas is produced before final combustion, a complete gasification unit (pre- and post-treatment steps and gas conditioning components) can significantly decrease the concentrations of harmful gases produced through other combustion systems. Compared to other renewable energy options, biomass gasification is a promising alternative to produce high quality energy from various types of feedstock available throughout the world.

Connecting Text

In Chapter 2, the basics of gasification technology, as a representative of an effective thermochemical conversion method, was elaborated. It explained what material would be eligible to be processed in the gasification reactor and what analysis should be performed prior to undertaking gasification. Additionally, different existing designs of reactor were presented and the down-draft reactor was selected as the configuration of interest for the rest of this study.

With the theoretical knowledge established in Chapter 2, Chapter 3 begins with the first set of experimental studies using a down-draft gasification system. The unit was first assembled in batch mode and then developed to continuous mode to improve the performance of the conversion process. After unit development, pelletized woody biomass was selected as the first biomass of interest to run in the reactor. Forests are a major source of wealth for Canadians, providing a wide range of economic, social and environmental benefits. Therefore, choosing woody biomass to run the gasifier for baseline tests matches with the available natural resources in Canada. This chapter elaborates the development, detailed technical aspects, and potential failure scenarios of the gasification process using woody biomass.

Chapter 3 is published as:

Madadian E., Lefsrud M., Perez Lee C., Roy Y., & Orsat V. (2016). Gasification of pelletized woody biomass using a downdraft reactor and impact of material bridging. *Journal of Energy Engineering*, 04016001.

CHAPTER 3

3. GASIFICATION OF PELLETIZED WOODY BIOMASS USING A DOWN-DRAFT REACTOR AND IMPACT OF MATERIAL BRIDGING

Abstract

Biomass gasification shows a great potential to displace fossil fuels. In this study, the gasification of pelletized hard wood using a 10 kW down-draft gasifier has been investigated. The variations of pressure and temperature parameters during the gasification process with air as a medium were controlled. The gasifier started in continuous mode to burn the wood pellet feedstock. The results from the continuous mode indicated average temperatures of 838 °C and 754 °C for combustion and reduction zones inside the gasifier, respectively, which shows a low temperature gasification process. Moreover, the pressure in the combustion zone varied on average from -1.30 kPa to -1.64 kPa, while the pressure on top of the main reactor showed average variation of less than 0.07 kPa. The pressure drop is assumed to be caused by bridging of the feedstock which results in a large part on the feedstock not flowing and burning inside the reactor. We have theorized that the shape of feedstock was assumed to be the major reason for the feedstock to bridge, in addition air leaks in the reactor, resulting from sealing challenges intensified the problem.

Keywords: biomass gasification, bridging, down-draft gasifier, wood pellet

3.1. Introduction

Gasification is one of the most effective energy conversion methods for the utilization of biomass (Umeki et al. 2010). The gasification technology converts carbonaceous into synthetic feedstock (Kim et al. 2015). Biomass is a major renewable energy source and is one of the most environmental friendly fuels that contain low sulfur and ash content (Brattsev et al. 2011). Biomass has higher volatile matter than coal making it an attractive clean fuel for reducing greenhouse gas emissions (Miccio et al. 2010). One of the applications of biomass is the production of gaseous fuel through the gasification of solid biomass materials (Papagiannakis and Zannis 2013). Biomass gasification is the most efficient and economical viable route for H2 production and a major focus of biomass gasification is to maximize the contents of H_2. Hydrogen is one of the most promising next generation fuels because it is abundant and environment-friendly (Kong et al. 2014). The higher amount of hydrogen can be achieved by water-shift reaction as a way to convert extra carbon monoxide to hydrogen. Biomass gasification is impacted by different operation parameters such as composition and moisture contents of feedstocks, type of gasifier, residence time, reactor pressure, gasifying agent, and most importantly temperature (Mohammed et al. 2011; Ahmed et al. 2012; Taba et al. 2012).

Wood pellets are densified biomass fuel typically made from material rejected by wood product manufacturers. By pelletizing residual forest waste, sawdust, planer shavings, and beetle-killed timber, millions of tons of waste can be put to work for the bioenergy economy while enhancing the environment by reducing greenhouse gas emissions (Murray 2010). Due to very low sulfur content and high reactivity of the wood fuel, the fraction of mineral ash content of the gasification products is very small (Brattsev et al. 2011).

Gasification performance depends on biomass characteristics and different biomass can result in different syngas high heating values, reaction temperatures, and tar content (Di Blasi et al. 1999; Rivas 2012). The use of limited air or oxygen in gasification partially oxidizes the biomass in an exothermic process that helps driving the endothermic reaction. However, the use of air can dilute the final syngas thus decreasing its heating value (Rivas 2012; Mahishi and Goswami 2007). High oxygen and moisture content results in a low heating value for the product syngas, typically less than 2.5 MJ m^{-3} (Madadian et al. 2014). Gasification coupled with syngas combustion for heat and power can achieve high efficiency and is recognised to make biomass heating cleaner and easier to control, compared to direct combustion of solid fuels (Dion et al. 2011; Reed et al. 1988; Quaak et al. 1999; Whitty et al. 2008).

In order to fully utilize bioresources in the field of gasification, it is necessary to study biomass gasification more detailed (Huo et al. 2014). One of the major limitations of biomass for energy is its low density, typically ranging from 60 to 80 kg m^{-3} for agricultural straws and grasses and 200 to 400 kg m^{-3} for woody biomass like wood chips (Sokhansanj and Fenton 2006; Tumuluru et al. 2010). Commercially, densification of biomass is performed using pellet mills, briquetting presses or other extrusion processes, to increase its density, which is typically between 20 to 400 kg m^{-3} for loose biomass (Malatji et al. 2011) up to tenfold and reduce feeding, storing, handling, and transporting problems (Tumuluru et al. 2010).

Gasification bed temperature is one of the most important operating parameters during gasification, affecting both the heating value and the producer gas composition (Alauddin et al. 2010). Taba et al. (2006) concluded that carbon conversion and cold gas efficiency (CGE) increase with the rise of temperature while hydrocarbons and tar contents are decreased. This efficiency depends on the thermodynamic behaviour of the reactions and the balance between endothermic

and exothermic reactions (Fermoso et al. 2009; Xiao et al. 2011; Taba et al. 2012). The operation temperature of the gasification process is rather high, commonly ranging from 750 °C to 1000 °C (Baláš et al. 2012).

The pressure gradient across the fixed bed is a function of system geometry, feedstock porosity, permeability and physical properties of the feedstock (Sharma 2011). Pressure sensors monitor the strength of the pressure gradient in the gasifier. In this study, the temperature and pressure were monitored during the operation of a downdraft gasification unit. Temperature and pressure are considered as the two most significant operational parameters impacting the efficiency during the gasification process. Variations in the temperature and pressure parameters in the gasifier could influence the calorific value as well as the carbon conversion.

The purpose of this research was to measure variations in temperature and pressure within the reaction vessel to determine the stability of the process.

3.2. Experimental

3.2.1. Biomass feedstock

Wood pellets from Valfei Products Inc. (hard wood, Shawinigan, Quebec) were used as the feedstock for the experiment. The wood pellets were cylindrical in shape, averagely 8 mm in diameter and 30 mm in length. The biomass materials, according to referenced American Society for Testing and Materials (ASTM), were proximate analysed for moisture content (ASTM E871-82), ash content (ASTM D1102-84), fixed carbon (ASTM E870-82) and volatile matter of the wood pellet (ASTM E872-82). The ultimate analysis was performed to measure the composition

of the biomass in mass percentage of carbon, hydrogen and oxygen (as the major components and all using ASTM D5373) as well as nitrogen (ASTM D5373) and sulfur (ASTM D3761).

3.2.2. Gasification medium

Air was used as gasification medium to perform the partial oxidation during the process. The air was introduced to the reactor through an air inlet as seen in Figure 1. Compressed air was provided using a compressor capable of providing 76 kPa pressure and 0.17 to 0.23 m^3 min^{-1} (commercially known as 6 to 8 cfm or ft^3/min) amount of air. All air supplied to the system was through an air compressor with venturi, no air blower was required for the system to operate properly.

3.2.3. Gasification process

The gasification process has been investigated using a pilot-scale downdraft gasifier (GEK Level 4, Model V3.1.0) purchased from All Power Labs Company (Berkley, California, USA). The nominal thermal output of the unit is 10 kW. The gasification unit is made up of three major parts: (1) Feeding; (2) Main reactor; and (3) Filtering (Fig. 3.1).

The feeding part consists of a cylindrical stainless steel drum (capacity of 0.141 m^3) followed by a drying bucket (0.039 m^3). The unit can be operated either in batch or continuous operation. During continuous operation, biomass is moved into the reactor using a screw conveyor connected to a motor. The feedstock in the drying bucket is dried using hot syngas, with an average temperature of 140°C, coming from the reactor connected at the bottom of the bucket. The drum can hold sufficient feedstock to support 60 hours of continuous operation.

The main reactor is a cylinder-shaped vessel (height of 0.4 m and diameter of 0.35 m) equipped with air nozzle supports to provide the reactant and gas pipes to transport the produced gas into the filtering system.

The gas pipes transfer the producer gas to the bottom of the reactor. The syngas then enters the cyclone, where tar is captured in a collection jar, and then into the drying bucket to dry the feedstock. Syngas leaves the drying bucket and enters the charcoal filtering chamber. During the start-up procedure, the bottom of the reactor is filled with wood charcoal, as bed material, up to 0.1 m below the reactor lid. The remainder of the vessel is filled with feedstock materials placing on top of the charcoal. At the bottom of the reactor is a reticular grate used to retain the feedstock in the combustion zone while allowing the ash to pass. A monometer is connected to the reactor frame for measuring the pressure inside the reactor during operation (Figure 3.1) (APL, 2012).

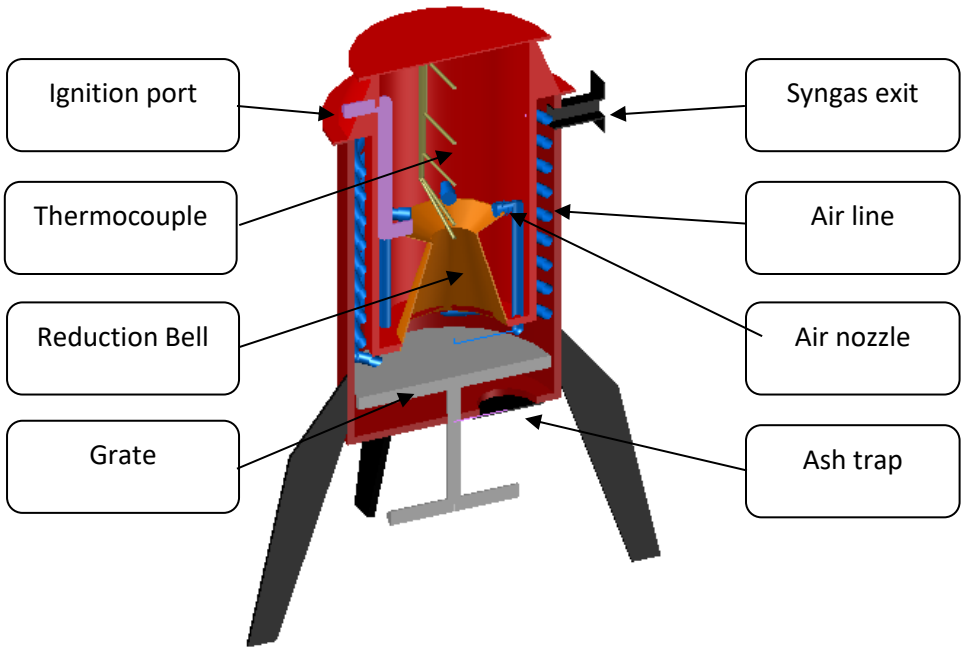

Figure. 3.1. Schematic cross section view of the main reactor of the downdraft gasifier. The materials are fed from the top and flow through the reduction bell. The gasifying agent (air) enters the unit using the air nozzles and flow into the main chamber

A charcoal filtering system is positioned downstream of the cyclone and drying bucket. The cyclone removes water, tar and particulates from the syngas. The filtering system is a cylindrical drum filled with charcoal media. Based on GEK operation instruction (APL, 2012), the first 0.05 m is filled with 0.025 m (1 inch) diameter charcoal while the remainder is filled with charcoal 0.012 m. A perforated foam disk is placed on the charcoal and two filter foams are placed on top of the disk.

A gasifier control unit (GCU Model v3.02, All Power Labs Co.) was used to monitor temperature and pressure during the operation. Data was obtained on the internal status of the gasifier through continuous monitoring (2 seconds intervals) of 4 thermocouples (K type) and 3 pressure sensors

were installed within the unit. The data from the GCU was directly logged onto a laptop. The thermocouples were located in the gasifier to measure the temperature layers of drying (T_1), pyrolysis (T_2), combustion or oxidation (T_3) and reduction or gasification (T_4) zones. Figure 3.2 showed the assembled GEK unit at Macdonald Campus, McGill University (Sainte-Anne-de-Bellevue, QC).

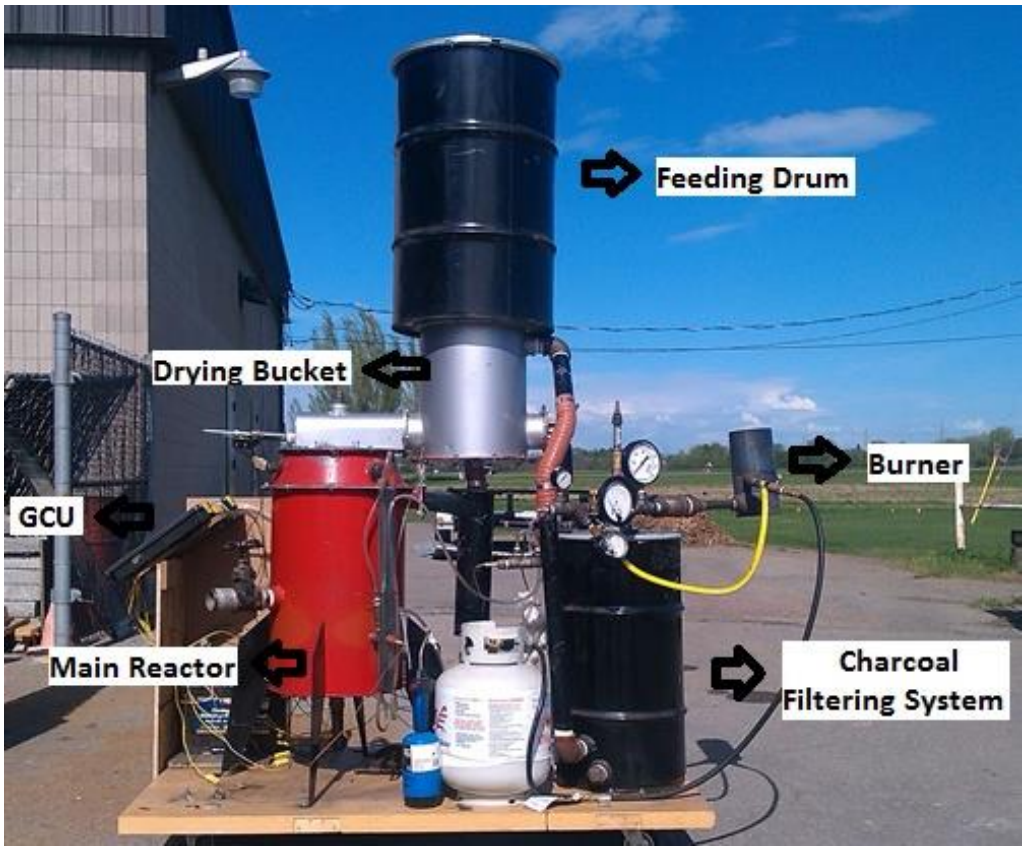

Figure 3.2. Downdraft gasification system assembled in Macdonald Campus, McGill University

Before starting the system, cold tests were conducted in order to check for any air leaks and establish the maximum pressure of the gasification unit. Cold tests were performed by connecting the compressor to the unit and increasing the air pressure to 1.2 kPa. The unit is started by injecting 60 ml of gasoline into the ignition port and using a propane torch to begin ignition through the ignition port which accesses the top of the charcoal and the injected gasoline. Ignition is complete when the temperature of the combustion zone (T_3) reaches 100 °C. It normally takes from 10 to 20 min depending on the ambient temperature of the lab.

After ignition, the combustion and gasification layers become established. Syngas exits the reactor at the bottom and enters the cyclone and flows into the charcoal filtering chamber and is combusted in a flare burner. At the end of the cycle, the generated ash is collected from the bottom of the reactor using a rotary handgrip collection system.

3.3. Results and Discussion

3.3.1. Time and consumption rate

All of the gasification runs for this experiment were performed in continuous mode, using the feed bucket. A complete gasification run was approximately 9000 seconds. The average feedstock consumption rate of the system was calculated at 23.66 g min^{-1} (volumetric feed rate of 0.68 cm^3 s^{-1}).

3.3.2. Biomass characterization

The average of the proximate analyses is reported in Table 3.1. The wood pellet feedstock showed low ash potential (1.2%) and an acceptable level of moisture content (3.3%) for meeting the GEK's

gasifier specification. The maximum moisture content of the feedstock should be 25% to allow the reactor to work at its optimum level.

Table 3.1. Proximate analysis of wood pellets feedstock (dry basis, hard wood, Valfei Products Inc.)

	Properties	Value*
Proximate analysis	Moisture content (%)	3.28 ±0.35
	Ash content (%)	1.2 ±0.21
	Fixed carbon content (%)	16.5 ±0.77
	Volatile matter (%)	68.5 ±6.63
	Bulk density ($kg.m^{-3}$)	580 ±0.90
Ultimate analysis	Carbon (%)	43.52
	Hydrogen (%)	7.04
	Oxygen (%)	45.71
	Nitrogen (%)	0.08
	Sulfur (%)	0.05
	Higher heating value (HHV) ($MJ\ kg^{-1}$)	18.31

3.3.3. Temperature

3.3.3.1. Drying and pyrolysis zones

For the top half of the reactor, the average temperatures were 88 °C and 178 °C in the drying (T_1) and pyrolysis (T_2) zones with standard deviation of 22 °C and 63 °C, respectively (Figures 3.3a and 3.3b).

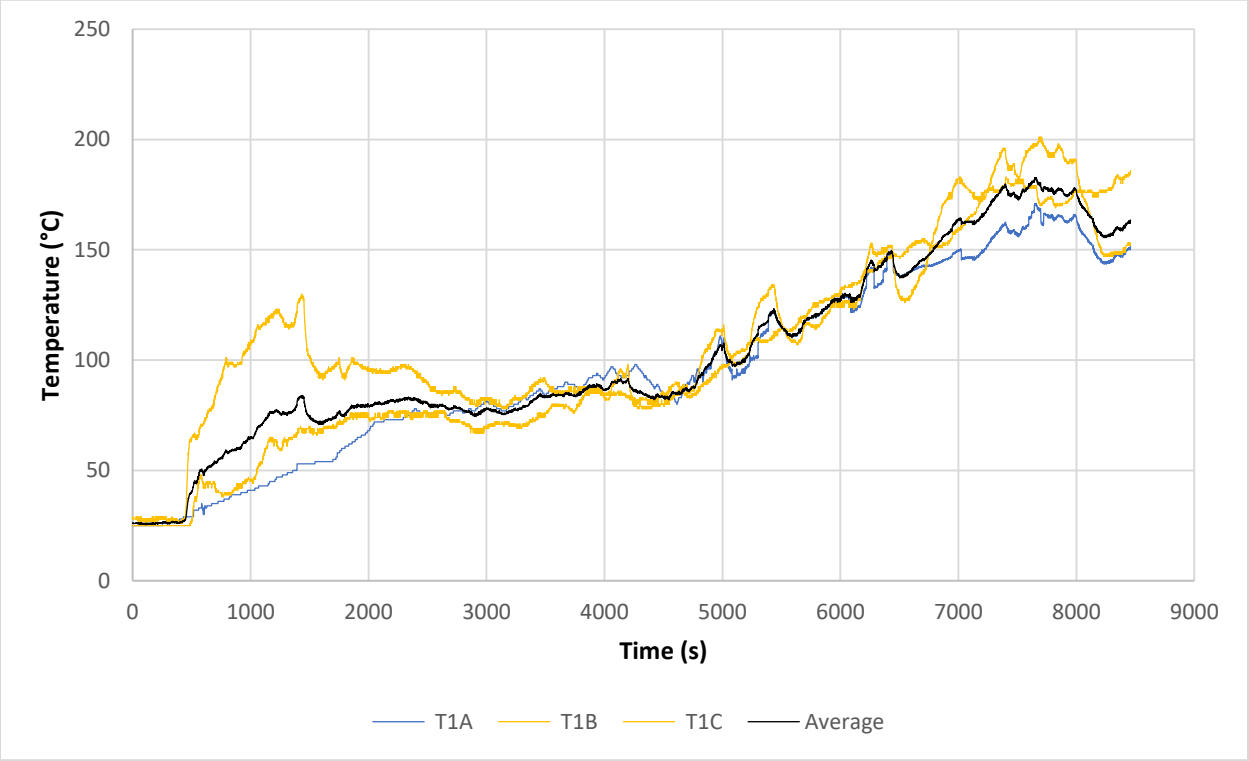

(a)

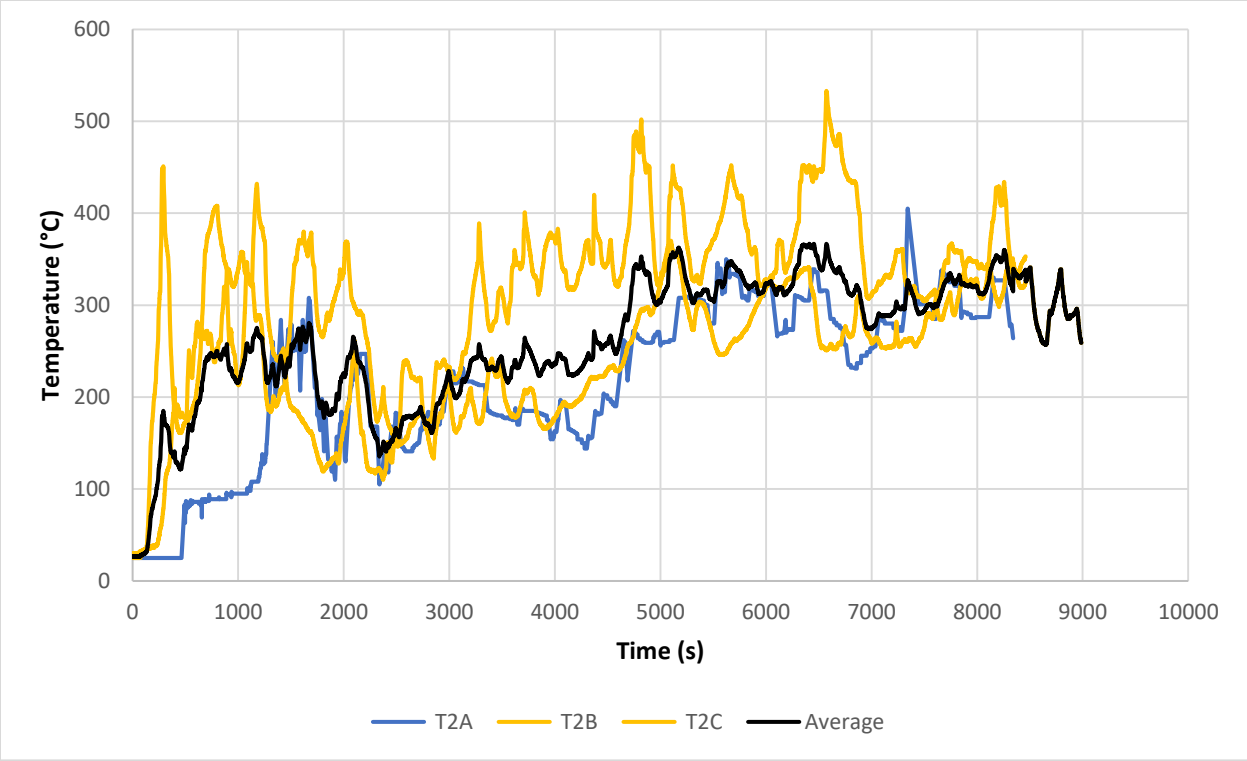

(b)

Figure. 3.3. Temperature variations through the gasification process in three repeated tests of A, B & C in (a) Drying zone (T_1) and (b) Pyrolysis zone (T_2)

In the drying and pyrolysis zones, the temperature of each replication showed an upward trend over the run. It has been observed that the outside air temperature has a significant impact on the reactor start up and operation. For outside temperature below -10 °C, the ignition flame needed to be maintained for a longer period of time inside the ignition port to ensure start up. In addition, the condition of the bed influenced the upward trend of the temperature. Cold pyrolyzed material left in the core of the reactor from a previous operation formed a relatively solid mass of material bounded together. This mass reduced the flowability of the biomass in the reactor and slowed

down the ignition process. A thin charcoal bed covered by fresh biomass helped the start-up which resulted in a more abrupt upward temperature trend. Heat transfer from the combustion zone to upper levels influenced the temperature trend of the drying and pyrolysis zones. Heat transfer usually depends on kinetic of the reactions and the conductibility of the material. The presence of gas pockets inside the feedstock reduced the heat conductivity of the feedstock influencing the temperature in the drying and pyrolysis zones. As soon as the flame was removed from the ignition port, the temperature follows a downward trend toward ambient temperature meaning that not enough heat is generated in the combustion zone to maintain the gasification. Low temperatures in the drying and pyrolysis zone imply a low heat generation in the combustion zone, meaning that the gasification is not occurring properly in the combustion and reduction zone.

As can be seen in Figure 3.3, there are some significant differences between the individual runs. However, the trend of each run is the same. One of the environmental parameters that could easily influence the start-up of the process of the gasifier was the ambient air temperature. This start-up variability was obvious when the experiments were performed during two different seasons, especially in Canada where the outside temperature is significantly different. Moreover, cleaning-up level between runs was another influencing factor on the temperature profile of the operations, as more caked on material reducing heat transfer. For this reason, the average of all the runs are demonstrated to make it simpler to observe the trends during the gasification process.

3.3.3.2. Combustion and reduction zones

The temperature in the combustion (T3) and reduction (T4) stages in the bottom half of the reactor, varied a significant amount with an average temperature of 838 °C and 754 °C for the combustion and reduction stages, respectively. The average values for replications A, B and C were 817 °C, 867 °C and 831 °C, respectively. However, all the replications followed a similar trend of increasing at the beginning then remaining constant with some small fluctuations (Figure 3.4a and Figure 3.4b). When the combustion temperature increased to approximately 800 °C (occurring in the first few minutes), the temperature stabilized for the remaining time of the operation.

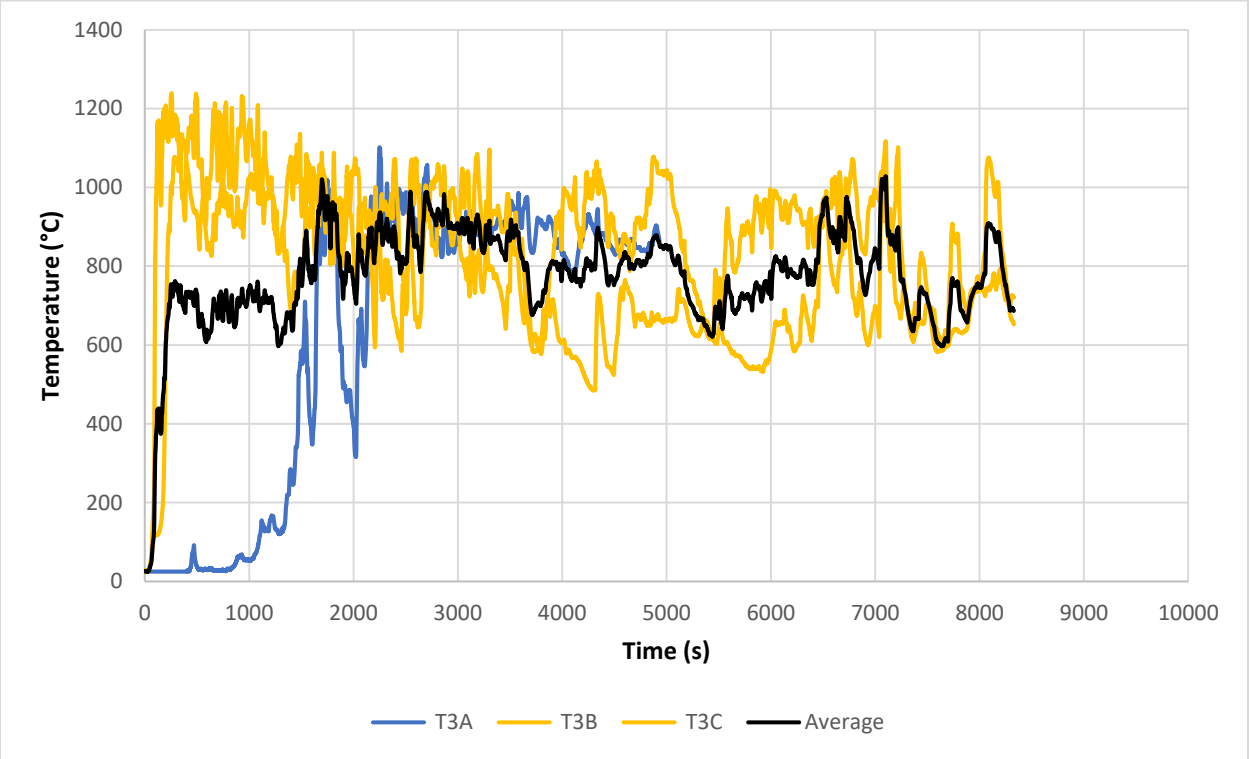

(a)

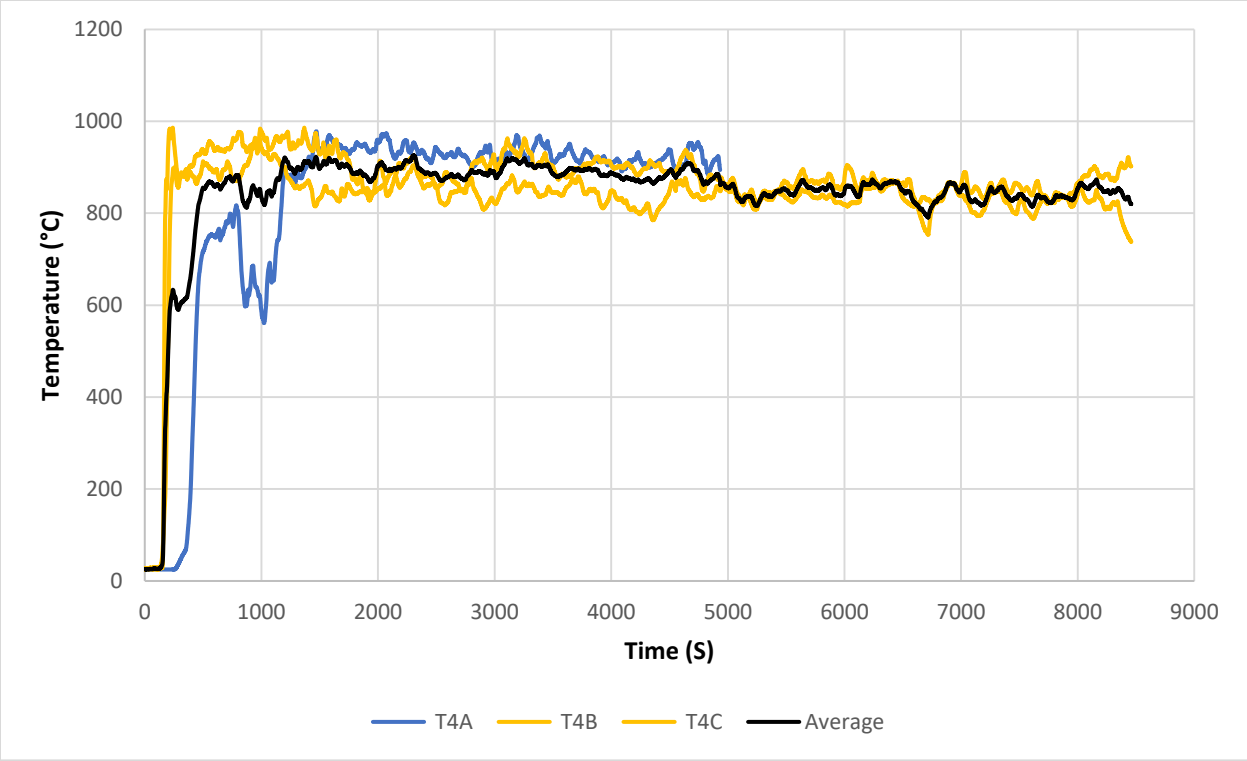

(b)

Figure 3.4. Temperature variations through the gasification process in three repeated tests of A, B & C in (a) Combustion zone (T_3) and (b) Reduction zone (T_4)

The temperature of the reduction zone showed more stable behavior compared to the combustion zone in all replications (Figure 3.4a & b). The average values in the reduction zone for replications A, B and C were 615 °C, 847 °C and 800 °C, respectively. This less stability in the reduction zone is mainly due to the instability of air flow in that zone. Moreover, most of the reactions in the combustion zone are exothermic and provided the required heat for these reactions (i.e. reducing CO_2 and H_2O to CO and H_2). During the experiment, the reduction zone showed more temperature

fluctuations with a standard deviation of 248 °C compared to the combustion zone which had a standard deviation of 165 °C.

As shown in Figure 3.4b, the temperature of the reduction zone increased immediately after starting the ignition in all replications excluding Test A which took around 900 seconds. The delay could be because of ambient conditions, especially outside air temperature which influenced the start-up time. As the fire stabilized in the reduction zone, it kept the temperature between 700 °C to 1200 °C.

The heat is generated through an exothermic reaction in the combustion zone and the syngas moves in a downward direction due to the vacuum pressure exerted by the venture. Gasification reactions are generally endothermic, but there are some exothermic reactions to help to initiate the endothermic reactions. Commonly, the reactions of carbon with oxygen and hydrogen are exothermic (Basu, 2010). The bottom half of the reactor reached a higher temperature than the top of the gasifier. The temperature changes during the operation of the gasifier are shown in Figure 3.4a. The reduction zone temperature was investigated to accomplish a high biomass carbon conversion and maintain a low tar content. A low reaction temperature (lower than 750 °C) can increase the quantity and composition of tar generated (Rivas 2012). Figure 3.5 shows the estimated average temperature profile of the different stages of the gasification during steady state conditions. The temperature was recorded in four identical time frames of 133 min that make it independent on the time in this graph. The graph is depicted base on the global steady state condition of the system after starting the operation. Obviously, the start-up time and the bridging scenario are not desired outcomes of gasification as observed from this graph and results in the system moving from steady state to transient and unsteady state conditions.

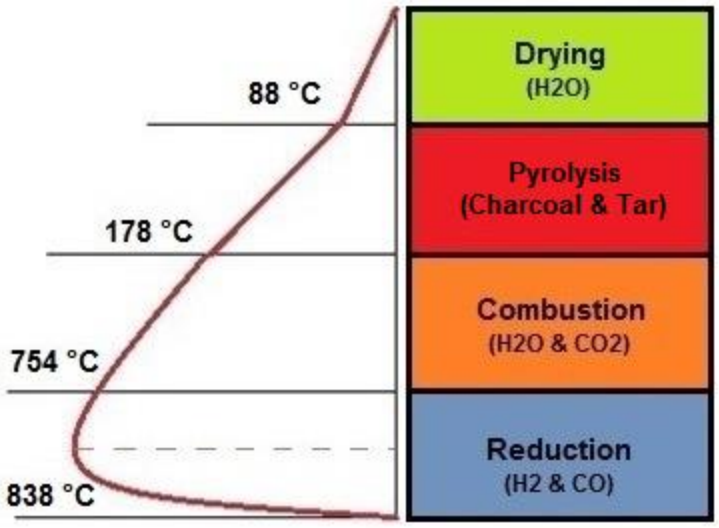

Figure 3.5. Temperature profile of different reactions inside the down-draft gasifier during steady state conditions. Drying takes some water out of the feedstock and make it ready to be pyrolyzed and produce charcoal and tar. These materials are partially combusted and liberate H_2O and CO_2 which are finally reduced to H_2 and CO

The average amount of ash generated within our three replicates were measured at 200 g which accounts for 1.2 % of the initial mass of the feedstock (16.5 kg) showing capability of wood pellets in producing very low amounts of ash.

3.3.4. Pressure

Pressure is one of the key factors for complete gasification of biomass. Pressure was monitored using two sensors placed at the top of the reactor (P_0) and at the bottom of the reactor which is located next to the reduction bell (P_1). The sensors measured the differential pressure between the two locations and the ambient outside air pressure. The results indicate a steady fluctuation between -1.00 kPa and -1.64 kPa, excluding changes recorded during air flow adjustment. There

was negligible pressure reduction when measuring the pressure between the top of the reactor and outside air pressure.

The reactivity of biomass feedstock during the gasification increases with increasing partial pressures. Pore diffusion (in biomass and between the pellets) is one parameter that can be used to control the gasification reactions. In our experiment, we used a compressor to produce a vacuum using a venturi and limit pressure differences across the reactor. However, this ideal pressure difference rarely occurred and there was some pressure difference caused by feedstock movement and air leaking into the unit.

3.3.5. Bridging

The pressure fluctuations between the top and bottom pressure sensors can be used to explain feedstock bridging. Bridging of the feedstock results in a stopping of the downward flow of the pellet biomass inside the main reactor. In this case, the combustion zone became destabilized due to improper feeding of the biomass within this zone. Moreover, the pressure values of the top and bottom sensors of the reactor showed a divergence with the bottom sensor monitoring a reduction in pressure and the top sensor remaining constant. This divergence is the result of the bridging which happens above the combustion zone and impedes the feedstock and air flow within the reaction chamber. This bridging can cause operational problems that lower the calorific value of the syngas through the reduction of CO and H_2 concentration into the syngas. Bridging can ultimately stop the gasification process. Based on earlier research (Cruangul and Sulairnari 2013), bridging happens due to two main reasons: (1) geometry and bulk density of feedstock, and (2) operational error. The bulk density and flow characteristics of feedstock will influence the conversion process (Woodcock and Mason 1988). Moreover, air leaks during the operation of the

gasifier can enhance the pressure imbalance within the reactor. The pressure changes of the three replicates are reported in Figure 3.6.

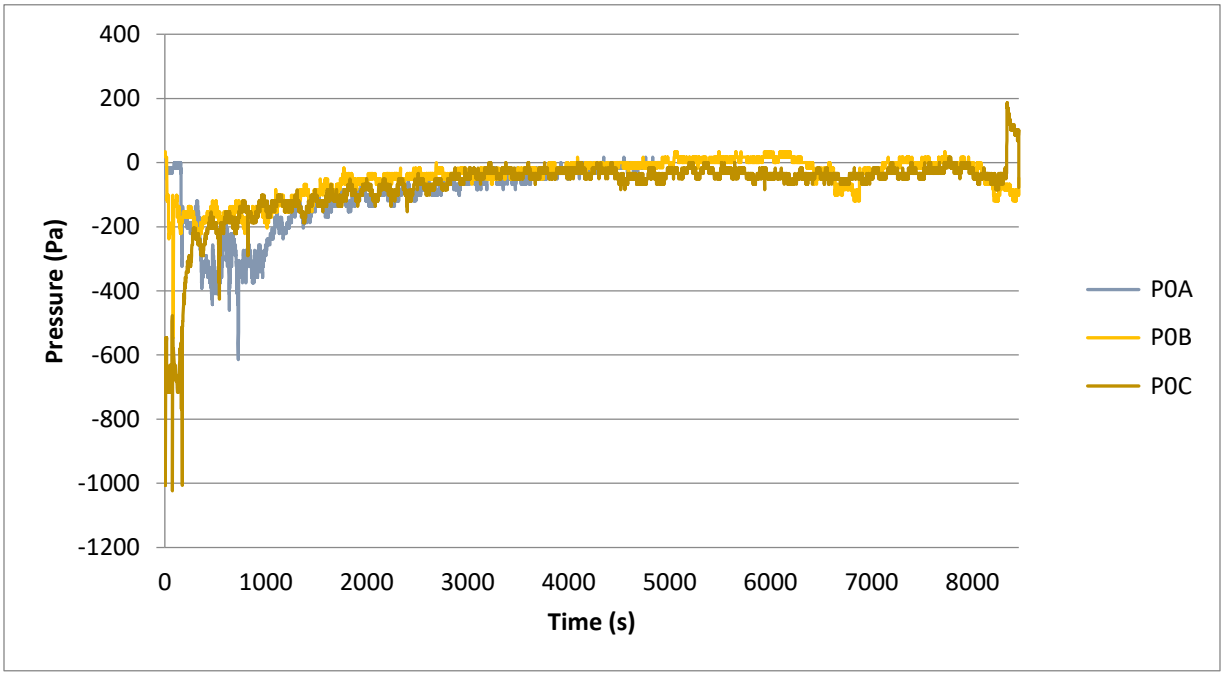

(a)

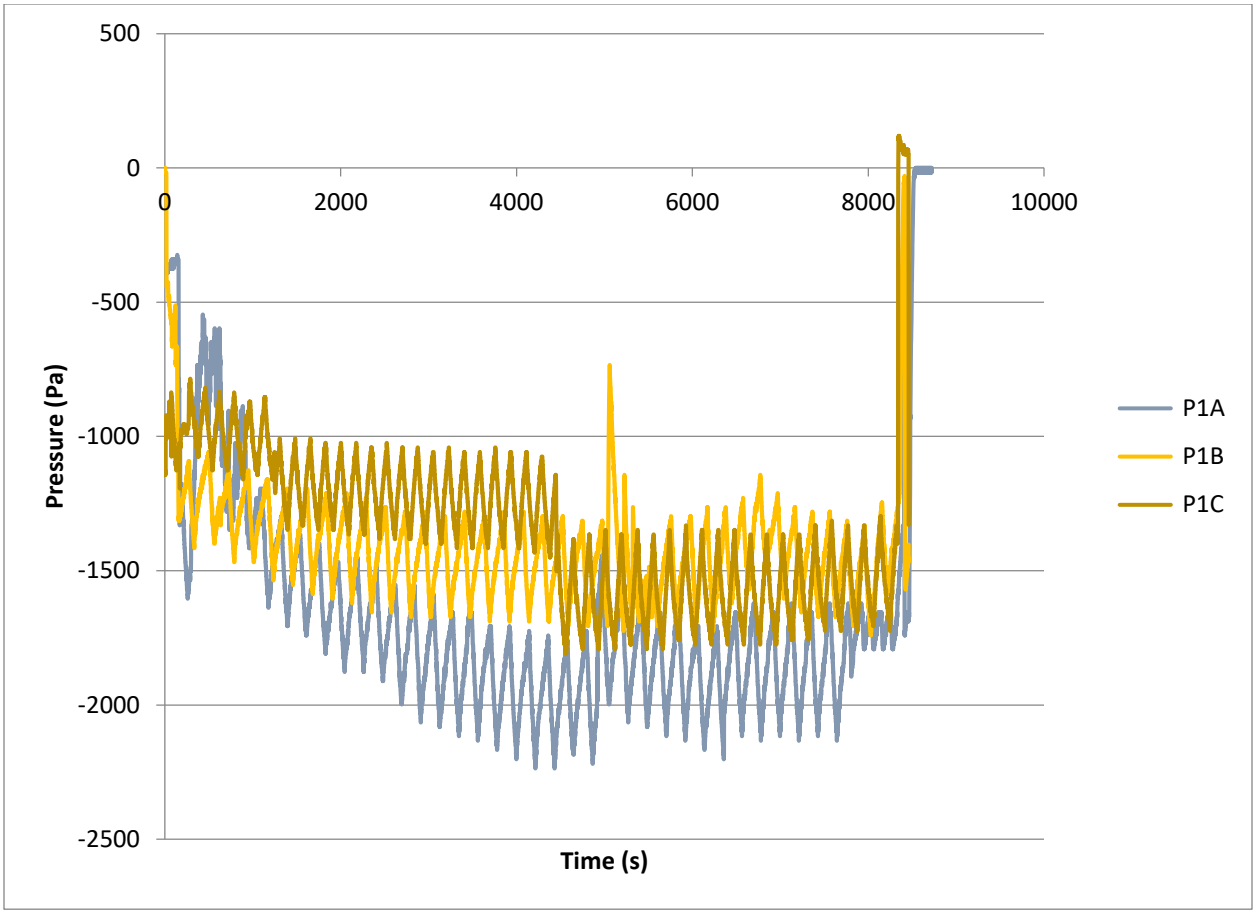

(b)

Figure 3.6. Pressure variations throughout the gasification process in three replications of A, B & C at (a) the top of the main reactor, and (b) the bottom of the reactor

The process took approximately 600 seconds to stabilize. As can be seen in Figure 6a, the pressure at the top of the reactor fluctuated between -0.06 kPa, -0.05 kPa and -0.07 kPa for the replications A, B and C, respectively. The difference was attributed to the amount of air leaks during each replication. Moreover, the pressure around the reduction bell of the reactor in Figure 6b fluctuated between -1.3 kPa to -1.6 kPa for all the replicates. At the end of the gasification process, P_1 dropped

dramatically to reach the minimum pressure level. In addition, the regular fluctuations in pressure graphs are mainly because of the compressor that was used to control the pressure using a venturi system.

In case of bridging, the external flare flame intensity dropped quickly and continued with non-continuous flow of the syngas. The flame instability resulted in an obvious noise change that could be used to record when the bridging was happening. When we heard this change in flame stability, we checked the temperature and pressure to validate that bridging was occurring. The material bridging was broken by applying three to five abrupt forces to the body of the reactor. This action immediately resulted in breaking the possible bridge bonding and intensifying the flame flow. This result can be observed in Figure 3.6b, replication B at ~5000 (spike in pressure) and then return to steady flow, but was observed for all replications.

In terms of visual observation, the bridging could be viewed after cool down of the reactor and when we opened the lid of the main reactor. We used a bar to break the surface material bridge and there was an obvious gap between the top layer of the bridge and the lower feedstock.

The temperature variation caused by the bridging was evident on the recorded data. Specifically, the temperature of the pyrolysis zone (T_2) started to increase, while the temperature of the combustion (T_3) and reduction (T_4) zones dropped slightly and simultaneously. This abnormal behaviour of the temperature profile in the reactor was attributed to the feedstock bridging that result in the gas being trapped in the upper section of the reactor and enhancing the temperature in the pyrolysis zone. As a result, the lower section of the reactor, in the combustion and reduction zones, did not have sufficient fuel to maintain optimum reaction rates. Therefore, there was less

gas and consequently lower temperatures were produced. The schematic of the bridging event is depicted in Figure 3.7.

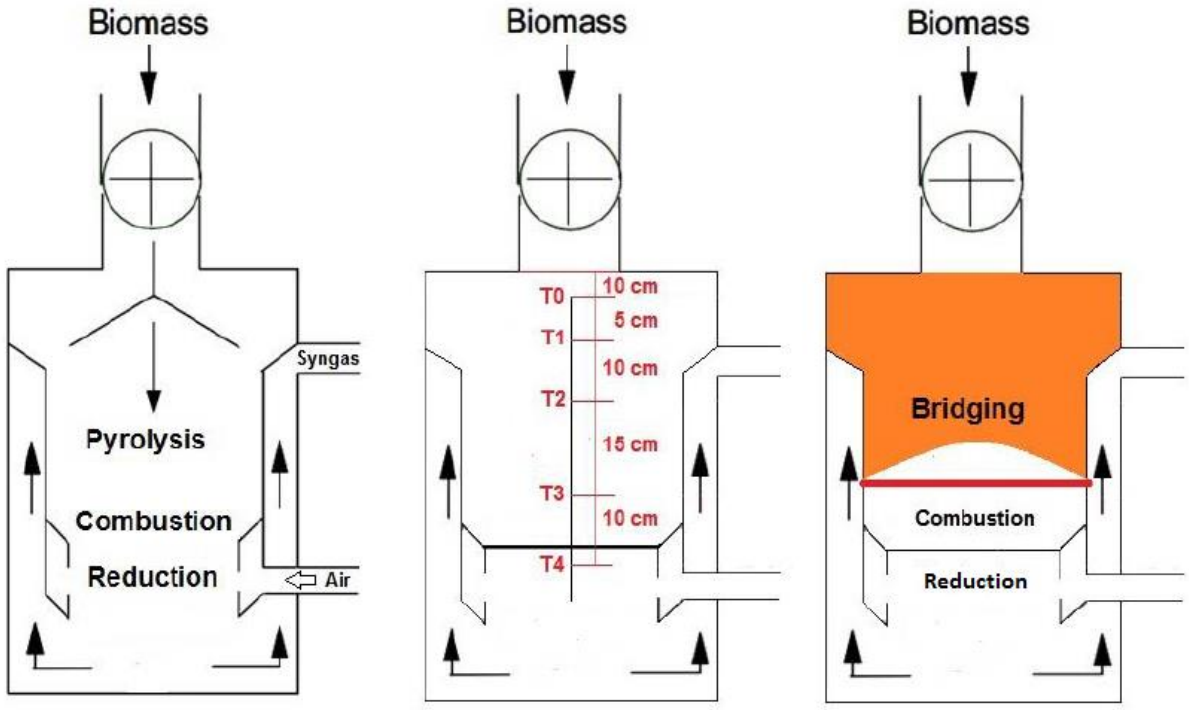

Figure 3.7. Schematic of bridging formation across the reactor (from left to right): the simple downdraft reactor, the location of thermocouples, and the location where the bridging takes place

The “degree of bridging” inside the reactor is a term defined by the author which is directly dependant on the magnitude of the pressure difference. Degree of bridging is a relative scale which requires further investigation to be considered as an absolute scale. Table 3.2 shows the average differential pressures generated across the height of the reactor in each replicate. As mentioned earlier, the pressure difference was concluded to be due to the bridging problem which occurred

due to the low bulkiness property of the feedstock. Tests A and C with the highest and lowest differential pressures of 1.58 kPa and 1.26 kPa, have the maximum and minimum degree of bridging between the replicates.

Table 3.2. The differential pressure between top and bottom of the reactor

Test	Average pressure at the top of the reactor, P_0 (kPa)	Average pressure at the bottom of the reactor, P_1 (kPa)	Pressure difference between top and bottom of the reactor, ΔP (kPa)
A	-0.06	-1.64	1.58
B	-0.05	-1.40	1.35
C	-0.07	-1.33	1.26

3.4. Conclusions

Gasification has an excellent potential for producing heat and power when operational parameters works perfectly. Temperature and pressure are two critical factors for gasification that have been investigated in this study. Temperature has a direct impact on the conversion efficiency in the gasifier and generation of tars. During the biomass gasification process, the highest temperature recorded was 838 °C reached in the combustion zone where the biomass feedstock is partially oxidized. During all three replications, pressure drops were observed in the lower reaction sensor when compared to the upper sensor. This change in pressure was determined to be due to the

feedstock bridging in the reactor which prevented flow of the feedstock inside the reactor. Bridging takes place above the combustion zone and inhibits descending flow of feedstock towards combustion and reduction zones. This bridging can cause operational problems that low quality of the syngas through the reduction of CO and H_2 concentration into the composition. Depending on the magnitude, bridging can influence the time of the gasification process and then finally can stop the process. Hence, the term of "degree of bridging" is defined by the author which is mainly dependent on the pressure drop factor. The operational parameters in a gasification process had slight differences between replications but the overall behaviour is always the same. The bulk density of material is also a crucial factor affecting the conversion operation in fixed bed gasifiers which is under investigation by the authors for further study possibilities.

Acknowledgements

This research is funded by BioFuelNet Canada, a network focusing on the development of advanced biofuels. BioFuelNet is a member of the Networks of Centres of Excellence of Canada program. The authors would also like to thank Valfei Product Inc. for supplying the wood pellet feedstocks.

Connecting Text

In Chapter 3, the first experimental study was carried out using pelletized woody biomass as a baseline test. The key operational factors (mainly temperature and pressure) were investigated across the down-draft reactor and the failure scenario of "bridging" was brought up. It was explained that depending on the magnitude, bridging could influence the time of the gasification process and then finally could stop the process. Hence, the term of "degree of bridging" was defined by the author which was mainly dependent on the pressure drop factor. The results of this chapter gave a good understanding of the technical parameters of the reactor using a pelletized biomass as the most common geometry available on the market.

In Chapter 4, a parametric study of the gasification of six biomass feedstocks (switchgrass, hardwood, softwood, fiber, cardboard and chicken manure), as representative of different types of biomass, was performed. In addition to what was discovered for woody biomass in Chapter 3, this chapter examines the quantity and quality of the syngas produced from the biomass feedstock and links them to the desired downstream application requirements.

Chapter 4 has been published for publication as:

Madadian E., Lefsrud M., & Orsat V. (2016). A comparative study of temperature impact on air gasification of various types of biomass in a research-scale down-draft reactor. *Energy & Fuels*, DOI: 10.1021/acs.energyfuels.6b03489.

CHAPTER 4

4. A COMPARATIVE STUDY OF TEMPERATURE IMPACT ON AIR GASIFICATION OF VARIOUS TYPES OF BIOMASS IN A RESEACH-SCALE DOWN-DRAFT REACTOR

Abstract

A parametric study of the gasification of six biomass feedstocks (switchgrass, hardwood, softwood, fiber, cardboard and chicken manure), as representative of different types of biomass, has been performed on an experimental, pilot-scale 10 kW down-draft gasification facility. A comparison was made of the performance of the gasifier as a function of feedstock, in terms of the syngas production and composition. The variation of syngas composition was analyzed in the range of 600^{o}C to 1000^{o}C. The results indicated that switchgrass, as a representative of energy crops, has greater potential to yield the main components of the syngas (i.e. hydrogen and carbon monoxide) in comparison with the other feedstocks. However, this did not guarantee the greatest suitability of the switchgrass for downstream applications due to low molar ratios of the ratio of hydrogen to carbon monoxide (H_2/CO) which was measured at 1.01. To enhance the utility efficiency of syngas, the downstream engines such as combustion engines require an adjusted ratio of H_2/CO to produce certain types of fuels which typically ranges from 1.5 to 3. By means of the catalytic water-gas shift reaction, an important portion of the CO content in the cracked gas can be used for additional hydrogen generation. The temperature variation of the down-draft reactor showed that the CO concentration increases with an increase in gasification temperature followed

by a drop of temperature dependent on the different biomass feedstocks. Conversely, CO_2 concentration follows an opposite trend that means an initial decreasing trend followed by an increase as the temperature increases. H_2 concentration follows a direct relationship with the gasifier temperature. The concentration of CH_4 varies very slightly with the increase in gasifier temperature. The results of this study showed that there were significant differences between the energy crops and chicken manure mixed with wood chip, in terms of composition. In general, the variations in syngas components were smaller at higher temperatures while H_2/CO showed greater variation between individual feedstocks.

Keyword(s): Biofuels, biomass feedstock, gasification, temperature variation, syngas composition

4.1. Introduction

The global demand for energy is rapidly increasing with increasing human population, urbanization and modernization. The growth in global energy demand is projected to rise sharply over the coming years (Asif and Muneer 2007). The worldwide fuel demand is recorded at 29.75 billion barrels of equivalent oil in 2011 and projected to be 34.90 billion barrels in 2030 (Zhao, Shen et al. 2014). Excessive consumption of fossil fuels, particularly in large urban areas, has resulted in generation of high levels of pollution during the last few decades. The level of greenhouse gases in the earth's atmosphere has drastically increased (Sarkar, Ghosh et al. 2012) which served as a stark reminder of the task facing politicians as the governments committed, in the Paris agreement on climate change 2015, to keep the increase in global average temperature to well below 2^{o}C above pre-industrial levels. In this context, the development of reliable, renewable energy systems is urgently required and is being encouraged by ambitious energy

policies such as the European Union's target to attain a 20% share of its energy consumption from renewable resources by 2020 (González-García, Iribarren et al. 2012).

Meeting current global demand for petroleum via current-generation of biofuels would require a doubling of the human share of net primary productivity, which would threaten species and habitats with extinction and sharply decrease global food security (Junginger, Faaij et al. 2006, Groom, Gray et al. 2008). High-efficiency extraction of hydrocarbons from lignocellulosic biomass is a necessary precondition for successful use of biofuels (e.g., EEA 2006). Biofuels made from lignocellulosic biomass comes from perennial species of wood, and crop residues and may prove to be more ecologically friendly than grain and grass feedstocks. Poplar and willow have been grown successfully with municipal-waste fertilizers and irrigated with municipal or industrial wastewater, thus decreasing waste streams while achieving inputs needed for high yields (Groom, Gray et al. 2008).

Biomass is available in many varieties, consisting of energy crops, forestry and agricultural residues, municipal solid waste (MSW), and animal wastes. Perennial energy crops such as switchgrass and miscanthus, and forest and agricultural residues are potential biomass feedstocks for bioenergy production (Djomo, Witters et al. 2015). Second generation biofuels derived from agricultural material, such as straw, have a high potential to contribute to covering the primary energy demand (Mikulandrić, Vermeulen et al. 2016). Forest residues like wood pellets are densified biomass fuel typically made from material rejected by wood-product manufacturers. By pelletizing residual forest waste, sawdust, planer shavings, and beetle-killed timber, millions of tons of waste can be put to work for the bioenergy economy while enhancing the environment by reducing greenhouse gas emissions (Madadian, Lefsrud et al. 2016). MSW generation keeps increasing because of the rapid economic development, continuous urbanization, and

improvements in the living standards (Madadian, Amiri et al. 2013, Zhao, Shen et al. 2014). The green energy derived from animal waste is considered to be carbon-neutral because animal feed is sourced from plants (Chang 2004). Theoretical calculations indicate that thermochemical processes (e.g., gasification) are inherently more productive in energy conversion than anaerobic digestion because most of the carbon can be utilized (Huang, Dong et al. 2011).

The conversion of biomass can be achieved through one of two major routes: biochemical conversion (fermentation, an/aerobic digestion) and thermochemical conversion (pyrolysis, gasification and liquefaction) (Basu 2013). Biochemical conversion may be conducted on two broad pathways: chemical decomposition and biological digestion. Biological processes are essentially microbial digestion and fermentation. A biochemical process converts biomass to ethanol and methane (Balat 2006). The thermo-chemical conversion processes have two basic approaches. The first is the gasification of biomass and its conversion to hydrocarbons. The second approach is to liquefy biomass directly by high-temperature pyrolysis, high-pressure liquefaction, ultra-pyrolysis, or supercritical extraction. These processes convert the waste biomass into energy rich products (Goyal, Seal et al. 2008).

Gasification is the most effective process for the production of hydrogen from biomass (Ahmad, Zawawi et al. 2016). Gasification utilizes various types of carbon-based feedstocks, such as natural gas, coal, petroleum, petcoke, biomass, and industrial waste (Ahmad, Zawawi et al. 2016). The gasification process consists of the thermochemical conversion of carbonaceous material into fuel gas rich in CO and H_2, called syngas. The composition of syngas is affected by gasification conditions, such as temperature, equivalent ratio, and pressure (El-Emam, Dincer et al. 2012, Pereira, da Silva et al. 2012).

The performance of gasification and quality of syngas depends upon numerous factors such as gasifying medium (air, steam or oxygen), heating rate, temperature, and equivalence ratio. In addition, the characteristics of the feedstock, i.e., the elemental composition, heating value, fixed carbon, volatile matters, moisture content and ash content would determine the performance of gasification (Skoulou, Zabaniotou et al. 2008, Inayat, Sulaiman et al. 2015). Recent studies showed that biomass gasification is impacted by different operation parameters such as composition and moisture contents of feedstocks, type of gasifier, residence time, reactor pressure, gasifying agent, and most importantly, temperature (Mohammed, Salmiaton et al. 2011, Ahmed, Ahmad et al. 2012, Madadian, Lefsrud et al. 2016). High oxygen and moisture content results in a lower heating value for the product syngas, typically less than 2.5 $MJ.m^{-3}$. This syngas poses problems for downstream combustors that are typically designed for a consistent medium-to-high heating value fuel (Madadian, Lefsrud et al. 2014). Out of different gasifier design, downdraft gasifier produces a relatively low content of tars in the gas (Reed and Markson 1983). As a consequence, it may be a preferable choice for small scale decentralized power generation systems via internal combustion engines (Sharma 2011)

Typically, gasification of biomass is performed at moderately high temperatures (700-900 °C), which results in the formation of carbon monoxide, hydrogen, water, carbon dioxide, methane and other light hydrocarbons (HCs), tar and char as shown in Reaction 1 (Carpenter, Bain et al. 2010).

$$Biomass + Air \rightarrow CO + H_2 + H_2O + CO_2 + CH_4 + HCs + tar + char \quad (1)$$

A high gasification temperature favors an increase in gas yield due to a high decomposition of cellulose and hemicellulose. Steam reforming and water-gas reaction favor higher H_2 concentration and lower CH_4 concentration in the syngas for gasification temperatures between

750 °C and 800 °C. At a higher temperature between 850 °C and 900 °C, the Boudouard reaction (Reaction 2) (Higman and Van der Burgt 2011, Basu 2013) favors higher CO concentration in the syngas (Kumar, Jones et al. 2009, Inayat, Sulaiman et al. 2015). Gas composition is dependent on feedstock composition, type of gasification reactor, gasification agents and operating condition (Madadian, Lefsrud et al. 2014).

$$C + CO_2 \rightarrow 2CO + 172\ kJ/mol \quad (2)$$

In this study, a systematic comparison has been made of the yields of gases and char from the gasification of switchgrass, hardwood, softwood, fiber, cardboard, and chicken manure.

4.2. Methodology

4.2.1. Characterization of biomass feedstock

Five types of feedstock were selected as representative of different categories of biomass. Gasification experiments were conducted using switchgrass, hardwood, softwood, fiber, cardboard and chicken manure. The biomass materials, according to the American Society of Testing Materials (ASTM), were proximately analyzed for moisture content (ASTM 2013), ash content (ASTM 2013), fixed carbon (ASTM 2013), and volatile matter in the wood pellet (ASTM 2013). An ultimate analysis was performed to measure the composition of the biomass in mass percentage of carbon, hydrogen, and oxygen (as the major components) (ASTM 2014) as well as nitrogen (ASTM 2014) and sulfur (ASTM 2002) (Table 4.1).

- ***Wood pellet (hardwood and softwood)***

Pelletized woody biomass from Valfei Products (hardwood and softwood, Shawinigan, Quebec, Canada) were used as representative of forest residues. The wood pellet production consists of using recycled hardwood remnants and were cylindrical in shape, averaging 8mm in diameter and 30mm in length.

- ***Fibrous pellet***

The fibrous feedstock was sampled from pulp and paper waste stream which consists of cellulose fibers that are present in hardwood and softwood trees. The biomass feedstock was pelletized with 5 mm in diameter and length varying from 25 mm to 40 mm using a pellet mill machine. The feedstock was supplied from a company in Stanstead, Quebec, Canada.

- ***Cardboard briquette***

Food grade waxed cardboard and gable top cartons from municipal solid waste stream were collected, shredded and pressed using briquetting machine in the average dimension of 50 mm in diameter and 40 mm in length. The material was received from a company in Quebec City, Canada.

- ***Chicken manure***

Chicken manure, as representative of animal waste, was collected from a chicken barn in Quebec City, Canada. The moisture content of feedstock was measured at 48% and was dried to 26% using sun drying and then mixed with wood chip for a ratio of 50/50.

- ***Switchgrass***

Switchgrass (*Panicum virgatum*) is a perennial warm-season bunchgrass native to most of North America east of the Rocky Mountains and extends north to 55° N latitude in northeastern Canada (Mitchell, Vogel et al. 2012, Masnadi, Grace et al. 2015). The switchgrass bale was supplied from a farm in Ottawa, Canada. The switchgrass was pelletized, by the supplier and used a pellet mill machine, with 6 mm in diameter and average length of 30 mm.

Table 4.1. Proximate and ultimate analysis of different types of biomass feedstock

	Feedstock	Wood pellet (hardwood)	Wood pellet (softwood)	Fiber pellet (pulp and paper waste stream)	Switchgrass pellet	Chicken manure (unpelletised)	Cardboard briquette
Proximate Analysis (dry)	Moisture content (mass%)	3.2 ± 0.41	6.5 ± 0.32	4.2 ± 0.57	3.4 ± 0.51	26.1 ± 0.83	6.8 ± 0.33
	Volatile matter (mass%)	77.9 ± 5.74	76.1 ± 6.33	85.7 ± 6.72	80.9 ± 8.44	31.2 ± 4.12	81.2 ± 5.47
	Fixed carbon (mass%)	16.5 ± 0.74	17.5 ± 0.63	3.5 ± 0.34	11.9 ± 0.52	6.4 ± 0.37	8.3 ± 0.40
	Ash content (mass%)	1.4 ± 0.24	1.1 ± 0.27	4.2 ± 0.18	3.8 ± 0.27	14.4 ± 0.61	2.4 ± 0.23
Ultimate Analysis (As received)	Carbon (%)	43.52	46.54	44.94	48.21	41.19	44.29
	Hydrogen (%)	7.0	6.8	5.9	5.8	8.5	6.8
	Nitrogen (%)	0.23	0.12	0.18	0.32	24.83	0.52
	Sulfur (%)	0.08	0.05	0.19	0.05	10.29	0.44
	Oxygen (%)	43.53	40.29	38.46	38.45	24.17	37.63
	HHV (MJ/kg)	18.31	17.52	17.09	20.34	12.85	17.73
	LHV (MJ/kg)	13.74	12.27	12.22	14.82	9.03	12.35

4.2.2. Experimental set-up

The gasification process was carried out using a down-draft gasifier where the feedstock and the syngas flow is concurrent. The unit is a Gasifier's Experimenter's Kit (GEK) Level 4, Model V3.1.0 purchased from All Power Labs (Berkeley, California). The nominal thermal output of the unit is 10 kW. The main reactor is a cylinder-shaped vessel (height of 0.4 m and diameter of 0.35 m) equipped with air nozzle supports to provide the reactant and gas pipes to transport the produced gas into the filtering system (Figure 4.1).

Briefly, biomass was fed into the down-draft reactor in batch mode. The feeding rate varied depending on the flowability properties of the feedstock. The process started with ignition of bed charcoal impregnated with 60 ml of gasoline through an ignition port. This external heat initiated the combustion process around the air nozzle. The hot gas moved upward to reach the raw material and dry the feedstock. The dried material moved down through the reactor and pyrolysis occurred above 600 °C. The pyrolysis products (i.e. charcoal, tar and pyrolysis gas) moved downward to crack in the higher temperature combustion zone where CO_2 and H_2O are produced. The combustion gaseous product lost a molecule of oxygen, in the reduction zone, to produce CO and H_2 as the main components of the syngas. The air, as the gasifying agent, was introduced to the reactor through an air inlet in the middle of the chamber, in the combustion zone. The air entered in the reactor with an Equivalent Ratio that varied from 0.1 to 0.5. The generated ash was discharged at the end of each single run to avoid ash agglomeration.

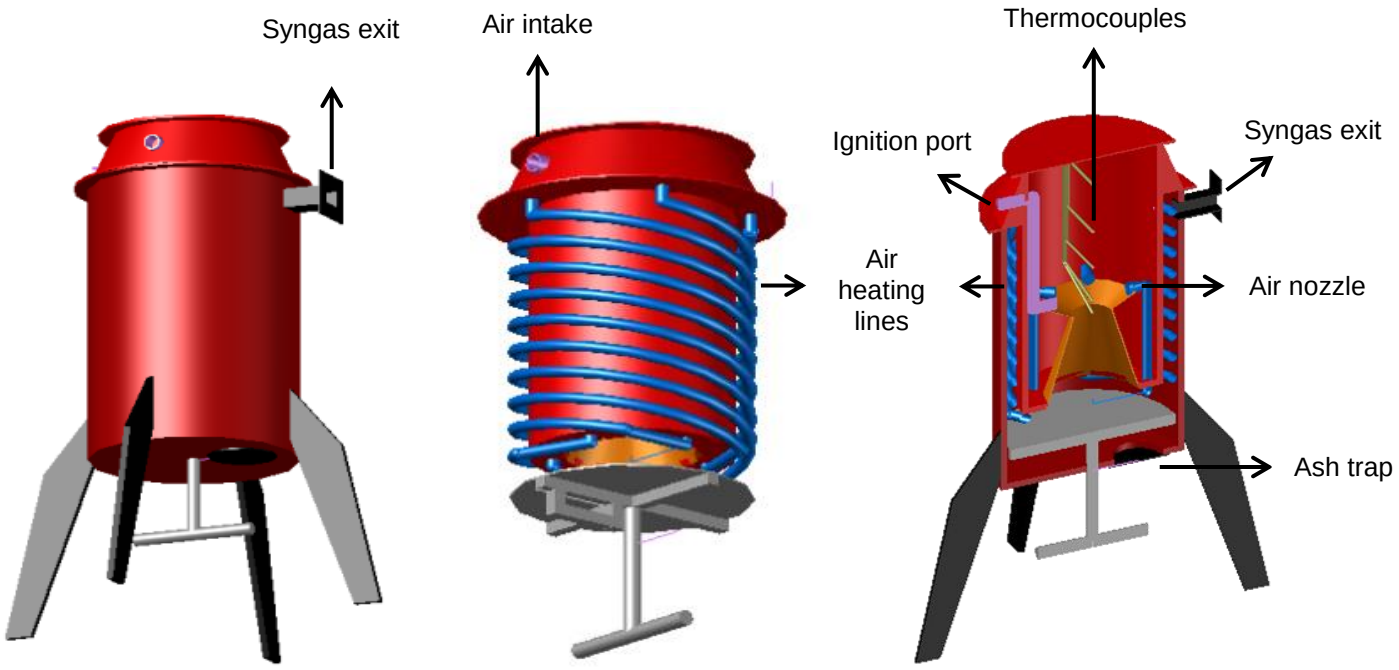

Figure 4.1. Schematic view of the GEK double layer down-draft gasifier. GEK compartments (a) external vessel of the reactor that minimizes heat loss during the gasification process, (b) internal vessel with air heating lines attached to preheat air before directing it to the reactor, and (c) cross-section of internal vessel where the fuel and gasifying agent (i.e. air) react and produce synthesis gas. The initial ignition is made through ignition port and then mixes with the air from coming out of the air nozzles. The thermocouples record the temperature across the reactor, and the ash generated is removed through the ash trap at the bottom.

The effluent of the reactor was sampled three times after each replication and analyzed with a gas chromatograph equipped with a Thermal Conductivity Detector (TCD) for quantification of H_2, CO, CO_2 and H_2O in the range of concentrations of interest. The experimental procedure involved

collection and recording of temperature readings along the gasifier bed using five Type-K thermocouples. The thermocouples were mounted in the middle section at five different locations along the length of the gasifier where drying (T_1), pyrolysis (T_2), combustion (T_3) and reduction (T_4) processes took place. The height of these locations from the lid of the reactor are 15 cm, 25 cm, 40 cm and 50 cm, respectively. Temperature readings were collected using USB based gasifier control unit (GCU) (Model v3.02, All Power Labs, Berkeley, California) every two seconds and the readings were automatically stored in a computer. These results were obtained at an air to biomass ratio of 0.3 (i.e. the optimum air-fuel ratio) and different reactor bed temperatures.

4.3. Results and Discussion

4.3.1. Effect of temperature on syngas composition

The gasification temperature controls the equilibrium of the chemical reactions (Cimini, Prisciandaro et al. 2005, Begum, Rasul et al. 2013). The gas compositions were recorded at five different instant temperatures of 600 °C, 700 °C, 800 °C, 900 °C and 1000 °C during the operation and at an air-biomass ratio of 0.3. All the feedstock reached temperatures over 1000^{o}C while the average bed temperature measured was different for each feedstock.

As shown in Figure 4.2, switchgrass showed great potential in producing CO and H_2. Concentration of CO increased (37% to 41%) with increasing gasifier temperature to almost 700 ^{o}C and then decreased to 35% until 900 ^{o}C where it increased again. Similarly, CH_4 increased to 13% up to 800 ^{o}C and then decreased to 7% and continued at this level without any change. CO_2 showed a decreasing trend; conversely, H_2 increasingly reached a maximum of 30% and then continued with a slight positive slope. According to Le Chatelier's principle and dynamic equilibrium, an increase in temperature is compatible with endothermic methane reforming reaction products, which means higher char conversion and more H_2 production (Beheshti,

Ghassemi et al. 2015). The other impurities such as nitrogen oxide (NO_x) or ethylene (C_2H_2) drastically dropped from 27% to 10% and then started increasing at 800 ^oC to 19%. The presence of noxious gases is because of using air as gasifying agent.

In the case of chicken manure, H_2 showed an increasing trend at a much lower concentration up to 14% at 1000 ^oC. CO concentration peaked slightly to 20% at 800 ^oC and then decreased with the same slight slope; on the contrary, CO_2 decreased to almost 12% at 700 ^oC and increased to 18% at higher temperatures. The concentration of CH_4 did not change significantly and ranged 16% to 18%. The other gas components, however, formed a major part of the syngas in the range from 38% to 45%.

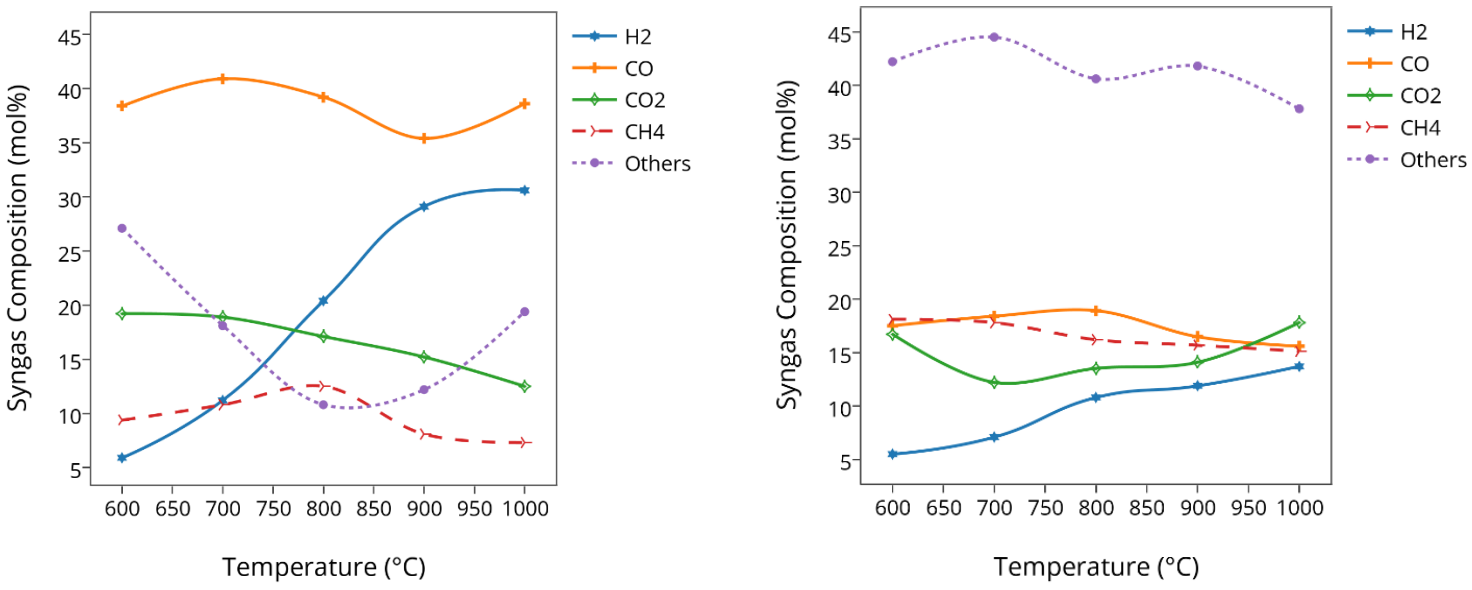

(a) (b)

Figure 4.2. The average change in syngas composition with respect to temperature profile during gasification of a) switchgrass, and b) chicken manure

Hardwood and softwood pellets showed almost identical trends in changing the composition of the syngas with respect to the temperature profile. As can be seen in Figure 4.3, CO concentration in hardwood increased from 22%, peaked to 29% at 800 ^{o}C, and then dropped to 17% at 1000 ^{o}C. CO_2 decreased from 14% to 11% at 700 ^{o}C and increased to 23% at 1000 ^{o}C. The hydrogen content of syngas increased from 7% to 26%. Likewise, the CH_4 decreased at 700 ^{o}C from 17% to 9%. The other components of the syngas drastically decreased to 24% by increasing H_2 and CO_2 at higher temperatures. The softwood trends were the same as the hardwood except CO which had fluctuations from 25% to 20%.

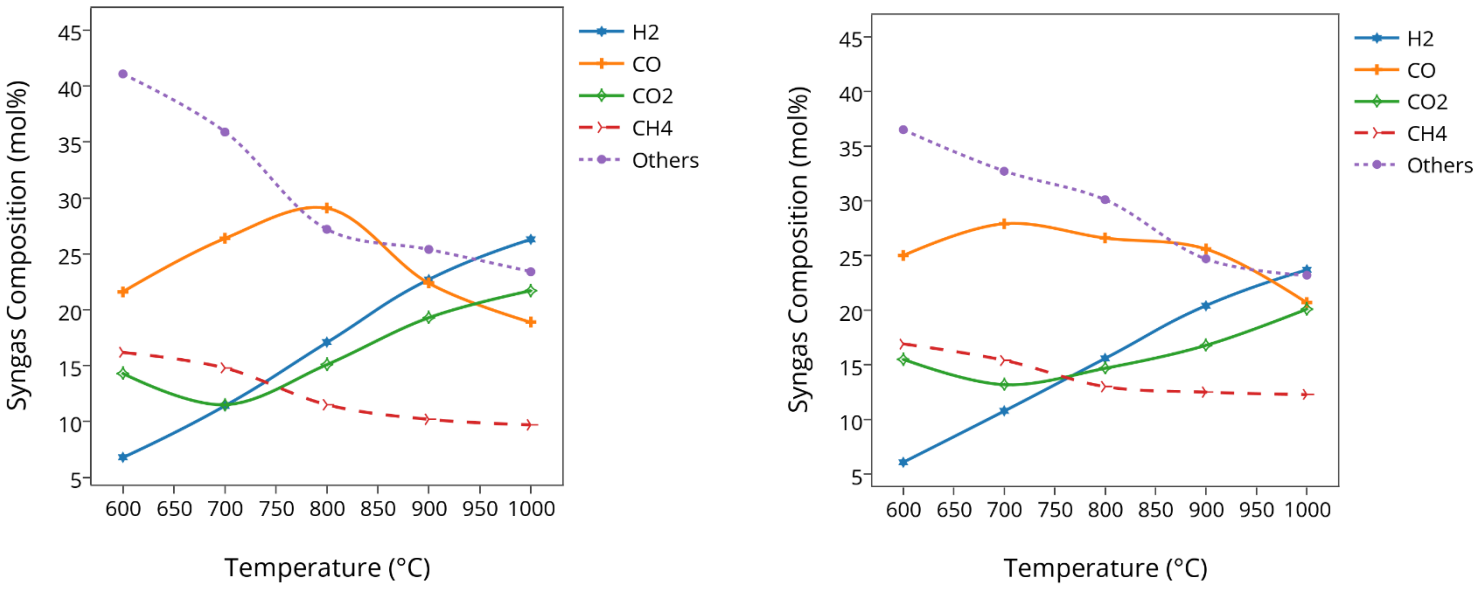

(a) (b)

Figure 4.3. The average change in syngas composition with respect to temperature profile during gasification of a) hardwood, and b) softwood

Fiber H_2 increased from 5.1% to 23%. The concentration of CO decreased from almost 25% to 23% from 600 ^oC to 1000 ^oC, with a slight increase at 700 ^oC where it reached 26%. Conversely, CO_2 decreased to almost 13% at 700 ^oC and then increased to 19% at 1000 ^oC. The methane content of the syngas decreased slightly from 16% to 14%. The other components dropped from 36% to 25% from 600 ^oC to 1000 ^oC.

Cardboard H_2 concentration of syngas increased from 5.2% to 25% while CO dropped to 16% after peaked to 22% at 700 ^oC. With the same trend, CO and CH_4 dropped from 18.6% to 13%. CO_2 decreased to 20% and then increased to 29% at the higher temperature of 1000^oC. The other components also decreased continuously to finally reach the same concentration as CO at 16% (Figure 4.4).

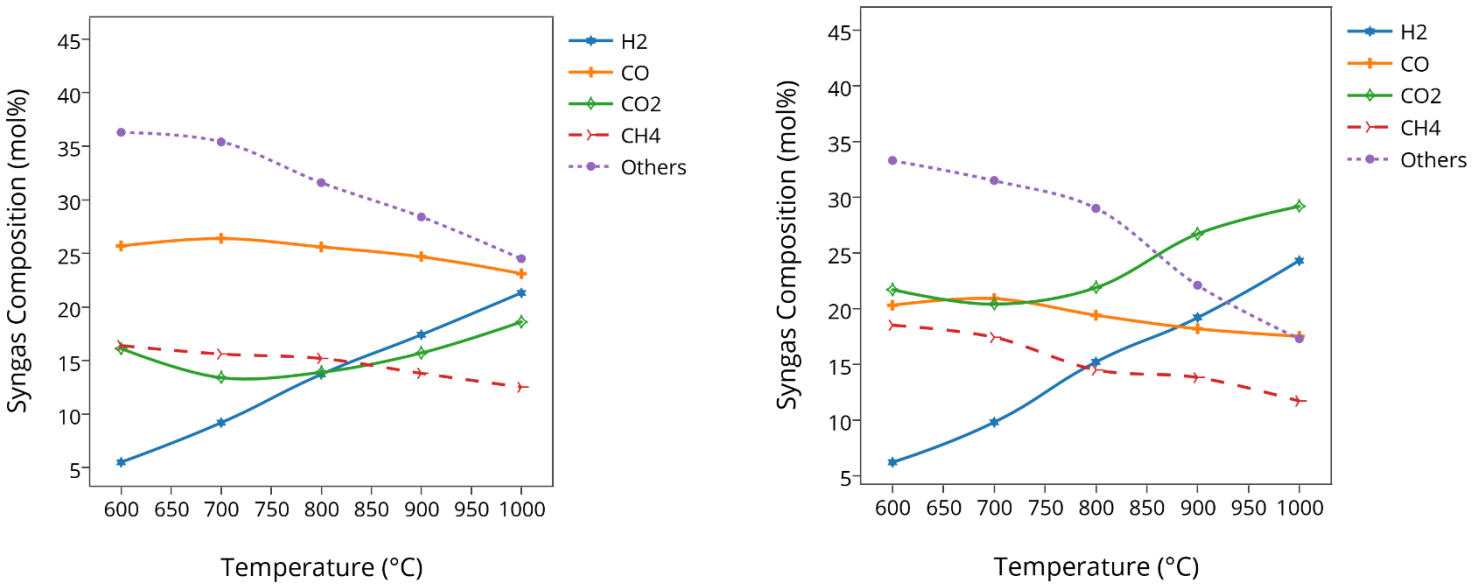

(a) (b)

Figure 4.4. The average change in syngas composition with respect to temperature profile during gasification of a) fiber, and b) cardboard

Perhaps most importantly, gasification of biomass leads to the formation of tars. These materials are condensable organic compounds, and as such, they can foul catalysts, plug lines, and damage compressors. Although we did not measure the tar content, the higher moisture content in some feedstock such as chicken manure could intensify the amount of tar generated after each run and increased the chance of clogging the pipes and junctions. The moisture in the structure of the fuel has undesirable effect on the gasification process. Since the high amount of moisture in fuel uses the energy and results in decreasing the temperature of gasification, which results in a less efficient process. In terms of energy efficiency, it obviates the need (capital, energy and time) for feedstock dewatering and drying as needed for other conversion technologies such as direct combustion and pyrolysis (Duan and Savage 2010, Zhao, Shen et al. 2014).

Furthermore, the content of H_2 exhibits an increasing trend with temperature. This is an expected result because most H_2 production reactions are endothermic. The content of CH_4 decreases with temperature because higher temperatures increase the steam reforming reaction of CH_4. The content of CO first increased and then decreased with temperature in most cases.

4.3.2. Temperature profile of different biomass feedstock

The average temperature profile of each biomass feedstock was recorded during steady state conditions during the gasification process. Due to different operational duration for each feedstock, the temperature was recorded in four identical time frames. This makes the temperature independent on the time in the graphs. The graphs are depicted based on the global steady-state condition of the system after starting the operation. These profiles are provided under the designated conditions including the pre-treatment of feedstock (moisture percentage, particle size and component of feedstock), and operating conditions (pressure and equivalence ratio).

As shown in Figure 4.5, the temperature profiles have a ballistic behavior within the reactor. The average temperature in every zone is recorded. The initial location was called as T_0 and is always set at the ambient temperature of 25 ^oC since the feedstock just enter into the reactor and there is no exposure to an external source of heat. By starting the ignition, the temperature increases in the combustion zone and quickly influenced the upper zones of drying (T_1) and pyrolysis (T_2). The average temperature in the drying zone was recorded below 100 ^oC for all feedstocks. However, the pyrolysis zones ranged between 300 ^oC to 500 ^oC. The temperature of all feedstocks peaked in the combustion zone (T_3) where the main exothermic reactions take place followed by a slight drop in the reduction zone (T_4) where the reducing environment led to a decreased amount of oxygen.

Amongst feedstocks, the highest temperature profile belonged to switchgrass at 502 ^{o}C, 915 ^{o}C and 851 ^{o}C at pyrolysis, combustion and the reduction zones, respectively. The chicken manure demonstrated the lowest temperatures of 364 ^{o}C, 783 ^{o}C and 685 ^{o}C, at the mentioned zones, respectively. The reason for this difference can be due to the high moisture content of the manure even after drying and mixing with wood chips (50/50). Comparing softwood to hardwood, hardwood has a slightly higher temperature within the reactor that can be attributed to the lower moisture content. Furthermore, the cardboard showed a very close temperature profile to paper fiber while having a higher moisture content. In spite of the higher moisture content of cardboard, the similarity between the temperature profiles of cardboard and paper fiber could be due to the better flow of cardboard briquette than fiber pellet within the reactor. The amount of energy input needed to dewatering the biomass increases with the moisture content (Sokhansanj and Webb 2016) and result is lowering the temperature. (Madadian, Lefsrud et al. 2016) reported on the bridging problem due to pelletized geometry of woody biomass in the down-draft reactor. They concluded that less bulky material increased the chance of material bridging near the throat of the reactor and stopped the downward flow of feedstock.

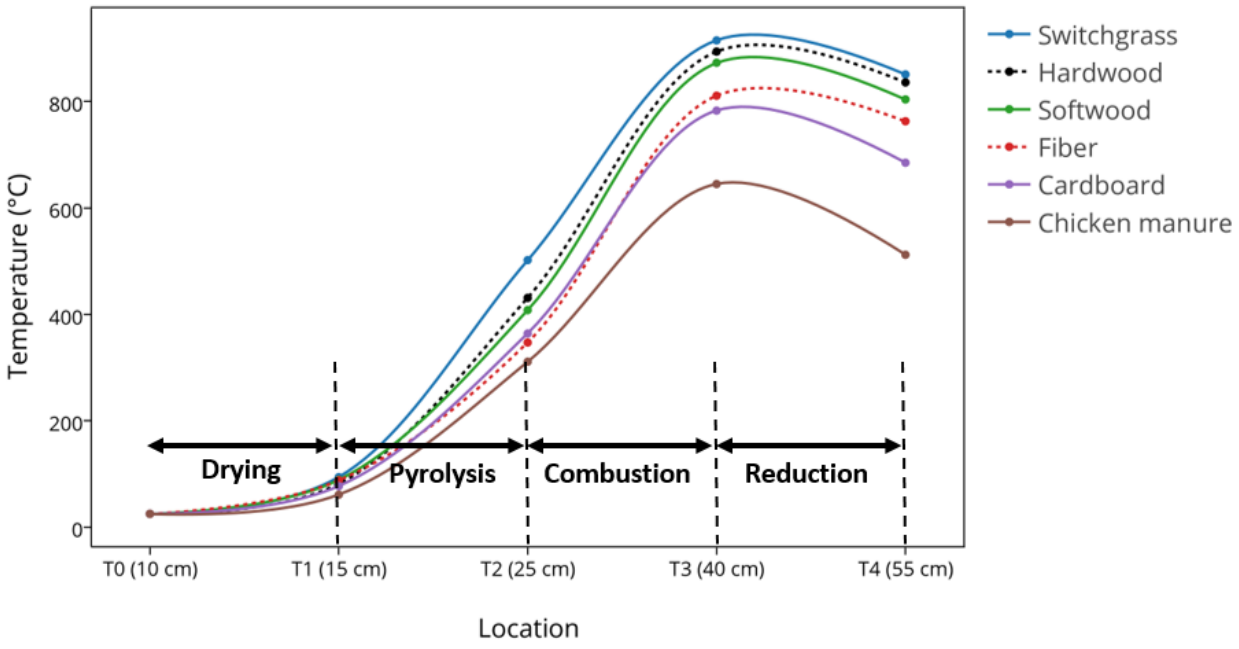

Figure 4.5. Temperature profile of different types of biomass feedstock within down-draft gasifier. There was higher temperature dispersion observed in combustion and reduction zones, where the temperature peaked, than those in drying and pyrolysis zones

4.3.3. Effect of temperature on syngas production

The influence of reactor temperature was studied by recording composition of produced syngas corresponding to values of the oxidation zone temperature for each biomass feedstock. The average of these gas composition values recorded over the steady operation period was used to calculate the calorific value of syngas. Operation of the pilot facility required long run times in order to obtain the steady-state results that are relevant for continuous operation. More than an hour was required for the temperatures and product concentrations to come to steady state after the conditions were set. Once the process was deemed to be at steady state, data were typically collected at that condition.

As shown in Figure 4.6, the highest bed temperature was 915 ^{o}C from switchgrass where the highest amount of hydrogen and CO was produced (29.6 and 37.2%). Both types of wood (hard and soft) produced similar amounts of syngas components except H_2 where it was 3% higher in hardwood. This similarity can be mainly due to comparable bed temperatures 894 ^{o}C and 873 ^{o}C for hardwood and softwood, respectively. As for fiber and cardboard, the amounts of H_2 and CO generated in cardboard were slightly more (5.3% and 2.1%) than the ones in cardboard. This result was expected since both feedstock originated from the pulp and paper stream. However, the greater flowability of cardboard briquette than fiber pellet due to higher bulk density (Madadian, Lefsrud et al. 2016) can be the reason for greater char conversion and producing more hydrogen and carbon monoxide. In addition, the lower moisture content and higher lignin content of the fiber pellet might be the reason for generating the higher temperature from the fibrous feedstock.

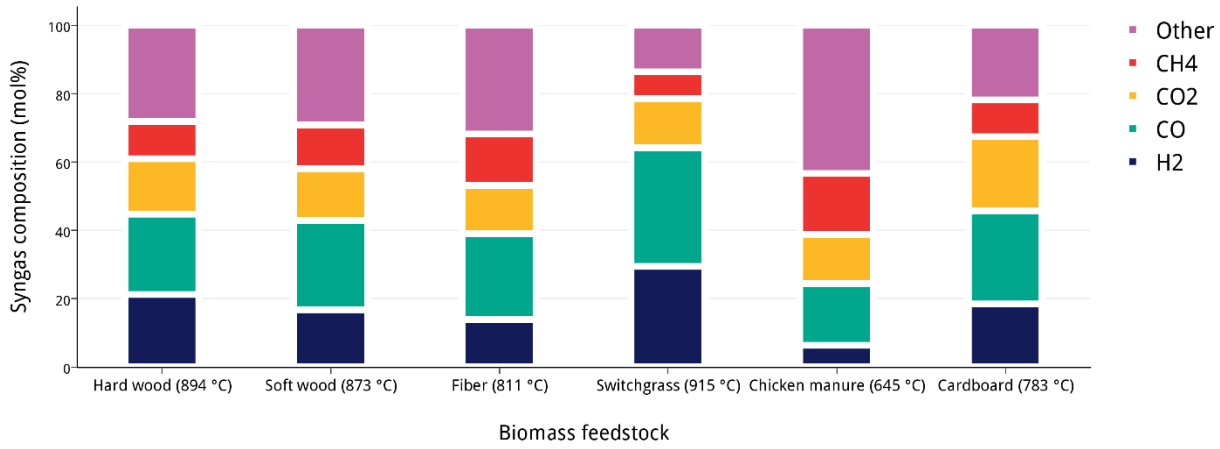

Figure 4.6. The syngas composition of different types of biomass feedstock at different bed temperatures. Switchgrass as representative of energy crops showed higher hydrogen and carbon monoxide than other feedstocks.

In the case of chicken manure, the high moisture content of feedstock did not allow the entire thermal energy spent to decompose the biomass. Therefore, a part of the energy was used to remove the water content from the manure. The temperature of the manure reactor only rose to 645 ^{o}C which is normally considered as a low-temperature gasification process. As a result, the heat required to move forward gasification endothermic reaction was not adequate. Lack of required heat to move the water-gas (Reaction 3) (Klass 1998, Basu 2013) and steam reforming (Reactions 4 and 5) (Higman and Van der Burgt 2011, Basu 2013) reactions forward led to lower production of hydrogen.

$$C + H_2O \leftrightarrow CO + H_2 + 131\ kJ/mol \quad (3)$$

$$CH_4 + H_2O \leftrightarrow CO + 3H_2 + 206\ kJ/mol \quad (4)$$

$$CH_4 + 0.5\ H_2O \rightarrow CO + 2H_2 - 36\ kJ/mol \quad (5)$$

4.3.4. Effect of temperature on H_2/CO molar ratio

The ratio of hydrogen to carbon monoxide was calculated in the range 0.15 to 1.39 for all cases under different temperatures. The amounts of H_2 and CO were recorded through syngas composition analysis explained in the methodology section. As shown in Figure 4.7, there is an increase in the H_2/CO ratio with an increase in the temperature profile within the reactor. The standard deviation between H_2/CO ratios from 600 ^{o}C to 1000 ^{o}C calculated at 0.067, 0.069, 0.093, 0.147, and 0.252 which shows greater difference between the ratios increased for different among the feedstocks at higher temperatures. The difference can relate to the effect of the higher temperatures that favors higher production of hydrogen. It is after 800 ^{o}C that the CO production

dropped as indicated in Section 4.3.1. Cardboard, hardwood, softwood, switchgrass, fiber and chicken manure produced the greatest to smallest H_2/CO ratio in this order.

Cardboard briquette showed a great potential to produce higher H_2/CO especially at higher temperatures. This can relate to the shape of the feedstock which has a smoother flow in the reactor. Based on Fourier's law, the greater area increases the conductive heat transfer. Hence, we hypothesized that the larger surface area of the cardboard briquette could result in higher conductivity which increases the carbon conversion rate.

As for switchgrass, the H_2/CO ratio is the lowest before 800 ^oC and it increased to the values of 0.82 and 1.01 by reaching the higher temperatures of 915 ^oC (average bed temperature) and 1000 ^oC (instantly). This relatively low ratio is due to the incomplete water-gas shift reaction (Reaction 2) and excess of CO which did not converted to H_2 and CO_2. Therefore, the catalytic reactions are required to enhance the hydrogen content of the syngas to adjust the H_2/CO ratio for appropriate downstream applications.

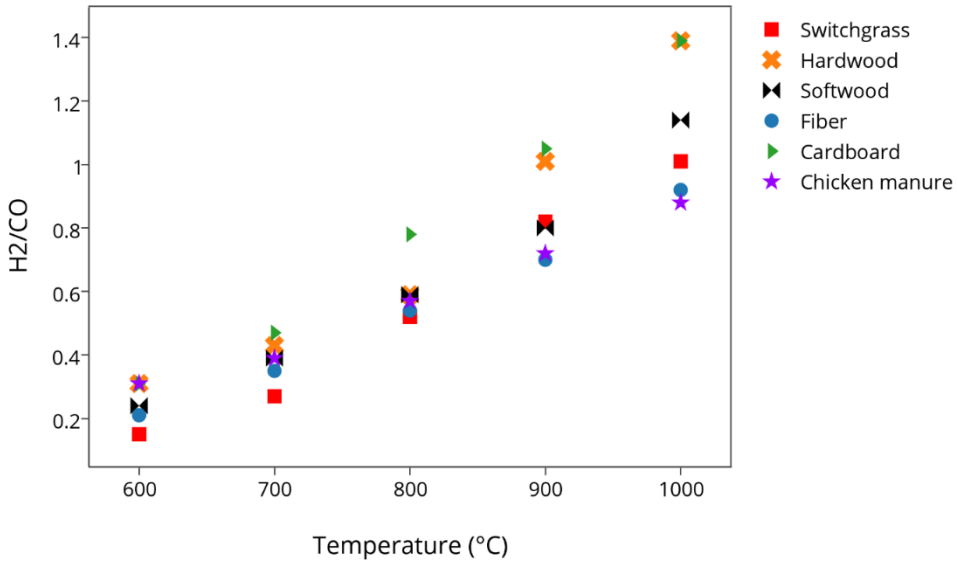

Figure 4.7. The hydrogen to carbon monoxide ratio of different biomass feedstock at different bed temperatures. H_2 and CO were individually measured through syngas composition analysis.

4.4. Conclusion

As a basis for investigating biomass gasification and to demonstrate the key characteristics of biomass thermochemical conversion, different types of feedstocks (switchgrass, wood, paper fiber, cardboard and chicken manure) were gasified in a pilot scale fixed bed reactor. The results showed that switchgrass as a representative of energy crops to have great potential in syngas yield, however, the H_2/CO might not necessarily suit for downstream applications. The reason can be due to incomplete vital reactions such as water-gas shift reactions which results in the generation of CO_2 and H_2 from carbon monoxide and water vapor. Although it is important how much H_2 and CO is generated, their ratio is much more important which can be adjusted using catalytic reactions downstream from the gasification main process. Feeding the syngas into the catalytic water-gas

shift reaction can be a solution to enhance the H_2/CO ratio. Additionally, CO concentration increases with an increase in gasification temperature followed by a slight drop. However, CO_2 concentration follows an opposite trend. H_2 concentration increases with the increase in gasifier temperature. The concentration of CH_4 varies slightly with the increase in gasifier temperature. Gasification does not individually guarantee the sustainability of purpose grown feedstocks and it requires an integrated approach towards post-gasification to valorize the produced syngas and promote greater use of the biomass feedstock.

Acknowledgments

This research is funded by BioFuelNet Canada, a network focusing on the development of advanced biofuels. BioFuelNet is a member of the Networks of Centres of Excellence of Canada program. The authors would like to thank Valfei Products for supplying the wood pellets, and EMISPEC Co. in Quebec City for supplying the cardboard briquettes. We would also like to show our gratitude to Mr. Yvan Gariepy, Mr. Yves Roy and Mr. Camilo Perez Lee for their pearls of wisdom with us during the course of this research.

Connecting Text

In Chapter 4, a parametric study of different classes of biomass feedstocks was conducted and the results showed how different types of biomass differ to produce a high-quality syngas. The size and physical shape of the feedstock differed and it impacted the results as indicated in Chapter 3. By prioritizing the existing biomass when converted to bioenergy using gasification technology, the baseline tests for individual feedstock were accomplished.

In Chapter 5, a composite biomass composed of paper fiber and plastic waste originating from a municipal waste stream is tested to investigate the role of adding dissimilar agents on the productivity of the gasification technology. The study also elaborates the failure scenario of "Clinkering" and investigates the thermo-chemical properties of the generated by-products through gasification of composite fiber and plastic.

Chapter 5 has been submitted for publication as:

Madadian E., Crowe C., & Lefsrud M. (2016). Evaluation of Composite Fiber-Plastics Biomass Clinkering Under Gasification Conditions. *The Journal of Cleaner Production* (Under revision).

CHAPTER 5

5. EVALUATION OF COMPOSITE FIBER-PLASTICS BIOMASS CLINKERING UNDER GASIFICATION CONDITIONS

Abstract

Cross contamination and non-recyclables remain after the separation of valuables in the recycling process, especially with commingled or single stream recycling systems. Therefore, some carbonaceous fractions of recyclables, such as plastics and fibers, are left as a potential biomass feedstock for thermochemical or thermal conversion processes. However, this fraction of waste is more likely to be highly contaminated and challenging, or may become unpredictable during its reuse in the thermal conversion process for heat and power applications. The current study aims to find how the increase in plastic specifically in the recycled fiber stream may affect the performance of a downdraft gasifier. Therefore, the effect of plastic combined with fiber feedstock during gasification has been investigated. For this purpose, three different plastic percentages of 2%, 5%, and 10% mixed with fiber were studied. The results showed that higher plastic-containing feedstock has higher energy content; however, the higher plastic content causes mechanical performance issues inside the reactor and does not necessarily guarantee greater calorific value syngas. Furthermore, gasifying the higher plastic percentage results in a temperature drop and an increase in the pressure difference across the reactor. This change in temperature and pressure is the result of thermal reactions of fiber material mixed with plastic that generates firm clinkers and interrupts the normal conditions in the reactor. The clinker predominantly contains aluminum,

silicon, calcium and sodium that originate from the source of fiber and plastic. This research has shown that a mixture of silicon with aluminum, calcium and sodium under high temperatures result in the generation of a solid clinker that ultimately moves through the reactor and deposits at the bottom of the reactor.

Keywords. Gasification, Fiber, Plastic, Clinker, Slag, Aluminum, Calcium, Silicon

5.1. Introduction

Biomass has great potential to supply part of the future energy demand of the world. The wastes from pulp and paper processing are one possible source of biomass and a promising source of energy. Waste paper itself can have a calorific value of 17 MJ/kg as reported in the current study, and consists of almost 1/3 of total waste generated in the US, where 50% of this postconsumer paper waste is actually recovered (USEPA 2015). Paper is often externally sized with various materials to increase their strength, resistance to picking, scuffing, resistance to penetration of water, organic solvents, oils, inks and various types of aqueous solutions as well as for improving their smoothness and optical characteristics (Gupta 2007).

There are inorganic compounds present in the woody biomass, and remain in waste paper. There are over 70 metal and earth elements found in woody biomass, with potassium and calcium being the major metals in woody biomass, followed by magnesium and phosphorus (Alén 2000). In hardwoods, for example, calcium contributes 0.08–0.2% of dry stemwood mass and 0.85–3.05% stem bark mass. Magnesium contributes 0.02–0.04% of dry hard wood stem mass and 0.07–0.11% dry hardwood stem bark mass (Liu 2015). The heterogeneity of woody biomass in composition presents both an opportunity of valued products and difficulty or complexity in the convertibility.

Utilization or conversion of all the components is the key to a sustainable economy or for the future supply of energy, chemicals and materials (Liu 2015). Woody biomass is composed of four components: extractive, hemicellulose, lignin and cellulose. Each component has a different degree of degradability by chemical, thermal or biological means, with hemicelluloses being the easiest one to degrade while cellulose being the most difficult to degrade (Liu 2015).

As for plastics in post-consumer biomass waste, the United Nations Environmental Program states that between 22 percent and 43 percent of the plastic used worldwide is disposed of in landfills, which can be a threat to underground resources. Plastic recovery from the waste stream and converting them to chemicals and fuels can minimize the environmental threats.

Many methods for the utilization of waste plastics have been developed (Delattre, Forissier et al. 2001, Okuwaki 2004). Due to heterogeneity of post-consumer plastic waste, specifically referring to varying size fractions, cross contaminates (e.g., metal and fiber), and fillers used in plastic are unsuitable for reclamation. In this case thermal cracking into hydrocarbons may provide a suitable means of recycling (Buekens and Huang 1998). The suitable treatment of non-recyclable plastic waste is one of the key questions of waste management facilities and is important from energetic, environmental, economical and political aspects (Miskolczi, Bartha et al. 2006). One of the more promising of these methods is the use of gasification of plastics for power generation and bulk chemical production (Namioka, Saito et al. 2011). In spite of high calorific value of polymer waste during direct combustion, the environmental threats due to noxious gaseous emissions, such as dioxins and furans, are detrimental. However, gasification could generate a mixture of hydrocarbons and synthesis gas which has broad range of applications (i.e. H_2 and CO) (Panda, Singh et al. 2010, Madadian, Lefsrud et al. 2014). Besides the various applications available, the gasification process emits fewer emissions such as dioxins and furans, HCl in addition to the option

of syngas cleaning prior to the combustion of the syngas, could help to reduce high temperature corrosion common in direct combustion of waste, resulting in and improved efficiency. Thermal pyrolysis of polyolefin, as a representative of polymer, is a high energy, endothermic process requiring temperature of at least 350 ^{o}C and up to 500^{o}C. There are some other studies applying higher temperatures in order to produce higher product yields (Garforth, Lin et al. 1998, Mastral, Esperanza et al. 2002, Demirbas 2004). Gasification, as a thermochemical conversion pathway, guarantees higher temperatures. Pyrolysis and gasification of plastics and other carbonaceous fuels have been studied extensively in the past (Kaminsky, Sinn et al. 1979, Schoeters and Buekens 1979, Ferrero 1989). Madadian et al. (2016) studied the gasification of pelletized virgin woody biomass using the down-draft reactor applied in the current study and indicated an average temperature of 838^{o}C and 754^{o}C around combustion and reduction zones inside the gasifier. Pyrolysis and gasification of plastics and other carbonaceous fuels have also been studied extensively in the past (Kaminsky, Sinn et al. 1979, Schoeters and Buekens 1979, Ferrero 1989).

To date, experimental indices based on feedstock composition have been used to predict ash deposition and slagging potential (Lee, Kim et al. 2016). Ash deposits or agglomerates are a major problem in the continuous operation of a thermo-chemical conversion reactor such as a gasification and combustion system (Namkung, Kim et al. 2016). There are several major factors in the bed representative agglomeration phenomenon such as particle size, feeding mode, reaction environment (oxidation/reduction), temperature, fluidization velocity, and contents of alkaline earth and alkali mineral (Namkung, Kim et al. 2016). Although downdraft gasifiers are known to have their limitations such as a feed size requirement, low ash content, decreased scale-up potential and increased risk for bridging and clinkering, this technology normally produces less tars and is less complex which could be applied for smaller scale systems (McKendry 2002).

In the current study a fixed-bed 10kW downdraft gasifier was used in order to examine the effects of an incremental increase in plastic added to municipal solid waste fiber. The purpose of this study was to determine the influence of post-consumer plastic blended with post-consumer fiber in a downdraft gasifier. We hypothesize that the presence of plastic can foster the energy content of the composite pellet by utilizing all the components of the fiber material (i.e. extractive, hemicellulose, lignin and cellulose) and that there may be a limiting threshold of plastic contamination permitted in the fuel to maintain a stable reaction and continuous flow in the down-draft gasifier examined.

5.2. Methodology

5.2.1. Raw material characteristics

The composition of the current experimental biomass includes a blend of the fibrous and plastic portions of post-consumer solid waste in Montreal, Quebec, Canada. The majority of the feedstock (90-100%) is comprised of fiber, which includes newspaper, cardboard, office paper, flyers, etc. Plastics are included as the remainder and consists of a blend of mixed polymers that include HDPE, LDPE, PET, trace PVC, etc. The plastics portion combined with fiber does not account for the level of plastic contamination that already exists in recycled municipal solid waste fiber. This portion may be as high as 2-5 wt%.

The proximate and ultimate analysis of biomass feedstock were carried out according to the American Society of Testing Materials (ASTM) for moisture content (ASTM 2013), volatile matter and ash content (ASTM 2013) and fixed carbon content (calculated by difference). Also, the percentages of carbon, hydrogen and nitrogen (ASTM 2014) and oxygen (calculated by difference) of samples were determined using a Gas Chromatography apparatus (GC-14B, SHIMADZU) with a flame-ionization detector. The sulfur content of the samples was measured

according to German Institute for Standardization (DIN) (DIN 2012). The results are shown in Table 5.1.

Table 5.1. Proximate and ultimate analysis of composite pelletized wood fiber and plastic

	Testing item		Waste plastic [1]	Recylced fiber (unpelletized) [1]	Pelletized composite recycled fiber with 0% plastic	Pelletized composite wood fiber with 2% plastic	Pelletized composite wood fiber with 5% plastic	Pelletized composite wood fiber with 10% plastic
Proximate Analysis	MC	wt%	4.78	6.27	6.3	6.24	6.20	6.12
	VM	wt%	94.19	85.78	85.7	85.95	86.20	86.62
	FC	wt%	< 0.01	3.45	3.45	3.38	3.28	3.11
	Ash	wt%	1.03	4.5	4.2	4.43	4.33	4.15
Ultimate Analysis	C	wt%	77	44.95	44.94	45.59	46.55	48.16
	H	wt%	13.97	5.92	5.92	6.08	6.32	6.73
	N	wt%	0.29	0.18	0.18	0.18	0.19	0.19
	S	wt%	0.19	0.19	0.19	0.19	0.19	0.19
	O	wt%	2.93	38.18	38.46	37.48	36.42	34.66
	HHV	MJ kg^{-1}	40.01	17.09	17.09	17.55	18.24	19.38

5.2.2. Experimental setup

The gasification process was performed using a downdraft gasifier with the nominal thermal output 10kW, (Gasifier's Experimenter's Kit Level 4, Model V3.1.0 purchased from All Power Labs, Berkeley, California). The installation consists of a downdraft fixed bed gasifier (35 cm diameter and 40 cm length). The air flow is controlled by a system of pressure regulators and valves and its value is estimated through the differential pressure measured over a calibrated nozzle. In the reactor, both gas and biomass feedstock move downward as the reaction proceeds. The main reactor is equipped with air nozzle supports to provide the reactant and gas pipes to transport the

produced gas into the filtering system. The biomass gradually moves down along with air passing through the series of thermo-chemical reactions in the reactor in order to produce synthesis gas, which leaves the reactor at the bottom through the grate (Figure 5.1a). During the course of the experiment, the temperature profile over the entire gasifier is measured by five thermocouples, K-type, installed as shown in Figure 5.1.

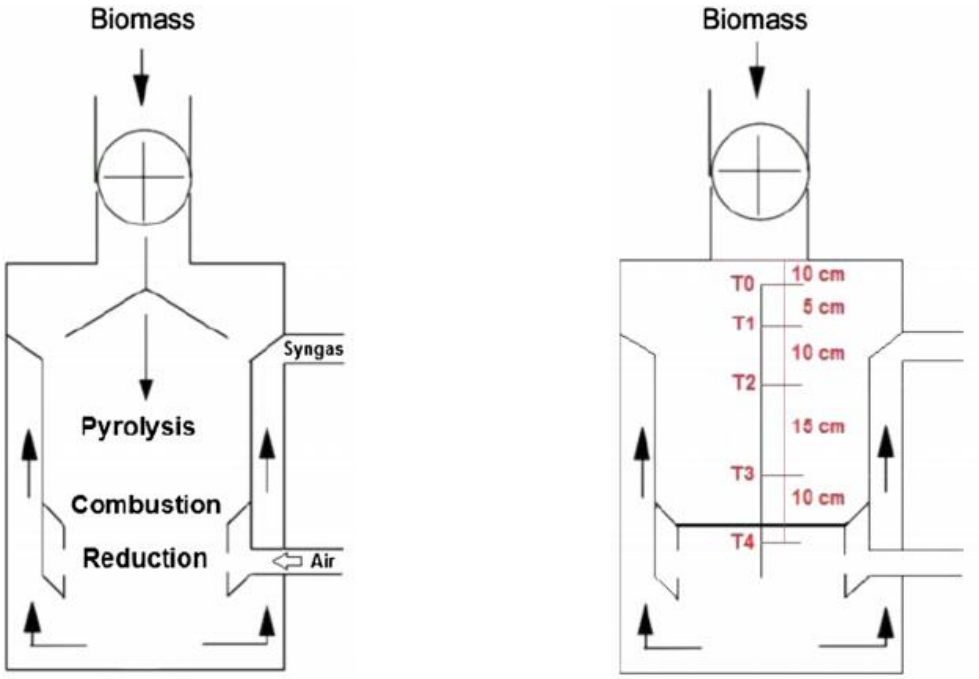

(a) **(b)**

Figure 5.1. Schematic of the down-drafter gasifier: (a) Location of different zones where thermochemical reactions occurs; (b) location of thermocouples.

5.3. Results and Discussion

5.3.1. Gasification and temperature profile

The temperature distribution in the reactor is measured by type K thermocouples. Due to the process dynamics, the temperature recorded fluctuations more in the first 30 min which then

stabilized. In the stable mode, the measuring tolerance of the thermocouple in the highest temperature point (combustion zone) is in the range of ±15^{o}C. Hence temperatures presented within this study are given as average. The downdraft gasifier has four distinct reaction zones: (1) drying, (2) pyrolysis, (3) oxidation and (4) reduction. Figure 5.2 presents the temperature profile at different zones within the main reactor.

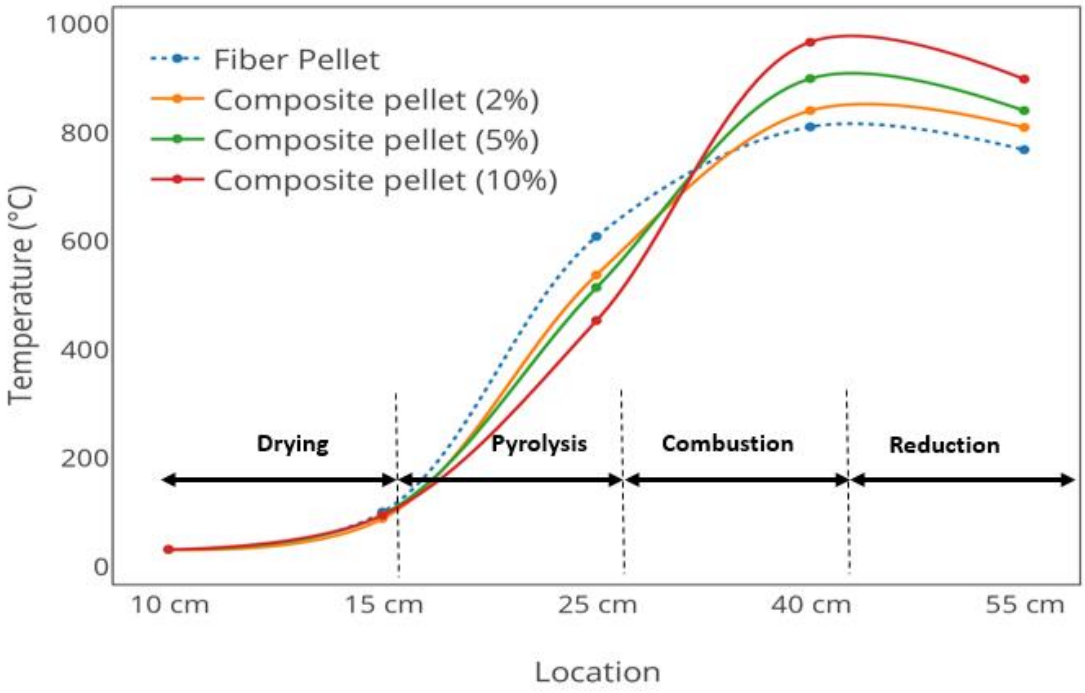

Figure 5.2. Temperature profile of pelletized composite fiber and different percentage of plastics (i.e. 0% 2%, 5% and 10%). The temperatures are recorded within the main reactor of the gasifier and at four different zones namely drying, pyrolysis, gasification and combustion.

As shown in Fig 5.2, the pellets with the lower percentage of plastic showed higher temperature up to the pyrolysis zone where the temperature did not exceed 600^{o}C. However, by proceeding to the next levels, the pellets with higher plastic content revealed higher temperature. This may be

due to decomposition temperature of the plastics at higher temperatures that helps to increase the temperature at combustion and reduction zones as well. The average temperature of composite pellets with 0%, 2%, 5% and 10% plastic content was recorded at 804^{o}C, 835^{o}C, 893^{o}C and 960^{o}C respectively, in the course of the combustion zone. A pressure increase and subsequent pressure drop originating from the liberation of material that has bridged within the reactor, results in a temperature change specifically between the combustion and reduction zones. This observation as an indication of material bridging within the downdraft gasifier was previously reported in Madadian et al. (Madadian, Lefsrud et al. 2016). As a result, instability within the reactor was shown to affect the feedstock decomposition and ash formation within the reactor.

The first change occuring in the feedstock during gasification is drying. Then, the solid temperature begins to increase until biomass is pyrolyzed. Subsequently combustion is initiated at the same time that pyrolysis is in course. Volatiles and pyrolyzed char react with oxygen. The combustion of volatiles increases the gas temperature, which in turn heats the solid. Once the oxygen is consumed, the pyrolysis can continue until all the biomass has been consumed. On the other hand, the high amount of thermal energy in the process allows the reduction reactions to begin (Di Blasi 2000, Tinaut, Melgar et al. 2008).

5.3.2. Clinker formation

Here we observe that by increasing the plastic content in the composition of composite matrix led to the production of a metallic chunk of semi-burnt pellet mixed with some other elements are formed. The clinker forms initially in combustion zone (Figure 5.3a) where the highest temperature resides. By increasing clinker formation, some move downward with the help of biomass flow and deposit on top of the bed material (Figure 5.3b). As a consequence, the developed clinker is less porous compared to the original one formed in combustion zone. This can be due to longer distance

in which they travel (i.e. from combustion to reduction zone) resulting in increased retention time in a high temperature zone which would lead to more viscous slag, along with lower heat transfer when entering the reduction zone. Dimensions of the clinker are shown in Figure 5.3c.

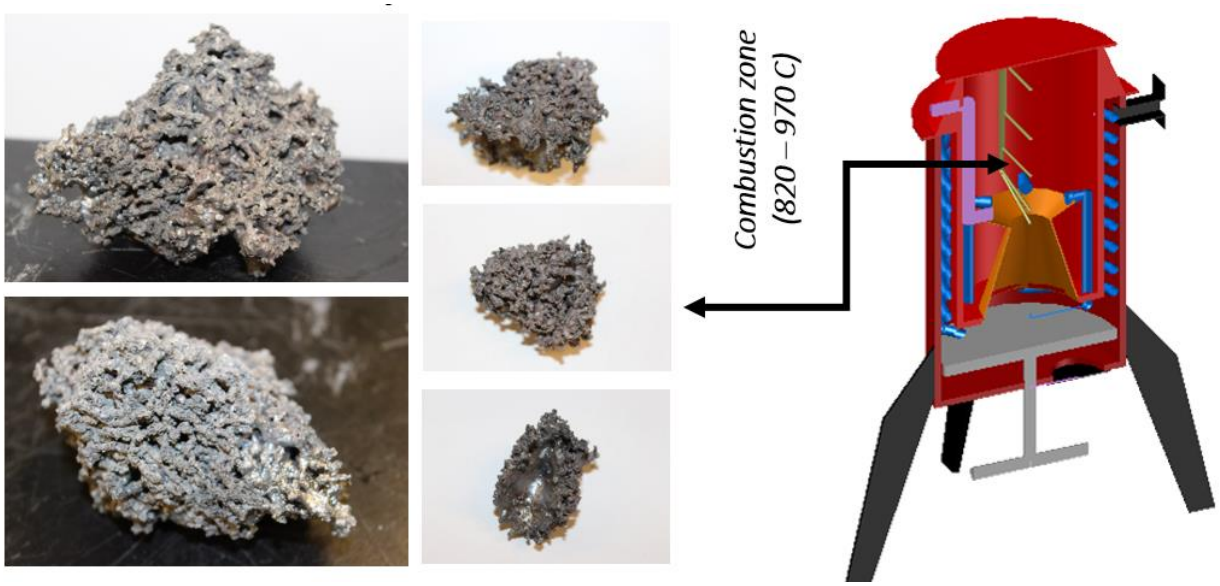

(a)

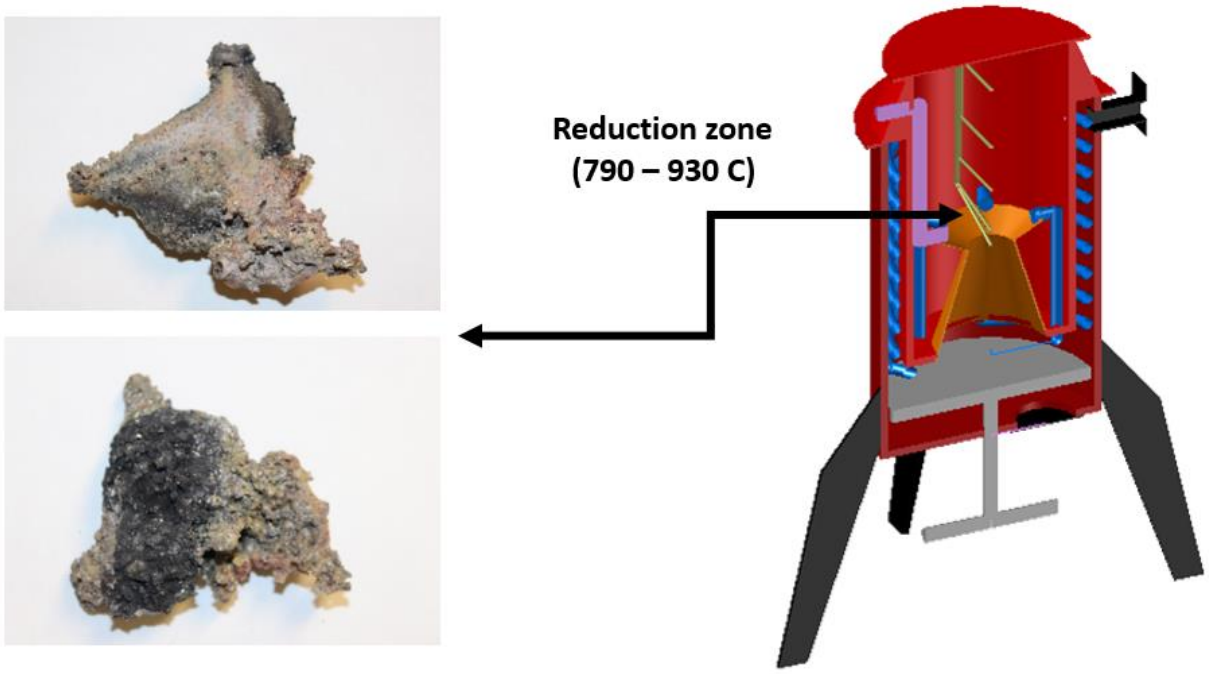

(b)

(c)

Figure 5.3. Clinker formed during the course of composite pellet of fiber and plastic gasification in a down draft reactor. The clinkers are formed in two different levels: (a) combustion zone where the highest temperature and rate of heat transfer takes place, (b) reduction zone where the bed materials are located and there is no downward motion and increased residence time for the

clinker, and (c) scaled picture of clinker generated in combustion 9cm×7.5cm (left) and reduction 8cm×6.5cm (right) zones

5.3.3. Morphology investigation by scanning electron microscope (SEM)

Scanning electron microscopy (SEM) is the most common tool used to observe micro-structural transformations occuring during thermal degradation of the biomass (Bahng, Mukarakate et al. 2009). Figure 5.4 represents the SEM images of clinker formed during gasification of composite pellets with different percentage of plastics.

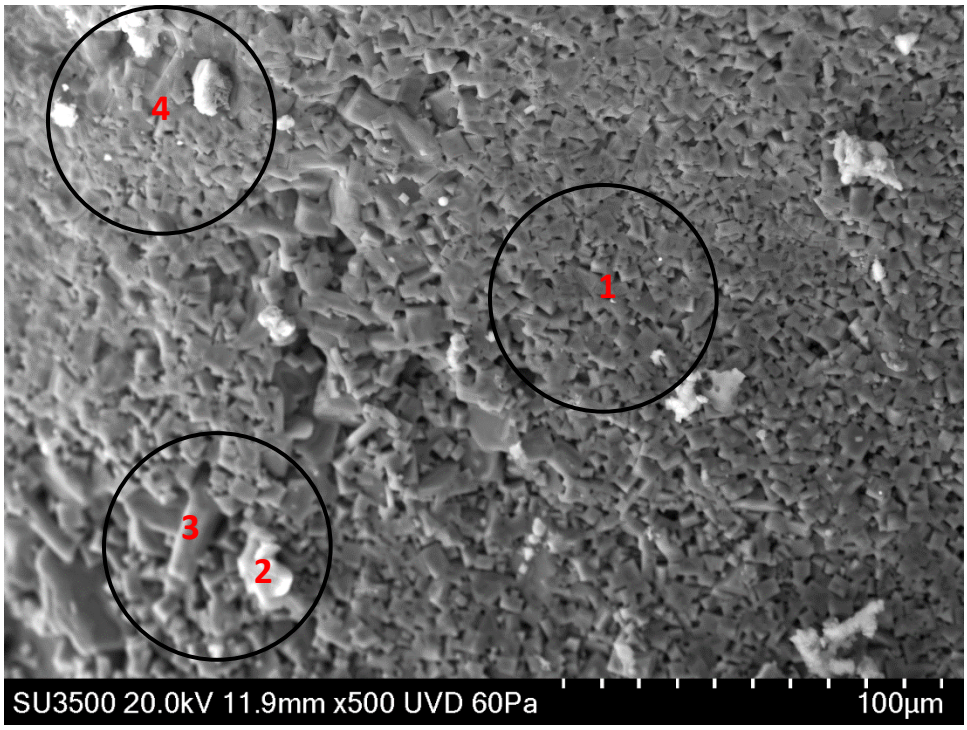
4
1
3
2
SU3500 20.0kV 11.9mm x500 UVD 60Pa
100µm

(a)

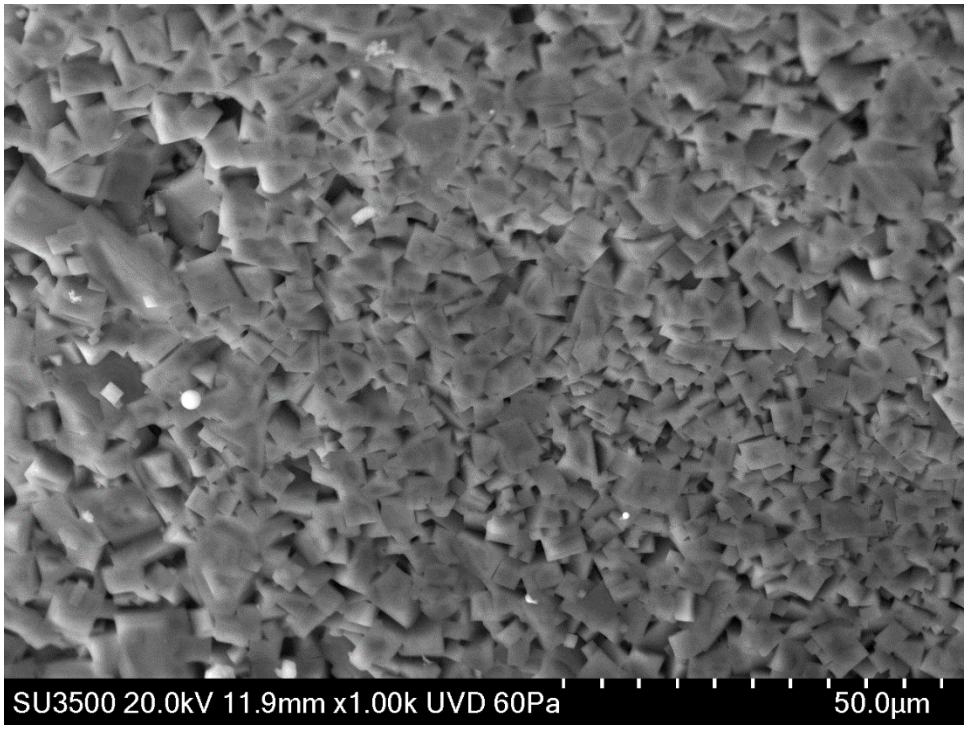
SU3500 20.0kV 11.9mm x1.00k UVD 60Pa
50.0µm

(b)

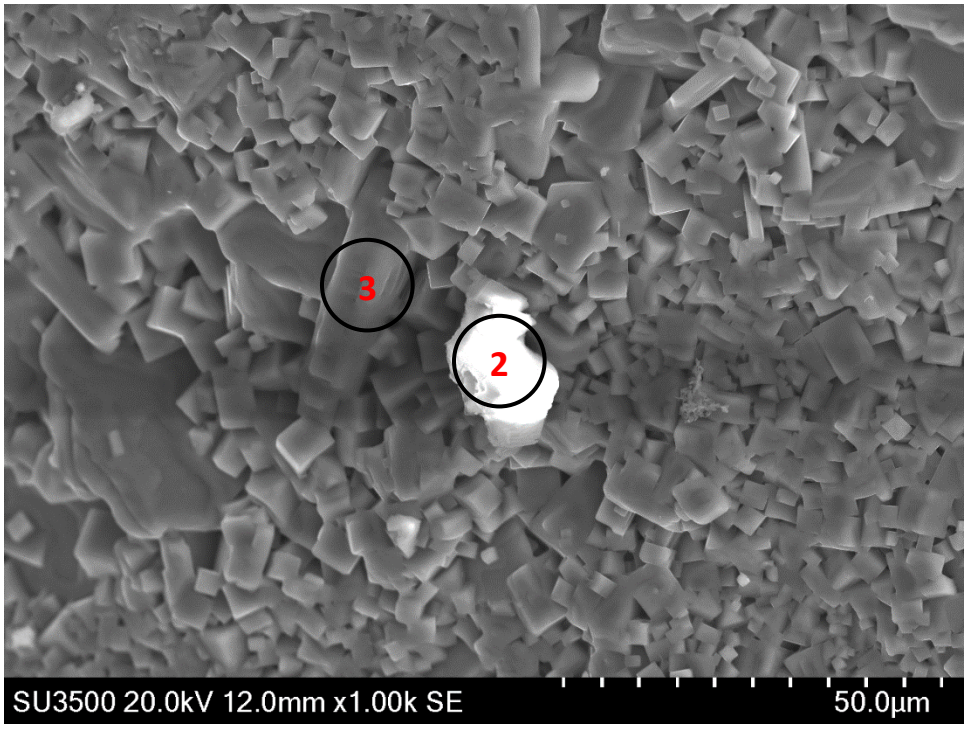

(c)

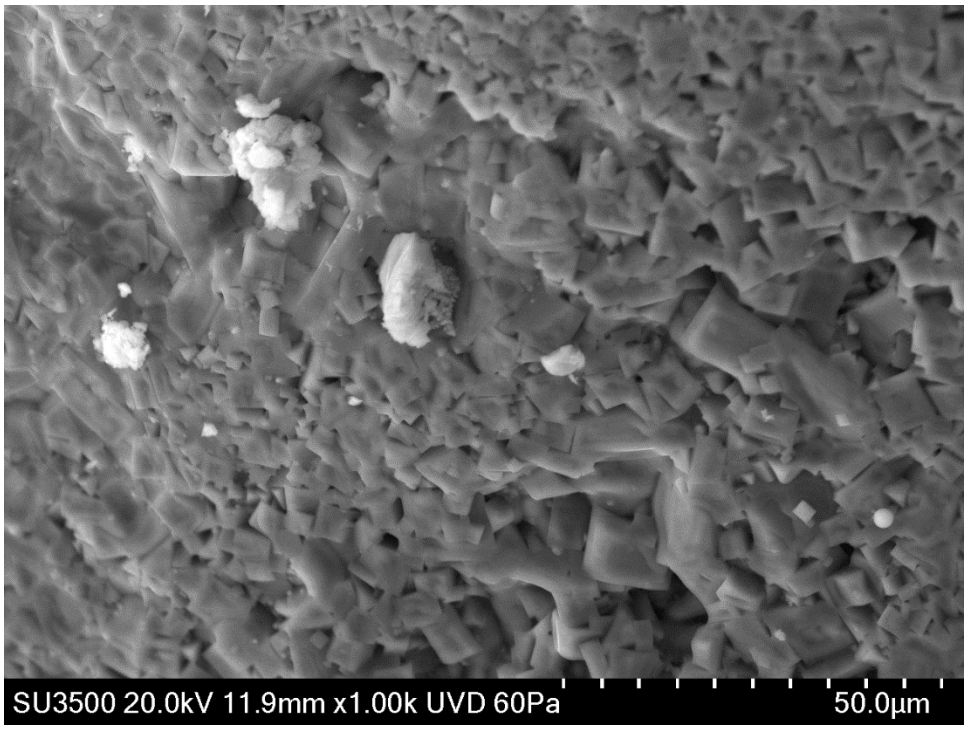

(d)

Figure 5.4. SEM images of clinker formed during gasification of composite fiber and plastic. There are four different spectra selected from the (a) main image, (b) spectrum 1, (c) spectra 2 and 3, and (d) spectrum 4 using Hitachi S-4800 Type II Ultra-High Resolution Field Emission

Table 5.2. Clinker analysis using SEM Hitachi S-4800 Type II Ultra-High Resolution Field Emission in PPM

Label	C	O	Na	Mg	Al	Si	P	Ca	Ti	Fe	Cu
Spectrum 1	15.18	48.96	0.97	0.87	4.78	8.81	-	18.91	0.53	0.34	0.66
Spectrum 2	15.27	49.56	0.90	0.79	4.63	8.76	0.16	18.33	0.52	0.29	0.81
Spectrum 3	32.27	40.61	0.73	0.47	3.14	5.59	0.11	14.55	0.32	0.58	1.64
Spectrum 4	23.50	46.18	0.91	0.57	3.83	6.78	-	16.10	0.38	0.49	1.27

As can be seen in the figures, there is 15% to 32% of unburned carbon that varies in the clinker composition. Consistent with our macro elemental analysis in Table 5.2, this microanalysis

confirms that these particles contain mostly Al, Si and Ca. In addition, carbon, copper, iron and magnesium vary relative to the magnitude of compared to the other elements detected in the clinker among the 4 spectrums.

5.3.4. Metallic and non-metallic content

The clinkers are analyzed using an ICP-MS instrument (Agilent 7500 Series ICP-MS, USA) and neutron activation analysis (NAA) techniques to measure the concentration of metal and non-metal content of the clinker at low concentrations. The results show that there are 26 different elements detected in the clinker structure, five of which indicated highest concentration. The five main elements are aluminum, calcium, sodium, potassium and silicone. Table 5.3 summarizes the elemental composition, which illustrates the level of alkalinity and contamination in the sample. In addition, it is expected that the levels of problematic Cl increase as the percentage of plastic increases due to post-consumer plastics containing chlorinated polymer contaminants such as PVC, saran and neoprene.

Table 5.3. Clinker analysis using ICP-MS instrument in PPM

	Fiber and Plastic Pellet	Blended Fiber (Pure Fiber)	Clinker
Cl	2200	2000	
Si	17425	17500	
Na	928 ± 1.6	1393 ± 134.8	11318
Mg	427 ± 12.7	503 ± 47.6	8358
Al	1463 ± 62.1	3022 ± 385.5	111967
K	87 ± 11.7	384 ± 39.2	1427
Ca	17255 ± 29.9	21892 ± 30.6	289278
V	1 ± 0.0	2 ± 0.3	25
Cr	1 ± 0.0	3 ± 0.2	202
Mn	48 ± 0.4	29 ± 1.7	491
Co	0	1 ± 0.7	11
Ni	2 ± 0.6	2 ± 0.1	175
Cu	64 ± 2.5	31 ± 4.4	431
Zn	11 ± 4.5	25 ± 3.2	45
Rb	0	1 ± 0.1	3
Sr	20 ± 0.6	21 ± 3.1	302
Y	0	2 ± 3.3	8
Ag	0	0	0
Cd	0	0	3
Ba	8 ± 0.1	13 ± 1.3	802
Tl	0	0	0
Pb	1	2	0
Fe	176	274	7426
As	0	0	2
Se	0	0	1

In order to figure out the source of the major elements detected in the ICP-MS analysis, a similar analysis is carried out for different types of fibrous material which are commonly seen in the municipal waste stream. The tested materials are brown paper towels, cardboard, print paper, and magazine paper (Table 5.4).

Table 5.4. ICP-MS analysis of commonly seen material in the municipal waste stream in PPM

Material	Na	Mg	Al	K	Ca	Si	Cl	Total
Brown hand paper	491.9958	573.8172	1328.933	114.9205	7540.277	UND*	UND*	10049.944
Cardboard	1338.72	1939.40	4222.37	252.92	24830.72	UND*	UND*	32584.13
Print paper	529.58	796.86	529.66	48.33	47524.66	UND*	UND*	49429.09
Magazine paper	1232.05	1561.69	4249.72	19.42	87773.24	UND*	UND*	94836.12

*Undetermined

The composition of the clinker resembles to the one from Al-Si and Al-Mg-Si Alloys in which silicon particles reinforced with aluminum matrix composites are formed by improving Si supersaturation in aluminium matrix. Al-Si alloys are widely used in different fields of industry (Nikanorov, Volkov et al. 2005). Due to the low specific weight, high corrosion resistance and outstanding technological properties, Al-Si alloys are widely used in automotive, motorcycles and military industries. Al-Mg-Si alloys are among the most widely used and currently studied alloys for applications leading to significant light weigh in structural components such as those of passenger cars and trucks (Fallah, Langelier et al. 2016).

5.3.5. Thermal conductivity

As shown in Figure 5.5, the thermal conductivity of blended fiber was 0.0594 W m^{-1} K^{-1} which is slightly higher than shredded plastic 0.0535 W m^{-1} K^{-1}. These results revealed that plastic has a lower thermal conductivity compared to fiber, and the composite pellets with a higher percentage of plastics have a lower bulk thermal conductivity. The lower thermal conductivity of plastics helps to procrastinate the early disintegration of the pellet. This may explain why we experienced lower temperatures within the reactor during pyrolysis for the 10% composite pellet compared to the fiber pellet (Figure 5.2). Therefore, we could evaluate how to maximize the utilization of wood fiber components can be achieved based on the different ratios of plastic.

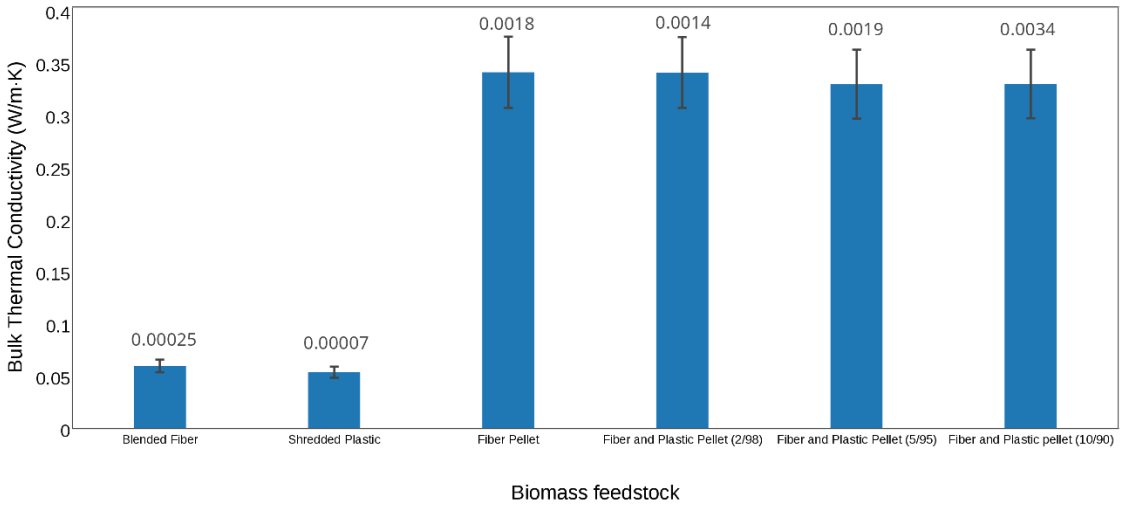

Figure 5.5. Thermal conductivity of individual blended fiber and shredded plastic, and composite fiber pellets using the Hot Disk Transient Plane Source (TPS) technique

5.3.6. The mechanism of clinker formation

During gasification of composite pellets, we observe that the average temperature profile in the heart of the reactor (i.e. combustion zone) was raised by increasing the amount of plastic in the composite matrix. This increment is from 800^{o}C for individual fiber pellet (0% plastic) to almost 960^{o}C for composite pellet consisting of 10% plastics. Additionally, the mass of clinker formed during gasification increases namely 217 g, 642 g, and 912 g for composite pellets of 2%, 5% and 10% plastics. There was however no clinker formation seen in the case of fiber pellet without plastic. Here, we observe increasing 4.64% in clinker mass by increasing 125 ^{o}C in the temperature (Figure 5.6).

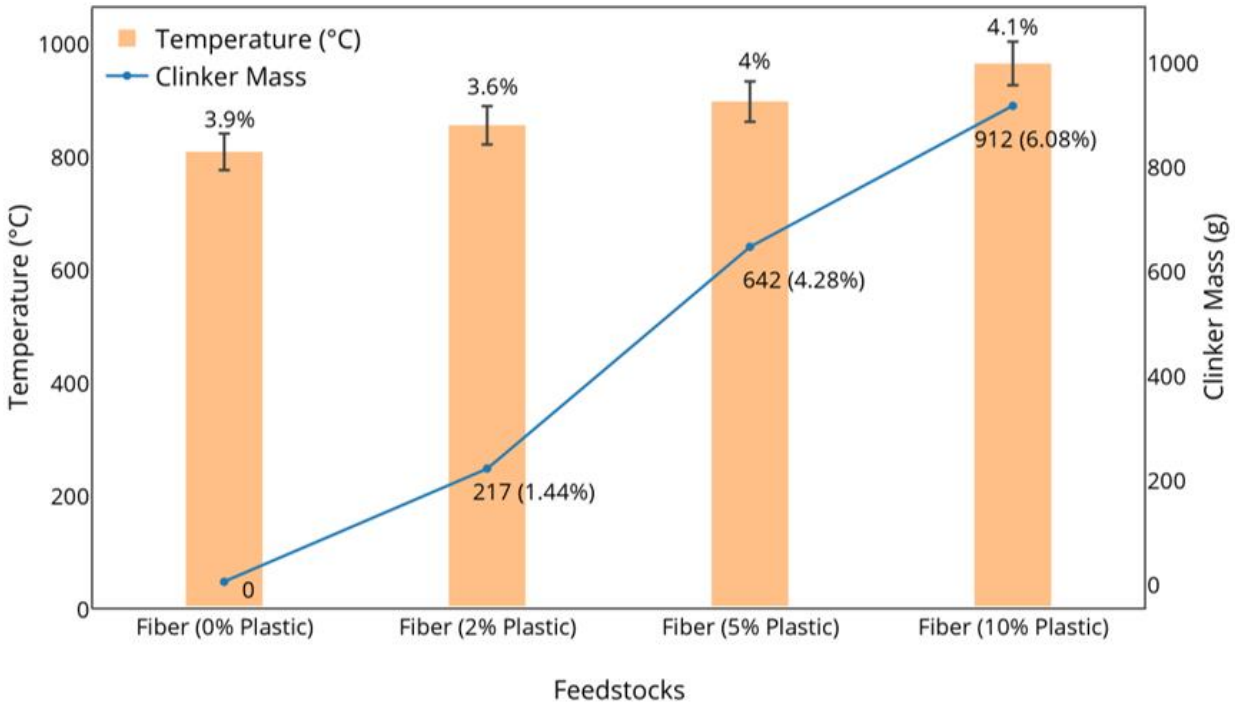

Figure 5.6. Gasification temperature and corresponding amount of clinker formed for composite pellets with different plastic content

We hypothesize that by increasing temperature, the rate of heat transfer increased inside the fuel, which ultimately resulted in releasing volatiles and propagates the formation of char in the pyrolysis zone. The outflow of volatiles leads to heat transfer between volatiles and cooler unpyrolysed fuel. After passing the pyrolysis zone, the temperature will increase and results in evolving organic content of the composite pellets.

In general, during a high temperature gasification process, the organic content of the biomass feedstock is completely consumed within the combustion zone, while the minerals transformed into ash. Normally, by exposing the ash to higher temperatures, it transforms to liquid, viscous slag owing to the melting and reactions of its component mineral matter, meanwhile, the molten ash particles accumulate on the internal walls of the gasification chamber, then the wall is covered by a layer of solid slag, over which the liquid slag will flow under the force of gravity and out of the bottom of the gasifier into a water quenching system. However, the current gasification system did not reach high enough temperatures to transform the ash to fluid, viscous slag, which resulted in severe ash agglomerates.

Tars are additional ash products formed from the agglomeration of organic aerosols during the conversion process and are grouped into three classes: (a) low molecular weight released by evaporation, (b) average molecular weight released by evaporation and produces both gaseous and heavier compounds, and (c) high molecular weight that form gases and char (Euh, Kafle et al. 2016). When the combustion gas temperature cools below the dew point of tar, it is condensed and causes fouling and blocking in the equipment (Euh, Kafle et al. 2016).

To determine the important parameters in clinkering, the thermal behavior of different composite biomass was analyzed in a furnace. Samples with different plastic contents were kept in an alumina crucible. The temperature of the furnace was set at 200^{o}C, 300^{o}C and 500^{o}C. The temperature was

raised up to the desired value and then the alumina crucible, including the sample, was fed into the furnace. The sample was heated for 2 hours and was then withdrawn from furnace to analyze the evolved elements at each temperature.

Table 5.5. The ICP-MS analysis of individual and composite fiber and plastic heated under different temperatures in an ash furnace in PPM

	Material	**Na**	**Mg**	**Al**	**K**	**Ca**
200ºC	Fiber	1462 ± 56	443 ± 27	2215 ± 84	420 ± 10	14713 ± 1296
	0%	742 ± 21	535 ± 16	1325 ± 9	142 ± 4	17097 ± 622
	2%	1036 ± 10	465 ± 16	2433 ± 75	122 ± 4	23767 ± 964
	5%	862 ± 24	474 ± 21	1458 ± 60	126 ± 15	19566 ± 1622
	10%	689 ± 14	350 ± 4	1069 ± 24	153 ± 1	10702 ± 471
300ºC	Fiber	2146 ± 84	1024 ± 49	4281 ± 172	960 ± 27	23418 ± 1355
	0%	1264 ± 147	699 ± 99	2163 ± 375	165 ± 20	29419 ± 3887
	2%	1442 ± 40	639 ± 23	3162 ± 225	182 ± 16	31407 ± 619
	5%	775 ± 22	725 ± 33	1418 ± 49	155 ± 9	23226 ± 1174
	10%	723 ± 13	448 ± 26	1291 ± 7	233 ± 15	11809 ± 733
500ºC	Fiber	7696 ± 300	4936 ± 133	60325 ± 1938	3861 ± 88	125601 ± 14089
	0%	9677 ± 616	5600 ± 108	63901 ± 1411	1317 ± 20	215300 ± 4246
	2%	9185 ± 288	4071 ± 57	74168 ± 2956	1240 ± 67	195499 ± 3397
	5%	6962 ± 96	6834 ± 880	56044 ± 2112	1351 ± 55	193404 ± 2218
	10%	11327 ± 76	6222 ± 166	72031 ± 1074	2851 ± 149	156999 ± 3630

As shown in Table 5.5, the amount of the six major elements increase by raising temperature of the ash furnace. Perhaps this is due to the decomposition temperature of each element which are above 300^{o}C. Therefore, the greater amounts of major elements are shown comparatively up to 500 ^{o}C comparing. This trend is similar for all the composite pellets used. This area of research demonstrates how the proportion of aluminum specifically begins to increase between 300-500 ^{o}C, and more notably in fiber and 10% plastic.

5.3.7. Char coalescence

The inorganic matter in the fuel itself can present complications during gasification or thermal decomposition of the fuel. For example, the composition of the fuel includes alkali metal species, such as K and Na, which are released to the vapor phase, and halogens like chlorine commonly found in biomass and plastics is then converted to HCl; these have been well documented to describe the corrosive nature of this species during the conversion process (McKendry 2002, Van Loo and Koppejan 2008, Becidan, Wang et al. 2015). The condensation of alkali metal vapors and increased HCl concentrations lead to corrosion and deposit formation. These alkali compounds in the fuel can vaporize at temperatures commonly found in the oxidation zone in the gasifier above 700C, and subsequently form small particles as they cool and condense, sticking to metal surfaces, which leads to corrosion (Kumar, Barrett et al. 2009). This resulting temperature above 700C in the oxidation zone is above the melting point of some biomass ash and impurities such as aluminum. The likelihood of clinker formation increases with a higher ash content, notably 5% or greater, especially if the ash contains high alkali oxides and salts (McKendry 2002).

In addition to the fuel composition itself, temperature, pressure in the reactor, and particle shape, all have significant roles in the formation of deposits during gasification. A complex, multivariable approach should be considered when examining the formation of deposits. For example, Wei et

al. (Wei, Schnell et al. 2005) examined the effect of pressure and species formation in 3 feedstocks: straw, sludge and wood. Increased atmospheric pressure and high temperature (greater than 1200K) increased the release of HCl, however in wood, these conditions decreased the release of HCl. This study would suggest that beyond the composition, the operational parameters should be adjusted to further optimize the reactor performance in efforts to minimize detrimental specie formation, common with alkali earth metals and Cl.

In the current experiment a high mineral matter with impurities and increased ash content, led to problematic clinker formation and slagging. Additionally, the shape (i.e., densified pellets) may have contributed further to the severity of the formation of clinkers in this type of reactor, and will be examined in more depth in future research. The temperature profile indicated that during the operation of the down-draft gasifier, clinker agglomerates were encountered at temperature in excess of 800 °C. The agglomeration was severe, and the gasifier bed was occupied with the agglomerated chunks and these solids had to be broken inside the bed in order to discharge them from the reactor.

5.4. Conclusion

The gasification of composite fiber mixed with different percentages of plastics was carried out. When the plastic level is less than 5% the amount of aluminum seen goes down. What we are assuming is that the plastic is increasing the reaction temperature and causing the aluminum and other material to form a slag. At the highest plastic levels tested (10%) we get one big ball of slag comprised of aluminum, silicone, calcium, sodium and potassium, with around 15 kg start sample we end up with an average of around 912 g of the slag. At the slightly lower plastic levels (2%) we end of with a slag chunk that looks exactly like the individual pellets in a semi melted chunk. Similar to a bunch of chocolate chips out on a warm counter, they are slightly melted

together. They are porous with all the volatiles released. At less plastic level (<2%), then we do not see any of the slag occurring. Finally, the current study provides an in-depth analysis of an experimental study on the gasification of waste and a plastic contamination threshold. This study examines and proves how the thermal conductivity and chemical composition affect the flowability or efficiency within the reactor due to slag formation. A future study will further examine the physical shape of the biomass itself and how this property may be optimized in order to improve efficiency in an experimental downdraft gasifier.

Acknowledgments

This research is funded by BioFuelNet Canada, a network focusing on the development of advanced biofuels. BioFuelNet is a member of the Networks of Centres of Excellence of Canada program.

Connecting Text

In Chapter 5, the gasification of composite fiber paper and plastic waste was investigated. The chapter aimed to find how the increase in plastic specifically in the recycled fiber stream would affect the performance of a downdraft gasifier. This research showed that a mixture of silicon with aluminum, calcium and sodium under high temperatures would result in the generation of a solid clinker that ultimately moves through the reactor and is deposited at the bottom of the reactor. At the highest plastic levels tested (10%) one big ball of aluminum slag with an average of around 912 g was generated from a 5 kg start sample.

In the next two chapters (Chapters 6 and 7), the thermo-chemo-mechanical analysis of the composite material discussed in Chapter 5 is investigated. In Chapter 6, the thermogravimetric analysis, differential scanning calorimetry and thermal conductivity test using the new technique of Hot-Disk Transient Plane Source (TPS) technique are examined.

Chapter 6 has been submitted for publication as:

Madadian E., Akbarzadeh A.H., & Lefsrud M. (2016). Pelletized Composite Wood Fiber Mixed with Plastic as Advanced Solid Biofuels: Thermo-Chemical Analysis. *Waste and Biomass Valorization*, (Under revision).

CHAPTER 6

6. PELLETIZED COMPOSITE WOOD-FIBER MIXED WITH PLASTIC AS ADVANCED SOLID BIOFUELS: THERMOCHEMICAL ANALYSIS

Abstract

Biomass has great potential to supply a part of the future energy demands of the world. Wastes from pulp and paper processing and lumber production in the forestry industry are one alternative resource of biomass and a promising source of clean sustainable energy. Composite pellets of plastics and wood fibers are one of the industrialized alternative biomass with improved multiphysical properties. In the past few decades, thermochemical conversion pathways have attracted a great deal of attention as a principal technique to convert biomass to energy. In this paper, mechanical, thermal, and chemical analysis along with scanning electron microscope (SEM) imaging were used to study the performance of composite pellets. The bio-based fibers were mixed with several volume fractions of plastic, i.e. 0%, 2%, 5%, and 10%, in the form of pelletized advanced solid fuel. The pristine fiber pellet containing no plastic was tested as a baseline for the thermo-chemical properties of composite wood pellets. Thermogravimetric analysis (TGA) and differential scanning calorimetry (DSC) were used for the thermal analysis of the pelletized samples. The TGA results were used to explore the thermal reactivity of fibers and plastics under high temperature conditions. The DSC results showed that the glass transition of the composite pellets, taking place under endothermic reactions, was developed by increasing the plastic content of composite pellets. Thermal conductivity of composite pellets was measured

using the Hot-Disk Transient Plane Source (TPS) technique. The TPS results showed that composite pellets with higher volume-fractions of plastics possessed a lower thermal conductivity. This is due to the lower thermal conductivity of shredded plastics than the blended fibers in the matrix of the pellets. The presence of plastic changed the thermal behavior of fiber by enhancing the energy content of the composite pellets while altering the chemical composition of the gas emission during the thermo-chemical conversion of biomass. Finally, the results of pelletized fiber-plastic composites were compared with undensified fibers and plastics to identify the accessible boundaries for the thermo-chemical properties of fiber-plastic solid fuels. The results of this study helped to improve the efficiency of the thermo-chemical conversion of the composite pellets, specifically gasification, through an improved understanding of the thermal behavior of the biomass within the reactor.

Keywords: Bioenergy, Composite solid fuel, Differential scanning calorimetry, Thermal analysis, Thermogravimetric analysis, Microstructural analysis

6.1. Introduction

Renewable energy constitutes 16.7% of global energy consumption (Shahrukh, Oyedun et al. 2015). About 8.7% of the total renewable energy consumption is originating from biomass (Shahrukh, Oyedun et al. 2015). Traditional bioenergy represents approximately 15% of total global energy use and 80% of current bioenergy use which counts for approximately 35 EJ yr^{-1} (Creutzig, Ravindranath et al. 2015). To overcome the negative environmental impacts of greenhouse gas emission affecting climate changes, carbon neutralized sources of energy should be used (Singh, Krishna et al. 2016). Biomass is a renewable and clean energy resource with carbon

neutrality and low sulfur content, which can potentially supply up to 14% of the world's energy consumption (Zhang, Zheng et al. 2016). Biomass is a complex heterogeneous mixture of key organic components, such as cellulose, hemicellulose, and lignin, along with accessory organic and synthetic composites (Nanda, Mohanty et al. 2013).

The majority of biomass stored in the technosphere is derived from forest species. This makes wood products the most important biomass for the scientific community and the Intergovernmental Panel on Climate Change (IPCC) to understand the carbon/climate benefits associated with the temporary storage of carbon in wood-based products (Guest, Cherubini et al. 2013). The advantage of using biomass is that there is no extra carbon entered to the environment and the natural carbon cycle. As a consequence, there will not be any additional emissions after their conversion to produce bioenergy. By densifying the residual forest wastes, not only much more volume of waste materials are effectively exploited but also the environment is protected via the reduction of greenhouse gases emissions (Madadian, Lefsrud et al. 2016).

Plastics are frequently used for packaging; however, they are recycled at one of the lowest rates for recycled materials; it is also getting more and more difficult to increase the recycling rate because the remaining waste streams are increasingly complex and quite difficult to separate (Adrados, De Marco et al. 2012). The plastic content of the rejected wastes, after recycling metals, glass, and fiber, in material recovery facilities is composed of many intermingled varieties such as polyethylene (PE), polypropylene (PP), polystyrene (PS), polyvinyl chloride (PVC), polyethylene terephthalate (PET), acrylonitrile butadiene styrene (ABS), and aluminum, (Adrados, De Marco et al. 2012). Lopez et al. (López, De Marco et al. 2011) studied the thermal behavior of different plastics through a thermogravimetric analysis and indicated that PE, PP, PS and PET only have one peak in their mass loss which implies one step degradation during thermal conversion, while

PVC showed two temperature peaks as a result of its two-step decomposition mechanism. The temperature peaks, where the main change in the mass of the material takes place, range from 300 ºC to 500 ºC depending on the plastic type. Miskolczi et al. (Miskolczi, Angyal et al. 2009) examined the pyrolysis of waste polymers where the main physico-chemical change occurred at 520 ºC. However, the determination of the ignition and burn-out temperatures of a solid fuel can be influenced by the operating conditions such as heating rate and retention time (Lu and Chen 2015).

The biomass conversion to energy depends on the biomass inherent material properties, determining the conversion process, the subsequent processing difficulties that may arise, and the emission produced during the conversion (McKendry 2002, López-González, Fernandez-Lopez et al. 2014). The primary aspect in utilizing biomass as a fuel is to understand its material composition and thermo-physical properties. Characterization of biomass is essential since the chemical composition of biomass affects the conversion processes differently. There are several methods of analyses for material characterization of biomass feedstock that can be used to understand the conversion behavior of biomass for the production of renewable energy.

6.1.1. Thermal analysis

The importance of thermo-physical properties, as a function of temperature, is critical to analyze the ultimate thermal behavior during thermo-chemical conversion pathways (Lazaro, Peñalosa et al. 2013). Fu et al. (Fu, Akbarzadeh et al. 2016) explored the thermal response of a sandwich panel with a cracked core foam to obtain the temperature distribution and heat flux intensity factor. The thermo-analytical methods, including thermogravimetric analysis (TGA) and differential scanning calorimetry (DSC), provide valuable information on the kinetics of thermo-chemical conversion techniques (Bahng, Mukarakate et al. 2009). TGA is essential for the kinetics study of

heterogeneous thermo-chemical reactions (Mabuda, Mamphweli et al. 2016). In the TGA process, samples are subjected to a predetermined temperature range in an inert atmosphere. Isothermal or dynamic modes of TGA are used to measure material degradation, oxidation or reduction thermo-chemical reactions, evaporation, sublimation, and other heat-related changes which occur during the biomass conversion (Bahng, Mukarakate et al. 2009).

Differential scanning calorimetry (DSC) is another thermo-analytical technique for measuring the energy added to a sample and reference as a function of temperature. DSC is one of the most powerful techniques to thermally characterize solid fuels and can be used to measure the materials melting point, melting enthalpy, and specific heat (Barreneche, Fernández et al. 2015). The results of these analyses provide an understanding of the chemical structure and major organic compounds in the biomass (Yaman 2004). The design and operation of biomass in conversion systems rely substantially on biomass characteristics, namely, heating value, moisture content, ash content, elemental and chemical composition (Yin 2011).

6.1.2. Microstructural analysis

There are a variety of microscopic techniques to explore the microstructural arrangement of the biomass feedstock. The most commonly used methods for the microstructural analysis are scanning electron microscopy (SEM), light microscopy (LM), environmental scanning electron microscopy (ESEM), SEM with energy dispersive X-ray analysis (SEM/EDX), transmission electron microscopy (TEM), X-ray diffraction (XRD), and small-angle neutron scattering (SANS) (Bahng, Mukarakate et al. 2009). Nadeem et al. (Nadeem, Manzoor et al. 2016) explored the mechanism of the biosorption process of lead (Pb II) onto immobilized waste biomass using SEM and EDX analyses. Therefore, the use of SEM in this study helped us to realize the arrangement of the constituents and their interlocking pattern throughout the matrix of the composite.

6.1.3. Thermo-chemical Conversion

Thermo-chemical conversion of biomass is considered as one of the most promising routes for biomass utilization. Thermo-chemical processes typically include: gasification, combustion, pyrolysis, and liquefaction (López-González, Fernandez-Lopez et al. 2014). Gasification is a thermo-chemical process for converting carbonaceous based materials into gaseous products called syngas (Madadian, Lefsrud et al. 2014). Gasification can be applied on a broad range of feedstock with different energy content, using a gasifier with different beds and gasifying agents (Lugato, Vaccari et al. 2013). Pyrolysis is one of the processes taking place during the biomass gasification. Gasparovic et al. (Gašparovič, Koreňová et al. 2010) studied the thermo-chemical conversion of wood wastes contained main components of hemicellulose, cellulose and lignin. They concluded that wood pellet decomposition proceeds in three distinct stages: water evaporation, active and passive pyrolysis, and wood decomposition. The decomposition of hemicellulose and cellulose takes place in active pyrolysis at temperature ranges from 473 K to 653 K and 523 K to 653 K respectively. Lignin is decomposed within both temperature ranges (Slopiecka, Bartocci et al. 2012). Most of lignocellulosic materials can be considered as a mixture of 40-80 wt% of cellulose, 15-30 wt% of hemicellulose, and 10-25 wt% of lignin (Carrier, Loppinet-Serani et al. 2011). Lignin concentration, as one of the three fundamental components of lignocellulosic materials, does not have a detrimental effect on thermo-chemical product yield (Naik, Goud et al. 2010) as it does in biochemical conversion pathways which is due to its highly hydrophobic nature (Mottiar, Vanholme et al. 2016).

The present study was aimed to investigate the thermo-chemical degradation analysis of composite wood fiber and plastic pellets in the temperature range of pyrolysis and gasification. The wood fibers were blended with plastics with dissimilar volume fractions. We hypothesized that the

presence of plastic in the composite pellets can potentially enhance the calorific value of the solid fuel. Thus, it was of great importance to analyze the pyrolytic behavior of the composite pellets. The thermo-chemical properties of composite pellets were analyzed using TGA, DSC, Hot-Disk TPS, and the gasification conversion process.

6.2. Methodology

In this section, a series of thermo-chemical characterization analyses for composite plastic pellets are presented. We aimed to explore the correlation between multiphysics properties of pellets with their thermal behavior during the thermo-chemical conversion pathways.

6.2.1. Biomass feedstock

In this study, pelletized wood fiber mixed with several volume fractions of plastics was compared in terms of their proximate and ultimate analysis. Selected composite pellets were cylindrical with an average diameter of 5 mm and the length of 25 mm. Four volume fractions of plastics, including 0%, 2%, 5%, and 10%, were considered in this analysis. Pelletized fiber containing 0% plastic along with unpelletized fibers and plastics were examined as a baseline for the characterization of composite pellets. The plastic ingredients were randomly obtained from municipal solid wastes, while the wood fibers originated from waste streams generated from the pulp and paper industry. The proximate and ultimate analysis of the biomass feedstock were carried out according to the American Society of Testing Materials (ASTM) for moisture content (ASTM 2013), volatile matter and ash content (ASTM 2013), and fixed carbon content (ASTM, 2013f). The percentages of carbon, hydrogen and nitrogen (ASTM 2014), and oxygen (calculated by difference) of both pelletized and unpelletized samples were determined using a gas chromatography apparatus (GC-14B, SHIMADZU) with a flame-ionization detector. The sulfur content of the samples was measured according to the German Institute for Standardization (DIN 2012).

6.2.2. Thermal analysis techniques

6.2.2.1. Thermogravimetric analysis

The dynamic feedstock mass changes were measured using a thermogravimetric analyzer (TA Instruments Q500 TGA) as a function of temperature and time under a controlled atmosphere. The instrument was first calibrated for both temperature and weight signals. Since the temperature range was constant for all materials, the calibration was performed only once. Curie point method was used for temperature calibration. For this purpose, a metallic crucible (with known Curie point) was placed in the furnace and the whole set was exposed to a magnetic field. The effect of magnetic field made the material appear lighter. Once the Curie point was reached, the crucible seemed to gain weight, thus providing a calibration for the TGA (TA Instruments guideline, Delaware, USA).

For each experimental run, an average of 5 to 8 mg of sample was loaded on a platinum crucible in the TGA device. The heating range of 25ºC to 700ºC was chosen for the analysis as a normal temperature range to reach for pyrolysis and gasification, and the heating rate was controlled at 20 ºC min^{-1}. Although the maximum temperature during gasification may reach above 1000 ºC, the principal feedstock decomposition occurred at the average temperature of 700 ºC (Madadian, Lefsrud et al. 2016). Nitrogen was used as the inert carrier gas during the thermogravimetric analysis, with a purge rate of 40 mL min^{-1}, to simulate the pyrolysis condition. Air was used as the reactive sample purge gas to move the process forward after 550 ºC as recommended by the manufacturer. The measurements were replicated three times per sample to account for the variability in the sample domain.

6.2.2.2. Differential scanning calorimetry

The DSC characterization of the composite fiber pellets mixed with plastics was conducted by applying a 20 ºC min^{-1} dynamic heating rate between 25 ºC and 220 ºC. The measurements were performed under a controlled lab temperature of 25 ºC and humidity of 30%. A heat-cool-heat temperature programming protocol was used in the DSC experiments to evaluate the behavior of the samples under thermal disturbances (Amorim, Ferreira et al. 2015).

6.2.2.3. Bulk thermal conductivity

The thermo-chemical conversion of biomass feedstocks is a function of their thermodynamic properties. Biomass particles are subject to heat conduction along and across their fiber, which influences their thermal behavior as a result of their thermal conductivity (Basu 2013, Akbarzadeh and Pasini 2014). The thermal conductivity (W m^{-1} K^{-1}) of composite pellets and bulk materials (shredded fibers and plastics) were measured at 21 °C according to the Hot Disk Transient Plane Source (TPS) technique and using the Thermtest TPS 2500S Thermal Constants Analyzer (Thermtest thermophysical Instruments, New Brunswick, Canada). The TPS 2500S system offers the ability to measure samples of limited dimensions with measurement time periods of 1 second. The TPS technique is the most versatile technique available for the measurement of thermal conductivity, thermal diffusivity, and heat capacity of materials since it is capable of testing solids, liquids, pastes, and powders of varying size and geometry. The Hot Disk technique offers significant advantages over other techniques, as it has the ability to identify the presence of contact resistance, inherent in any interfacial testing method, and remove the effects of this contact resistance completely (Ahadi, Andisheh-Tadbir et al. 2016).

According to ISO/DIS 22007-2.2, a test sample surrounded the TPS sensor and the heat evolved in the sensor freely diffusing in all directions. The solution to the thermal conductivity equation

assumed the sensor to be in an infinite sample medium, so the measurement and subsequent analysis of data must account for the limitation caused by the smallest distance from the TPS sensor to any sample boundary.

In order to obtain the best contact with the sensor, 320 grit sandpaper was used to flatten these surfaces. Holes were cut into two XPS (extruded polystyrene) blocks and the pellets were inserted into the blocks, which held the pellets in place during thermal testing. One XPS block/pellet was placed below the sensor while one XPS block/pellet was placed above the sensor, and pressure was then applied in order to press the flat surfaces of the pellets against the sensor. A measurement time was chosen such that no heat introduced during the course of a measurement penetrated beyond the boundaries of the sample being tested. The functionality of XPS blocks was to hold the sample in place to assure satisfactory contact between the sample and the sensor. For thermal testing of the blended fiber and shredded plastics samples, a sensor was placed in a hollow metal cylinder, surrounded by the sample (Figure 6.1).

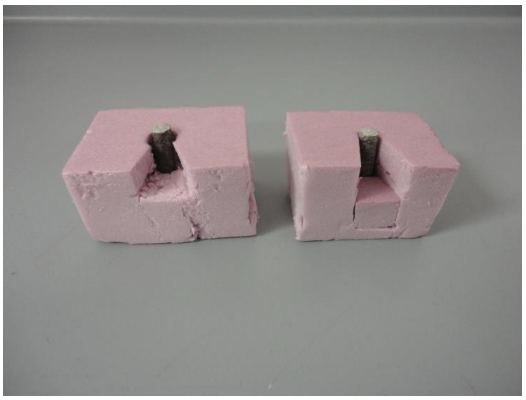

(a)

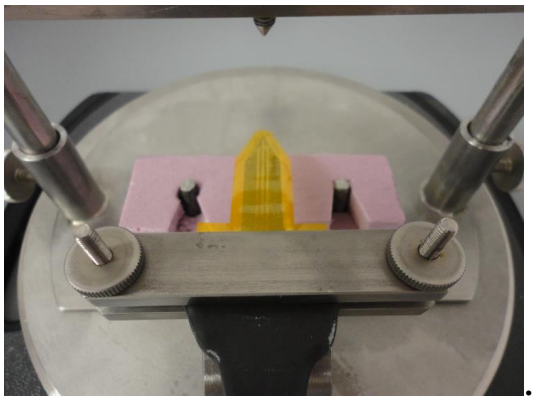

(b)

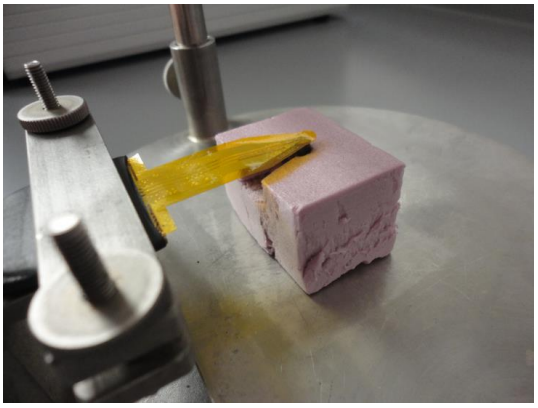

(c)

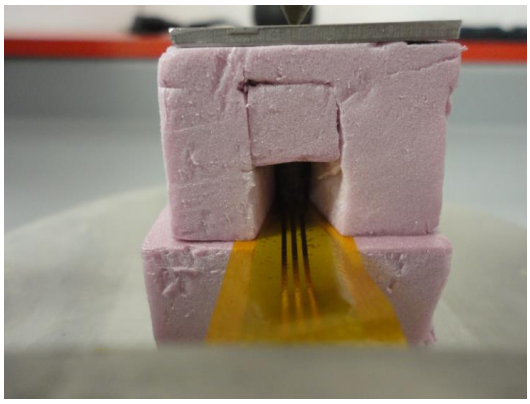

(d)

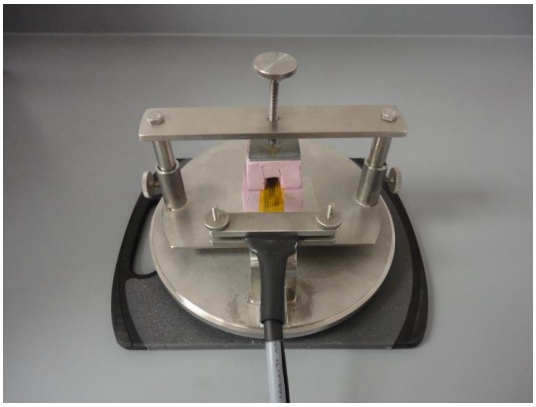

(e)

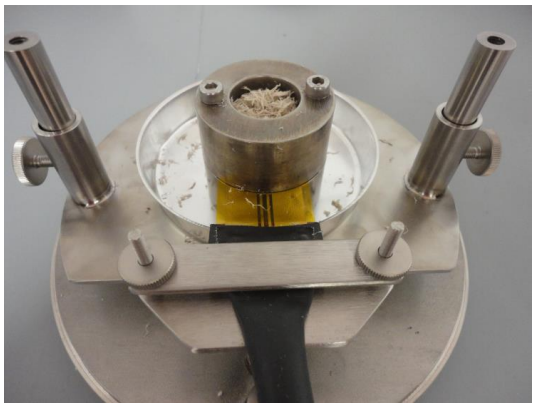

(f)

Figure 6.1. Bulk thermal conductivity test of individual and composite wood fiber and plastics by TPS technique: (a) Custom-cut XPS blocks used to hold pellet samples in place during the thermal conductivity test, (b) TPS sensor clamped in place above pellets in XPS blocks, (c) Bottom sample piece placed under TPS sensor, (d) Top places above TPS sensor. Pressure is applied on the top of the setup in order to ensure satisfactory contacts between the sensor and samples, (e) Top view of experimental setup, with samples pieces held in place by

XPS blocks and clamped in place over the sensor, and (f) Experimental setup used for testing blended fiber and shredded plastic with sensors embedded in the material.

6.2.3. Gasification of composite pellets

Gasification of composite pellets with different plastic contents were carried out in a pilot-scale fixed-bed reactor (GEK Level 4, Model V3.1.0, All Power Labs, Berkeley, California). The main reactor was a cylindrical-shaped chamber and had a height of 80 cm and a diameter of 40 cm. The gasifier was equipped with air nozzle supports to provide the reactant and gas pipes to transport the produced gas into the filtering system (Figure 6.2) (Madadian, Lefsrud et al. 2016).

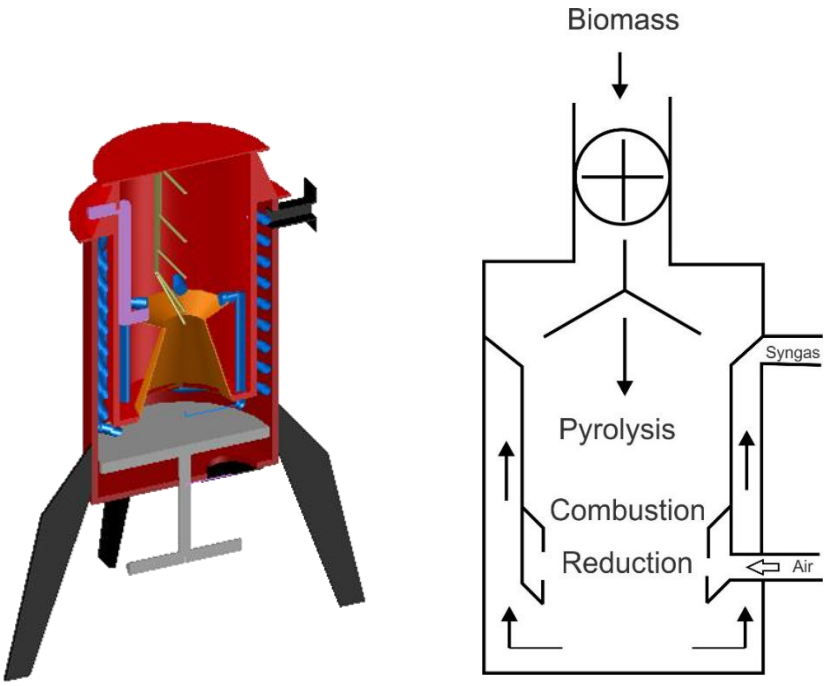

(a) **(b)**

Figure 6.2. Schematic view of the GEK down-draft gasifier: (a) External vessel of the reactor that minimizes heat loss during the gasification process, (b) Different zones in which thermo-chemical reactions take place during the gasification

There are four thermal stages taking place across the down draft reactor namely drying, pyrolysis, combustion, and reduction. Combustion is the heart of the reactor where vital reactions take place, resulting in the production of carbon dioxide and water. The behavior of composite pellets with four different volume fractions of plastics (0%, 2%, 5%, and 10%) in the combustion zone of the reactor during the gasification process was demonstrated in Figure 6.3. The composite pellets were abbreviated as $CF_{P0\%}$, $CF_{P2\%}$, $CF_{P5\%}$ and $CF_{P10\%}$ according to their volume fraction of plastics.

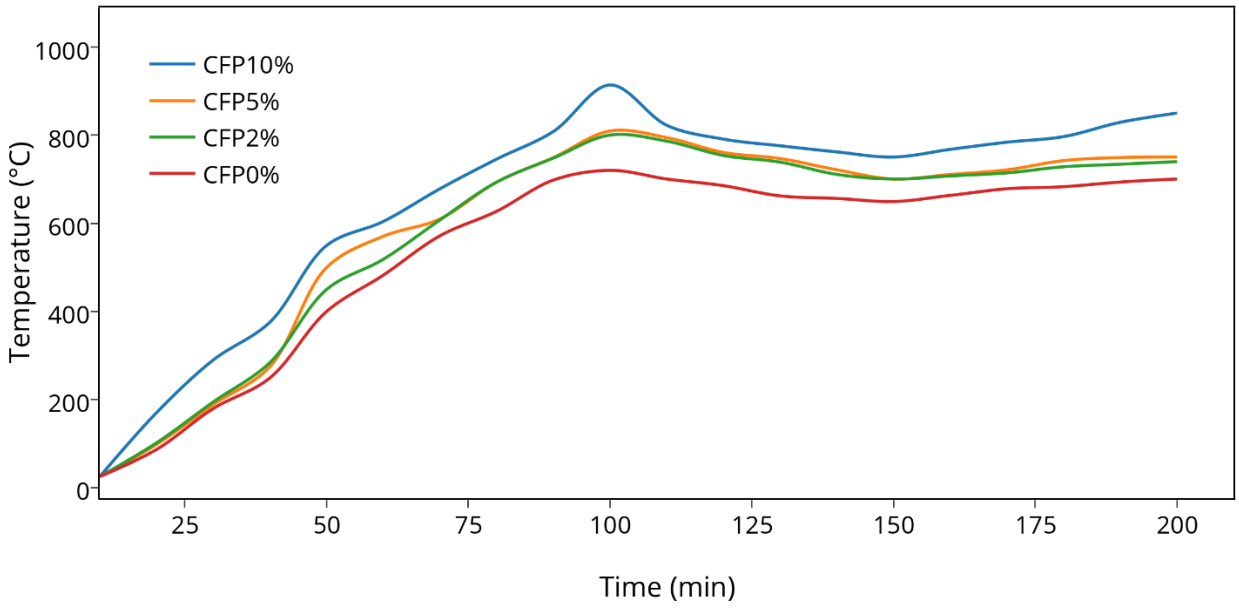

Figure 6.3. Temperature variation of composite pellet gasification within the combustion zone of the down draft reactor.

The gasification results showed that the pellets containing higher plastic contents produced a higher temperature in the combustion zone. A higher temperature in the combustion zone caused the complete combustion of the biomass feedstocks and resulted in the production of a greater amounts of combustion products (i.e. CO_2 and H_2O). As a consequence, greater amounts of synthesis gas (i.e. syngas) would be produced.

6.2.4. Morphology investigation by scanning electron microscopy (SEM)

Scanning electron microscopy (SEM) is the most commonly used tool to observe micro-structural transformations that occur during the thermal degradation of biomass feedstock (Bahng, Mukarakate et al. 2009). Figure 6.4 represents the SEM images of composite pellets with different volume fractions of plastics. Size, shape and interlocking between constituents of the composite pellets alter the multiphysical properties of the composite pellet. In addition, size particle and characterization of the constituents may affect thermal and mechanical stability, chemical reactivity, flowability, and material strength of composites (Alkan, Sarı et al. 2009), such as composite pellets. Figures 6.4a and 6.4b show the microstructure of shredded plastics and blended fibers mixed in the composite pellet. The shredded plastics had a filamentous texture with lower effective surface area compared to blended fibers. On the contrary, blended fibers demonstrated higher continuity within their molecules with a greater surface area compared to plastic constituents. Figure 6.4c showed a densified blended fiber pellet where the components were

compressed and there was less void space within the matrix. Figures 6.4d, 6.4e, and 6.4f show densified composite of pellets with different percentage of plastics 2%, 5% and 10%, respectively. Since, the arrangement of blended fibers and plastics was random during densification, there was no certain rule to define the distribution of the components of composite pellets. The samples were coated with a fine layer of carbon to improve the imaging quality and to inhibit charging and reduce the potential thermal damages.

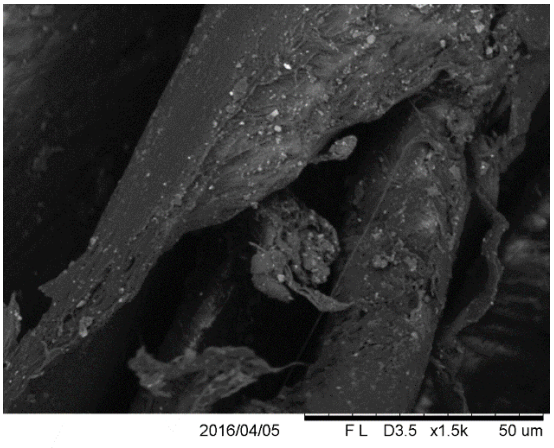

(a)

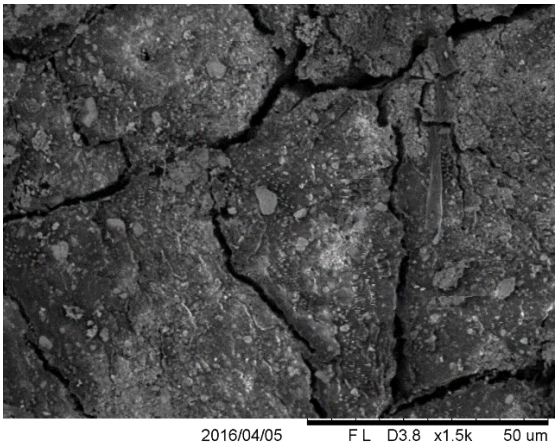

(b)

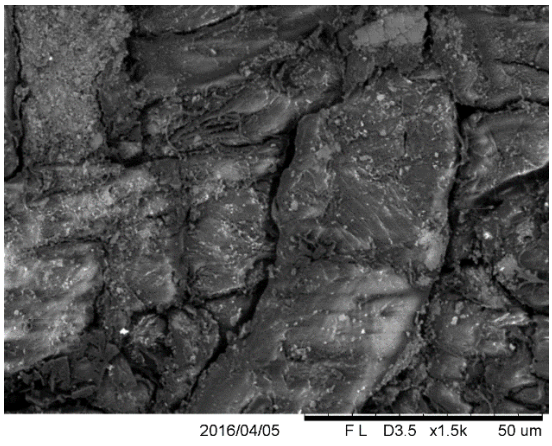

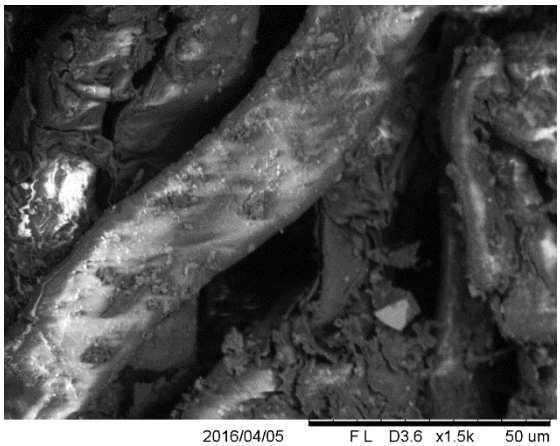

(c) **(d)**

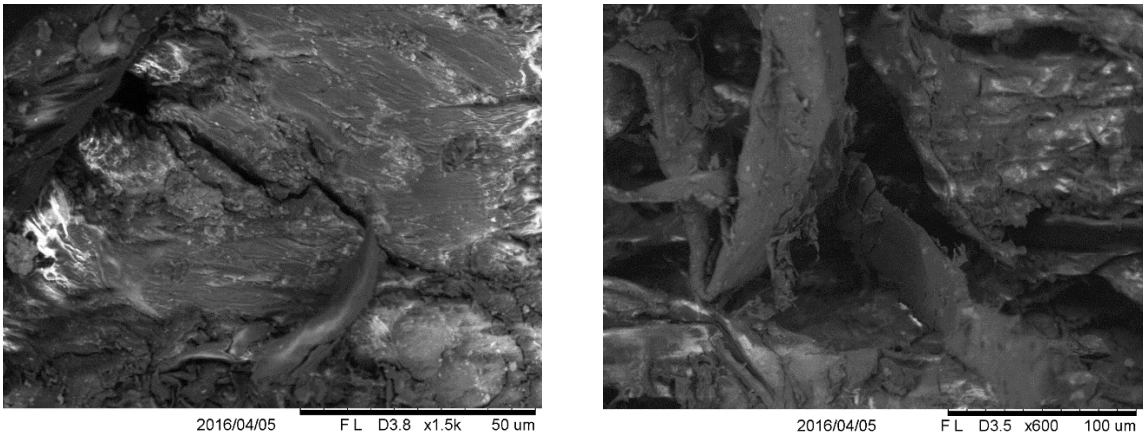

(e) **(f)**

Figure 6.4. SEM images of (a) shredded plastics, (b) blended fiber, (c) pelletized wood fiber containing 0% plastic ($CF_{P0\%}$), (d) pelletized composite wood fiber containing 2% plastic ($CF_{P2\%}$), (e) pelletized composite wood fiber containing 5% plastic ($CF_{P5\%}$), and (f) pelletized composite wood fiber containing 10% plastic ($CF_{P10\%}$).

6.3. Results and Discussion

In this section, we present the result of the thermo-chemical experiments explained in the methodology section. The material characterization was used to interpret the behavior of composite pellets during thermo-analytical tests. The thermal conductivity experiment results justified the outcomes of the thermo-analytical experiments.

6.3.1. Biomass characterization

With respect to elemental analysis, proximate analysis parameters include sulfur, moisture, volatile matter, ash, and fixed carbon. Ultimate analysis is dependent on quantitative analysis of various elements present in the composite wood pellet such as carbon, hydrogen, sulfur, oxygen, and nitrogen (Madadian, Lefsrud et al. 2016). The results of proximate and ultimate analysis of biomass samples are shown in Table 6.1.

Table 6.1. Proximate and ultimate analysis of composite pelletized wood fiber and plastic.

	Testing item	Waste plastic [1]	Fiber (unpelletized) [1]	Pelletized composite fiber with 0% plastic	Pelletized composite fiber with 2% plastic	Pelletized composite fiber with 5% plastic	Pelletized composite fiber with 10% plastic
Proximate Analysis	Moisture content (%)	4.78	6.27	6.3	6.24	6.20	6.12
	Volatile matter (%)	94.19	85.78	85.7	85.95	86.20	86.62
	Fixed carbon (%)	0.00	3.45	3.45	3.38	3.28	3.11
	Ash content (%)	1.03	4.50	4.2	4.43	4.33	4.15
Ultimate Analysis	Carbon (%)	77.00	44.95	44.94	45.59	46.55	48.16
	Hydrogen (%)	13.97	5.92	5.92	6.08	6.32	6.73
	Nitrogen (%)	0.29	0.18	0.18	0.18	0.19	0.19
	Sulfur (%)	0.19	0.19	0.19	0.19	0.19	0.19
	Oxygen (%)	2.73	37.99	38.46	37.48	36.42	34.66
	HHV (MJ/kg)	40.01	17.09	17.09	17.55	18.24	19.38

1 As-received basis

6.3.2. TGA of undensified fiber and plastics

The TGA and derivative of thermogravimetric (DTG) analysis of unpelletized fiber and plastics continuously monitored the mass change of the feedstock as function of temperature and time. For this purpose, we used the following linear temperature-time relationship

$$T_t = T_0 + ct \qquad (1)$$

where T_t, T_0, and c are the temperature at time t, the initial temperature, and the heating rate, respectively.

These samples were examined individually as baseline to have better understanding of the mixtures decomposition behavior (Figure 6.5). A typical weight loss step normally happens in the range of 200-300ºC and develops gradually from the initial horizontal TGA curve.

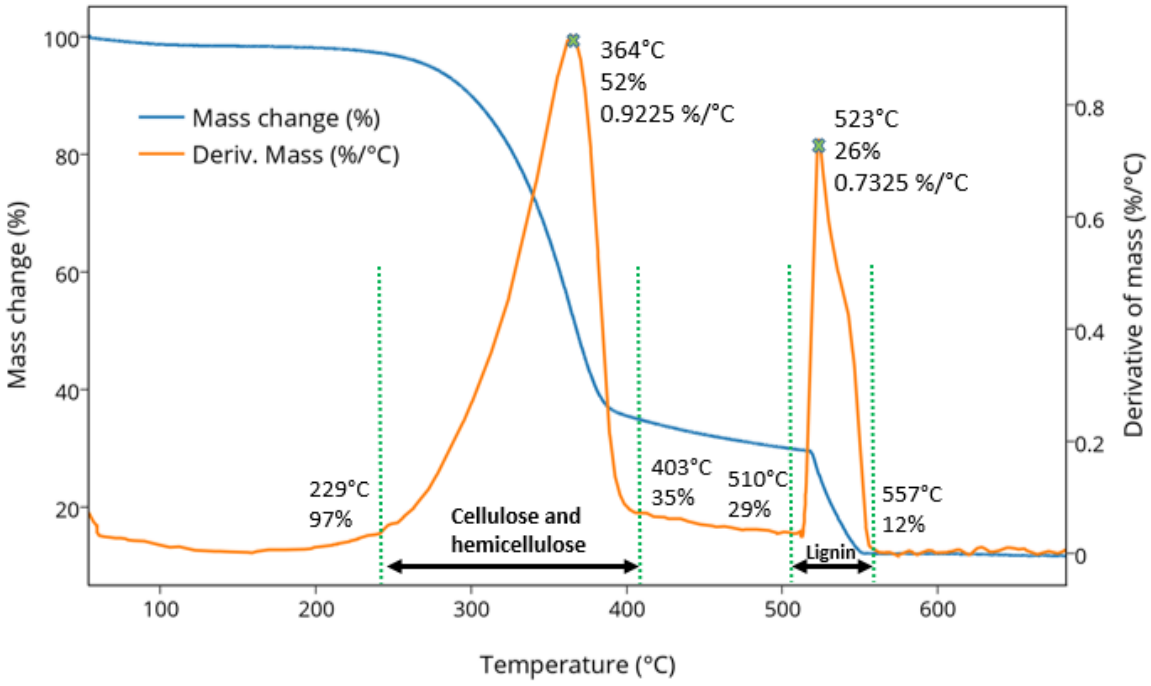

(a)

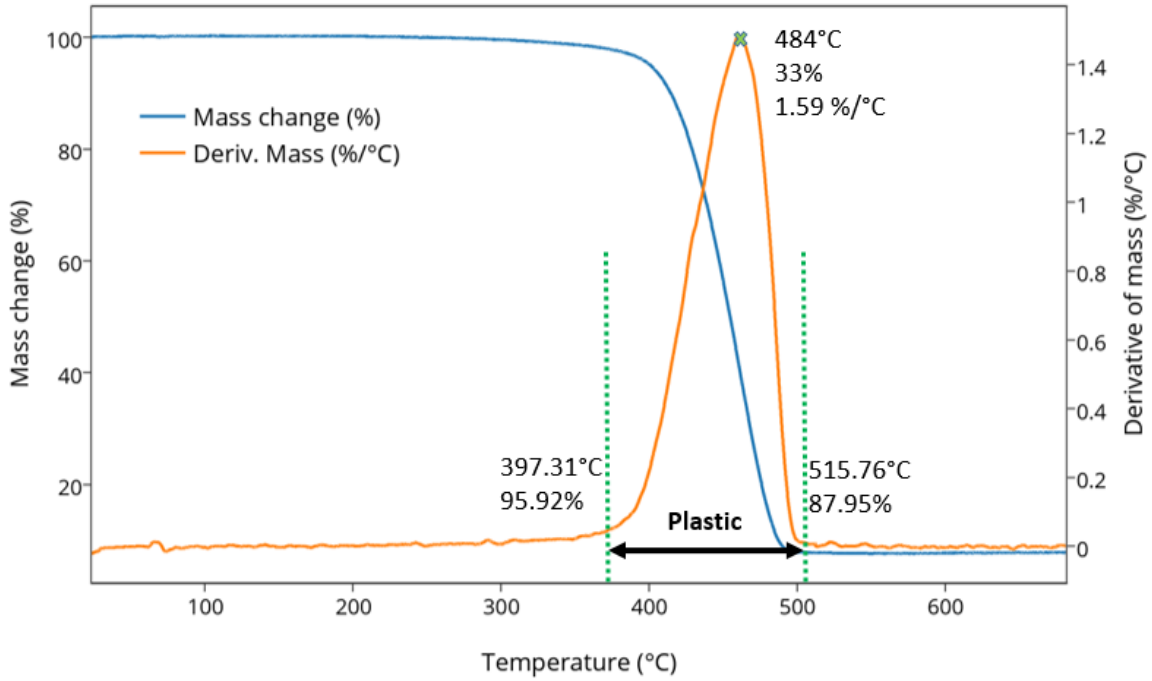

(b)

Figure 6.5. Thermal degradation of undensified (a) wood fiber and (b) plastics using thermogravimetric analysis

As a whole, the thermal degradation of unpelletized wood fiber was characterized in two main phases. As shown in Figure 6.5a, the first phase of reactions developed during the range of 252-402 ºC. The first temperature peak occurred at 365 ºC in the DTG curve derivative and indicated the point of greatest rate of change on the mass loss. The point is mathematically called as point of inflection where the decomposition intensity reaches the maximum of 0.9224 wt % $ºC^{-1}$ followed by a drastic drop. This can be attributed to decomposition of hemicellulose and cellulose parts of the wood fiber. Due to the negligible moisture content of the material, there was no horizontal drop at around 100 ºC. The second phase developed in the interval between 510-560 ºC

and hit a higher temperature peak of 524 ºC while a lower decomposition intensity of 0.7378 wt % $ºC^{-1}$. The remaining lignin part of the lignocellulosic feedstock decomposed in this phase.

As for plastics, the thermal degradation took place in a single phase. This phase ranged between 382-502 ºC and reached the peak and decomposition intensity at 461 ºC and 1.484 wt % $ºC^{-1}$, respectively (Figure 6.5b). The results showed that plastics have higher tendency to decompose when the temperature reached closer to the decomposition temperature

6.3.3. Composite wood fiber and fuel

6.3.3.1. TGA analysis

With regard to the composite wood fiber mixed with several ratios of plastics, Figures 6.6 and 6.7 show their thermal degradation behavior under thermal conditions of pyrolysis and gasification.

The plastic free fiber pellet ($CF_{P0\%}$) demonstrated almost exactly the same trend as unpelletized fiber (Figure 6.6a). The thermal degradation of the pelletized fiber was characterized in two main stages. The first stage evaluation indicated that about 70 wt% of the volatile matter was released in the range of 230-423 ºC. The temperature reached a peak at 376 ºC with a decomposition intensity of 0.8854 wt% $ºC^{-1}$ which was almost the same as the one for unpelletized fiber. The second stage was developed in the interval of 509-567 ºC in which the temperature peaked at 524 ºC with the degradation rate of 0.7269 wt% $ºC^{-1}$. The results implied that there was no noticeable change between the pyrolytic behavior of the pelletized and unpelletized wood fiber as shown in the thermogravimetric analysis.

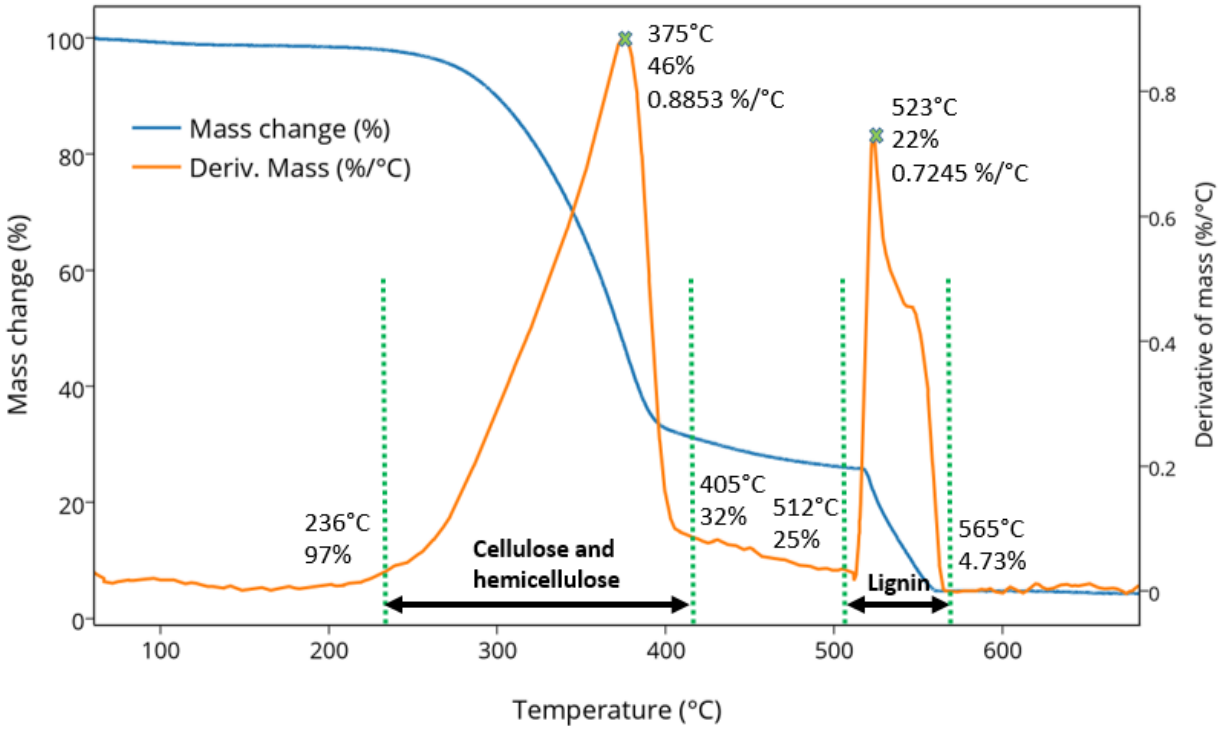

(a)

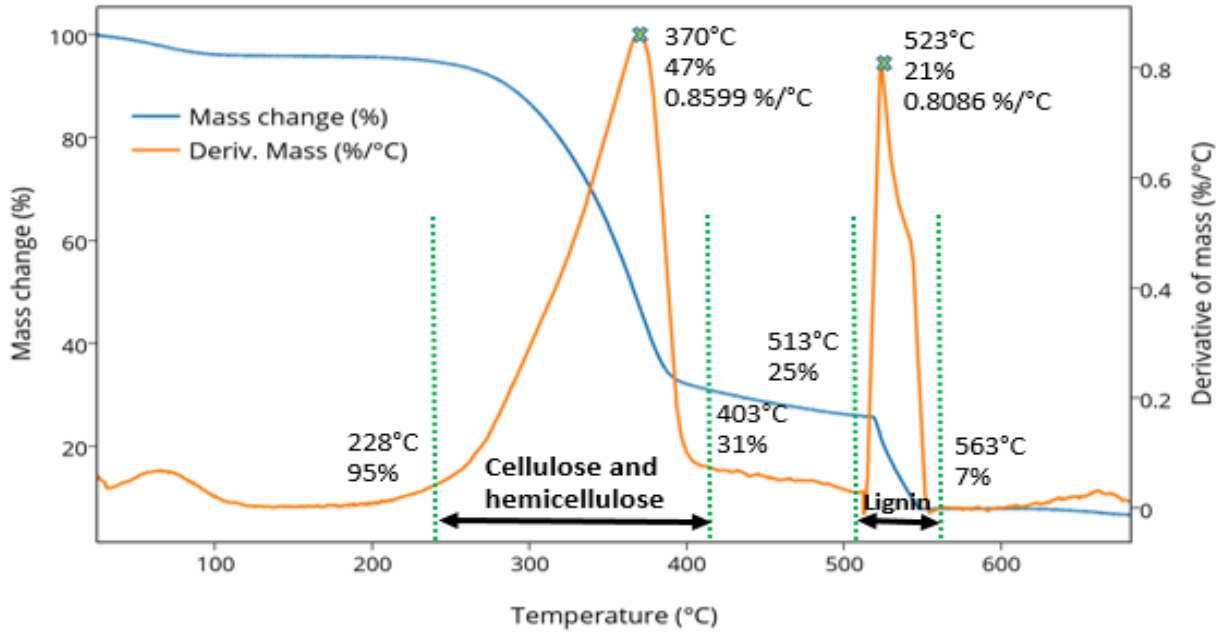

(b)

Figure 6.6. Thermal degradation of (a) pelletized wood fiber ($CF_{P0\%}$), and (b) pelletized composite wood fiber containing 2% plastics ($CF_{P2\%}$) using thermogravimetric analysis.

The pyrolytic behavior of the pelletized composite wood fiber containing 2% plastics indicated to some extent a similar trend as for the fiber pellet. As shown in Figure 6.6b, the thermal degradation of $CF_{P2\%}$ was characterized in two principle phases. The first temperature peak was reached at 370 º and in the interval 228-409 ºC. This showed that there is no effect of plastic content on the decomposition of fiber in this phase. The decomposition intensity of this stage was measured at 0.8603 wt% $ºC^{-1}$. It is within the second phase, which exhibited a similar reaction as the plastics, a higher temperature peak at 524 ºC was denoted in a time period of 2 min. Decomposition intensity was measured at 0.8086 wt% $ºC^{-1}$ which was slightly higher than that of its corresponding value for $CF_{P0\%}$. The higher decomposition rate was due to the existence of plastics in the pellet. The result was consistent with the results presented for plastics waste in which the decomposition took place in a single stage. The peak exhibited in the second phase is the consequence of the overlap of the decomposition of plastics and remaining lignin from the lignocellulosic wood fiber. The cellulose and hemicellulose were removed in the first degradation phase. It should be noted that the additional 2% plastics did not make any change in the number of thermal change. This difference is mainly due to the different thermal peaks of fiber and plastics which were measured at 365 ºC and 524 ºC for cellulose and hemicellulose respectively in fiber and 461 ºC for plastics.

With regard to the pelletized composite wood fiber containing more than 5% plastics (i.e. $CF_{P5\%}$ and $CF_{P10\%}$), their thermal degradation was characterized in three main stages as shown in Figure 6.7a and Figure 6.7b. As shown, the first temperature peak is reached at 372 ºC for $CF_{P5\%}$ and $CF_{P10\%}$, and at almost the same decomposition rate of 0.72 wt% $ºC^{-1}$. This similarity

implies that the plastic content does not influence the behavior of the first stage of thermal degradation of the composite pellets since the plastics degrade around 461 ºC. It is the second temperature peak recorded at 485 ºC, for both composite pellets, that justifies the plastics degradation in the range of 408-513 ºC. The decomposition intensity of $CF_{P5\%}$ in the second stage was slightly lower than $CF_{P10\%}$. Additionally, the third stage was peaked at similar temperatures 523 ºC for both $CF_{P5\%}$ and $CF_{P10\%}$ and at almost similar intensity of 0.672 and 0.599 wt.% $ºC^{-1}$, respectively.

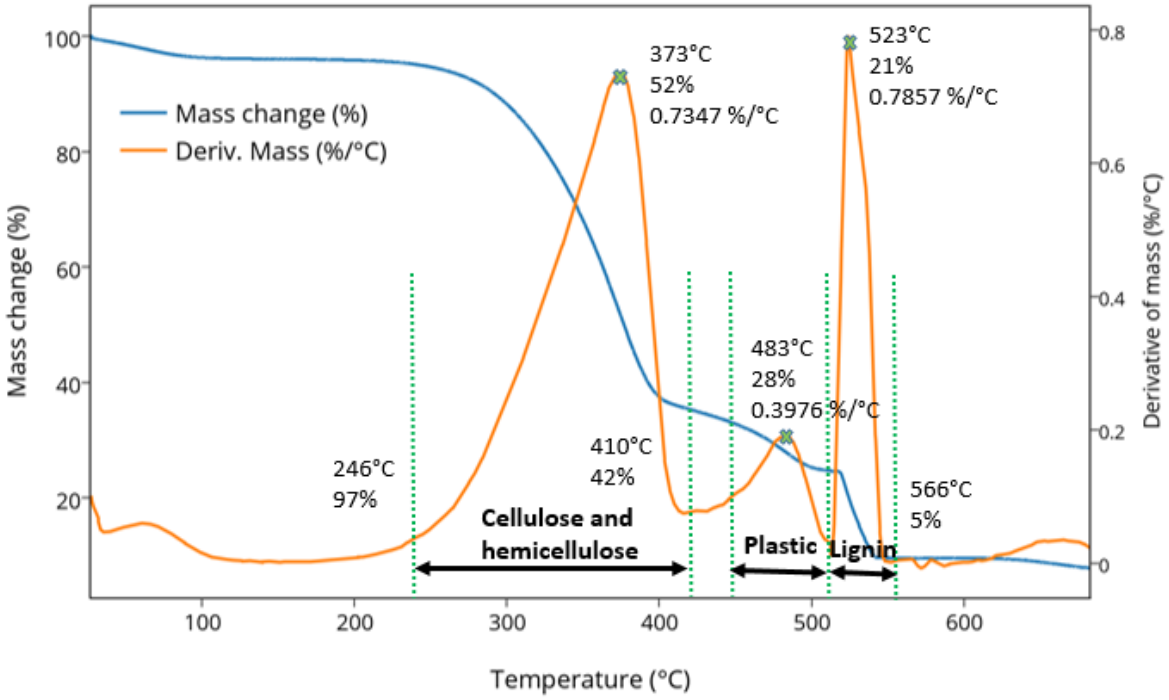

(a)

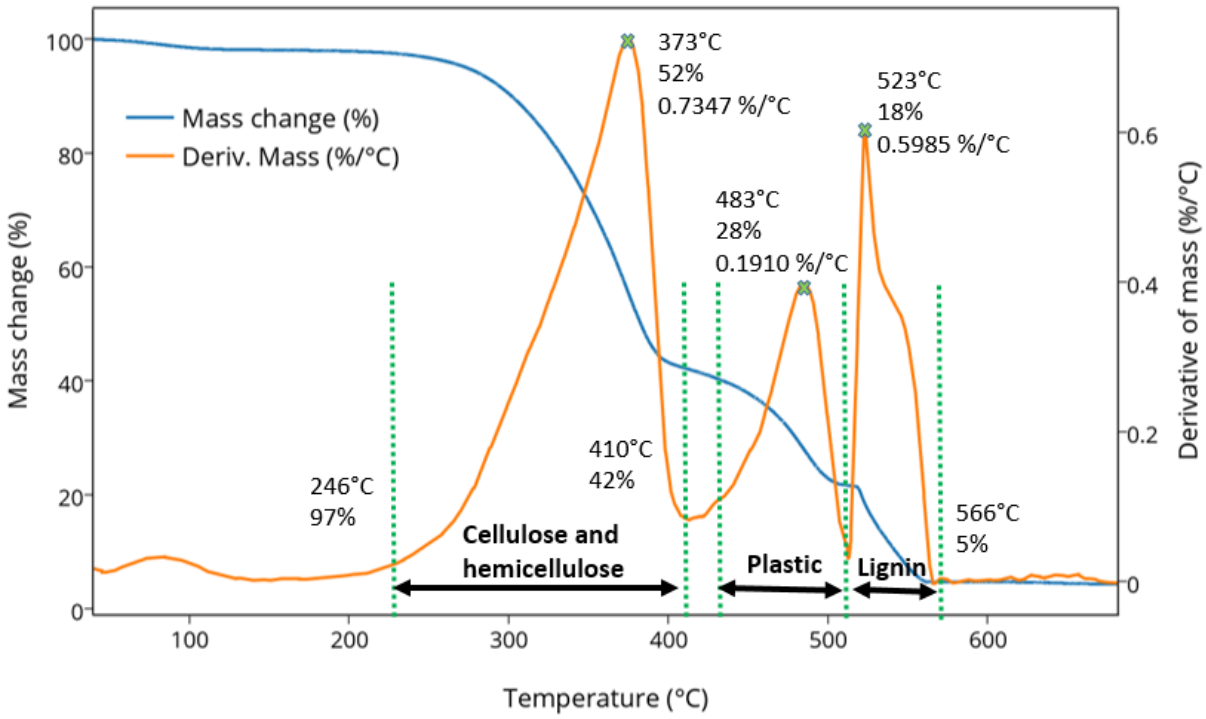

(b)

Figure 6.7. Thermal degradation of (a) pelletized composite wood fiber containing 5% ($CF_{P5\%}$) plastics, and (b) pelletized composite wood fiber containing 10% ($CF_{P10\%}$) plastics using thermogravimetric analysis.

6.3.3.2. DSC analysis

The DSC thermograms of the biomass feedstocks are plotted in Figures 6.8 to 6.10. As shown, the ordinate axis of the DSC data was reported in units of milliwatts (per gram) when the instrument underwent sensitivity or enthalpy calibration. The thermogram abscissa was expressed in terms of temperature. There are four main parameters discussed here for each thermogram, namely enthalpy change (ΔH), extrapolated peak onset temperature (T_{onset}), average specific heat ($C_{p\ ave}$) and maximum specific heat ($C_{p\ max}$). All the parameters except specific heat values were calculated directly by the TA Universal Analysis Software (TA Instruments, Delaware, USA). The

extrapolated peak onset temperature helps to define the melting point, because compared with the peak temperature, the extrapolated onset temperature is less dependent on heating rate, sample thermal conductivity, sample mass, and sample thickness (Sun and Simon 2007).

In case of blended fiber and shredded plastics, the DSC thermograms demonstrated only a peak in the downward direction representing endothermic behavior of the material when undergoing a linearly increasing temperature from 25^{o}C to 220^{o}C. Integration of the DSC peaks provided a measure of the total amount of energy consumed or released during the reaction, in this case -103.73 J g^{-1} and -106.67 J g^{-1} for blended fiber and shredded plastics, respectively, which show that both are only consuming energy using the mass of the samples just before the reaction. The higher enthalpy of plastics implied its greater heat content change than with blended fiber. The endothermic reactions for blended fiber initiated at 71^{o}C which is quite close to the one for shredded plastics at 78^{o}C. Additionally, blended fiber exhibited its glass transition event with a wider enthalpic relaxation peak at 107°C comparing to shredded plastics in which the glass transition demonstrates a sharp peak at 121°C. The average specific heat for the blended fiber was 10.71 mJ $^{o}C^{-1}$ and it reached to 17.049 mJ $^{o}C^{-1}$ at the reaction's peak. Although the maximum specific heat value of plastic (17.14 mJ $^{o}C^{-1}$) was similar to blended fiber, its lower average value (6.28 mJ $^{o}C^{-1}$) showing lower potential to hold the heat and energy (Figures 6.8a and 6.8b).

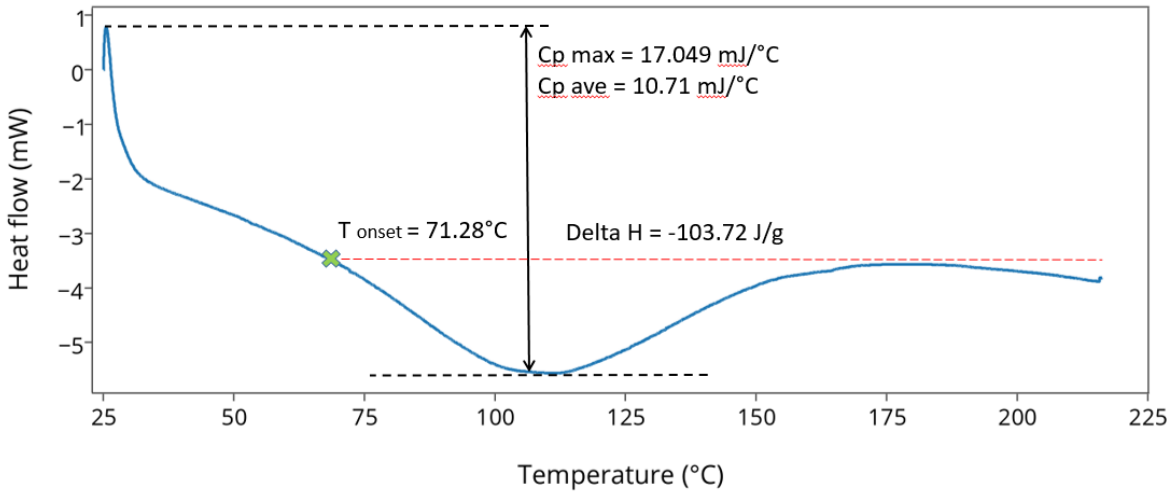

(a)

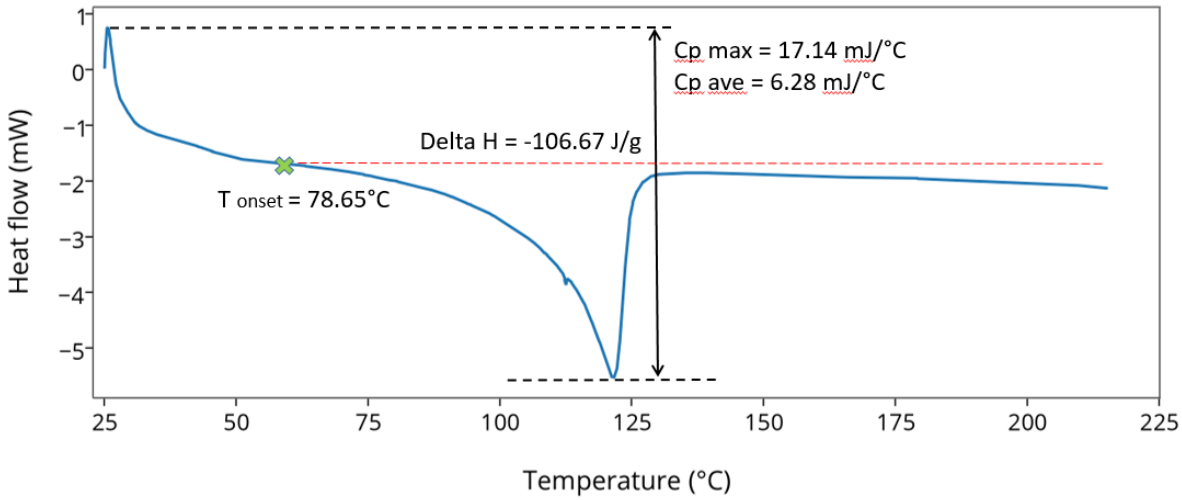

(b)

Figure 6.8. Thermodynamic parameters thermogram of (a) undensified wood fiber, and (b) shredded plastics using Differential Scanning Calorimetry, heating rate 20 ºC min^{-1} in a nitrogen atmosphere.

In respect to pelletized composite biomass, $CF_{P0\%}$ began to undergo the endothermic reaction at a temperature of 74.85°C and the peak temperature occured at 118°C. This represented the maximum rate of heat absorption at the given heating rate conditions (20 $^{o}C\ min^{-1}$).

Similar phenomenon was observed in the cases of 2% plastic contained composite pellet ($CF_{P2\%}$), for which glass transition temperature began at a temperature of 82.74°C and peaked at 127°C. The greater enthalpy change for $CF_{P2\%}$ (-224.67 J g^{-1}) than $CF_{P0\%}$ (-273.15 J g^{-1}) indicated that adding plastic increased the ability of heat content change considering the higher enthalpy of shredded plastics than blended fiber as shown in Fig. 9a and Fig. 9b. The additional plastic content enhanced the heat capacity values as $CF_{P0\%}$ demonstrated 15.99 mJ $^{o}C^{-1}$ and 25.39 mJ $^{o}C^{-1}$ for average and maximum heat capacity compared to the ones from $CF_{P2\%}$ at 21.76 mJ $^{o}C^{-1}$ and 33.84 mJ $^{o}C^{-1}$.

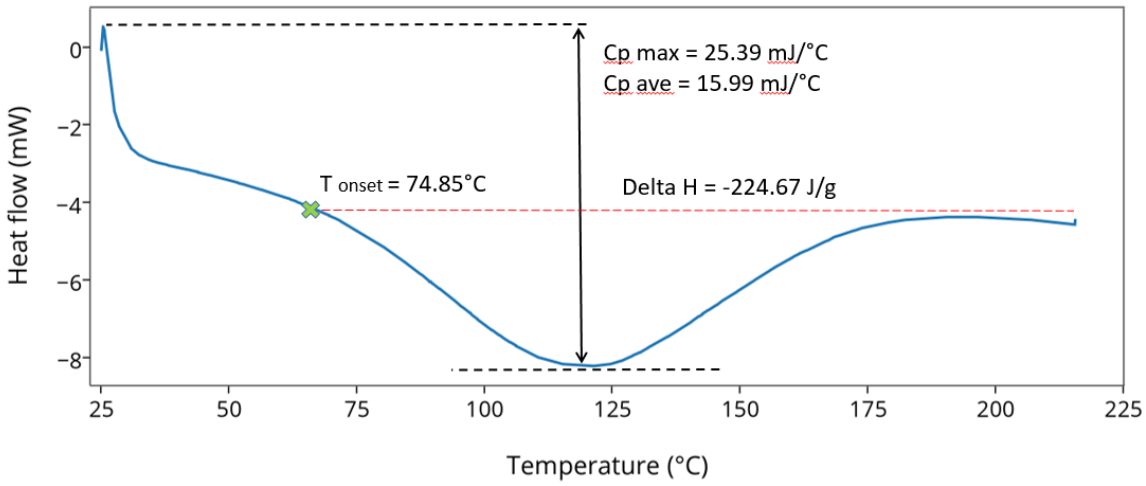

(a)

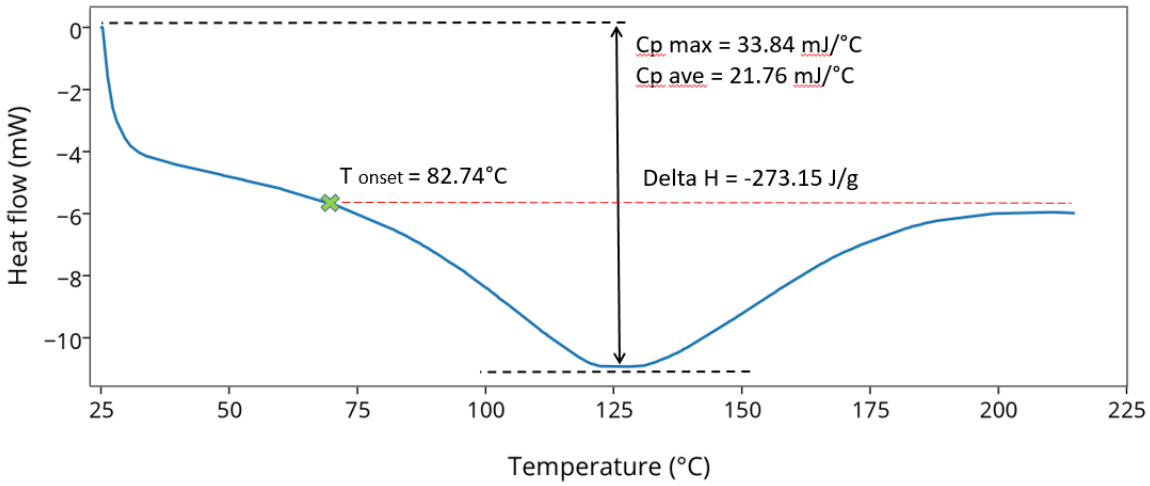

(b)

Figure 6.9. Thermodynamic parameters thermogram of: (a) pelletized wood fiber ($CF_{P0\%}$), and (b) pelletized composite wood fiber containing 2% plastics ($CF_{P2\%}$) using Differential Scanning Calorimetry with a heating rate of 20 ºC min^{-1} in a nitrogen atmosphere.

Displayed in Figures 6.10a and 6.10b are the results of the DSC analysis obtained on the $CF_{P5\%}$ and $CF_{P10\%}$. The curves showed a displacement at around 50°C arising from the glass transition and peaks at extrapolated onset temperature of about 74°C and 82°C for melting, respectively. In the figures, the transition is particularly well defined. Similar to the other composites, $CF_{P5\%}$ and $CF_{P10\%}$ also show endothermic behavior by increasing temperature. The glass transition began and peaked at similar temperatures of 64°C and 130°C. Furthermore, increasing the plastic content over 2% (i.e. 5% and 10%) led to drastic rise in the enthalpy changes in which case they were -301.38 J g^{-1} and -444.05 J g^{-1} for $CF_{P5\%}$ and $CF_{P10\%}$, respectively.

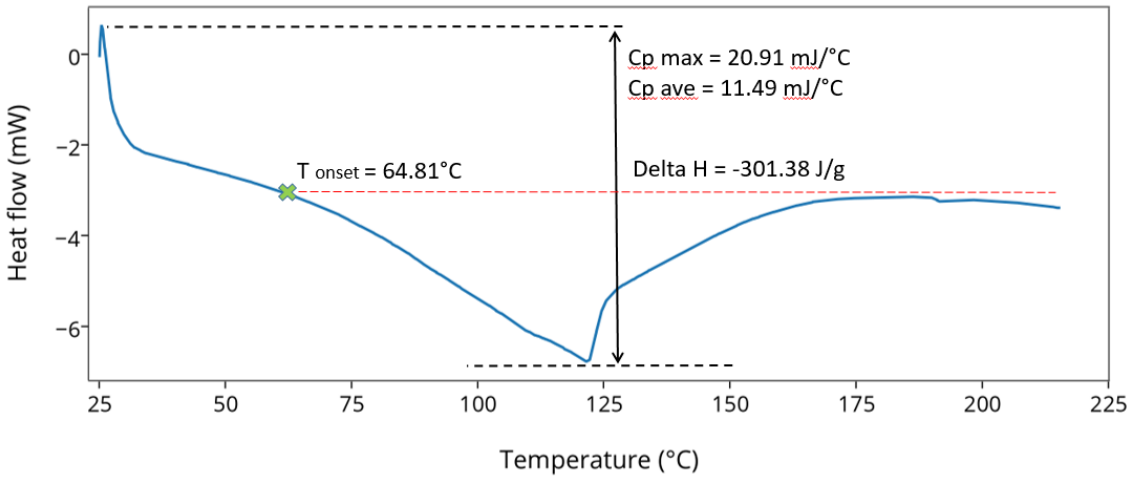

(a)

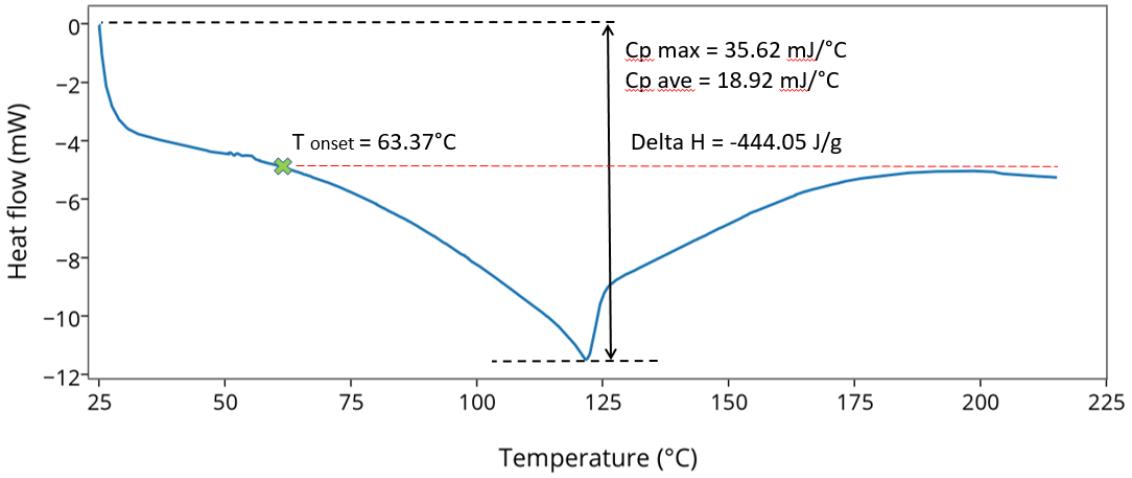

(b)

Figure 6.10. Thermodynamic parameters thermogram of pelletized composite wood fiber (a) containing 5% ($CF_{P5\%}$) plastics, and (b) containing 10% plastics ($CF_{P10\%}$) using differential scanning calorimetry, heating rate 20 $^{o}C.min^{-1}$ in a nitrogen atmosphere.

As noted previously, for each of the individual and composite wood fiber and plastic pellets, three samples each were subjected to DSC analysis for a total of 18 thermograms. Values of onset and peak temperatures for the peaks were compared by ANOVA to determine if there are any

significant differences among the composite pellets with different plastic contents. Mean values were considered to be significantly different for $\alpha < 0.05$. Table 6.2 summarizes the means and standard deviations (S.D.) of the onset and peak temperatures for the endothermic transformation found by DSC thermograms for the individual and composite biomass feedstocks.

Table 6.2. Onset and peak temperatures (°C) for the endothermic transformation (i.e. peaks in downward direction) observed for individual and composite pellets of fiber and plastics

Biomass	**DSC**		
	Onset	Peak	Average specific heat ($C_{p\ ave}$)
Blended fiber	71.28 (1.07)[a]	107.43 (1.40)[a]	10.71 (0.84)[a]
Shredded plastics	78.65 (0.92)[b]	121.71 (1.52)[b]	6.28 (0.75)[b]
$CF_{P0\%}$	74.85 (1.05)[a]	118.38 (1.18)[b]	15.99 (0.89)[c]
$CF_{P2\%}$	82.74 (0.84)[b]	127.14 (2.47)[c]	21.76 (1.50)[d]
$CF_{P5\%}$	64.81 (0.90)[c]	130.73 (1.14)[c]	11.49 (1.04)[a]
$CF_{P10\%}$	63.37 (0.82)[c]	129.96 (2.74)[c]	18.92 (0.92)[d]

[a, b, c, d] Values are mean (S.D.) for n = 3, and means in a given column with the same letters (a, b, c, d) are not significantly different ($\alpha > 0.05$).

6.1.1. Thermal conductivity

As shown in Figure 6.11, the thermal conductivity of blended fiber was measured as 0.0594 W $m^{-1}K^{-1}$ which was slightly higher than shredded plastics 0.0535 W $m^{-1}K^{-1}$. Granted that plastics had lower thermal conductivity compared to fiber, the composite pellets with higher percentage of plastics had lower bulk thermal conductivity, therefore,

$$k_{belnded\ fiber} > k_{Shredded\ plastic} \quad (2)$$

$$k_{\mathrm{CF_{P0\%}}} > k_{\mathrm{CF_{P2\%}}} > k_{\mathrm{CF_{P5\%}}} > k_{\mathrm{CF_{P10\%}}} \quad (3)$$

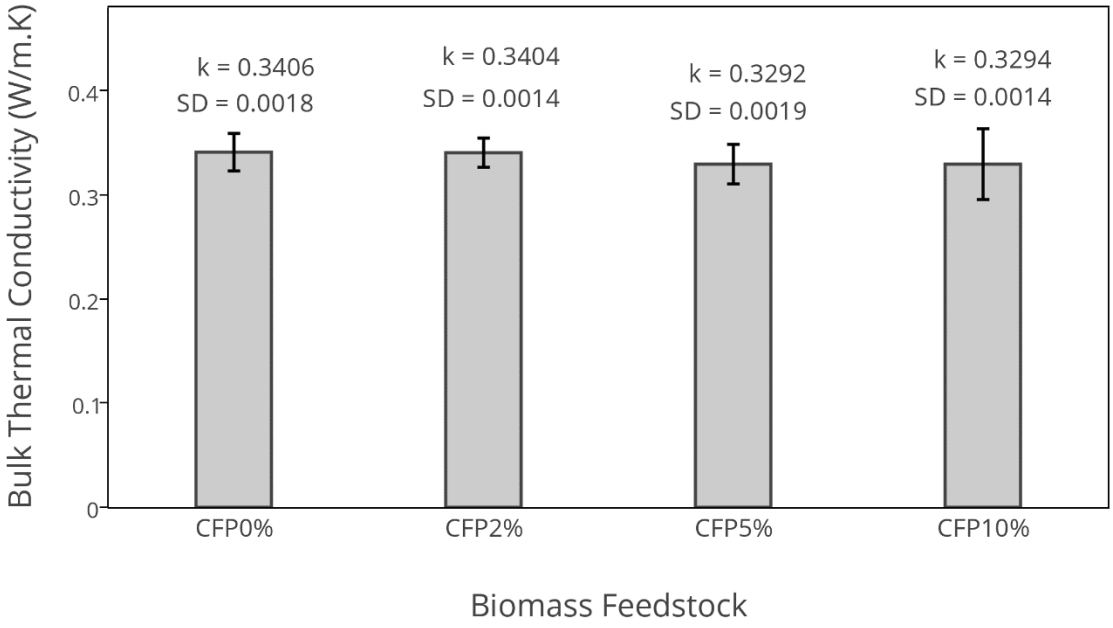

(a)

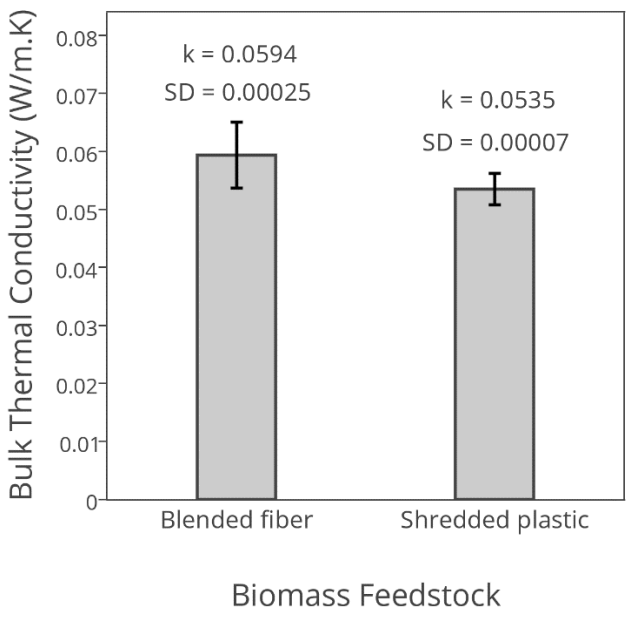

(b)

Figure 6.11. Bulk thermal conductivity: (a) Individual blended fiber and shredded plastics and (b) Composite wood pellets using the Hot Disk Transient Plane Source (TPS) technique. The values and their standard deviations are presented as k and SD.

6.4. Conclusion

The thermo-chemical investigation of composite pellets of blended fibers and plastic sheds light to better understand the thermochemical conversion of pelletized wood pellets. Although the behavior of composite pellets is a function of their constituent, their pelletized mixture may behave differently within the higher temperatures occurring during the thermochemical conversion. We specifically draw the following conclusions:

- Both physical properties and composition and history of composite constituents may affect the thermal analysis parameters such as glass transition.

- The higher plastic content increased the temperature and consequently should increase the specific heat value, however, due to the presence of unknown plastics from municipal solid waste stream, there were few discrepancies. The specific heat depends to some extent on the type and source of biomass.
- The higher volume fractions of plastic (i.e., 5% and 10%) in the composite pellet have greater impacts on its thermal degradation.
- The enthalpy changes for glass transitions of all composite pellets were endothermic.
- The glass transition developed by increasing the plastic content of the pelletized composite biomass. However, the extrapolated peak and onset temperatures defining the points at which composite pellets changed from a glassy state to a more pliable state, were found to be independent of composite plastic content. This phenomenon may be associated with the unknown types of plastics with different thermal decomposition rates used in the manufacturing process of composite materials.
- Increasing plastic volume fraction slightly reduced the thermal conductivity of the composite pellets which tailors the thermal energy content of the composite pellets.

Acknowledgment

This research is funded by BioFuelNet Canada, a network focusing on the development of advanced biofuels. BioFuelNet is a member of the Networks of Centres of Excellence of Canada program. We also gratefully acknowledge the technical support by *Thermtest thermophysical instruments* in New Brunswick on conducting thermal conductivity tests.

Connecting Text

In Chapter 6, the thermochemical characteristics of composite material (fiber and waste) were analyzed and it was concluded that adding more plastic to the matrix of the composite pellets would increase the number of degradation stages. Using Hot Disk Transient Plane Source (TPS) technology, it was shown that composite pellets with higher volume-fractions of plastics possessed a lower thermal conductivity. Finally, the results of pelletized fiber-plastic composites were compared with undensified fibers and plastics to identify the accessible boundaries for the thermo-chemical properties of fiber-plastic solid fuels.

In Chapter 7, the main focus will be on the physico-chemo-mechanical behaviour of pelletized composite material. The fundamental physical analysis of composite pellets is examined along with the mechanical performance to understand the contribution of mechanical (and/or gravitational) load on the pellets.

Chapter 7 has been published for publication as:

Madadian E., Akbarzadeh A.H., Orsat V., & Lefsrud M. (2016). Pelletized Composite Wood Fiber Residues Mixed with Plastic Wastes as Advanced Solid Biofuels: Physico-Chemo-Mechanical Analysis. *Waste and Biomass Valorization*, DOI:10.1007/s12649-017-9921-1.

Chapter 7

7. Pelletized Composite Wood Fiber Residues Mixed with Plastic Wastes as Advanced Solid Biofuels: Physico-Chemo-Mechanical Analysis

Abstract

Characterization and prediction of the physico-chemo-mechanical properties of pelletized wood fiber composites are essential for design considerations and optimization of thermochemical conversion pathway of biomass in order to produce bioenergy. The purpose of this study is to evaluate the physico-chemo-mechanical performance of composite wood residues pellets blended with plastic wastes as potential feedstocks for producing advanced biofuels through gasification technology. The biomass feedstocks were blended in 5% volume fraction of plastics and pelletized in different diameters. The composite pellets were compressed longitudinally and laterally using a universal testing machine to evaluate their mechanical properties. The pellets were treated identically at 3% moisture content as received, and ambient temperature 25^{o}C. The compression test results showed that pellets with larger diameters have higher elastic limits. With respect to transverse direction, there was no certain relationship between stress-strain values and pellet size. The incompatibility in the relation between the increase of yield stress and diameter was attributed to the unknown type of plastics used in composites plastic wood pellets. As a consequence, we predicted the type of plastics used in the composites using the rule of mixture considering the young's modulus of composites, the wood fiber, and the volume fractions of the constituents. We measured the angle of repose of the composite wood pellets, which ranged between 25^{o} for the

largest sample (14mm diameter) to 41^{o} for the smallest pellets; it implies that the pellets with smaller diameters have lower chance of slumping in the feeding drum during the gasification of pellets. It was shown that the angle of repose would increase with the moisture content in all the composite pellets. Larger pellet sizes with higher bulk density demonstrated a smaller angle of repose. In this paper, we presented the results from chemical analysis and inductively coupled plasma mass spectrometry (ICP-MS) to identify the existing minerals in composite pellets which may not only change their thermophysical properties but also the environmental impact of the syngas produced during the thermochemical conversion of biomass through gasification. The chemical analysis was presented in conjunction with microscopic imaging to understand the microstructural interaction between plastic and wood fibers in the composite pellets. Lastly, the experimental measurements of temperature profile of gasification for composite pellets with different sizes demonstrated the size-effect of the thermochemical behavior of pelletized biomass in the reactor, a phenomenon which needs further detailed investigations.

Keywords: Mechanical characterization, Angle of repose, Gasification, Elemental chemical analysis, Pellet size

7.1. Introduction

To deal with the scarcity of conventional fuels and to reduce air pollution and greenhouse gas emission, bioenergy and biofuels are gradually becoming more attractive to the public. The use of biomass for energy production incorporates the benefits of reduced CO_2 emissions from combustion of fossil fuels, reduced SO_2 formation through a decrease in fuel bound sulfur, and reduced NOx formation through a reduction in fuel bound nitrogen (Verma, Bram et al. 2012).

Emission and conversion efficiency of biomass energy systems vary as a function of fuel quality, implemented technology, and operational conditions such as temperature and pressure. The physico-chemical and thermal properties of biomass solid fuels, such as bulk and energy density, heating value, chemical composition, moisture content and ash contents, are essential properties of new composite pellets to be evaluated for their commercial residential application (Verma, Bram et al. 2009, Verma, Bram et al. 2012).

Pellets are compressed solid fuels of high density and high combustion efficiency. Its geometry and cylindrical form facilitates transportation over long distances, compact storage, and control feeding to boilers and burners. These attractive properties have resulted in soaring demand for wood pellets in Europe and North America (Di Giacomo and Taglieri 2009, Heinimö and Junginger 2009, Acda 2015, Guo, Wang et al. 2016). Global wood pellet production has grown rapidly since 2000, and is currently over 11 million tons per year (Lamers, Junginger et al. 2012). Wood pellet production and consumption increased in2003 to 2007 by 30% and 28% respectively in Canada (Peng, Bi et al. 2010). As of 2012, Canada had 42 pellet plants with 3 million tonnes annual production capacity (Canada 2016).

The quality of pelletized fuel is typically assessed in terms of its density and durability. High density of pellet represents higher energy per unit volume of material, while durability is the resistance of pellets to withstand various shear and impact forces applied during handling and transportation. High bulk density increases storage and transport capacity of pellets. Since feeding of boilers and gasifiers generally is volume-dependent, variations in bulk density should be avoided (Larsson, Thyrel et al. 2008).

The possibility of using municipal solid wastes (MSW) in the development of composites is very attractive, especially with respect to the large quantity of plastic waste generated daily. Hence, the

development of new value added products, to utilize the recovered plastics, is assuming greater importance (Diop and Lavoie). The addition of recycled wood fibers to waste plastics renders the resulting composites viable from both the mechanical properties and the environmental points of view (Ashori and Nourbakhsh 2009). Over the past few decades, polymers have replaced many conventional materials, such as metal and wood, in many applications. (Nuñez, Sturm et al. 2003, Kuo, Wang et al. 2009). Plastic waste is one of the major components of global municipal solid waste (Cui, Lee et al. 2008). The worldwide production of plastics is approximately 100 million tons per year resulting in a significant proportion in municipal solid waste (Hannequart 2004, Adhikary, Pang et al. 2008). Most of the research on wood and recycled high-density polyethylene (HDPE) composites has concentrated on the use of either a single type of plastic from the waste stream, or a simulated mixing of waste plastics or mixing of recycled and virgin plastics (Adhikary, Pang et al. 2008).

Physical properties of biological materials are a prerequisite for the design of equipment for handling, dehulling, expression etc. These physical properties include shape, size, bulk density, apparent density, angle of repose, porosity and mass (Tunde-Akintunde, Olajide et al. 2005). Low durability of pellets results in problems like disturbance within pellet feeding systems, dust emissions, and an increased risk of fire and explosions during pellet handling and storage (Temmerman, Rabier et al. 2006). Compression testing is widely used to determine the stress/strain behavior of solids. It has the inherent advantage of simplicity in which circular cylinders are usually used and the specimen is loaded between relatively rigid platens to give a stress state of simple compression provided there is no constraint to movement at the loaded interfaces (Williams and Gamonpilas 2008). The stress-strain relationship is the most fundamental part of constitutive relationships. According to Hooke's Law, which has been generally used to describe this stress–

strain relationship for elastic mechanical processes, a stress– strain relationship should be linear. However, this linearity does not always apply to every case, and related moduli are stress-dependent for many applications (Zhao and Liu 2012). The mechanical properties of biomass feedstock may impact the thermal conversion. For instance, particle structure only affect the rate and duration of drying stage in the pyrolysis. Compressing particles in the palletization process bends the fibers and partially block some wood channels (Rezaei, Yazdanpanah et al. 2016, Sokhansanj and Webb 2016).

The demand for wood-plastic composites (WPCs) is experiencing a substantial growth in recent years (Zhong, Poloso et al. 2007). By increasing the popularity of composites application in the industry, a lot of research is being conducted to evaluate the mechanical properties of the composites. Predicting the overall mechanical properties of the composite is very important for material design and applications. There have been many attempts to correlate the overall mechanical properties of the composite and the properties of its constitutes (Kim 2000).

It is important to understand the fundamental mechanism of the biomass compression process, which is required to design energy efficient compaction equipment to mitigate the cost of production and enhance the quality of the product. To a great extent, the strength of manufactured compacts depends on the physical forces that bond the particles together. To fulfil this purpose, this study addressed the compressive properties of composite pellets with different size as well as the impact of adding plastics on the composite pellets. The motivation for the work described here arose from considering mechanical properties of composite wood fiber and plastics in conjunction with the results from thermochemical properties; these would help in identifying functionality of the composite pellets for further use in biorefineries.

7.2. Methodology

In this section, we considered a series of physico-chemo-mechanical characterization techniques for composite pellets with alternative sizes. The physical characteristics of pellets were mainly defined through bulk density, moisture content, and porosity of the pellets. The mechanical behavior of pellets was investigated by conducting uniaxial compression and angle of repose tests. Using elemental and inductively coupled plasma mass spectrometry (ICP-MS), chemical analysis was conducted for pelletized composite samples. In addition, we aimed to define the impact of the properties of pellets with the thermal behavior during gasification as representative of the thermo-chemical conversion pathway.

7.2.1. Biomass Feedstock

The test material used in this study was pelletized wood fiber mixed with plastics. The biomass feedstocks were taken from the municipal solid waste stream of Quebec City in Quebec, Canada. The fibrous material was initially provided in the blended form and then mixed with shredded plastics with volume fraction of 5% and densified into pellet. The composite pellets were cylindrical in shape in the range of 5 mm, 8 mm, 10 mm and 14mm in diameter corresponding with 9 mm, 17 mm, 18 mm and 20 mm in length, respectively (Figure 7.1).

Figure 7.1. Composite pellets of wood fiber and plastics in different sizes: 14mm, 10mm, 8mm, and 5mm (from left to right).

Many parameters can be measured to characterize pellets. In this study, the compressibility, moisture content, dimensions of pellets, bulk and true densities, and angle of repose were measured. The volatile matter, fixed carbon content and ash content of the material as proximate analysis and thermo-mechanically impact of the biomass behavior were measured. The biomass material, according to American Society for Testing Material (ASTM), were proximately analyzed for moisture content (ASTM 2013), ash content (ASTM 2013), fixed carbon (ASTM 2013), and volatile matter in the wood pellet (ASTM 2013). All samples were cured at ambient laboratory temperature and 50% relative humidity.

The physical properties of biomass feedstocks contributed to their convertibility function in combustors and gasifiers. Their physical characteristics can be both directly and indirectly related to the way in which they flow in reactors. The bulk density of pellets was calculated, according to ASTM D6683-14 (ASTM 2014), from the mass and volume of compacts (Table 7.1).

Table 7.1. Physical characteristics of biomass feedstocks

Feedstock	Moisture content* (mass%)	Volatile matter (mass%)	Fixed carbon (mass%)	Ash content (mass%)	Bulk density ($kg.m^{-3}$)	True density ($kg.m^{-3}$)	Porosity
Blended fiber	6.27	85.78	3.45	4.5	-**	-**	-**
Shredded plastics	4.78	94.19	0	1.03	-**	-**	-**
Wood fiber pellet (5mm)	6.3	85.7	3.45	4.2	287	471	0.39
Composite pellets	5mm 7	86.20	3.28	4.33	5mm 280	5mm 459	5mm 0.38
	8mm 8				8mm 274	8mm 423	8mm 0.35
	10mm 13				10mm 285	10mm 411	10mm 030
	14mm 15				14mm 302	14mm 427	14mm 0.29

* As received / **Not applicable

True density is the density of the solid material excluding the volume of any open and closed pores, while bulk density is the characteristic of volume of divided material such as powders, grains, and granules. Porosity (P) was calculated from the relationship between bulk (ρ_b) and true (ρ_t) densities as follows (Mohsenin 1970, Basu 2013). The measurement of true density of the biomass feedstocks was estimated using elemental analysis and the true density of their constituent elements.

$$\rho_t = \frac{Total\ mass\ of\ biomass}{Solid\ volume\ of\ biomass} \times 100 \quad (1)$$

$$P = \frac{\rho_t - \rho_b}{\rho_t} \times 100 \quad (2)$$

7.2.2. Mechanical Properties

The mechanical strength of pellets was described in terms of compressibility and flowability of material. The compressive characteristics of the pellets defined the extreme load that can be potentially applied to biomass feedstock during either storage or conversion process. Flowability is an index which influences compressibility and play a vital role during the biomass conversion. Madadian et al. (Madadian, Lefsrud et al. 2016) addressed flowability issue of biomass particles during gasification of wood pellet as a challenge that impacted the convertibility performance and efficiency of the process. The pellets were dried to provide similar conditions for measuring their mechanical performance.

7.2.2.1. Uniaxial Compression Test

Uniaxial compressive strength testing was performed according to ASTM D143 - 09, standard test methods for small clear specimens of timber. These test methods represent procedures for evaluating the different mechanical and physical properties, controlling factors such as specimen size, moisture content, temperature, and rate of loading. An INSTRON Universal Testing Machine

(M 4502, INSTRON Corp., Canton, MA) was used to perform the compression analysis under a pressure of 150 MPa and record the force-deformation of the composite pellets was recorded. During the compression of the pellets, a 10 kN load cell in the INSTRON machine was used to the pellets through a plunger (diameter 8.5cm) with the crosshead speed of 10 mm min^{-1}. It is of worth mentioning that the load applied on the samples varied which is what is recorded to compute the stress-strain curves. Ten samples of each size were selected for the compression test and the loading was conducted longitudinally and conversely. The tests were performed for three replications.

7.2.2.2. Angle of Repose

Angle of repose was measured using a steel truncated cone with a height of 500mm with a detachable base panel. The cone was filled with the composite pellets at different desired moisture contents and the base panel was quickly removed allowing the pellets to flow and assume its natural slope. The angle of repose was calculated by dividing the height of poured pellet pile by half the width of the base of the cone. The inverse tangent of this ratio is the angle of repose. The experiment was repeated 10 times for each feedstock to calculate the mean angle of repose.

The effect of moisture content and pellet diameter on angle of repose is shown in Table 7.2. The angle of repose ranged from 25^o to 41^o depending on moisture and size of the pellet. The results showed that the angle of repose would increase with the moisture content in all the composite pellets. Also, larger pellet size with higher bulk density demonstrated smaller angle of repose. The angle of repose was the highest at 41^o for the composite pellet of 5 mm in diameter with 8% moisture content, and the lowest at 25^o for the dried composite pellet of 14mm in diameter.

Table 7.2. Angle of repose for different size of composite pellet with different moisture contents

		Angle of repose (°)			
		Composite pellet (5mm)	**Composite pellet (8mm)**	**Composite pellet (10mm)**	**Composite pellet (14mm)**
Moisture content (%)	8	**41.50 ± 1.62**	**39.27 ± 1.26**	**38.03 ± 1.37**	**35.44 ± 1.4**
	6	**38.32 ± 1.43**	**35.46 ± 1.14**	**36.13 ± 1.25**	**32.08 ± 1.28**
	4	**34.76 ± 1.10**	**32.54 ± 1.34**	**31.49 ± 1.19**	**30.21 ± 1.53**
	0	**31.14 ± 1.16**	**30.11 ± 1.08**	**28.52 ± 1.2**	**25.84 1.02**

7.2.3. Toughness and Strain Energy

The toughness and strain energy of the composite pellets can be used as indicators of the strength of the material. Toughness is a material's resistance to fracture and is measured as the energy needed to cause fracture (Ritchie 2011). Toughness addresses the ability to absorb mechanical energy up to the point of failure. Toughness of polymers is often measured using Charpy and Izod impact test (Panda, Mohanty et al. 2013). A method for the determination of fracture toughness has been developed by calculating strain energy release rate directly from the results of impact tests on multiple specimens with different notch depths (Panda, Mohanty et al. 2013).

7.2.4. Chemical Properties

Elemental and inductively coupled plasma mass spectrometry (ICP-MS) analysis were conducted to identify the chemical composition of the composite pellets (Table 7.3). Conducting elemental analysis sheds lights on chemical compounds of pelletized feedstock which make an impact on the behavior of pellets during thermochemical conversion of composite pellets. The elemental analysis presented the portion of each chemical elements contributing in the biomass pellets and ICP-MS results complimented by addressing the amount of mineral in the composite pellet.

Table 7.3. Elemental and ICP-MS analysis of biomass feedstock

	Testing item	Shredded plastics	Blended wood fiber	Wood fiber pellet (5mm)	Composite pellet
Elemental analysis (mass%)	Carbon	77	44.95	44.94	46.55
	Hydrogen	13.97	5.92	5.92	6.32
	Nitrogen	0.29	0.18	0.18	0.19
	Sulfur	0.19	0.19	0.19	0.19
	Oxygen	2.93	38.18	38.46	36.42
ICP-MS analysis (ug/g)	Aluminum	-*	3022	3022	1507
	Magnesium	100	503	503	436
	Calcium	-*	21892	21892	17276
	Sodium	-*	1393	1393	927
	Potassium	-*	384	384	95

* Not applicable

As shown in Table 7.3, a few metallic elements contributing to the composite pellets in addition to the principal constituent elements of fiber and plastics. The detected metallic components were aluminum, magnesium, calcium, sodium and potassium. The presence of these metallic elements could cause changes to the porosity by changing the mass of the pellet and consequently changing the true density as shown in Equation 1. The high percentage of aluminum contents may emanate from aluminum sulfate which is the most extensively used chemical compound used in the papermaking industry. In the pulp and paper industry, the use of mineral fillers such as clay and calcium carbonate for paper production is a well-established practice which contributes to the cost and energy savings (Huang, Shen et al. 2013). There are a variety of minerals used in making acid and alkaline papers such as talc (a magnesium silicate mineral), hydrous kaolin, calcined carbonate, silica and silicates and titanium dioxides (Chauhan, Bhardwaj et al. 2013). These elements ultimately emerged in the wood fiber pellet coming from paper waste stream.

7.2.5. Gasification of different size of composite pellets

Gasification of composite pellets with different sizes were carried out in a pilot-scale fixed-bed reactor (GEK Level 4, Model V3.1.0, All Power Labs, Berkeley, California). As shown in Figure 7.2, the larger the size of composite pellets the higher will be the thermal energy production through the gasification process. The temperature was recorded via five different thermocouples (K type) installed throughout the reactor. The thermocouples located in the gasifier to measure the temperature layers of drying (T1), pyrolysis (T2), combustion (T3), and reduction (T4) zones. The temperature results of composite pellets with different sizes were very close similar in the drying and pyrolysis zones, while in combustion there was a great jump in temperature of the reactor for the biomass feedstocks. The maximum temperature in the combustion zone for composite pellets of 14mm, 10mm, 8mm and 5mm diameters were measured as 974 ^{o}C, 796 ^{o}C, 622 ^{o}C, and 617 ^{o}C, respectively. The temperature difference may be attributed to different flowability properties of feedstock in the gasifier reactor. The followability of composite pellet was tested through conducting angle of repose analysis along with the compressive strength test.

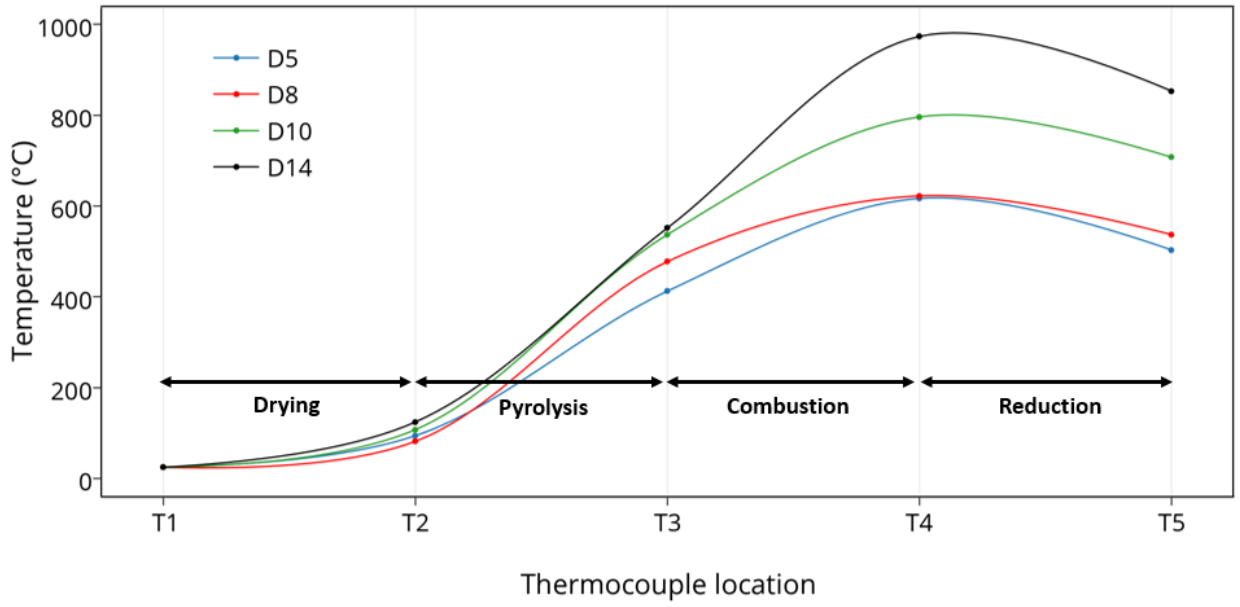

Figure 7.2. Thermal behavior of composite fiber of blended fiber mixed with shredded plastics with volume fraction of 5% in the main zones of the gasifier reactor (i.e. drying T1-T2, pyrolysis T2-T3, combustionT3-T4 and reduction T4-T5) during gasification process.

7.2.6. Microscopic Imaging

To investigating physical interaction between constitutes of the composite pellet, microscopic imaging was performed using an optical microscope with high depth function (digital microscope KEYENCE VHX-series 5000, Canada). Figure 7.3a and 7.3b show cross sections of two different points of the composite pellet. Section A-A indicates a regular surface of densified fibrous material, however there were impurities from waste stream shown up in the wood fiber pellet (Section B-B). In the case of composite pellets, Figure 7.3c clearly showed the interlocking between fiber and plastics in Section C-C. The distribution of plastics in the composite pellet did not follow a regular rule and was randomly blended with the fibrous material. Figure 7.3d

demonstrated surface area of regular hard wood pellet (Section D-D) where the uniformity was much higher than the one for wood fiber and composite pellet.

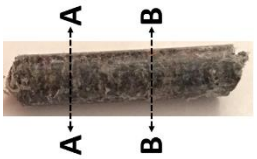

(a)

(b)

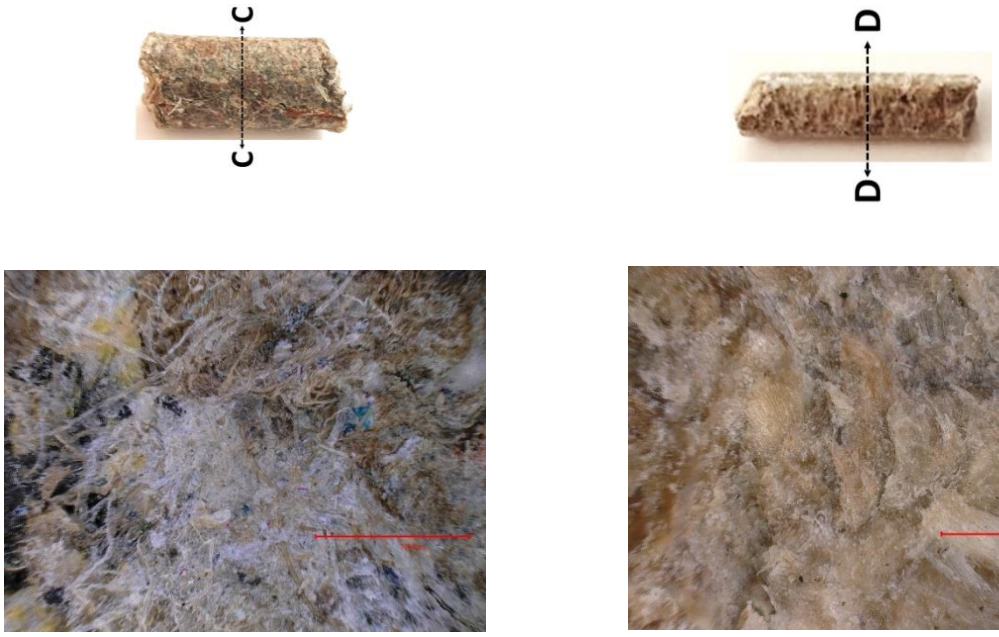

(c) **(d)**

Figure 7.3. Microscopic images of wood fiber pellet, composite pellet, and wood pellet using digital microscope (KEYENCE VHX-series 5000): (a) Cross section A-A, a regular fibrous surface of material in wood fiber pellet, (b) Cross session B-B, fibrous impurities shown up in the material in wood fiber pellet coming from paper waste stream, (c) Cross section C-C, interlocking of fiber and plastics within structure of composite pellet (d) Cross section D-D, a regular surface of wood pellet structure.

7.3. Results and Discussion

Stress versus strain relationships for all the tests were derived from experimental load-displacement curves by dividing the applied load by the initial cross-sectional area and the displacement by the initial length of the specimen. The strain-stress curves were drawn using force-displacement calculations from the initial point where the platen start to exert pressure on the pellet up to the maximum load at which the pellets fail in tension. Young's modulus, yielding point,

ultimate strain/stress and toughness were obtained from the experimental data. Figure 7.4 shows the strain-stress curve of composite pellets in different size.

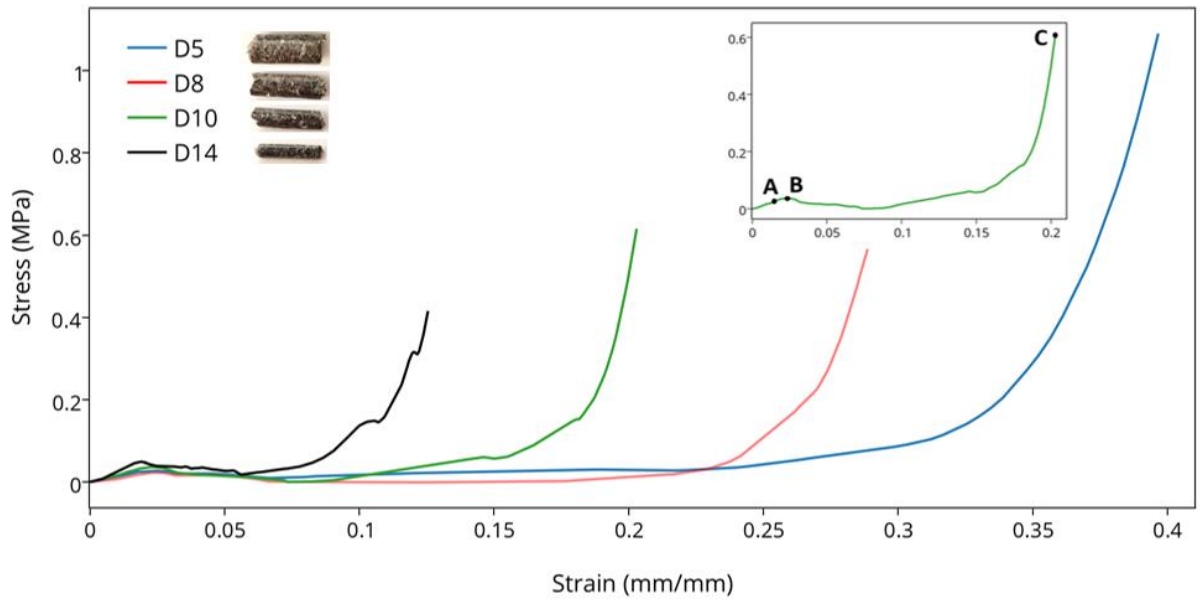

Figure 7.4. The strain-stress curve for composite pellets of wood fiber and plastics with different size in longitudinal direction. The INSTRON machine was set to exert a maximum load of 10kN longitudinally and the instant force and its corresponding displacement were recorded every second.

As shown in Figure 7.4, there are 3 points considered for each size of pellets. Point A refers to the point at which the curve levels off and plastic deformation began to occur. At this points the specimen was still able to return to their original length upon release of the load. Point B is yield point at which an abrupt rise take place in strain without a corresponding increase in stress. Point C is ultimate strength where a material withstands the maximum stress. This value was calculated by dividing the load at failure by the original cross sectional area.

The results indicated that larger pellets have higher elastic limit yield stress but lower ultimate stress under vertical force in longitudinal direction. The higher elasticity may be explained due to lower porosity of the composite pellet; however, the lower ultimate strength of the bigger pellets did not follow the same trend and fell in the plastic zone. In the elastic limit, the material regains its shape and size when the external pressure was removed, while the higher ultimate strength meant that the materials not only lost its elasticity, but also broke down. As can be seen in Table 7.4, the higher elasticity did not result in higher ultimate strength in the composite pellets. Pellet 14mm had the highest elastic limit at 0.043 MPa while the lowest ultimate strength of 0.415 MPa. Similarly, the composite pellet 5mm showed the weakest and strongest elastic limit and ultimate limit at 0.024 MPa and 1.089 MPa, respectively.

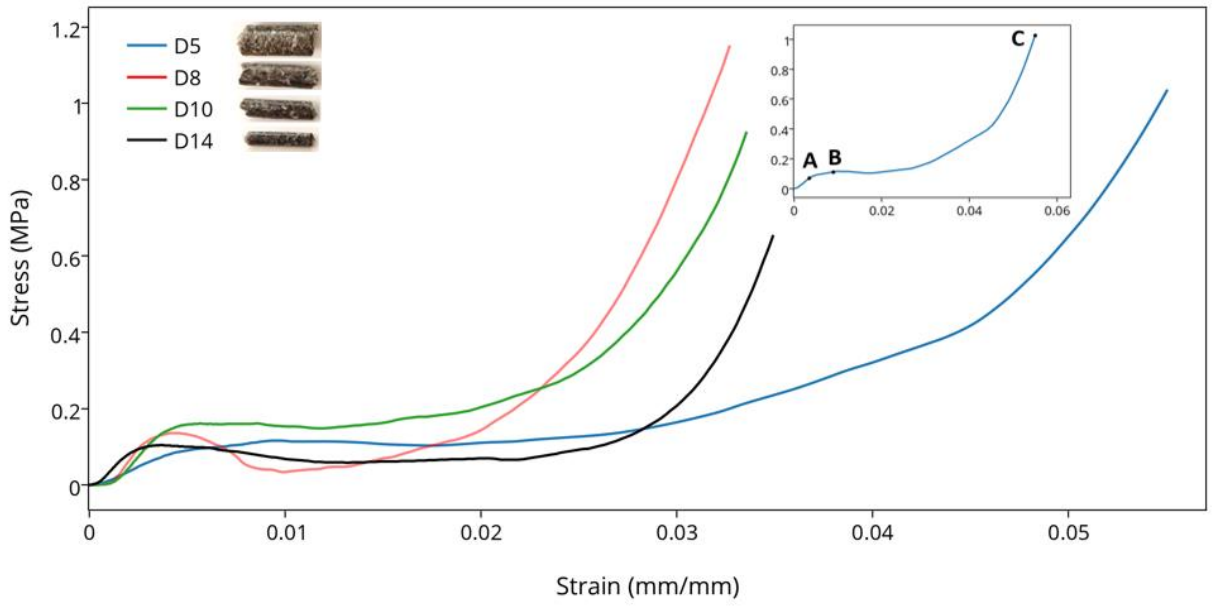

Figure 7.5. The strain-stress curve for composite pellets of wood fiber and plastics with different size in transverse direction. The INSTRON machine was set to exert a maximum load of 10kN transversely and the instant force and its corresponding displacement were recorded every second.

The behavior of wood fiber plastic composites was directly related to their hierarchical microstructures. It is well-known that the structures at microscopic scales often play a unique role in determining the physical properties of the materials d transferring and amplifying molecular functions to a property at macroscopic length scales (Wang, Lin et al. 2013). Therefore, the mechanical properties of composites were observed by several microstructural parameters such as properties and distribution of the filler as well as interfacial bonding. The interfaces may affect the effectiveness of load transfer from the wood fiber to plastics. Similar to longitudinal direction, Points A, B and C refer to elastic limit, yield point and ultimate strength, respectively (Figure 7.5).

In transverse direction, the values of elastic limit, yield and ultimate strengths did not follow a certain trend. This may be due to the original loading in densification stage where the material compacted longitudinally and the sinew of the composite was placed vertically. It may be also due to random distribution of constituents particularly the plastics whose types were unknown. Additionally, the stress values of points A, B and C in the longitudinal direction were recorded as 0.042 MPa, 0.049 MPa, and 0.416 MPa which lower than the ones loaded transversely given by 0.088 MPa, 0.105 MPa, and 0.65484, respectively. The force-deflection process and the corresponding deflection to Points A, B and C for both directions are demonstrated in Figure 7.6 and their corresponding values are presented in Table 7.4.

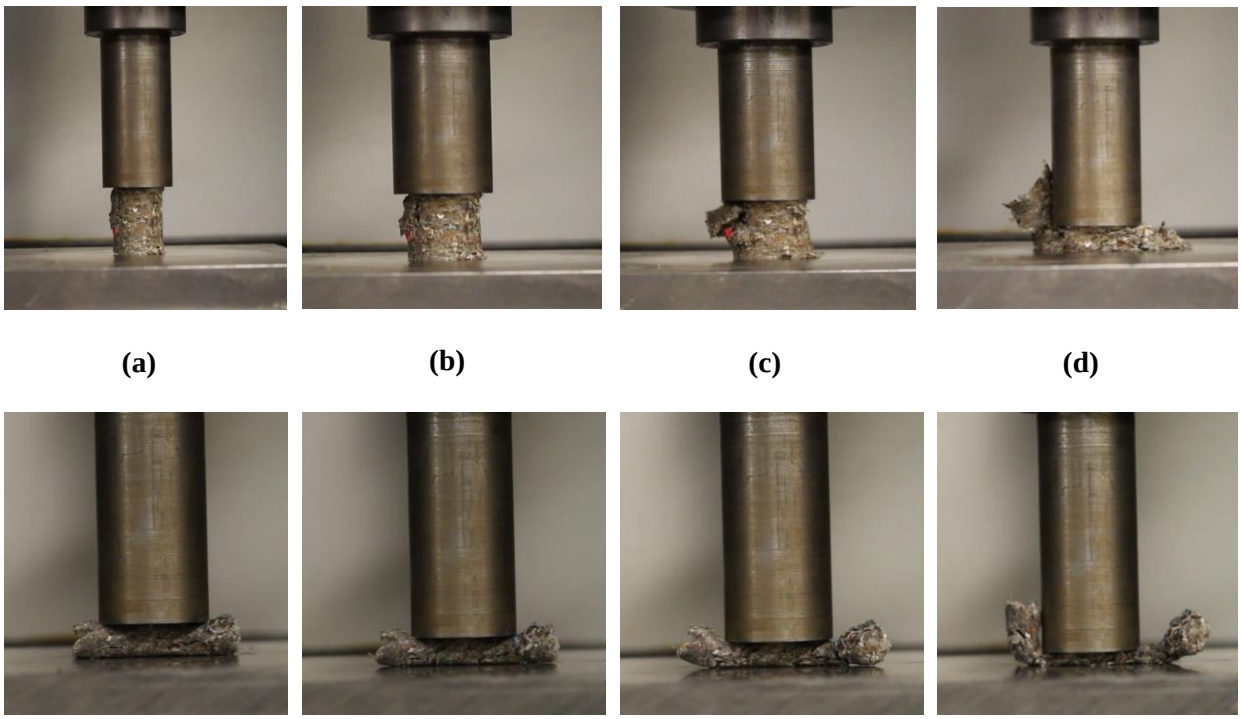

(a) **(b)** **(c)** **(d)**

(e) (f) (g) (h)

Figure 7.6. The loading process during compression test of the wood fiber and plastic composite pellets to identify compressive strength of the materials. During the compression of the pellets, a load was applied to pellets through a plunger (diameter 8.5cm) with the crosshead speed of 10 $mm.min^{-1}$. (a) the loading exerts vertical force and there is a linear relationship between force and deflection, (b) the first crack forms by increasing forcing longitudinally and yielding takes place (Point B), (c) the plastic limits begins where the material is not able to return to its original length upon release of the load, (d) the ultimate limit happens and the pellet is completely crashed. (e) The loading exerts force in transverse direction to the pellet and the deflection is elastic, (f) by enhancing the load the material reaches to its yielding point, (g) The plastic limit begins and there is no linear relationship between force and deflection anymore, (h) The pellet reaches its ultimate strength where the material is completely destroyed.

Table 7.4. Mechanical specification of composite wood pellets and plastics under compressive pressure in longitudinal and transverse directions

	Longitudinal						**Transverse**					
	Elastic limit (Point A)		Yield strength (Point B)		Ultimate strength (Point C)		Elastic limit (Point A)		Yield strength (Point B)		Ultimate strength (Point C)	
	σ_e (MPa)	ε_e (%)	σ_y (MPa)	ε_y (%)	σ_u (MPa)	ε_u (%)	σ_e (MPa)	ε_e (%)	σ_y (MPa)	ε_y (%)	σ_u (MPa)	ε_u (%)
Composite pellet (5mm)	0.0228	0.0203	0.0271	0.0251	1.0897	0.3965	0.0716	0.0036	0.1139	0.0112	1.0358	0.0551
Composite pellet (8mm)	0.0229	0.02202	0.0229	0.0268	0.6413	0.2875	0.1020	0.0044	0.1358	0.00449	1.1519	0.0327
Composite pellet (10mm)	0.0306	0.0239	0.0367	0.0234	0.6152	0.2030	0.1165	0.0046	0.1602	0.0045	0.9258	0.0336
Composite pellet (14mm)	0.0424	0.0167	0.0489	0.0197	0.4159	0.1256	0.0876	0.0023	0.1041	0.0037	0.6548	0.0349

The resulting multiphsyical properties of the composite pellets were expected to be the combination of the properties of the constituent materials. The different types of loading may apply on different elements of the composite to take the load. This implied that the material properties of composite materials may be different under compression in different directions. As a consequence, we performed the compression test for individual wood fiber for Young's modulus of which measured as 0.76 and 12.14 MPa in longitudinal and transverse directions, respectively. Although we were aware of the presence of different constituent of the composite pellets (i.e. wood fiber and pellet), it was impossible to realize the type of plastics blended with the fibrous material. This was due to the general waste stream where the plastics originated. Using the rule of mixture for composite material, the Young's modulus of plastics was calculated and used in each composite pellet. According to rule of mixtures, the Young's modulus of the composite is resulting from Young's modulus of each component depending on its contribution in the pellet. The rule of mixture may be written as (Akbarzadeh, Abbasi et al. 2011, Chen, Wu et al. 2013):

$$E_C = E_F V_F + E_P V_P \qquad (3)$$

where E_C, E_F and E_P represent Young's moduli of the composite pellet, fiber, and plastic, respectively; and V_F and V_P are the volume fraction of fiber and plastic in composite pellet.

The values of Young's modulus for composite pellets were experimentally measured and presented in Figure 7.5. As indicated earlier, the longitudinal and transverse Young's modulus of prestine wood fiber were 0.756 MPa and 12.142 MPa. The volume fraction of wood fibers and plastic in the tested composite pellets were 0.9 and 0.1. Therefore, the modulus of plastics for each composite is caculated in Table 7.5.

Table 7.5. Modulus of elasticity for plastic constituent of the composite pellets in longitudinal and transverse directions

	Longitudinal				Transverse			
	5mm	8mm	10mm	14mm	5mm	8mm	10mm	14mm
Modulus of Elasticity for plastic(MPa)	4.45	3.45	6.05	18.55	89.14	122.74	146.34	271.84

The values of longitudinal modulus of elasticity for plastic content of the composite pellets were calculated in the range of 4.45 MPa to 18.55 MPa. As for the transverse modulus of elasticity, the calculated values were much higher than the longitudinal and ranges from 89.14 MPa to 271.84 MPa. Table 7.6 shows Young's modulus values of different types of plastics. Comparing computed results to the values from Table 5, indicated possibility of presence of ethylene vinyl acetate (EVA) and Surlyn in the composite pellets. EVA is an elastomeric polymer that produces materials which are rubber-like in softness and flexibility. Surlyn is an ionomer which comprises the copolymers of ethylene and acrylic acid being metal neutralized and is used in structure of thermoplastic material (Gkinosatis 2009).

Table 7.6. Modulus of elasticity for alterantive types of plastics (Curbell Plastics 2016).

	PBT	ETFE	EVA	FEP	HDPE	Nylon	PET	PFA	PTFE	Surlyn	UHMW
Young's modulus (MPa)	2275	999	17	655	1378	2826	2757	620	496	29-51	758

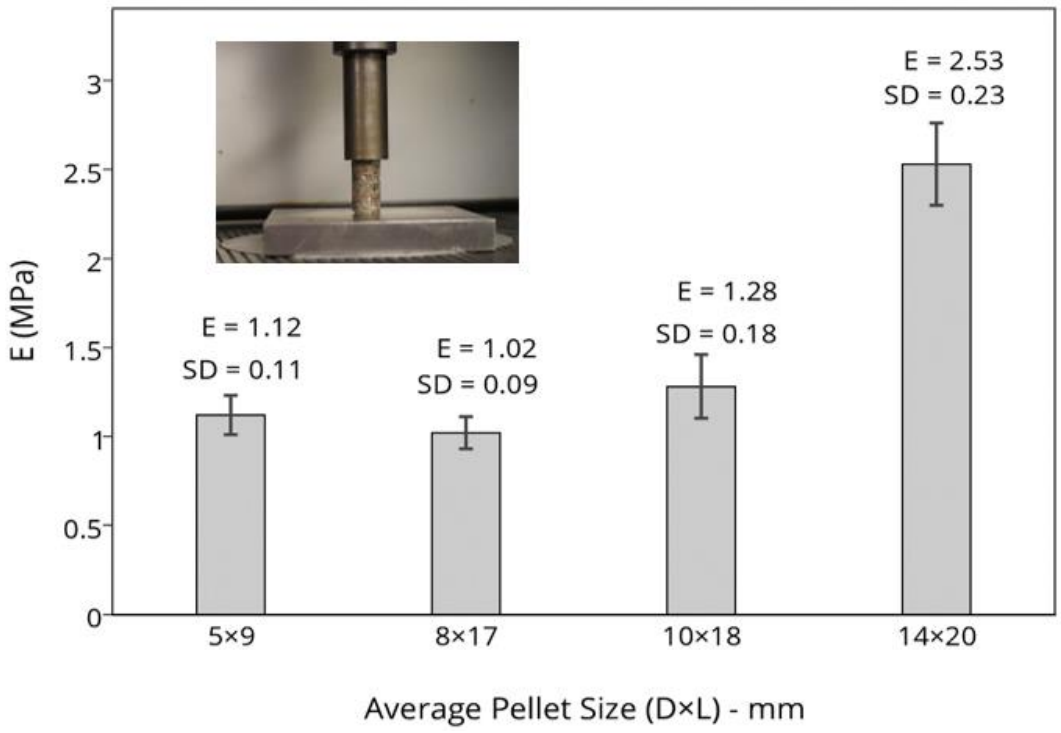
E (MPa)
3
2.5
2
1.5
1
0.5
0
E = 1.12
SD = 0.11
E = 1.02
SD = 0.09
E = 1.28
SD = 0.18
E = 2.53
SD = 0.23
5×9
8×17
10×18
14×20
Average Pellet Size (D×L) - mm

(a)

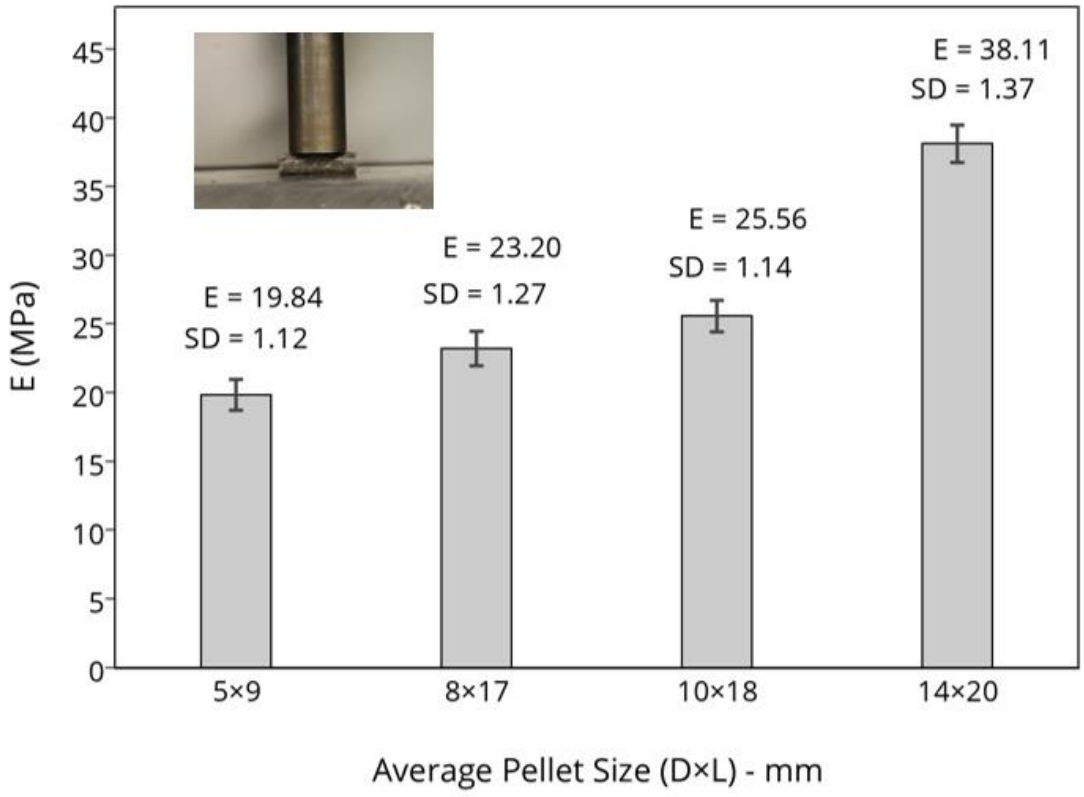

(b)

Figure 7.7. Young's modulus of composite pellets with 5% volume fraction of plastics through compression test in: (a) Longitudinal direction and (b) Transverse direction. The values and their standard deviations are presented as E and SD.

As shown in Figure 7.7, the Young's modulus for both logitudinal and transverse directions belonged to the largest size of pellet. Similarly, it may be due to higher porosity of larger pellet size. A reduction of porosity in a solid material increases its strength in general has been reported since 1972 (Chen, Wu et al. 2013). Popovics (Popvics 1973) showed that porosity has a role in the relationship between mechanical properties of concrete, such as the compressive strength-modulus of elasticity relationship.

The toughness of the composite pellets was defined in this research with respect to the domains of the stress-strain curves. We determined the toughness values by integrating the corresponding stress-strain curves. The explicit mathematical description of toughness may be written as (Tso, Chiang et al. 2007),

$$\frac{E_s}{V} = \int_0^{\varepsilon_f} \sigma d\varepsilon \qquad (4)$$

where E_s is strain energy absorbed by the material (J), V is the composite pellet volume (mm^3), σ and ε are corresponding stress (MPa) and strain and ε_f is the strain recorded at ultimate strength where failure occurs.

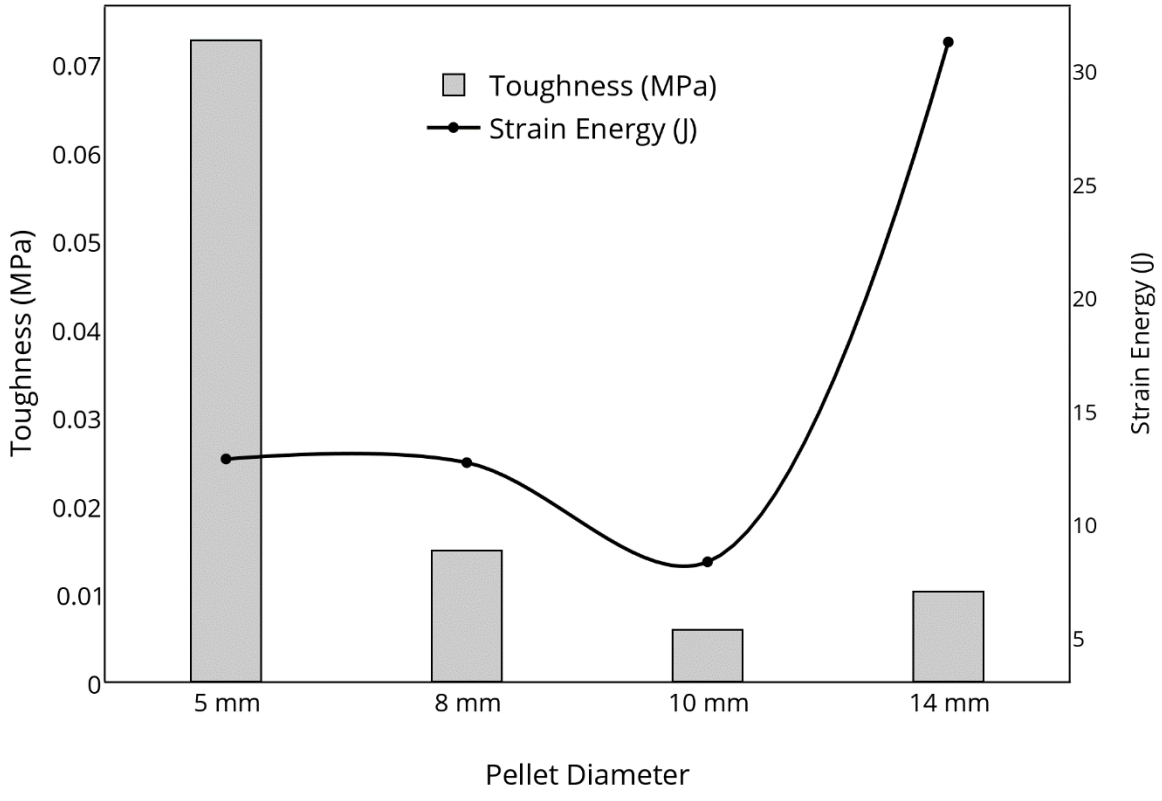

(a)

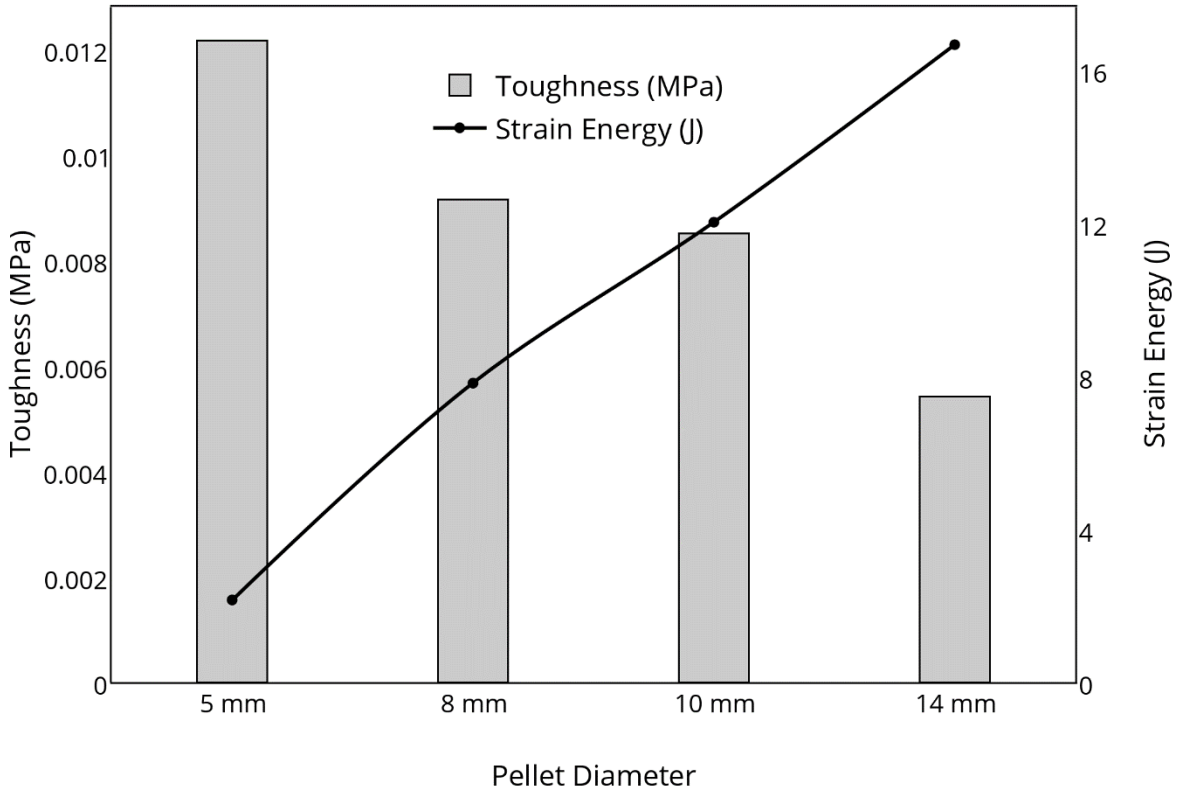

(b)

Figure 7.8. The toughness and strain energy of composite pellets obtained via compression tests in: (a) longitudinal direction and (b) transverse direction.

As shown in Figure 7.8, the wood fiber and plastic composite material have extremely low toughness particularly in transverse direction. It was observed that the larger size of the composite pellet had lower toughness. Therefore, the greatest toughness in both directions belonged to the smallest composite pellets. As explained for Young's modulus, the bigger size of materials demonstrated higher modulus of elasticity. This may be due to the difference in definitions of stiffness and toughness. The stiffness refers to ability of a material to resist deformation and

toughness implies the amount of energy the material absorbs per unit volume before it breaks (Corinaldesi, Nardinocchi et al. 2016, Guo, Wang et al. 2016). As a consequence, the greater Young's modulus resulted in greater stiffness. But nevertheless, the results showed that the pellets with higher stiffness had lower toughness. The larger size of pellets had higher resistivity in the elastic zone and by continuing loading and reaching a yielding point and plastic zone, they did not follow the same trend. The smaller size of pellets was less resistant under elastic loading and reached quicker to yielding point, but showed higher tolerance in plastic zone and reaches the failure point slower.

As indicated in Equation 4, strain energy had a direct relationship with toughness. In the case of longitudinal direction, however, the strain energy of pellets 5mm and 8mm were almost exactly the same at 0.025 MPa and was higher than pellet 10mm which counts for 0.014 MPa and much lower than the one for pellet 10mm at 0.073 MPa. The incompatibility between toughness and strain energy of the pellets loaded in longitudinal direction was only because of different volumes of composite pellets. With respect to transverse direction, there was no such incompatibility observed. This was due to insignificant difference between toughness of different pellets comparing to the one from longitudinal direction. Therefore, the volume variation did not change the order in toughness and strain energy in transverse direction.

7.4. Conclusion

Physico-chemo-mechanical properties of composite pellets made of wood fibers and plastic were investigated in this study. The investigated biomass feedstock was in the form of cylindrical pellets of different diameters. Due to the non-homogeneity of composite pellets and their material

constituents, physical, chemical, and mechanical behavior of the composite pellets did not only change by the volume fraction of material constituents but also varied with the pellet geometry and the position of experimental tests within the pellets. The physico-chemo-mechanical properties of biomass feedstocks played a significant role in the performance of the thermochemical conversion pathways, such as gasification and combustion, for producing sustainable clean energy from advanced solid biofuels. Due to the heterogeneity and size-dependency of composite pellets, the mechanical behavior of the composite pellets was specifically studied in both longitudinal and lateral directions. The results of physico-chemo-mechanical investigation of composite wood fiber and pellets were closely tied in to the thermal application of them in a gasifier. The major findings of this research can be summarized as below:

- The mechanical behavior of composite pellets is different in the longitudinal and lateral compressive analysis. In the longitudinal compressive test, the elastic limit and yield strength of pellets with larger diameters are higher while the ultimate strength is lower. However, pelletized composite biomass loaded transversely do not show specific trends for strength and elastic limit as a function of sample size.
- The chemical analysis showed the existence of minerals (specifically aluminum and calcium) in the composition of the composite plastic pellets which could cause changes in their multiphysics properties as well as their thermal energy value.
- The strength of composite pellets was affected by their porosity and heterogeneity. In the composite pellets, multiple types of plastics were randomly distributed through the composite pellets.
- With respect to physical properties, the angle of repose increased with the moisture content and decreased with the bulk density in all the composite pellets. These characteristics impacted

the flow properties of the composite pellets inside the downdraft gasifier and resulted in reaching higher temperature during the thermochemical conversion.

- The results of gasification of composite pellets indicated the better thermochemical conversion performance of pellets with larger diameters due to a greater flowability indicated by a lower angle of repose.

Acknowledgment

This research is funded by BioFuelNet Canada, a network focusing on the development of advanced biofuels. BioFuelNet is a member of the Networks of Centres of Excellence of Canada program. We would like to also acknowledge the contribution of Dr. Nima Gharib from the Material Engineering Department of McGill University for conducting the microscopic imaging of the pelletized composites.

Connecting Text

In Chapter 7, the physico-chemo-mechanical performance of composite wood residue pellets blended with plastic wastes as potential feedstocks for producing advanced biofuels through gasification technology was investigated. The composite pellets were compressed longitudinally and laterally using a universal testing machine to evaluate their mechanical properties. The results showed that pellets with larger diameters have higher elastic limits. With respect to transverse direction, there was no certain relationship between stress-strain values and pellet size. The incompatibility in the relation between the increase of yield stress and diameter was attributed to the unknown type of plastics used in composites plastic wood pellets.

Although the primary goal of this study was set on experimental work, in Chapter 8, a thermodynamic model is applied to study the effect of equivalence ratio on the reactions temperature and producer gas during the decomposition of biomass feedstock in a down-draft gasifier. The purpose is to facilitate the estimation of the behaviour of the process by changing the design and key operational factors from the knowledge gained within the work performed in Chapters 1 to 7.

Chapter 8 has been submitted for publication as:

Madadian E., Amiri L., & Lefsrud M. (2016). Pelletized Composite Wood Fiber Residues Mixed with Plastic Wastes as Advanced Solid Biofuels: Physico-Chemo-Mechanical Analysis. *Energy and Fuels* (Under revision).

CHAPTER 8

8. THERMODYNAMIC BEHAVIOR OF WOOD PELLET GASIFICATION USING A DOWNDRAFT REACTOR

Abstract

Thermochemical biomass conversion technologies use renewable feedstocks to produce gaseous (syngas), liquid (tar) or solid (biochar) fuels for the production of electric power, heat, chemicals or other types of fuel. Biomass gasification has emerged as a promising conversion technology to meet increasing global energy demands. In this study, a thermodynamic model programmed with MATLAB and CANTERA was used to study the effect of equivalence ratio (ER) on reaction temperature and producer gas during the decomposition of biomass feedstock (wood pellets) in a downdraft gasifer. The composition of the producer gas was estimated by minimizing the Gibbs free energy for calculation of the equilibrium constants. A Newton-Raphson algorithm was used to find the final equilibrium state. This process began with an initial estimate for temperature of the chemical composition at equilibrium. Higher heating value and ER variations were calculated for various moisture contents. Model predictions were satisfactorily consistent with experimental data. The results of this study can be directly applied to develop gasification reactors in biorefineries to enhance process efficiency and use the products in different energy and environmental sectors.

Keywords: Gibbs energy, Thermochemical equilibrium, Equivalence ratio, Partial combustion, Gasification products

8.1. Introduction

Atmospheric greenhouse gas (GHG) concentrations have doubled in the past century due to anthropogenic emissions. It is widely accepted that this rapid increase is the main reason for global climate change (Chareonpanich, Kongkachuichay et al. 2017). Although renewable energy sources have begun to be used, fossil fuels remain the dominant energy source in the world. It is more difficult to apply renewable energy systems to the transportation sector than to land-based facilities. As a consequence, fossil fuel use in the transportation sector is a top priority for research endeavors (Deniz and Zincir 2016). The International Energy Agency has identified biomass-based technologies as important future "game changers" to reduce dependence on fossil fuels and lower GHG emissions (Mandil).

Sources of biomass to produce biofuels include agricultural and forestry residues, animal waste, municipal solid wastes, energy crops and algae. Woody biomass for energy production could play an important role in the emerging bio-economy, including the mitigation of climate change (Gustavsson, Haus et al. 2017), energy security, jobs and revenue generation (Mansuy, Paré et al. 2017).

Biomass conversion technologies use mechanical, chemical, biochemical and thermochemical routes (Arvidsson, Morandin et al. 2015). Gasification is a thermochemical process to efficiently produce gaseous (synthesis gas or "syngas"), liquid (tar) and solid (carbon-rich biochar) biofuels (Hansen, Müller-Stöver et al. 2017) from a wide range of agricultural residues (containing carbon, hydrogen and oxygen) (Jarungthammachote and Dutta 2008). Gasification is a high-temperature, partial oxidation process. Apart from the feed biomass, it requires a gasifying agent such as steam, oxygen, air or a mixture of these gases (Kaushal and Tyagi 2017). Gasification processes operate

at sub-stoichiometric conditions, with the oxygen supply maintained at approximately 35% of that theoretically required for complete combustion (Mendiburu, Carvalho et al. 2014).

Gasification typically follows a sequence of four thermochemical steps. The feedstock is initially dried, then heated by thermal degradation (pyrolysis). The pyrolysis products are oxidized and then reduced by the gasifying medium to form the final gasification product (Basu 2013). In most commercial gasifiers, the thermal energy necessary for drying, pyrolysis, and endothermic reactions comes from the exothermic combustion reactions allowed in the gasifier (Basu 2013). Typical gasification reactions are listed in Table 8.1. The net energy produced is 71 kJ mol^{-1}.

Table 8.1. Typical gasification reactions

Reaction type	Reaction
R1 (Boudouard)	$C + O_2 \leftrightarrow 2CO + 172\ kJ.mol^{-1}$
R2 (Water-gas)	$C + H_2O \leftrightarrow CO + H_2 + 131\ kJ.mol^{-1}$
R3 (Hydrogasification)	$C + 2H_2 \leftrightarrow CH_4 - 74.8\ kJ.mol^{-1}$
R4	$C + 0.5\ O_2 \leftrightarrow CO - 111\ kJ.mol^{-1}$
R5	$C + O_2 \leftrightarrow CO_2 - 394\ kJ.mol^{-1}$
R6	$CO + 0.5\ O_2 \leftrightarrow CO_2 - 284\ kJ.mol^{-1}$
R7	$CO + H_2O \leftrightarrow CO_2 + H_2 - 41.2\ kJ.mol^{-1}$
R8	$CH_4 + H_2O \leftrightarrow CO + 3H_2 + 206\ kJ.mol^{-1}$

Many studies have evaluated the thermodynamics of gasification. For example, Puig-Arnavat et al. studied the impacts of various operational factors based on a modified thermodynamic equilibrium model (Puig-Arnavat, Bruno et al. 2012), kinetics (Puig-Arnavat, Bruno et al. 2010) and artificial neural networks (Puig-Arnavat, Hernández et al. 2013). Thermodynamic equilibrium models have been used widely (Puig-Arnavat, Bruno et al. 2010). However, in reality thermodynamic equilibrium never occurs during gasification, particularly at high temperature (~800°C) (Chowdhury, Bhattacharya et al. 1994, Altafini, Wander et al. 2003). If the installation is working properly, we can assume that the products leaving the gasifier are all gases, predominantly chemical species of low molecular weight such as CO, CO_2, H_2O, H_2, N_2 and CH_4 and traces of other chemical substances (Melgar, Perez et al. 2007).

Compared to combustion, gasification has higher efficiency due to exergy (i.e. the energy that is available to be used) losses, mainly from lower internal thermal energy exchange of expended exergy. The losses due to internal thermal energy exchange may be lowered by changing the gasifying agent (Jangsawang, Laohalidanond et al. 2015). The gas composition evolved from biomass gasification strongly depends on the gasification process, the gasifying agent, and the feedstock composition (Jangsawang, Laohalidanond et al. 2015).

8.1.1. Tar and Biochar Formation and Modelling

Fast pyrolysis is optimized to produce tar, whereas slow pyrolysis or carbonization is used to produce biochar. These processes are commercially important because the products can be used in a variety of processes such as combined heat and power generation and biofuel and chemical (methanol and hydrogen) production (Sattar, Leeke et al. 2014). In addition, biochar has great potential to be used in soil amendment and/or as a low-cost sorbent to sequester carbon, enhance soil fertility, and benefit the environment (Yao, Gao et al. 2015).

The amount of tar in syngas depends on the gasification temperature and the gasifier design. Average tar concentrations in gases from downdraft and updraft biomass gasifiers are 1 and 50 g Nm^{-3}, respectively (Basu 2013). Several studies have developed models of tar formation during biomass gasification, which can be categorized as single compound, lumped and detailed kinetic models (Simell, Hirvensalo et al. 1999, Morf, Hasler et al. 2002, Li and Suzuki 2009). The most frequent tar species studied and modelled are primary (e.g. acetol, acetic acid and guaiacols), secondary (e.g. phenols, cresols and toluene), and tertiary tars (e.g. naphthalene) (Simell, Hirvensalo et al. 1999). Hence, for modelling high-temperature air gasification of woody biomass, the tar composition was assumed to be a mixture of acetol, toluene and naphthalene.

The current research highlights the impact of pivotal operational conditions (equivalence ratio and temperature) and feedstock properties on gasification of woody biomass to produce syngas, tar and biochar. Among the three main gasification products, it is most common to model syngas behavior during gasification. However, it is much more difficult to model evolution of tar and biochar, because unlike syngas, their chemistry is non-homogeneous. There is also much less agreement regarding the proper mechanisms and rate parameters for the reactions in which tar and biochar participate (Broer and Brown 2015). These difficulties have often deterred modellers from considering the possibility that significant amounts of nitrogen might be bound in the char and tar (Broer and Brown 2015). Published estimations of tar production by primary pyrolysis are typically used often what it is assumed that tar undergoes a single step secondary cracking reaction that converts it to a few common carbon-, oxygen-, and hydrogen-bearing species (Broer and Brown 2015). In this study, it was assumed that biomass gasification produces CO, CO_2, H_2, CH_4, H_2O, N_2, tar, and biochar (Figure 8.1); no model is proposed for tar and biochar production. However, the results of other studies are compared with the experimental results.

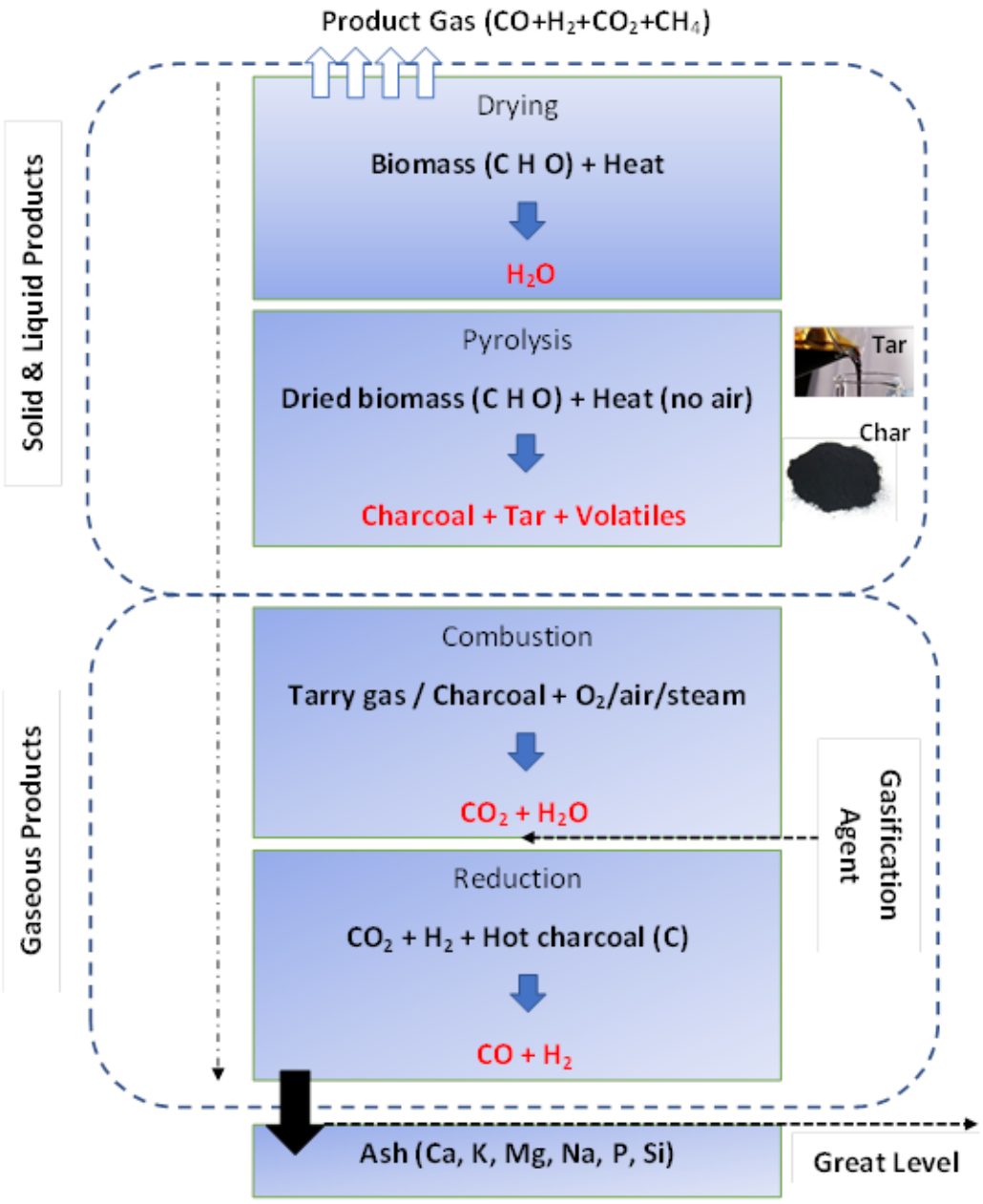

Figure 8.1. Gasification stages and products

8.2. Methods

A chemical equilibrium-based model was selected for evaluation using CONTERA. As a steady state simulation tool, CONTERA along with MATLAB has been widely used to implement equilibrium model to model biomass gasification in fixed-bed gasifiers. The simulation model was validated using experimental data from gasification of wood pellets in a laboratory-scale downdraft gasifier reported by the author (Madadian, Lefsrud et al. 2016).

8.2.1. Experimental Data

The equivalence ratio (ER) indicates the oxygen feed during gasification, thus it is a crucial factor affecting the performance of the gasification process. Seven experiments were performed to alter the ER with different air (i.e. not oxygen or steam) feeding rates during gasification of wood pellets [38]. The air for gasification was force-fed by a blower. The flow rate was metered by a rotameter and regulated with a valve (Axial Flow Fan, CTF Model, China). The amount of feedstock introduced into the reactor was weighed for estimation of the average fuel consumption rate.

8.2.2. Air Gasification Model

The basis of gasification is to supply less oxidant than would be required for stoichiometric—whereby all carbonaceous fuel is converted to CO_2 and there is no excess O_2 left—combustion of a solid fuel (Doherty, Reynolds et al. 2009). The resulting chemical reactions produce a mixture of combustible carbon monoxide (CO) and hydrogen (H_2), the main elements of syngas. Chemical equilibrium is usually explained either by minimization of Gibbs free energy (the chemical potential that is minimized when a system reaches equilibrium at constant pressure and temperature) or by using an equilibrium constant (Jarungthammachote and Dutta 2007). In this study, gasification was modeled based on the former concept. The total Gibbs free energy of a system is defined as (Ghassemi and Shahsavan-Markadeh 2014):

$$G = \sum_{i=1}^{N} \mu_i \, n_i \qquad (1)$$

Where n_i and μ_i are number of moles and chemical potential of ith species, respectively. Gibbs minimization takes place under the following constraint (Janajreh, Raza et al. 2013):

$$\sum_{i=1}^{N} n_i \, a_{ik} = A_k \qquad (K=1,2,3,\ldots,w) \qquad (2)$$

Where a_{ik} is the number of atoms of the kth element present in each molecule of the chemical species I; A_k is the total number of atomic masses of the kth element in the system; and w is the total number of atoms present in the system.

The chemical potential is calculated using Equation 3 (Alshammari and Hellgardt 2012):

$$\mu_i = RT \left[\ln\left(\frac{\varphi_i P}{P_0}\right) + lnX_i + G_i^0(T, P_0) \right] \qquad (3)$$

Where T, P and R are temperature, pressure and gas constants, respectively; and X_i is the ratio of number of moles in ith species over the total number of moles.

To minimize the total Gibbs energy to predict chemical changes, the standard free energies of formation of each chemical species at a specific temperature must be known (Materazzi, Lettieri et al. 2013):

$$\Delta G^0 = \Delta H^0 - T\Delta S^0 \qquad (4)$$

Where ΔH^0 and ΔS^0 are the enthalpy and entropy of formation at standard conditions, respectively.

By combining Equations 1–4 and using the Lagrange multipliers method, the following equations are obtained:

$$\sum_k \lambda_k (\sum_k n_i \, a_{ik-} A_k) = 0 \quad (5)$$

$$\mu_i + \sum_k n_i \, a_{ik} = 0 \quad (6)$$

The ER for gasification is generally defined as the relation of the real mass of air used in the process to the stoichiometric mass of air necessary to achieve complete combustion. Thus, the gasification ER is the inverse of the ER in combustion calculations (Mendiburu, Carvalho et al. 2014):

$$ER = \frac{m_{air-real}}{m_{air-stq}} \quad (7)$$

Based on the assumption that the air gasification product contains CO_2, CO, H_2, CH_4, and H_2O, the global reaction in the downdraft gasifier can then be written as Equation (8). It is also assumed that there is no unburned carbon left in the end of the process:

$$CH_aO_bN_c + dH_2O + e(O_2 + 3.76N_2) = n_{H2}H_2 + n_{CO}CO + n_{CO2}CO_2 + n_{H2O}H_2O + n_{CH4}CH_4 + (\frac{c}{2} + 3.76e)N_2$$

Where *a*, *b* and *c* are the number of atoms of hydrogen, oxygen, and nitrogen per number of atom of carbon in the feedstock, respectively; *d* is the amount of moisture per kmol of feedstock; and *e* is the amount of oxygen per kmol of feedstock.

The performance of gasification is quantified by means of the syngas higher heating value (HHV) and cold gas efficiency (CGE) (Ghassemi and Shahsavan-Markadeh 2014), computed using the following equation (Cohce, Dincer et al. 2014, Ghassemi and Shahsavan-Markadeh 2014, Tapasvi, Kempegowda et al. 2015). The lower heating value (LHV) of solid fuel in MJ kg^{-}

[1] was derived using the higher heating value formula presented by Channiwala and Parikh (Channiwala and Parikh 2002):

$$\eta_{cg} = \frac{LHV_{syngas}}{LHV_{biomass}+Q_{air}+Q_{steam}} \quad (8)$$

$$HHV = 12.75\,[H_2] + 12.63\,[CO] + 39.84\,CH_4 \quad (9)$$

$$LHV = HHV - 9m_H h_{fg} \quad (10)$$

Where η_{cg} is the value of CGE; H_2, CO, CH_4 are percentage of mass of hydrogen, carbon monoxide and methane in the syngas; m_H is mass fraction of hydrogen in solid fuel, and h_{fg} is enthalpy of vaporization of water. The HHV is the heat released by a substance by combustion. The CGE is the ratio between the chemical energy in the product gas and the chemical energy in the fuel. LHV is defined with moisture evaluation heat taken into consideration.

8.3. Results and Discussion

This section first presents validation of the simulation based on experimental results from the literature. Next, the results of a parametric study of important operating parameters are presented.

8.3.1. Model Validation

The measured and modelled performance parameters and syngas HHV and composition are presented in Table 8.1. Overall, model predictions of gasification products are in good agreement with the experimental data. The model under-estimated most parameters, with the exception of water and gas yield which could mostly be attributed to CO_2.

Table 8.2. Experimental and model results under typical operation conditions

Property		Experimental	Modelled	Difference (%)
Temperature (ºC)		875	823	–5.9
Equivalence ratio (%)		0.37	0.32	–13.5
Higher heating value (MJ Nm^{-3})		10.5	7.5	–28.6
Tar yield (%)		9.5	7.1	-33.8
Biochar yield (%)		17	14	–17.6
Gas yield (%)		62	66	6.5
Syngas Composition	H_2	29.20	25.53	–12.6
	CO	25.74	22.19	–13.8
	CO_2	11.45	12.15	6.1
	CH_4	5.78	4.86	–15.9
	Other (including H_2O)	27.69	35.27	27.4

`

8.3.2. Parametric Study

8.3.2.1. Effect of ER on CGE and HHV at different temperatures

The CGE was higher at higher reactor temperatures within the temperature range (500–900°C) chosen from published work (Kihedu, Yoshiie et al. 2014, Ong, Cheng et al. 2015, Madadian, Lefsrud et al. 2016) (Figure 8.2). The CGE was similar at 800 and 900°C. For all five temperatures, the CGE increased with increasing ER until a certain ER (2.9), then it declined. The maximum CGE ranged from 68% at 500°C to 82% at 800 or 900°C. At higher temperatures, reactions shifted toward production of syngas, which has higher HHV. At low ERs, where the gasification condition is much below the stoichiometry, a lower gasification performance was observed. As ER

increased, the value of CGE also increased up to a certain point considered as optimum ER (0.31). Higher ER signifies higher air flow rate for a specific biomass consumption rate. Hence, above the optimum ER, the calorific value of the syngas gas deteriorated due to the presence of more combustion products. A similar trend was observed by Sheth and Babu (Sheth and Babu 2009) during gasification of wood waste in a downdraft reactor.

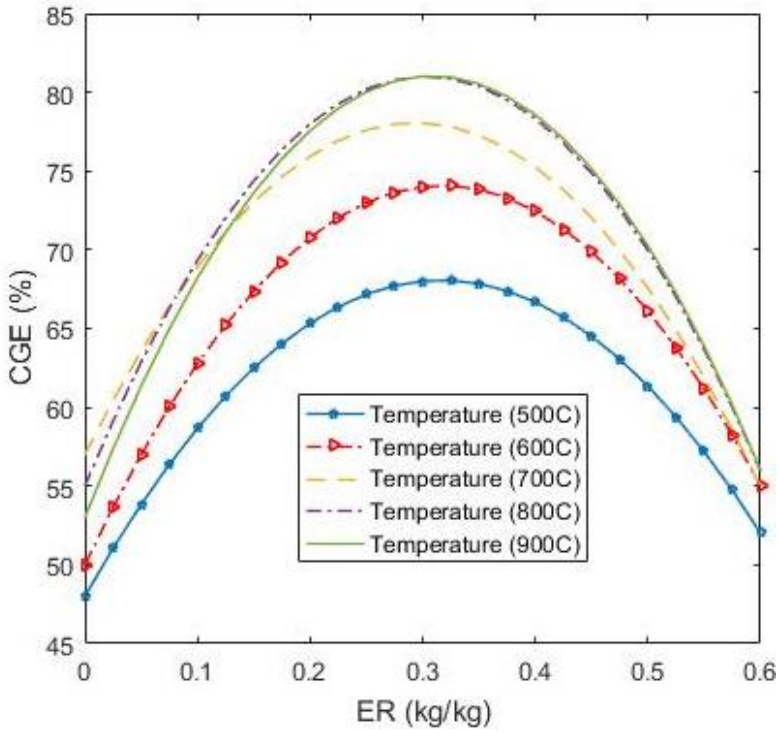

Figure 8.2. Cold gas efficiency (CGE) versus equivalence ratio (ER) at five reactor temperatures during gasification of woody biomass

The HHV decreased linearly with ER at each of the five chosen temperatures (Figure 8.3). This is due to the reduction of the syngas main components (i.e. H_2 and CO) at higher ERs.

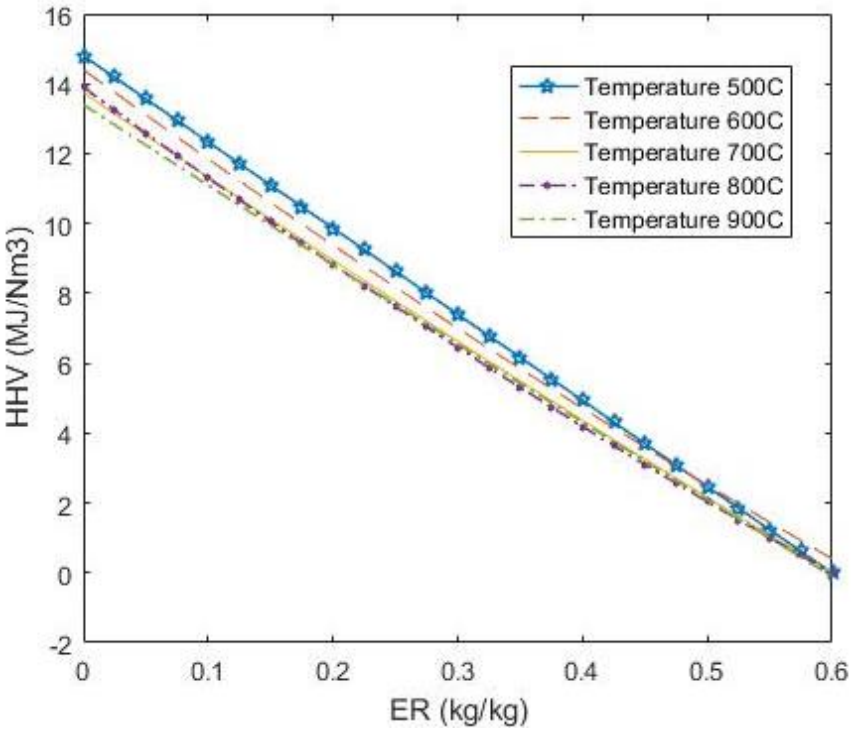

Figure 8.3. Higher heating value (HHV) of gaseous product versus equivalence ratio (ER) at five reactor temperatures during gasification of woody biomass

8.3.2.2. Effect of ER on CGE and HHV at different moisture contents

Not surprisingly, moisture content within the range of 5 to 35% had a negative effect on gasifier performance: for a given ER, the HHV was highest at 5% moisture and lowest at 35% moisture. At the optimum ER (0.31), HHV ranged from 3.8 at 35% moisture to 8.7 MJ Nm^{-3} at 5% moisture. The production of syngas decreases, thus HHV and CGE also decrease. The HHV takes into account the latent heat of vaporization of water in the combustion products. Thus, the latent heat might be the reason for the lower HHV with higher moisture content. It might be expected that both of energy and environmental aspects of combustion process can be improved at higher fuel

water content, up to a certain point, but it must be checked separately for gasification process (Ghassemi, Beheshti et al. 2015).

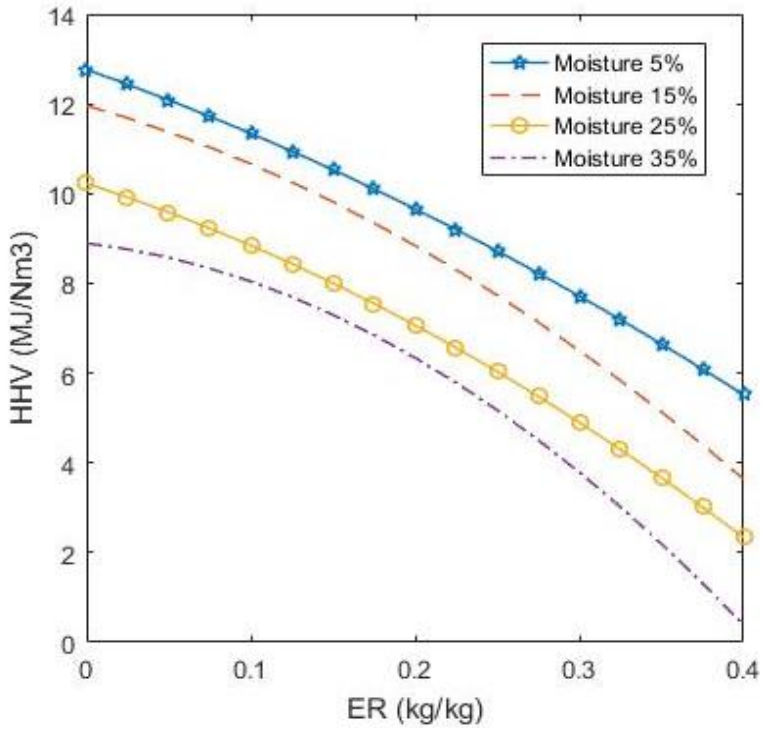

Figure 8.4. Higher heating value (HHV) of gaseous product versus equivalence ratio (ER) at four biomass moisture contents during gasification of woody biomass

Overall, there is a negative linear relationship between HHV and ER (Figure 8.5) because of the significant decrease in the quality of syngas when ER increases. CGE exhibits a parabolic behavior with respect to ER; the maximum CGE (87%) was observed at an ER of 0.33. At ERs lower than 0.33, an inverse relationship between HHV and CGE was observed. At ERs above 0.33, increasing ER decreased both HHV and CGE.

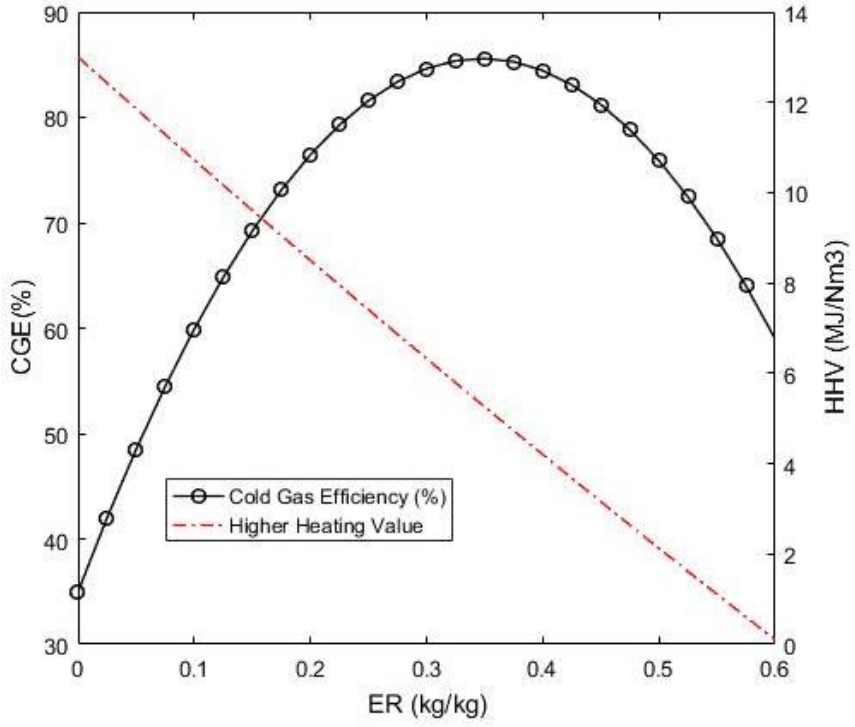

Figure 8.5. Overall relationships between cold gas efficiency (CGE) and higher heating value (HHV) versus equivalence ratio (ER) during gasification of woody biomass

8.3.2.3. Effect of ER on syngas composition and reactor temperature

With increasing ER, the volume fraction of CO in syngas increased gradually, peaked at 20.1% at ER = 0.28 and then gradually decreased (Figure 8.6). The CO_2 content of syngas showed an inverse trend to CO. This trend may be explained through the endothermic Boudouard reaction (Table 8.1) whereby at higher temperatures, more O_2 reacted with biochar to produce CO. For ERs greater than 0.29, there was insufficient char available for the Boudouard reaction. Consequently, the amount of CO decreased and CO_2 content increased at higher ERs and temperatures. With continued increases in ER above the optimum, more air entered the reactor, which resulted in an increase in N_2 content, to a maximum of 52%. Gasification with pure oxygen would generate a

syngas free of N_2 and with a higher calorific value (Arena 2012). The increasing presence of air with increasing ER also consumed H_2 via hydrogen oxidation. Increasing ER and passing the stoichiometric air-to-fuel ratio point resulted in a higher reactor temperature.

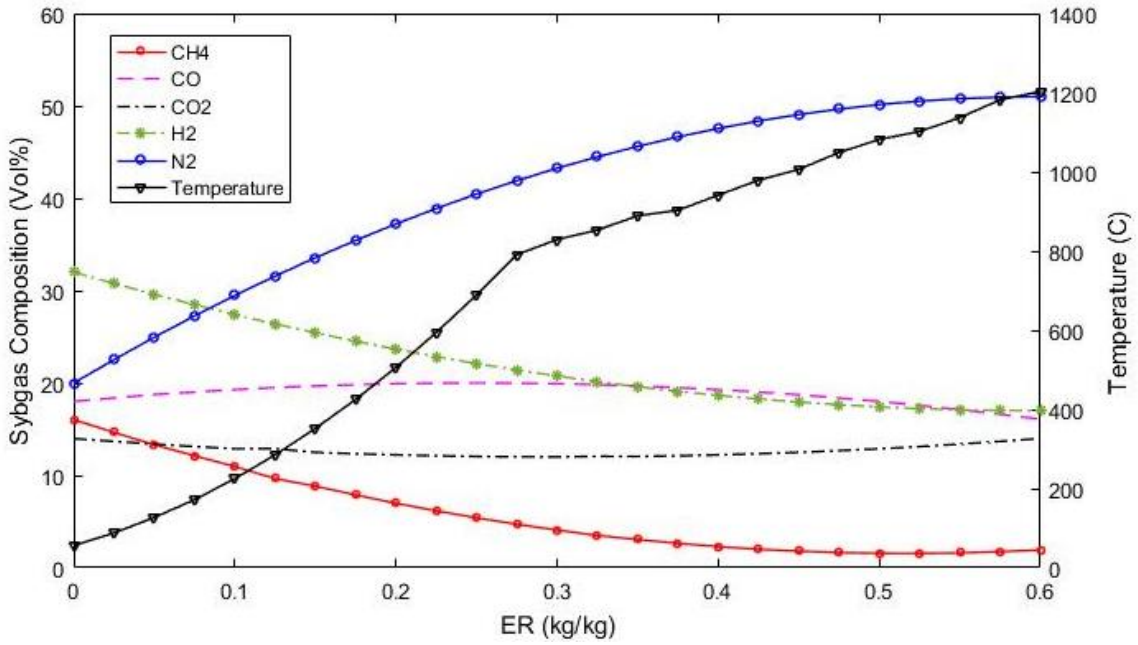

Figure 8.6. Volume fraction of syngas composition and temperature with respect to equivalence ratio (ER)

Methane showed a decreasing trend with increasing ER, possibly due to the steam-methane reforming reaction (R8 in Table 8.1), which led to negligible production of methane as ER increased (Figure 8.6). This endothermic reaction is favored by increasing temperature. Hence, CH_4 content decreased while CO content increased (Doherty, Reynolds et al. 2009). Additionally, it is assumed that most of the carbon in fuel is converted to CO and CO_2. The product composition strongly depends on the amount of oxidizer, which consequently affects ER. The primary products of the gasification process are CO_2 and CO, and their amounts will be considered as an indicator

for the stoichiometry or as set points for ER. Considering the crossover point between CO and H_2 at approximately 800°C in Figure 8.6, the optimum ER should be set at approximately 0.31 to 0.34.

When the amount of air was low, the order of produced gases was $H_2 > CO > CH_4 > CO_2$. As ER increased, the production of H_2 and CH_4 gradually decreased, while CO and CO_2 production barely changed. The CO_2 production increased by admitting a large amount of air into the reactor. When ER was comparatively large, more CO was produced than H_2. From a thermodynamics standpoint, the addition of oxidant decreased H_2 yield and increased CO yield, which can be further balanced using the water-gas shift reaction. A similar trend was reported by Jin et al. (Jin, Lu et al. 2010) for H_2 production by partial oxidative gasification of biomass.

By increasing ER, the higher heating value (LHV) of the gas linearly dropped from 13 MJ Nm^{-3} to 6.4 MJ Nm^{-3} at ER 0.31 and kept decreasing at higher ER values. The change in HHV reflected the same trend to LHV. Low producer gas LHV due to the nitrogen dilution makes it difficult to use producer gas in some high efficiency combustion applications such as gas turbines or fuel cells. Additionally, as indicated in Equation 9 and Figure 8.4, by increasing of ER, the content of H_2 as a valuable gas dropped, and there was no significant change in CO and CO_2, which resulted in decreasing HHV.

8.3.2.4. Effect of ER on product yields

In the model, the ER was varied between 0 and 0.60 in increments of 0.15, assuming an average reactor temperature of approximately 900°C (temperature of optimum ER). The air flow rate entering the reactor was varied to investigate the effect of ER. With changes in ER, different amounts of syngas, tar and biochar were generated, corresponding to four zones (Figure 8.7). In

Zone A (ER < 0.18), gas, tar and biochar yields increased up to 44, 18 and 15%, respectively, as drying and pyrolysis took place. In Zone B (ER 0.18–0.27), the gas yield increased to 58%, whereas both the tar and biochar yields slightly decreased to 12%. In Zone C (ER 0.27–0.36), the gas yield peaked at 64%. Biochar production continued to decline due to the corresponding temperature range (820–910°C) where chars are transformed to tars. In Zone D (ER 0.36–0.60), biochar and tar yields followed the same trend as Zone C, whereas gas production dropped significantly. Although Zone D is not of interest in the study of gasification, this may help to understand the process of ash sintering, which can result in failure scenarios such as clinkering in the reactor. This trend was observed by Mohammed et al. (Mohammed, Salmiaton et al. 2011) during air gasification of empty fruit bunches.

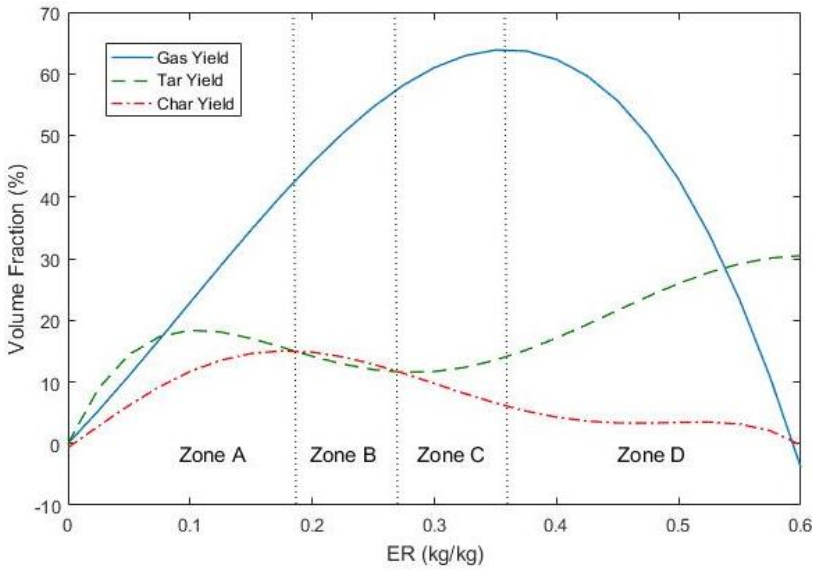

Figure 8.7. Volume fraction of gas, tar and biochar products with respect to equivalence ratio (ER)

Zone C is the zone of the reactor where pivotal reactions take place. To improve gas production and reduce the amount of tar in Zone C, the catalytic gasification is essential. Catalysts such as

nickel enhance the quantity and quality of the syngas (Xiao, Cao et al. 2013). Additionally, the main step for producing biochar was shown to be in Zones B and C where pyrolysis took place.

8.4. Conclusion

The elemental parameters affecting an actual gasification reactor and those predicted by a thermochemical equilibrium model for pelletized wood fuel showed similarities. Temperature and ER were critical parameters to consider when optimizing the gasification process. The ER strongly affects reaction temperature under the autothermal conditions. Increasing the reaction temperature causes rise in ER, potentially leading to a significant increase in GHG emissions. Increase in ER results in CO and H_2 partial oxidation where these two gases reacted individually with oxygen to form CO_2 and H_2O, respectively. Also, air increases the N_2 content of syngas. ER variation also affected the relative contribution of gaseous, tar and biochar gasification products. The volume fraction of the products also varied with respect to temperature.

Acknowledgment

This research is funded by BioFuelNet Canada, a network focusing on the development of advanced biofuels. BioFuelNet is a member of the Networks of Centres of Excellence of Canada program.

Connecting Text

Chapters 1 to 8 provided information about the technical details of advanced biofuel production through thermochemical conversion pathways, particularly gasification. The purpose was about investigating the question “How to develop the gasification unit? And how to optimise the conversion process after all the technical failures are solved. In Chapter 8, the process modeling was presented where a thermochemical equilibrium model was used and the composition of the producer gas was estimated by minimizing the Gibbs free energy for the calculation of the equilibrium constants.

In the final chapter of this study, a summary of all the results in earlier chapters are presented. Chapter 9 also presents the contribution of this work to the scientific knowledge and the application of the outputs to develop biorefinery approaches and step forward towards a sustainable green economy. In the end of this chapter, several recommendations are made which may be helpful for future research in the field of renewable energy.

CHAPTER 9

9. General Conclusions and Recommendations

9.1. General Summary

Owing to the depletion of fossil resources and the increasing demand on fuels, it is important to develop renewable resources to produce fuels and chemicals for energy security. Biofuels have emerged as one of the most strategically important sustainable fuel sources and are considered an important way of progress for limiting greenhouse gas emissions, improving air quality and finding new energetic resources. Advanced biofuels are referred to as liquid, gas and solid fuels predominantly produced from biomass which are not in conflict with food security. A variety of fuels can be produced from biomass such as ethanol, methanol, biodiesel, Fischer-Tropsch diesel, hydrogen and methane. Renewable and carbon neutral biofuels are necessary for environmental and economic sustainability.

Biobased materials, including biomass and wood pellets, are one of the most promising sustainable energy resources to replace expensive fossil fuels, which are threatening our environment and global climate. Biobased residues and waste, as renewable multifunctional resources, can not only be used for heating and power generation but also for greenhouse carbon dioxide enrichment and the improvement of soil structure or soil aeration via biochar production.

The work began with a general overview of the energy situation of the world and how the convectional fuels impact the future of the globe environmentally and economically. As a

solution, application of renewable energy specifically biofuels were explained and how it can be promoted in a green economy. Then the existing techniques to convert the biomass feedstock to bioenergy were presented. The thermochemical conversion pathways were selected due to their high efficiency and popularity comparing to the older biochemical techniques. This was followed by choosing gasification as an environmentally friendly method which enables producing a wider range of products depending on the ultimate application. A comprehensive introduction to the gasification technology was made in Chapter 2. To elaborate the technology more in detail, baseline tests were carried out on individual feedstocks using a down-draft gasifier. The results of baseline tests indicated the potential deficiencies of material decomposition in a down-draft gasification unit while key operational factors were investigated. The study was followed by testing different types of feedstock each represented a certain class from existing biomass such as agricultural and forestry residue, energy crops, municipal solid waste and animal waste. The potential of bioenergy production from each of which was investigated. The shape and size of feedstock were also a factor examined during gasification of individual feedstocks. The failure scenario of "Bridging" was observed in this stage. Next, multiple feedstocks were examined for seeking the possible improvement in the quantity and quality of the produced gas. The failure scenario of "Clinkering" was observed in this stage which could be considered as an individual project to work on. Finally, thermo-chemo-mechanical analysis of composite materials were examined to understand the thermal, chemical and mechanical behaviour of biomass during the conversion process. To fulfill this goal, thermogravimetric analysis, differential scanning calorimetric, Hot Disk Transient Plane Source (TPS) technique, mechanical strength tests, and inductively coupled plasma mass spectrometer (ICP-MS) were applied.

9.2. Contributions to knowledge:

This study presents informative tools for improving advanced biofuel production through gasification technology and using different types of biomass feedstock. The outcome of this study has contributed to both scientific knowledge and particularly to biorefinery concepts in more ways than one. A few of the several commendable contributions are as follows:

1- This study provides a comprehensive technical perspective of potential ways to rectify deficiencies of the gasification technology. This helps to improve the efficiency of the process to produce higher quality syngas. The results of this work are practical for scaling up the unit in bigger scale biorefineries.

2- This study provides comprehensive data on gasification behaviour, kinetics and ignition performance of different types of biomass feedstock.

3- The results of this study can be used as a guideline to optimise productivity of bioenergy production in biorefineries dealing with gasification and combustion technologies, and to facilitate building of integrated gasification combined cycle (IGCC).

4- The present work is expected to contribute towards expanding current data on gasification of advanced composite biomass feedstocks. This is the first thermogravimetric assessment of composite material, particularly wood fiber and waste, which has investigated their role in the gasification technology efficiency.

5- For the first time, a complete multiphysics characterization of composite pellets (i.e. forestry and agricultural wastes and residue composed with plastics) has been performed to identify compositions with dominant effect on thermal, chemical and mechanical properties of biofuels.

6- The present works also elaborate the experimental study on the product (mainly syngas) of thermochemical conversion, for the utilization of forestry/agricultural residues and waste to correlate the multiphysics characteristics with final product and generated thermal energy.
7- The failure scenarios during gasification of individual feedstocks and composite materials, using a down-draft reactor, are identified and suggested solutions have been made. The "Bridging" scenario is correlated to the physical properties (shape and size of feedstock) while the "Clinkering" Scenario is linked to the thermal properties and chemical composition of the composite materials.

9.3. General Recommendations

This study focused on the development of gasification technology to enhance the efficiency of biomass conversion within the process. The following recommendations are offered for future research:

1- Although this study worked on gasification of different types of biomass feedstock and identified the potential failure scenarios, it is still essential to elaborate the post-gasification process for syngas conditioning to produce enriched gas. This will have a significant contribution to approaching integrated gasification combined cycle (IGCC) concept.
2- Developing/re-designing the down-draft gasification unit is recommended to examine the possibility of process optimisation. The new design might apply a coupled reactor in

which one produces the syngas and the other one works as a downstream unit to condition the produced gas.

3- Designing a burner is recommended to enhance the efficiency of the process where the syngas comes out. A good burning process helps to preserve the syngas produced in the reactor and boost the performance of the technology.

4- Developing a feeding system which is independent of the physical properties of feedstock is strongly recommended. This will help to reduce the cost related to supply chain.

5- A detailed investigation of tar and char modeling through different types of reactor configurations could help to understand the formation process and hesitate the detrimental effects of by-products.

References

Acda, M. N. (2015). "Physico-chemical properties of wood pellets from coppice of short rotation tropical hardwoods." Fuel **160**: 531-533.

Acton, D. and L. Gregorich (1995). "The health of our soils-towards sustainable agriculture in Canada. Centre for Land and Biological Resources Research, Research Branch, Agriculture and Agri-Food Canada, Ottawa, Ont. xiv+ 138 pp.

Adhikary, K. B., et al. (2008). "Dimensional stability and mechanical behaviour of wood–plastic composites based on recycled and virgin high-density polyethylene (HDPE)." Composites Part B: Engineering **39**(5): 807-815.

Adrados, A., et al. (2012). "Pyrolysis of plastic packaging waste: A comparison of plastic residuals from material recovery facilities with simulated plastic waste." Waste Management **32**(5): 826-832.

Aghaei, J. and M.-I. Alizadeh (2013). "Demand response in smart electricity grids equipped with renewable energy sources: A review." Renewable and Sustainable Energy Reviews **18**: 64-72.

Ahadi, M., et al. (2016). "An improved transient plane source method for measuring thermal conductivity of thin films: Deconvoluting thermal contact resistance." International Journal of Heat and Mass Transfer **96**: 371-380.

Ahmad, A. A., et al. (2016). "Assessing the gasification performance of biomass: A review on biomass gasification process conditions, optimization and economic evaluation." Renewable and Sustainable Energy Reviews **53**: 1333-1347.

Ahmed, T. Y., et al. (2012). "Mathematical and computational approaches for design of biomass gasification for hydrogen production: A review." Renewable and Sustainable Energy Reviews **16**(4): 2304-2315.

Akbarzadeh, A., et al. (2011). "Dynamic analysis of functionally graded plates using the hybrid Fourier-Laplace transform under thermomechanical loading." Meccanica **46**(6): 1373-1392.

Akbarzadeh, A. and D. Pasini (2014). "Phase-lag heat conduction in multilayered cellular media with imperfect bonds." International Journal of Heat and Mass Transfer **75**: 656-667.

Alén, R. (2000). "Structure and chemical composition of wood." Forest products chemistry **3**: 11-57.

Alkan, C., et al. (2009). "Preparation, characterization, and thermal properties of microencapsulated phase change material for thermal energy storage." Solar Energy Materials and Solar Cells **93**(1): 143-147.

Alshammari, Y. M. and K. Hellgardt (2012). "Thermodynamic analysis of hydrogen production via hydrothermal gasification of hexadecane." International Journal of Hydrogen Energy **37**(7): 5656-5664.

Altafini, C. R., et al. (2003). "Prediction of the working parameters of a wood waste gasifier through an equilibrium model." Energy Conversion and Management **44**(17): 2763-2777.

Altun, S. (2011). "Fuel properties of biodiesels produced from different feedstocks." Energy Education Science and Technology Part A-Energy Science and Research **26**(2): 165-174.

Amen-Chen, C., et al. (2001). "Production of monomeric phenols by thermochemical conversion of biomass: a review." Bioresource Technology **79**(3): 277-299.

Amorim, P. H. O., et al. (2015). "Investigation on the thermal behavior of β-blockers antihypertensives atenolol and nadolol using TG/DTG, DTA, DSC, and TG–FTIR." Journal of Thermal Analysis and Calorimetry **120**(1): 1035-1042.

Arena, U. (2012). "Process and technological aspects of municipal solid waste gasification. A review." Waste Management **32**(4): 625-639.

Arvidsson, M., et al. (2015). "Biomass gasification-based syngas production for a conventional oxo synthesis plant—greenhouse gas emission balances and economic evaluation." Journal of Cleaner Production **99**: 192-205.

Ashori, A. and A. Nourbakhsh (2009). "Characteristics of wood–fiber plastic composites made of recycled materials." Waste Management **29**(4): 1291-1295.

Asif, M. and T. Muneer (2007). "Energy supply, its demand and security issues for developed and emerging economies." Renewable and Sustainable Energy Reviews **11**(7): 1388-1413.

ASTM (2002). "Standard test methods for total fluorine in coal by the oxygen bomb combustion/ion selective electrode method. ASTM D3761-96." West Conshohocken, PA.

ASTM (2013). "Standard test method for ash in wood. ASTM D1102-84." West Conshohocken, PA.

ASTM (2013). "Standard test method for moisture analysis of particulate wood fuels. ASTM E871-82." West Conshohocken, PA.

ASTM (2013). "Standard test method for moisture analysis of particulate wood fuels. ASTM E871-82. "West Conshohocken, PA.

ASTM (2013). "Standard test method for volatile matter in the analysis of particulate wood fuels. ASTM E872-82." West Conshohocken, PA.

ASTM (2013). "Standard test method for volatile matter in the analysis of particulate wood fuels. ASTM E872-82." West Conshohocken, PA.

ASTM (2013). "Standard test methods for analysis of wood fuels. ASTM E870-82." West Conshohocken, PA.

ASTM (2014). "ASTM D6683-14, Standard Test Method for Measuring Bulk Density Values of Powders and Other Bulk Solids as Function of Compressive Stress." West Conshohocken, PA.

ASTM (2014). "Standard test methods for determination of carbon, hydrogen and nitrogen in analysis samples of coal and carbon in analysis samples of coal and coke. ASTM D5373." West Conshohocken, PA.

ASTM (2014). "Standard test methods for determination of carbon, hydrogen and nitrogen in analysis samples of coal and carbon in analysis samples of coal and coke. ASTM D5373." West Conshohocken, PA.

Awudu, I. and J. Zhang (2012). "Uncertainties and sustainability concepts in biofuel supply chain management: A review." Renewable and Sustainable Energy Reviews **16**(2): 1359-1368.

Bahng, M.-K., et al. (2009). "Current technologies for analysis of biomass thermochemical processing: a review." Analytica Chimica Acta **651**(2): 117-138.

Bain, R. L., et al. (1998). "Biomass-fired power generation." Fuel Processing Technology **54**(1): 1-16.

Balat, M. (2006). "Biomass energy and biochemical conversion processing for fuels and chemicals." Energy Sources, Part A **28**(6): 517-525.

Barreneche, C., et al. (2015). "Thermophysical characterization and thermal cycling stability of two TCM: CaCl 2 and zeolite." Applied Energy **137**: 726-730.

Basu, P. (2010). Biomass gasification and pyrolysis: practical design and theory, Academic press.

Basu, P. (2013). Biomass gasification, pyrolysis and torrefaction: practical design and theory, Academic press.

Becidan, M., et al. (2015). "Norwegian waste-toenergy (wte) in 2030: challenges and opportunities." Chemical Engineering Transactions **43**: 2401-2406.

Begum, S., et al. (2013). "Performance analysis of an integrated fixed bed gasifier model for different biomass feedstocks." Energies **6**(12): 6508-6524.

Beheshti, S., et al. (2015). "Process simulation of biomass gasification in a bubbling fluidized bed reactor." Energy Conversion and Management **94**: 345-352.

Bessou, C., et al. (2011). "Biofuels, greenhouse gases and climate change. A review." Agronomy for Sustainable Development **31**(1): 1-79.

Bina, O. (2013). "The green economy and sustainable development: an uneasy balance?" Environment and Planning C: Government and Policy **31**(6): 1023-1047.

Brar, J., et al. (2012). "Cogasification of coal and biomass: a review." International Journal of Forestry Research **2012**.

Bridgwater, A. V. and G. Evans (1993). An assessment of thermochemical conversion systems for processing biomass and refuse, Energy Technology Support Unit Harwell.

Broer, K. M. and R. C. Brown (2015). "The role of char and tar in determining the gas-phase partitioning of nitrogen during biomass gasification." Applied Energy **158**: 474-483.

Buekens, A. and H. Huang (1998). "Catalytic plastics cracking for recovery of gasoline-range hydrocarbons from municipal plastic wastes." Resources, Conservation and Recycling **23**(3): 163-181.

Carpenter, D. L., et al. (2010). "Pilot-scale gasification of corn stover, switchgrass, wheat straw, and wood: 1. Parametric study and comparison with literature." Industrial & Engineering Chemistry Research **49**(4): 1859-1871.

Carrier, M., et al. (2011). "Thermogravimetric analysis as a new method to determine the lignocellulosic composition of biomass." Biomass and Bioenergy **35**(1): 298-307.

Chang, F. H. (2004). Energy and sustainability comparisons of anaerobic digestion and thermal technologies for processing animal waste. 2004 ASAE Annual Meeting, American Society of Agricultural and Biological Engineers.

Channiwala, S. and P. Parikh (2002). "A unified correlation for estimating HHV of solid, liquid and gaseous fuels." Fuel **81**(8): 1051-1063.

Chareonpanich, M., et al. (2017). "Integrated transdisciplinary technologies for greener and more sustainable innovations and applications of Cleaner Production in the Asia–Pacific region." Journal of Cleaner Production **142**: 1131-1137.

Chauhan, V. S., et al. (2013). "Effect of particle size of magnesium silicate filler on physical properties of paper." The Canadian Journal of Chemical Engineering **91**(5): 855-861.

Chen, X., et al. (2013). "Influence of porosity on compressive and tensile strength of cement mortar." Construction and Building Materials **40**: 869-874.

Chiang, K.-Y., et al. (2012). "Characterization and comparison of biomass produced from various sources: suggestions for selection of pretreatment technologies in biomass-to-energy." Applied Energy **100**: 164-171.

Chowdhury, R., et al. (1994). "Modelling and simulation of a downdraft rice husk gasifier." International Journal of Energy Research **18**(6): 581-594.

Ciferno, J. P. and J. J. Marano (2002). "Benchmarking biomass gasification technologies for fuels, chemicals and hydrogen production." US Department of Energy. National Energy Technology Laboratory.

Cimini, S., et al. (2005). "Simulation of a waste incineration process with flue-gas cleaning and heat recovery sections using Aspen Plus." Waste Management **25**(2): 171-175.

Cohce, M. K., et al. (2014). Economic Assessment of Three Biomass-Based Hydrogen Production Systems. Progress in Exergy, Energy, and the Environment, Springer**:** 899-912.

Corinaldesi, V., et al. (2016). "Study of physical and elasto-mechanical behaviour of fiber-reinforced concrete made of cement containing biomass ash." European Journal of Environmental and Civil Engineering **20**(sup1): s152-s168.

Creutzig, F., et al. (2015). "Bioenergy and climate change mitigation: an assessment." GCB Bioenergy **7**(5): 916-944.

Cui, Y., et al. (2008). "Fabrication and interfacial modification of wood/recycled plastic composite materials." Composites Part A: applied science and manufacturing **39**(4): 655-661.

Curbell Plastics, I. (2016). "Plastic Properties Table." https://www.curbellplastics.com/Research-Solutions/Plastic-Properties.

D'Sa, A. (2005). "Integrated resource planning (IRP) and power sector reform in developing countries." Energy Policy **33**(10): 1271-1285.

Del Río, P. and M. Burguillo (2009). "An empirical analysis of the impact of renewable energy deployment on local sustainability." Renewable and Sustainable Energy Reviews **13**(6): 1314-1325.

Delattre, C., et al. (2001). "Improvement of the microactivity test for kinetic and deactivation studies involved in catalytic cracking." Chemical Engineering Science **56**(4): 1337-1345.

Demirbas, A. (2004). "Pyrolysis of municipal plastic wastes for recovery of gasoline-range hydrocarbons." Journal of Analytical and Applied Pyrolysis **72**(1): 97-102.

Demirbas, A. (2005). "Potential applications of renewable energy sources, biomass combustion problems in boiler power systems and combustion related environmental issues." Progress in Energy and Combustion science **31**(2): 171-192.

Demirbas, A. (2009). "Global renewable energy projections." Energy Sources, Part B **4**(2): 212-224.

Demirbas, A. (2011). "Competitive liquid biofuels from biomass." Applied Energy **88**(1): 17-28.

Demirbas, M. F. (2009). "Biorefineries for biofuel upgrading: a critical review." Applied Energy **86**: S151-S161.

Demirbas, M. F. (2011). "Biofuels from algae for sustainable development." Applied Energy **88**(10): 3473-3480.

Deniz, C. and B. Zincir (2016). "Environmental and economical assessment of alternative marine fuels." Journal of Cleaner Production **113**: 438-449.

Di Blasi, C. (2000). "Dynamic behaviour of stratified downdraft gasifiers." Chemical Engineering Science **55**(15): 2931-2944.

Di Giacomo, G. and L. Taglieri (2009). "Renewable energy benefits with conversion of woody residues to pellets." Energy **34**(5): 724-731.

DIN (2012). "Solid mineral fuels – determination of sulfur content – Part 3: Instrumental methods, DIN 51724-3." German Institute for Standardization, Germany.

Diop, C. I. K. and J.-M. Lavoie "Isolation of Nanocrystalline Cellulose: A Technological Route for Valorizing Recycled Tetra Pak Aseptic Multilayered Food Packaging Wastes." Waste and Biomass Valorization: 1-16.

Djomo, S. N., et al. (2015). "Impact of feedstock, land use change, and soil organic carbon on energy and greenhouse gas performance of biomass cogeneration technologies." Applied Energy **154**: 122-130.

Doherty, W., et al. (2009). "The effect of air preheating in a biomass CFB gasifier using ASPEN Plus simulation." Biomass and Bioenergy **33**(9): 1158-1167.

Duan, P. and P. E. Savage (2010). "Hydrothermal liquefaction of a microalga with heterogeneous catalysts." Industrial & Engineering Chemistry Research **50**(1): 52-61.

Duku, M. H., et al. (2011). "A comprehensive review of biomass resources and biofuels potential in Ghana." Renewable and Sustainable Energy Reviews **15**(1): 404-415.

El-Emam, R. S., et al. (2012). "Energy and exergy analyses of an integrated SOFC and coal gasification system." International Journal of Hydrogen Energy **37**(2): 1689-1697.

Ertas, M. and M. H. Alma (2011). "Slow pyrolysis of chinaberry (Melia azedarach L.) seeds: Part I. The influence of pyrolysis parameters on the product yields." Energy Education Science and Technology Part A-Energy Science and Research **26**(2): 143-154.

Euh, S. H., et al. (2016). "A study on the effect of tar fouled on thermal efficiency of a wood pellet boiler: A performance analysis and simulation using Computation Fluid Dynamics." Energy **103**: 305-312.

Fallah, V., et al. (2016). "Cluster evolution mechanisms during aging in Al–Mg–Si alloys." Acta Materialia **103**: 290-300.

Ferrer-Castán, D., et al. (2016). "Water-energy dynamics, habitat heterogeneity, history, and broad-scale patterns of mammal diversity." Acta Oecologica **77**: 176-186.

Ferrero, G. (1989). Pyrolysis and Gasification, Kluwer Academic Pub.

Fouquet, R. (2016). "Lessons from energy history for climate policy: Technological change, demand and economic development." Energy Research & Social Science **22**: 79-93.

Fouquet, R. and P. J. Pearson (2012). "Past and prospective energy transitions: insights from history." Energy Policy **50**: 1-7.

Fridleifsson, I. B. (2001). "Geothermal energy for the benefit of the people." Renewable and Sustainable Energy Reviews **5**(3): 299-312.

Fu, J., et al. (2016). "Non-Fourier heat conduction in a sandwich panel with a cracked foam core." International Journal of Thermal Sciences **102**: 263-273.

Garforth, A., et al. (1998). "Production of hydrocarbons by catalytic degradation of high density polyethylene in a laboratory fluidised-bed reactor." Applied Catalysis A: General **169**(2): 331-342.

Gasparatos, A., et al. (2017). "Renewable energy and biodiversity: Implications for transitioning to a Green Economy." Renewable and Sustainable Energy Reviews **70**: 161-184.

Gašparovič, L., et al. (2010). "Kinetic study of wood chips decomposition by TGA." Chemical Papers **64**(2): 174-181.

Ghassemi, H., et al. (2015). "Mathematical modeling of extra-heavy oil gasification at different fuel water contents." Fuel **162**: 258-263.

Ghassemi, H. and R. Shahsavan-Markadeh (2014). "Effects of various operational parameters on biomass gasification process; a modified equilibrium model." Energy Conversion and Management **79**: 18-24.

Gkinosatis, D. (2009). Thin film for waste packing cassettes, US Patents (US20090191392 A1).

Goldemberg, J. (2000). World Energy Assessment: Energy and the challenge of sustainability, United Nations Pubns.

González-García, S., et al. (2012). "Life cycle assessment of two alternative bioenergy systems involving Salix spp. biomass: Bioethanol production and power generation." Applied Energy **95**: 111-122.

Goyal, H., et al. (2008). "Bio-fuels from thermochemical conversion of renewable resources: a review." Renewable and Sustainable Energy Reviews **12**(2): 504-517.

Griffiths, S. (2017). "A review and assessment of energy policy in the Middle East and North Africa region." Energy Policy **102**: 249-269.

Groom, M. J., et al. (2008). "Biofuels and biodiversity: principles for creating better policies for biofuel production." Conservation Biology **22**(3): 602-609.

Guest, G., et al. (2013). "Global warming potential of carbon dioxide emissions from biomass stored in the anthroposphere and used for bioenergy at end of life." Journal of Industrial Ecology **17**(1): 20-30.

Guidolin, M. and R. Guseo (2016). "The German energy transition: Modeling competition and substitution between nuclear power and Renewable Energy Technologies." Renewable and Sustainable Energy Reviews **60**: 1498-1504.

Guo, F., et al. (2016). "Low-Cost Coir Fiber Composite with Integrated Strength and Toughness." ACS Sustainable Chemistry & Engineering **4**(10): 5450-5455.

Guo, L., et al. (2016). "Compression and relaxation properties of selected biomass for briquetting." Biosystems Engineering **148**: 101-110.

Gupta, N. (2007). Effect of various fillers on physical and optical properties of agro-straw papers, Thapar Unuversity Patiala.

Gustavsson, L., et al. (2017). "Climate change effects of forestry and substitution of carbon-intensive materials and fossil fuels." Renewable and Sustainable Energy Reviews **67**: 612-624.

Hannequart, J. (2004). "Good practice guide on waste plastics recycling: A guide by and for local and regional authorities." Association of cities and regions for recycling (ACRR), Belgium.

Hansen, V., et al. (2017). "The effects of straw or straw-derived gasification biochar applications on soil quality and crop productivity: A farm case study." Journal of Environmental Management **186**: 88-95.

Harter, H., et al. (2017). "Developing a roadmap for the modernisation of city quarters–Comparing the primary energy demand and greenhouse gas emissions." Building and Environment **112**: 166-176.

Heinimö, J. and M. Junginger (2009). "Production and trading of biomass for energy–an overview of the global status." Biomass and Bioenergy **33**(9): 1310-1320.

Hernandez, D., et al. (2014). "Biofuels from microalgae: lipid extraction and methane production from the residual biomass in a biorefinery approach." Bioresource Technology **170**: 370-378.

Higman, C. (2013). State of the gasification industry–the updated worldwide gasification database. Gasification Technologies Conference, Colorado Springs, 16th October.

Higman, C. and M. Van der Burgt (2011). Gasification, Gulf Professional Publishing.

Huang, X., et al. (2013). "Filler modification for papermaking with starch/oleic acid complexes with the aid of calcium ions." Carbohydrate Polymers **98**(1): 931-935.

Huang, Y., et al. (2011). "Characterization of animal manure and cornstalk ashes as affected by incineration temperature." Applied Energy **88**(3): 947-952.

IEA., A. v. d. D., H. Boerrigter (2006). "Snthesis gas from biomass for fuels and chemicals."

Inayat, M., et al. (2015). The Study of Temperature Profile and Syngas Flare in Co-gasification of Biomass Feedstock in Throated Downdraft Gasifier. ICGSCE 2014, Springer**:** 203-210.

Janajreh, I., et al. (2013). "Plasma gasification process: Modeling, simulation and comparison with conventional air gasification." Energy Conversion and Management **65**: 801-809.

Jangsawang, W., et al. (2015). "Optimum Equivalence Ratio of Biomass Gasification Process Based on Thermodynamic Equilibrium Model." Energy Procedia **79**: 520-527.

Jarungthammachote, S. and A. Dutta (2007). "Thermodynamic equilibrium model and second law analysis of a downdraft waste gasifier." Energy **32**(9): 1660-1669.

Jarungthammachote, S. and A. Dutta (2008). "Equilibrium modeling of gasification: Gibbs free energy minimization approach and its application to spouted bed and spout-fluid bed gasifiers." Energy Conversion and Management **49**(6): 1345-1356.

Jefferson, P. G., et al. (2004). "Potential utilization of native prairie grasses from western Canada as ethanol feedstock." Canadian Journal of Plant Science **84**(4): 1067-1075.

Jin, H., et al. (2010). "Hydrogen production by partial oxidative gasification of biomass and its model compounds in supercritical water." International Journal of Hydrogen Energy **35**(7): 3001-3010.

Junginger, M., et al. (2006). "The growing role of biofuels-opportunities, challenges and pitfalls." International Sugar Journal **108**(1295): 618-619.

Kaminsky, W., et al. (1979). "Raw material recovery from scrap tires and plastic waste by pyrolysis." Recycling Berlin'79: 681-685.

Karakul, A. K. (2016). "Educating labour force for a green economy and renewable energy jobs in Turkey: A quantitave approach." Renewable and Sustainable Energy Reviews **63**: 568-578.

Kaushal, P. and R. Tyagi (2017). "Advanced simulation of biomass gasification in a fluidized bed reactor using ASPEN PLUS." Renewable Energy **101**: 629-636.

Kelly-Richards, S., et al. (2017). "Governing the transition to renewable energy: A review of impacts and policy issues in the small hydropower boom." Energy Policy **101**: 251-264.

Kihedu, J. H., et al. (2014). "Counter-flow air gasification of woody biomass pellets in the auto-thermal packed bed reactor." Fuel **117**: 1242-1247.

Kim, H. S. (2000). "On the rule of mixtures for the hardness of particle reinforced composites." Materials Science and Engineering: A **289**(1): 30-33.

Klass, D. L. (1998). Biomass for renewable energy, fuels, and chemicals, Academic press.

Kumabe, K., et al. (2007). "Co-gasification of woody biomass and coal with air and steam." Fuel **86**(5): 684-689.

Kumar, A., et al. (2009). "Thermochemical biomass gasification: a review of the current status of the technology." Energies **2**(3): 556-581.

Kumar, P., et al. (2009). "Methods for pretreatment of lignocellulosic biomass for efficient hydrolysis and biofuel production." Industrial & Engineering Chemistry Research **48**(8): 3713-3729.

Kuo, P.-Y., et al. (2009). "Effects of material compositions on the mechanical properties of wood–plastic composites manufactured by injection molding." Materials & Design **30**(9): 3489-3496.

Lamers, P., et al. (2012). "Developments in international solid biofuel trade—An analysis of volumes, policies, and market factors." Renewable and Sustainable Energy Reviews **16**(5): 3176-3199.

Larsson, S. H., et al. (2008). "High quality biofuel pellet production from pre-compacted low density raw materials." Bioresource Technology **99**(15): 7176-7182.

Lazaro, A., et al. (2013). "Intercomparative tests on phase change materials characterisation with differential scanning calorimeter." Applied Energy **109**: 415-420.

Lee, B.-H., et al. (2016). "Ash deposition characteristics of Moolarben coal and its blends during coal combustion." Korean Journal of Chemical Engineering **33**(1): 147-153.

Leung, D. Y., et al. (2010). "A review on biodiesel production using catalyzed transesterification." Applied Energy **87**(4): 1083-1095.

Li, C. and K. Suzuki (2009). "Tar property, analysis, reforming mechanism and model for biomass gasification—an overview." Renewable and Sustainable Energy Reviews **13**(3): 594-604.

Liu, S. (2015). "A synergetic pretreatment technology for woody biomass conversion." Applied Energy **144**: 114-128.

López-González, D., et al. (2014). "Kinetic analysis and thermal characterization of the microalgae combustion process by thermal analysis coupled to mass spectrometry." Applied Energy **114**: 227-237.

López, A., et al. (2011). "Influence of time and temperature on pyrolysis of plastic wastes in a semi-batch reactor." Chemical Engineering Journal **173**(1): 62-71.

Lu, J.-J. and W.-H. Chen (2015). "Investigation on the ignition and burnout temperatures of bamboo and sugarcane bagasse by thermogravimetric analysis." Applied Energy **160**: 49-57.

Lugato, E., et al. (2013). "An energy-biochar chain involving biomass gasification and rice cultivation in Northern Italy." GCB Bioenergy **5**(2): 192-201.

Mabuda, A., et al. (2016). "Model free kinetic analysis of biomass/sorbent blends for gasification purposes." Renewable and Sustainable Energy Reviews **53**: 1656-1664.

Madadian, E., et al. (2013). "Application of analytic hierarchy process and multicriteria decision analysis on waste management: a case study in Iran." Environmental Progress & Sustainable Energy **32**(3): 810-817.

Madadian, E., et al. (2014). "Green energy production: The potential of using biomass gasification." Journal of Green Engineering **4**(2): 101-116.

Madadian, E., et al. (2016). "Gasification of pelletized woody biomass using a downdraft reactor and impact of material bridging." Journal of Energy Engineering: 04016001.

Mandil, C. World Energy Outlook 2004. International Energy Agency (IEA), Paris, 2004.

Mansuy, N., et al. (2017). "Estimating the spatial distribution and locating hotspots of forest biomass from harvest residues and fire-damaged stands in Canada's managed forests." Biomass and Bioenergy **97**: 90-99.

Maria, E. and T. Tsoutsos (2004). "The sustainable management of renewable energy sources installations: legal aspects of their environmental impact in small Greek islands." Energy Conversion and Management **45**(5): 631-638.

Masnadi, M. S., et al. (2015). "Single-fuel steam gasification of switchgrass and coal in a bubbling fluidized bed: A comprehensive parametric reference for co-gasification study." Energy **80**: 133-147.

Mastral, F., et al. (2002). "Pyrolysis of high-density polyethylene in a fluidised bed reactor. Influence of the temperature and residence time." Journal of Analytical and Applied Pyrolysis **63**(1): 1-15.

Materazzi, M., et al. (2013). "Thermodynamic modelling and evaluation of a two-stage thermal process for waste gasification." Fuel **108**: 356-369.

McKendry, P. (2002). "Energy production from biomass (part 1): overview of biomass." Bioresource Technology **83**(1): 37-46.

McKendry, P. (2002). "Energy production from biomass (part 2): conversion technologies." Bioresource Technology **83**(1): 47-54.

McKendry, P. (2002). "Energy production from biomass (part 3): gasification technologies." Bioresource Technology **83**(1): 55-63.

Mediavilla, M., et al. (2013). "The transition towards renewable energies: Physical limits and temporal conditions." Energy Policy **52**: 297-311.

Melgar, A., et al. (2007). "Thermochemical equilibrium modelling of a gasifying process." Energy Conversion and Management **48**(1): 59-67.

Mendiburu, A. Z., et al. (2014). "Thermochemical equilibrium modeling of biomass downdraft gasifier: Stoichiometric models." Energy **66**: 189-201.

Mendiburu, A. Z., et al. (2014). "Thermochemical equilibrium modeling of a biomass downdraft gasifier: Constrained and unconstrained non-stoichiometric models." Energy **71**: 624-637.

Mendu, V., et al. (2012). "Global bioenergy potential from high-lignin agricultural residue." Proceedings of the National Academy of Sciences **109**(10): 4014-4019.

Meyer, M. A. and A. Weiss (2014). "Life cycle costs for the optimized production of hydrogen and biogas from microalgae." Energy **78**(0): 84-93.

Midilli, A., et al. (2007). "The role and future benefits of green energy." International Journal of Green Energy **4**(1): 65-87.

Mikulandrić, R., et al. (2016). "Modelling of thermal processes during extrusion based densification of agricultural biomass residues." Applied Energy.

Milne, T. A., et al. (1997). Biomass Gasifier" Tars": Their Nature, Formation, Destruction, and Tolerance Limits in Energy Conversion Devices. Proceedings of the 3rd Biomass Conference of the Americas: Making a Business from Biomass in Energy, Environment, Chemical, Fibers and Materials.

Miskolczi, N., et al. (2009). "Fuels by pyrolysis of waste plastics from agricultural and packaging sectors in a pilot scale reactor." Fuel Processing Technology **90**(7): 1032-1040.

Miskolczi, N., et al. (2006). High energy containing fractions from plastic wastes by their chemical recycling. Macromolecular Symposia, Wiley Online Library.

Mitchell, R., et al. (2012). "The feasibility of switchgrass for biofuel production." Biofuels **3**(1): 47-59.

Mohammed, M., et al. (2011). "Air gasification of empty fruit bunch for hydrogen-rich gas production in a fluidized-bed reactor." Energy Conversion and Management **52**(2): 1555-1561.

Mohsenin, N. N. (1970). "Physical properties of plant and animial materials. Vol. 1. Structure, physical characterisitics and mechanical properties." Physical properties of plant and animial materials. Vol. 1. Structure, physical characterisitics and mechanical properties.

Morf, P., et al. (2002). "Mechanisms and kinetics of homogeneous secondary reactions of tar from continuous pyrolysis of wood chips." Fuel **81**(7): 843-853.

Mottiar, Y., et al. (2016). "Designer lignins: harnessing the plasticity of lignification." Current Opinion in Biotechnology **37**: 190-200.

Nadeem, R., et al. (2016). "Biosorption of Pb (II) onto immobilized and native Mangifera indica waste biomass." Journal of Industrial and Engineering Chemistry **35**: 185-194.

Naik, S., et al. (2010). "Characterization of Canadian biomass for alternative renewable biofuel." Renewable Energy **35**(8): 1624-1631.

Najafi, G., et al. (2009). "Performance and exhaust emissions of a gasoline engine with ethanol blended gasoline fuels using artificial neural network." Applied Energy **86**(5): 630-639.

Namioka, T., et al. (2011). "Hydrogen-rich gas production from waste plastics by pyrolysis and low-temperature steam reforming over a ruthenium catalyst." Applied Energy **88**(6): 2019-2026.

Namkung, H., et al. (2016). "Effect of bed agglomeration by mineral component with different coal types." Journal of the Energy Institute **89**(2): 172-181.

Nanda, S., et al. (2014). "Pathways of lignocellulosic biomass conversion to renewable fuels." Biomass Conversion and Biorefinery **4**(2): 157-191.

Nanda, S., et al. (2013). "Characterization of North American lignocellulosic biomass and biochars in terms of their candidacy for alternate renewable fuels." Bioenergy Research **6**(2): 663-677.

Nigam, P. S. and A. Singh (2011). "Production of liquid biofuels from renewable resources." Progress in Energy and Combustion Science **37**(1): 52-68.

Nikanorov, S., et al. (2005). "Structural and mechanical properties of Al–Si alloys obtained by fast cooling of a levitated melt." Materials Science and Engineering: A **390**(1): 63-69.

Nuñez, A. J., et al. (2003). "Mechanical characterization of polypropylene–wood flour composites." Journal of Applied Polymer Science **88**(6): 1420-1428.

Obernberger, I. and G. Thek (2008). Combustion and gasification of solid biomass for heat and power production in Europe-state-of-the-art and relevant future developments. Proc. of the 8th European Conference on Industrial Furnaces and Boilers (keynote lecture).

Okuwaki, A. (2004). "Feedstock recycling of plastics in Japan." Polymer Degradation and Stability **85**(3): 981-988.

Ong, Z., et al. (2015). "Co-gasification of woody biomass and sewage sludge in a fixed-bed downdraft gasifier." AIChE Journal **61**(8): 2508-2521.

Pachauri, R. K., et al. (2014). Climate change 2014: synthesis Report. Contribution of working groups I, II and III to the fifth assessment report of the intergovernmental panel on climate change, IPCC.

Paisley, M. A. and D. Anson (1998). "Biomass gasification for gas turbine-based power generation." Journal of Engineering for Gas Turbines and Power **120**(2): 284-288.

Panda, A. K., et al. (2010). "Thermolysis of waste plastics to liquid fuel: A suitable method for plastic waste management and manufacture of value added products—A world prospective." Renewable and Sustainable Energy Reviews **14**(1): 233-248.

Panda, B. P., et al. (2013). "Mechanical Behavior and Fracture Toughness Evaluation of Multiphase Polymer Nanocomposites Using Impact and-Integral via Locus Method." Chinese Journal of Engineering **2013**.

Peng, J., et al. (2010). "An economical and market analysis of Canadian wood pellets." International Journal of Green Energy **7**(2): 128-142.

Pereira, E. G., et al. (2012). "Sustainable energy: a review of gasification technologies." Renewable and Sustainable Energy Reviews **16**(7): 4753-4762.

Popvics, S. (1973). Method for developing relationships between mechanical properties of hardened concrete. Journal Proceedings.

Prins, M. J., et al. (2007). "From coal to biomass gasification: comparison of thermodynamic efficiency." Energy **32**(7): 1248-1259.

Puig-Arnavat, M., et al. (2010). "Review and analysis of biomass gasification models." Renewable and Sustainable Energy Reviews **14**(9): 2841-2851.

Puig-Arnavat, M., et al. (2012). "Modified thermodynamic equilibrium model for biomass gasification: a study of the influence of operating conditions." Energy & Fuels **26**(2): 1385-1394.

Puig-Arnavat, M., et al. (2013). "Artificial neural network models for biomass gasification in fluidized bed gasifiers." Biomass and Bioenergy **49**: 279-289.

Raheem, A., et al. (2015). "Thermochemical conversion of microalgal biomass for biofuel production." Renewable and Sustainable Energy Reviews **49**: 990-999.

Reed, T. B. and M. Markson (1983). "A predictive model for stratified downdraft gasification of biomass." Progress in Biomass Conversion.

Rezaei, H., et al. (2016). "Pyrolysis of ground pine chip and ground pellet particles." The Canadian Journal of Chemical Engineering.

Ritchie, R. O. (2011). "The conflicts between strength and toughness." Nature Materials **10**(11): 817-822.

Rutter, P. and J. Keirstead (2012). "A brief history and the possible future of urban energy systems." Energy Policy **50**: 72-80.

Salam, P. A., et al. (2010). "Report on the status of biomass Gasification in Thailand and Cambodia." Prepared for: Energy Environment Partnership (EEP)(Mekong Region. Asian Inst Technol, Bangkok, Thailand).

Sarkar, N., et al. (2012). "Bioethanol production from agricultural wastes: An overview." Renewable Energy **37**(1): 19-27.

Sattar, A., et al. (2014). "Steam gasification of rapeseed, wood, sewage sludge and miscanthus biochars for the production of a hydrogen-rich syngas." Biomass and Bioenergy **69**: 276-286.

Schoeters, J. and A. Buekens (1979). Pyrolysis of plastics in a steam fluidised bed. International Recycling Congress, Berlin: Freitag Verlag.

Shahrukh, H., et al. (2015). "Net energy ratio for the production of steam pretreated biomass-based pellets." Biomass and Bioenergy **80**: 286-297.

Sharma, A. K. (2011). "Experimental investigations on a 20 kWe, solid biomass gasification system." Biomass and Bioenergy **35**(1): 421-428.

Sharp, J. D., et al. (2009). "Anticipating public attitudes toward underground CO 2 storage." International Journal of Greenhouse Gas Control **3**(5): 641-651.

Sheth, P. N. and B. Babu (2009). "Experimental studies on producer gas generation from wood waste in a downdraft biomass gasifier." Bioresource Technology **100**(12): 3127-3133.

Simell, P. A., et al. (1999). "Steam reforming of gasification gas tar over dolomite with benzene as a model compound." Industrial & Engineering Chemistry Research **38**(4): 1250-1257.

Sims, R. E. (2003). Bioenergy options for a cleaner environment: in developed and developing countries, Elsevier.

Singh, J. and S. Gu (2010). "Commercialization potential of microalgae for biofuels production." Renewable and Sustainable Energy Reviews **14**(9): 2596-2610.

Singh, R., et al. (2016). "Opportunities for utilization of non-conventional energy sources for biomass pretreatment." Bioresource Technology **199**: 398-407.

Skoulou, V., et al. (2008). "Syngas production from olive tree cuttings and olive kernels in a downdraft fixed-bed gasifier." International Journal of Hydrogen Energy **33**(4): 1185-1194.

Slopiecka, K., et al. (2012). "Thermogravimetric analysis and kinetic study of poplar wood pyrolysis." Applied Energy **97**: 491-497.

Sokhansanj, S. and E. Webb (2016). "Evaluating industrial drying of cellulosic feedstock for bioenergy: a systems approach." Biofuels, Bioproducts and Biorefining **10**(1): 47-55.

Statistics, N. C. f. H. S. D. o. V., et al. (1979). Vital statistics of the United States, United States Bureau of the Census.

Stigka, E. K., et al. (2014). "Social acceptance of renewable energy sources: A review of contingent valuation applications." Renewable and Sustainable Energy Reviews **32**: 100-106.

Stultz, S. C. and J. B. Kitto (1992). "Steam: it's generation and use." The Babcock & Wilcox Company, Barberton, Ohio USA.

Sun, J. and S. Simon (2007). "The melting behavior of aluminum nanoparticles." Thermochimica Acta **463**(1): 32-40.

Tapasvi, D., et al. (2015). "A simulation study on the torrefied biomass gasification." Energy Conversion and Management **90**: 446-457.

Temmerman, M., et al. (2006). "Comparative study of durability test methods for pellets and briquettes." Biomass and Bioenergy **30**(11): 964-972.

Thellufsen, J. Z. and H. Lund (2016). "Roles of local and national energy systems in the integration of renewable energy." Applied Energy **183**: 419-429.

Tinaut, F. V., et al. (2008). "Effect of biomass particle size and air superficial velocity on the gasification process in a downdraft fixed bed gasifier. An experimental and modelling study." Fuel Processing Technology **89**(11): 1076-1089.

Towler, B. F. (2014). The future of energy, Academic Press.

Tso, I. M., et al. (2007). "Does the giant wood spider Nephila pilipes respond to prey variation by altering web or silk properties?" Ethology **113**(4): 324-333.

Tunde-Akintunde, T., et al. (2005). "Mass-volume-area related and mechanical properties of soybean as a function of moisture and variety." International Journal of Food Properties **8**(3): 449-456.

USEPA (2015). "Division of Materials and Waste Management (DMWM)." Columbus, OH.

Van Loo, S. and J. Koppejan (2008). "Biomass combustion and co-firing." Earthscan, London/Sterling.

Verma, V., et al. (2009). "Small scale biomass heating systems: standards, quality labelling and market driving factors–an EU outlook." Biomass and Bioenergy **33**(10): 1393-1402.

Verma, V., et al. (2012). "Agro-pellets for domestic heating boilers: Standard laboratory and real life performance." Applied Energy **90**(1): 17-23.

Wang, L., et al. (2013). "Hierarchical microstructures self-assembled from polymer systems." Polymer **54**(14): 3427-3442.

Wei, X., et al. (2005). "Behaviour of gaseous chlorine and alkali metals during biomass thermal utilisation." Fuel **84**(7): 841-848.

Williams, J. and C. Gamonpilas (2008). "Using the simple compression test to determine Young's modulus, Poisson's ratio and the Coulomb friction coefficient." International Journal of Solids and Structures **45**(16): 4448-4459.

Wrangham, R. W., et al. (1999). "The raw and the stolen." Current Anthropology **40**(5): 567-594.

Xiao, X., et al. (2013). "Synthesis gas production from catalytic gasification of waste biomass using nickel-loaded brown coal char." Fuel **103**: 135-140.

Yaman, S. (2004). "Pyrolysis of biomass to produce fuels and chemical feedstocks." Energy Conversion and Management **45**(5): 651-671.

Yao, Y., et al. (2015). "Engineered biochar from biofuel residue: characterization and its silver removal potential." ACS Applied Materials & Interfaces **7**(19): 10634-10640.

Yin, C.-Y. (2011). "Prediction of higher heating values of biomass from proximate and ultimate analyses." Fuel **90**(3): 1128-1132.

Yue, D., et al. (2014). "Biomass-to-bioenergy and biofuel supply chain optimization: overview, key issues and challenges." Computers & Chemical Engineering **66**: 36-56.

Zanzi, R., et al. (2002). "Rapid pyrolysis of agricultural residues at high temperature." Biomass and Bioenergy **23**(5): 357-366.

Zhang, Y., et al. (2016). "Effect of fuel origin on synergy during co-gasification of biomass and coal in CO 2." Bioresource Technology **200**: 789-794.

Zhao, P., et al. (2014). "Clean solid biofuel production from high moisture content waste biomass employing hydrothermal treatment." Applied Energy **131**: 345-367.

Zhao, Y. and H.-H. Liu (2012). "An elastic stress–strain relationship for porous rock under anisotropic stress conditions." Rock Mechanics and Rock Engineering **45**(3): 389-399.

Zhong, Y., et al. (2007). "Enhancement of wood/polyethylene composites via compatibilization and incorporation of organoclay particles." Polymer Engineering & Science **47**(6): 797-803.